

博士論文

**A Study of Applicability and Properties of Recycled Aggregate Concrete with
Modified Fly Ash by Flotation Method**

浮遊選鉱法によって改質したフライアッシュを使用した再生骨材コンクリート
の特性と適用性に関する研究

2022年7月

林 航葳 リン ハンウェイ

LIN Hangwei

The University of Kitakyushu
Faculty of Environmental Engineering
Department of Architecture
Takasu Laboratory

A study of influence and applicability of modified fly ash obtained by flotation method on properties of recycled aggregate concrete

ABSTRACT

In general, this paper starts with the development of new flotation equipment to bring fly ash up to industrial standards by reducing the carbon content in fly ash. After those the mechanical and physical properties of concrete with different proportions and different aggregates are measured by different experiments, compared with normal concrete and an attempt is made to find out the connection between some of these properties. By comparing the measurements of compressive strength, drying shrinkage, static modulus of elasticity and dynamic modulus of elasticity of normal concrete with the predicted values of drying shrinkage of high strength concrete, it can be concluded that the application of fly ash in concrete after decarbonization using the new flotation method makes good results. The above results show that the application of MFAS prepared by the flotation method to concrete is feasible.

CHAPTER 1 RESEARCH BACKGROUND AND PURPOSE OF THE STUDY focuses on the production of fly ash and the hazards, briefly describes the classification system of fly ash, and discusses the development status of the flotation method of fly ash.

CHAPTER 2 PREVIOUS LITERATURE REVIEW mainly introduces the current status of research on fly ash concrete at home and abroad. The development of fly ash decarbonization technology is reflected through the development of fly ash flotation method and the international utilization of fly ash.

CHAPTER 3 RESEARCH METHOD mainly describes the experimental methods of this study. It includes the development process of the flotation method and the design of the concrete mix ratio introducing the development method of the new equipment.

CHAPTER 4 DEVELOPMENT OF FLOTATION DEVICE FOR REMOVING UNBURNT CARBON IN FLY ASH FOR USE IN HARDENED CEMENTITIOUS MATERIALS concluded that: We developed a prototype device for removing unburned carbon from fly ash by means of the flotation method and examined the operating conditions of the device experimentally.

CHAPTER 5 EFFECT OF INCORPORATING FLY ASH AND RECYCLED FINE AGGREGATE ON PROPERTIES AND CUMULATIVE PORE VOLUME OF CONCRETE concluded that: Incorporating RFA or low amount of FA as into concrete reduces its initial strength, but the compressive strength of concrete incorporating an appropriate amount of FA can reach that of concrete without FA as the age of concrete increases or the W/B ratio decreases.

CHAPTER 6 A STUDY ON PROPERTIES, STATIC AND DYNAMIC ELASTIC MODULUS OF RECYCLED CONCRETE UNDER THE INFLUENCE OF MODIFIED FLY ASH concluded that: The relationship between the compressive strength and static modulus of elasticity is recommended by an equation derived based on the formula of each national standard.

CHAPTER 7 STRENGTH AND DRYING SHRINKAGE OF HIGH-STRENGTH CONCRETE WITH RECYCLED AGGREGATES USING FLY ASH WITH THE FLOTATION OF DECARBONIZATION concluded that: By comparing the predicted formulas of various countries, the predicted formula of ACI is the closest to the actual value of this experiment.

ACKNOWLEDGEMENT

My deepest gratitude goes first and foremost to my tutor, Prof. Koji Takasu, who has taken his precious time off from his tight schedule, giving me suggestions and offering me constant encouragement, which contribute to the completion of my thesis.

Second, I would like to express my heartfelt gratitude to Prof. Weijun Gao who led me into the University of Kitakyushu and helped me a lot in the past years and thanks to Prof. Hidehiro Koyamada and Hiroki Suyama for the support on my experiment.

Third, I would like to thank my friends Dr. Shilun Liu and Murong Xu. They selflessly encouraged and helped me when I was constantly rejected by the publisher.

Thanks to all my friends in Takasu LAB, none of these would have been possible without your love and support.

Last my thanks would go to beloved family and my girlfriend (Dr. Yuan Peng), for their loving considerations and great confidence in me all through these years. I feel much grateful and heartily owe my achievement to them.

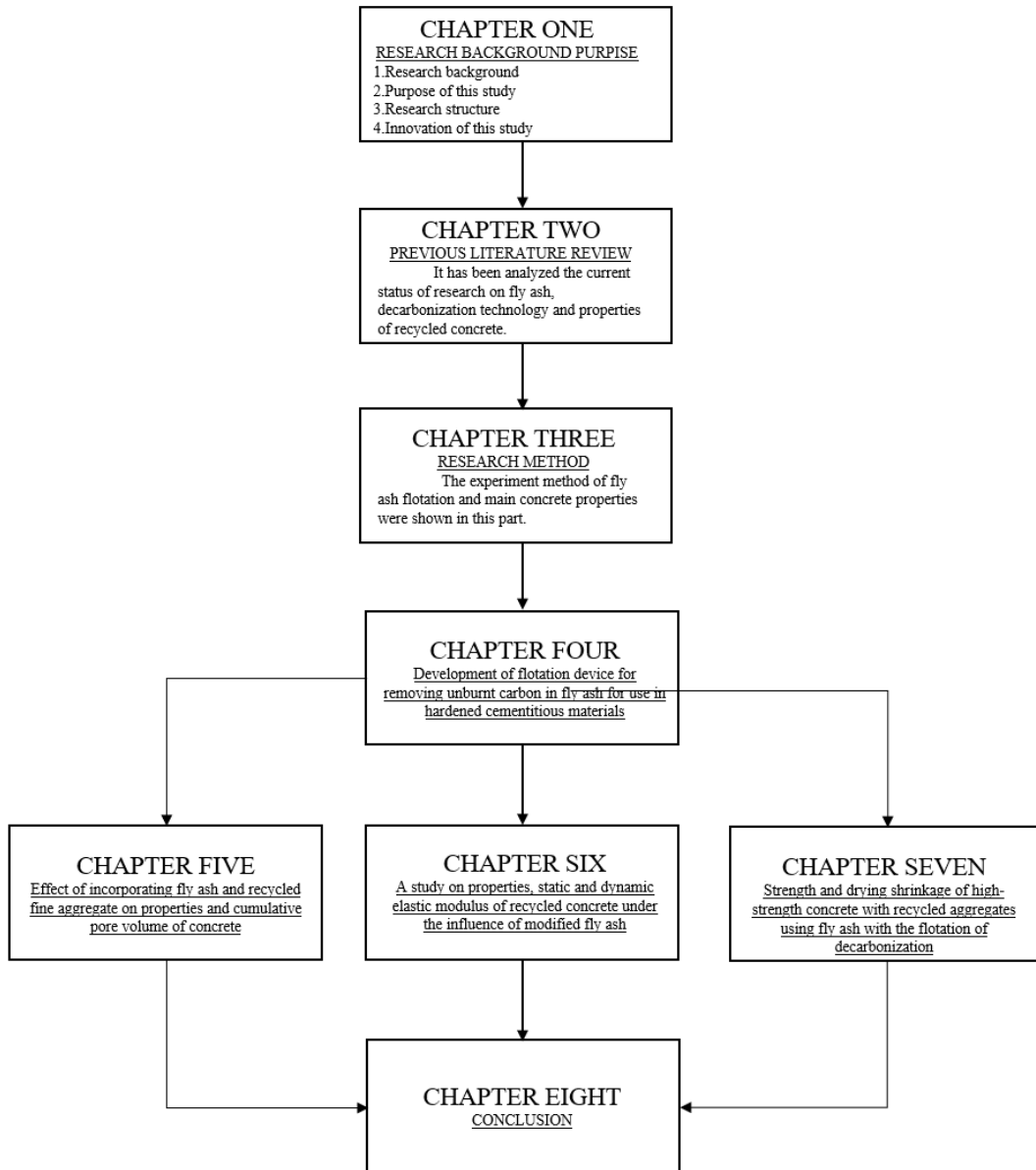
LIST OF CONTENTS

Chapter 1	1
RESEARCH BACKGROUND AND PURPOSE	1
1.1 Background	3
1.1.1 Production and harm of fly ash	3
1.1.3 Research significance of fly ash concrete	12
1.1.4 Effect of fly ash on properties of recycled concrete	14
1.1.5 The elastic modulus of fly ash concrete	17
1.2 Purpose of this study	19
1.3 Research structure	20
1.4 Innovation of this study	20
References	22
Chapter 2	25
PREVIOUS LITERATURE REVIEW	25
2.1 Research status of Fly ash flotation method	27
2.1.1 Research status of Fly ash	27
2.1.2 Decarbonization technology of fly ash	30
2.1.3 Flotation reagents for separating unburned carbon	38
2.1.4 Research progress on the structure and dynamics of foam	39
2.2 Research status of fly ash recycled aggregate concrete	42
2.2.1 Recycled aggregate	42
2.2.2 Research state of workability	48
2.2.3 Research state of compressive strength	49
2.2.4 Research state of drying shrinkage	54
2.3 Research state of static and dynamic modulus in concrete	59
2.4 The Current State of Research Regarding Cement Porosity	64
References	67
Chapter 3	75
RESEARCH METHOD	75
3.1 Flotation Method Experiment	77
3.1.1 Concrete Specimen Fabrication	80
3.1.2 concrete mix	80
3.1.3 Formulation	81
3.2 Fly ash recycled concrete experiment	83
3.2.1 Mixing of concrete	83
3.2.2 Compression Strength test	86
3.2.3 Drying shrinkage test	87
3.3 Modulus of Elasticity Experiment	89
3.3.1 Static Modulus of Elasticity test	89
3.3.2 Dynamic elastic modulus Test	91
3.4 Mercury intrusion porosimetry test for porosity	97

References.....	103
Chapter 4.....	105
DEVELOPMENT OF FLOTATION DEVICE FOR REMOVING UNBURNT CARBON IN FLY ASH FOR USE IN HARDENED CEMENTITIOUS MATERIALS	105
4.1 Introduction.....	107
4.2 Materials and Methods.....	109
4.2.1 Flotation Method Experiment	109
4.2.2. Concrete Specimen Fabrication	112
4.2.3. Concrete Specimen Tests	112
4.3. Results and Discussion	112
4.3.1. Removal of Unburned Carbon by the Flotation Method.....	112
4.3.2. Base Model Development and Performance Verification	115
4.3.3. Treatment Conditions	120
4.3.4. Properties of Concrete with MFAS	124
4.4. Conclusions.....	127
References.....	128
Chapter 5.....	131
EFFECT OF INCORPORATING FLY ASH AND RECYCLED FINE AGGREGATE ON PROPERTIES AND CUMULATIVE PORE VOLUME OF CONCRETE.....	131
5.1. Introduction.....	133
5.2. Experimental outlines	134
5.3. Experimental results and discussion	137
5.3.1 Influence of RFA and FA on the compressive strength of concrete	137
5.3.2 Influence of RFA and FA on the drying shrinkage of concrete	141
5.3.3 Cumulative pore volume.....	142
5.4. Conclusion	151
References.....	152
Chapter 6.....	155
A STUDY ON PROPERTIES, STATIC AND DYNAMIC ELASTIC MODULUS OF RECYCLED CONCRETE UNDER THE INFLUENCE OF MODIFIED FLY ASH.....	155
6.1 Introduction.....	157
6.2 Materials and experiments	158
6.2.1 Materials	158
6.2.2 Experiments	158
6.2.3 Test methods	159
6.3 Result and discussion.....	161
6.3.1 Result of f_c and ε_d	161
6.3.2 Result of E_c and E_d	163
6.3.3 Relationship between E_c and E_d	165
6.3.4 Relationship between f_c and E_c	167
6.3.5 Relationship between f_c and E_d	169
6.3.6 Influence of pore diameter on the correlation between Porosity and ε_d or E_d	170

6.4 Conclusions.....	175
References.....	176
Chapter 7.....	181
STRENGTH AND DRYING SHRINKAGE OF HIGH-STRENGTH CONCRETE WITH RECYCLED AGGREGATES USING FLY ASH WITH THE FLOTATION OF DECARBONIZATION.....	181
7.1. Introduction.....	183
7.2. Materials and method of experiment.....	184
7.2.1 Materials	184
7.2.2 Mix proportion	184
7.2.3 Test method.....	185
7.3. Result and discussion.....	186
7.3.1 Drying shrinkage test	186
7.3.2 Dry shrinkage prediction model.....	188
7.4. Conclusion	191
Reference	191
Chapter 8.....	193
CONCLUSION	193
8.1 Conclusion	194
8.2 Prospect.....	196

A study of influence and applicability of modified fly ash obtained by flotation method on properties of recycled aggregate concrete



Research flow chart of the thesis

Chapter 1

RESEARCH BACKGROUND AND PURPOSE

CHAPTER 1: RESEARCH BACKGROUND AND PURPOSE OF THE STUDY

1.1 Background

1.1.1 Production and harm of fly ash

Fly ash is a type of mineral substance that has latent volcanic ash activity. It is obtained at coal-fired power plants by spraying pulverized coal with preheated air into the furnace for suspension combustion. Dust collectors then collect the high-temperature flue gas that results from this process. It is a solid waste that is produced in the process of burning coal, and it is formed as a result of a series of changes that occur in the minerals that are found in coal..



Picture 1.1 Fly ash [1]

The value of fly ash is gradually being recognized by people as a result of the current situation both at home and abroad. In particular, the comprehensive utilization of fly ash has developed rapidly in recent years. This can be attributed to the fact that the situation is the same both at home and abroad. Asia has a very high per capita consumption rate for coal. The majority of the power plants burn coal as their primary fuel source. The growth of the power industry has led to the encouragement of joint ventures between the coal and electricity industries, which has also resulted in a significant rise in the amount of fly ash emissions. Exploitation brings about brand new difficulties.

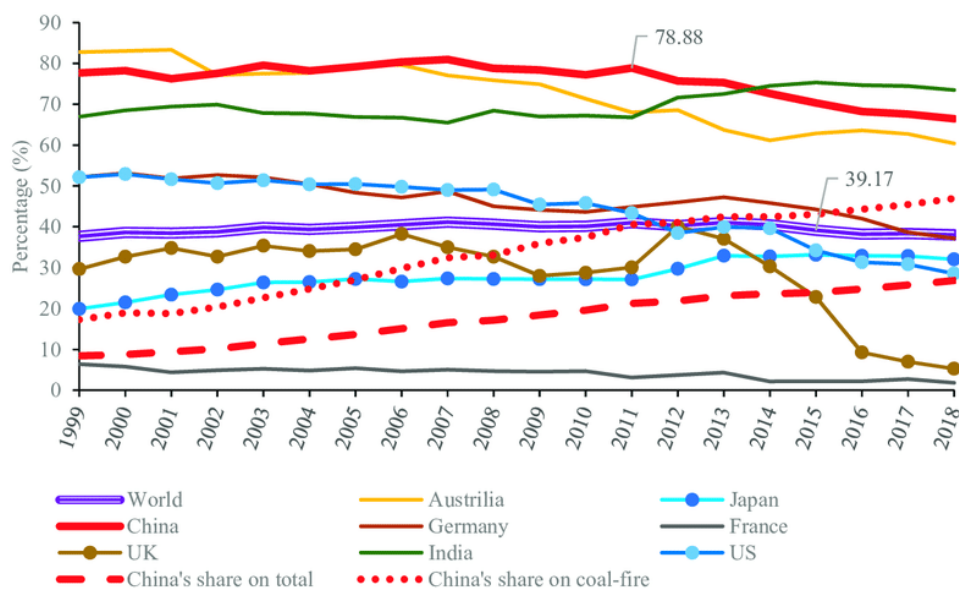


Fig 1.1 Proportion of coal-fired power generation to total power generation from 1999 to 2018.[2]

As a result of the situation that exists both in the United States and in other countries, people are gradually coming to recognize the value of fly ash. In particular, there has been a significant expansion in recent years in the use of fly ash in its comprehensive form. This is because the circumstance is the same both at home and in other countries where people are affected by it. Coal is consumed at a very high rate when compared to population in Asia. Coal is the primary fuel source for the vast majority of power plants, which can be found all over the world. The expansion of the power industry has encouraged joint ventures between the coal and electricity industries, which has led to a significant increase in the amount of fly ash emissions. This has also resulted in the encouragement of joint ventures between the coal and electricity industries. The exploitation of resources results in the emergence of brand-new problems.

Table 1.1 Generation and utilization of fly-ash in different countries.[3]

Country	Fly-ash production (million tons per year)	Fly-ash utilization (%)
India	112	38
China	100	45
USA	75	65
Germany	40	85
UK	15	50
Australia	10	85
Canada	6	75
France	3	85
Denmark	2	100
Italy	2	100
Netherlands	2	100

At the moment, population, resource depletion, and environmental damage are global problems that every nation must contend with. The environment is getting worse, the population is already quite

large, and there is already a lot of strain on the available resources. The comprehensive utilization of fly ash, which accounts for the largest discharge in terms of industrial waste residues, is a major issue with regards to the economy, the environment, and society. The pursuit of efficiency is not only an operational priority but also a long-term strategic issue for the sake of succeeding generations.

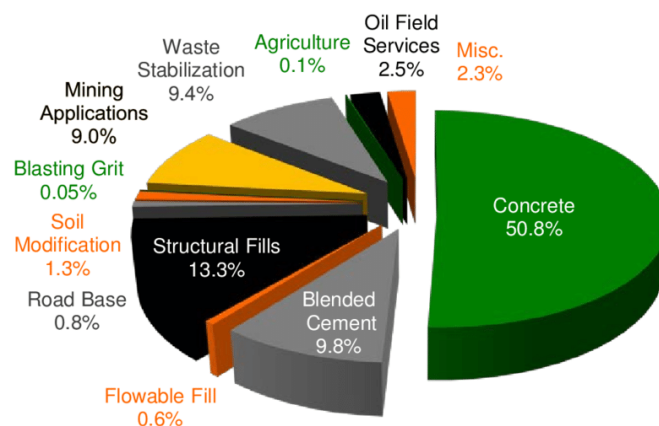


Fig 1.2 Coal fly ash use in 2012 in the U.S. by application [4]

Fly ash is a mineral-like industrial waste residue that possesses dormant pozzolanic activity. It is obtained by injecting pulverized coal into the furnace for suspension combustion with preheated air in a coal-fired power plant to produce high-temperature flue gas, and it is then collected by a dust collector. When pulverized coal particles are burned in the furnace, the temperature can reach at least 1300 degrees Celsius, and the byproducts take the form of molten droplets. They are kept in suspension in the flow of air by the action of turbulence, and they undergo rapid expansion by the action of the many different gas components that are present in the flue gas. The external air pressure is evenly pressed to these droplets from all directions as they move to the low temperature section with the flue gas. As a result, their surface can bear with the maximum tension to form a spherical shape. The rate of cooling of small droplets is quick, and they form vitreous bodies. The rate of cooling of large droplets is slow, and crystals can form inside of them. Some of the droplets are entombed by gas, which then forms hollow spheres of varying wall thicknesses around them. The thin-walled hollow spheres have the potential to shatter into fragments if they are rapidly cooled. The finished product of fly ash formation is a heterogeneous mixture that has a consistent look and is composed of fine but uneven particles.

There are roughly four stages involved in the production of fly ash, and they are as follows:

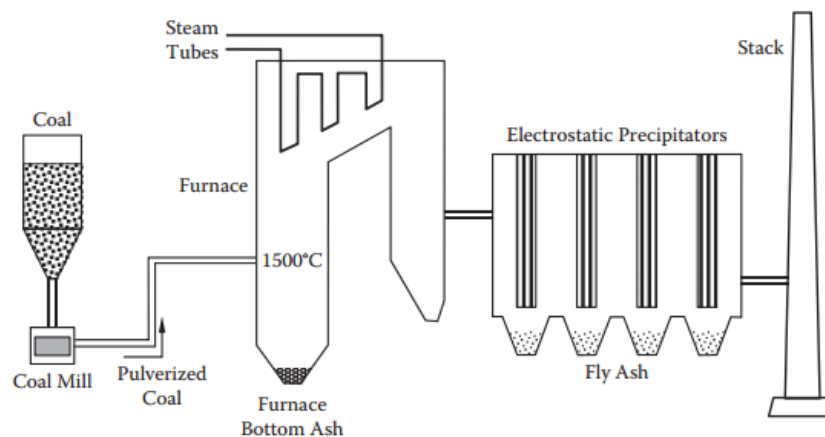
The first stage is when the air blows the pulverized coal into the boiler at a high speed to start the combustion process. This causes the volatile components in the coal to first escape from the gap between the mineral and the fixed carbon, which results in the formation of porous carbon particles.

The second stage is the complete combustion of organic matter contained within porous carbon particles, which, along with an increase in temperature, will cause the minerals contained within those porous carbon particles to become dehydrated, disassembled, and oxidized into inorganic oxides, which will ultimately result in the formation of porous glass.

The third stage: as the combustion process continues, the porous glass gradually melts and shrinks due to the action of surface tension. As a result, the porosity of the glass decreases, the sphericity of the glass increases, and the particle size decreases, resulting in the formation of a dense molten sphere

with a high density and small particle size. Make the particles with a certain viscosity expand rapidly, or expand at a stable speed to form a hollow molten sphere. At the same time, combustion and gasification occur in the molten particles with less carbon and a low melting point, and the generated gas is discharged outward at different speeds.

The molten sphere is expelled along with the flue gas during the fourth stage of the process. When it is rapidly cooled in the air, it solidifies into very fine spherical particles, which are then collected by the dust collection equipment for centralized discharge. These particles can be as small as a single atom. The physicochemical phase diagram of silicate indicates that the fourth stage of the process results in the formation of crystalline substances.



Picture 1.2 Schematic layout of a coal-fired electrical generating station [1]

As a form of fuel, ground pulverized coal is currently utilized in the boilers of contemporary thermal power plants. When pulverized coal is introduced into the furnace, the coal will be combusted into a fine particle fire mass in order to make the most efficient use of the heat energy it contains. Because different types of raw coal have varying amounts of ash in them, the ash that remains after combustion typically accounts for 15–40 percent of the total quality of the raw coal. The fine-grained dust collected from the smoke exhaust system with dust collection facilities is called fly ash or fly ash. Fly ash accounts for about 70–85 percent of the total mass of ash and slag, including some very fine particles, which are discharged into the atmosphere through the chimney opening. The other form of ash and slag produced by a pulverized coal boiler is known as bottom ash. Bottom ash is a coarse-grained dust that accumulates at the bottom of the boiler. The other is the granular ash that is bonded in the furnace, which falls into the bottom of the boiler, and some form large blocks, which are broken and discharged from the bottom of the boiler, which is called bottom ash or ash, accounting for about 15 percent to 30 percent of the total ash. The efficiency of the dust collection equipment determines the amount of very fine particles that are able to escape. Fly ash is a type of powdery mineral resource that is produced through an artificial process and does not occur naturally. It cannot be found anywhere else. Alternately, one could refer to it as a "renewable mineral powdery resource." According to the annual report of the United States Department of the Interior from 1974, coal ash is the seventh most abundant mineral in the country.

The production of a large amount of fly ash requires the occupation of a large amount of land in order to construct an ash storage yard, and the cost of managing fly ash transportation, management, and maintenance accounts for a significant portion of the total. When the winds pick up, dust kicks up

everywhere, polluting the air and the environment. As a result, a significant amount of money and equipment must be invested in order to spray and reduce the amount of dust.

The potential dangers posed by fly ash can be roughly categorized as water hazards, airborne hazards, and groundwater dangers. The extremely fine grain size of fly ash makes it easy for it to become airborne in the presence of wind and contribute to the formation of sandstorms and other forms of air pollution in the area surrounding landfills. The method that is currently used to treat fly ash is called landfilling, and the locations of landfills are typically chosen in low-lying areas such as mountains.

More damage is done by runoff or by underground infiltration; the use of fly ash as a fertilizer additive will cause soil alkalization and compaction, resulting in a decrease in soil fertility. This is due to the fact that fly ash is an alkaline substance.

Fly ash takes up a significant portion of the land, pollutes the water in rivers, lakes, and oceans, and causes significant damage to the ecological system and the soil. The proper way to get rid of fly ash

It has become one of the most significant factors that impedes the growth of the power industry in my country. It is imperative to utilize fly ash in a comprehensive manner, and doing so is an important part of the strategy for sustainable development that our nation is pursuing.

1.1.2 Classification and Decarbonization of Fly Ash

The formation of fly ash is influenced by a wide variety of factors, and the characteristics of the various types of fly ash can vary greatly. It is necessary to classify fly ash in great detail for a number of reasons, including those having to do with the use of fly ash as well as the protection of the environment.

Japanese Standard Classification :

Table 1.2 Chemical Composition and Physical Properties of JIS

Item	Grade A	Grade B	Grade C	
Density, min, g/cm ³	-	-	-	
Specific surface, min, m ² /kg	3000	3000	3300	
Initial setting time, min, min	60	60	60	
Final setting time , max, h	10	10	10	
Stability	Putt mehod	fine	fine	
	Le Chatelier's law, max, mm	10	10	10
Compressive strength min, N/mm ²	3d	12.5	10.0	7.5
	7d	22.5	17.5	15.0
	28d	42.5	42.5	40.0
Chemical requirements	MgO, max, %	5.0	6.0	6.0
	SO ₃ , max, %	3.5	4.0	4.5
	Loss on ignition, max, %	5.0	5.0	5.0

American Standard Classification

Table 1.3 Chemical Composition and Physical Properties of ASTM

Item		
Fineness		
Amount retained when wet screened on a 45-um(No.325) sieve, max%	20	
Air content of slag mortar, max%	12	
Sulfide sulfur(S), max, %	2.5	
Slag activity index, min, %	-	
7-Day Index		
Grade 80
Grade 100	75	70
Grade 120	95	90
28-Day Index		
Grade 80	75	70
Grade 100	95	90
Grade 120	115	110

In China's national standard "Fly Ash for Cement and Concrete" (GB1596-91), the fly ash that is used as an admixture for concrete and mortar is also separated into three categories. These categories are determined based on the fly ash's fineness as well as its loss on ignition. grades: Class I fly ash has a sieve residue of less than 12 percent and a loss on ignition of less than 5 percent; Class II fly ash has a loss on ignition of more than 12 percent.

Class II fly ash has a sieve residue of 45m square hole that is less than 20 percent, and it has a loss on ignition that is less than 8 percent. Class III fly ash has a 45m square sieve residue that is less than 45 percent, and it has a loss on ignition that is less than 15 percent.

According to the state of the fly ash, it is possible to classify fly ash as either modified fly ash, which is also known as humidity-adjusting ash, or aged ash. This categorization is done in the context of fly ash backfilling. When talking about "modified fly ash," people are referring to the process of transporting freshly discharged fly ash to its final destination after first mixing it with some amount of water.

Since the strength of fly ash after compaction increases with time, this type of fly ash is typically used for backfilling or soil reinforcement; in order to fulfill these functions, modified fly ash needs to meet particular strength requirements.

Because it is generally believed that aged ash has relatively poor properties, there is no requirement for its strength, and it is generally only used for backfilling. Aged ash is typically stored for a significant amount of time before being put to use. The water molecules that are contained within aged ash make up its equilibrium moisture content.

This classification is based on the self-hardening property of fly ash, but some researchers disagree with it. These researchers believe that old ash, not newly discharged fly ash, also possesses self-hardening properties, and therefore, this classification is incorrect. In point of fact, it is more appropriate to divide fly ash into dry ash, wet ash, and old ash according to the change in the moisture content of fly ash. Dry ash, wet ash, and old ash are all examples of ash.

The term "dry ash" refers to newly discharged fly ash that has been stored for no longer than six

months and has a moisture content that is no higher than three percent. The amount of time spent in storage does not have a significant impact on the fly ash's properties when it comes to low calcium fly ash.

Wet ash is a term that describes fly ash that has had a specific amount of water added to it during the discharge process. This type of fly ash also includes fly ash that has a moisture content that is lower than 3 percent after it has been treated.

Chen ash is another name for fly ash that has been stored outside in the open air. Even if this particular kind of fly ash is expelled dry, it almost always has a very high moisture content due to the fact that it absorbs rainwater or any moisture that is present in the air while it is being stored.

The equipment that is used is the primary determinant of the collection method for fly ash. Electrostatic dust collection is typically utilized by the equipment used for the collection of fly ash.

Electrostatic precipitators are superior to mechanical precipitators in terms of their ability to collect fine fly ash particles. These finer densities of fly ash are better from the point of use, and electrostatic precipitators are superior to mechanical precipitators. nature.

The collected fly ash from electrostatic precipitators can be separated into one, two, and three electric fields according to the difference in the electric field of the fly ash. The fly ash collected by the third-level electric field is of the finest particle size, making it an excellent mineral admixture for cement concrete.

The carbon particles that are present in fly ash have a dampening effect on the activity of fly ash, which is the primary reason for the negative impact that these carbon particles have on the overall utilization of fly ash. The carbon particles lower the strength of the concrete; because of their low density, the carbon particles float to the surface during the process of slurry formation, which results in an uneven distribution of the concrete and cement;

A theoretical foundation for the separation of fly ash can be found in the fact that coarse particles contain a higher concentration of carbon particles. The cyclone is able to separate the coarser particles from the finer ones. The fine particles contain very few carbon particles and are high-quality cement and concrete admixtures. The carbon particles are low in carbon particles. The carbon particles that are contained in the sorted coarse particles have a relatively high concentration, and these carbon particles are capable of being separated through additional sorting. The separated carbon particles have a higher added value because they can be used for adsorbents, catalyst carriers, and the production of carbon black. Wait.

Fly ash is now considered to be just as important a component of modern concrete as cement, aggregate, water, and admixture. Fly ash has emerged as an essential part of modern concrete. However, the residual carbon in fly ash will adsorb air-entraining agents, which will have an effect on the frost resistance of the concrete. Fly ash is considered an impurity.

This adsorption characteristic is a key factor in determining whether a certain fly ash can be used in concrete and the amount of ash that needs to be added to the concrete. The following three factors determine the amount of residual carbon that is adsorbed on the air-entraining agent: (1) the adsorption capacity of the fly ash is increased when the carbon content of the fly ash is higher; (2) the adsorption capacity of the carbon is increased when the specific surface area of the carbon is increased; (3) the adsorption capacity of the carbon is increased when the surface area of the small particles is increased, which in turn increases the available pore surface area and the adsorption capacity. In general, fly ash

with a carbon content that is higher than 5 to 6 percent (which is equivalent to fly ash that does not meet the standard for Class I ash in my country) is not suitable for the production of concrete, according to the experiences of people in other countries. Consequently, lowering the carbon content is very important in order to increase the utilization of fly ash in the manufacturing of concrete.

Due to certain technical difficulties in economic combustion, the pulverized coal that is used in power plant boilers that burn anthracite or inferior bituminous coal is unable to be completely burned. This leads to an increase in the carbon content of the fly ash, which typically ranges between 8% and 20%. Every year, millions of tons of coal are lost as a result of fly ash at power plants, which not only results in the wasteful loss of valuable coal resources but also creates a significant amount of waste.

In addition, the large quantity of carbon that is present in fly ash causes an increase in the quantity of fly ash that is discharged. Furthermore, and this is of the utmost importance, the presence of unburned carbon in fly ash will make it difficult to make comprehensive use of fly ash. It is not conducive to the protection of the environment and has a negative impact on the development of fly ash resources.

It is necessary to decarbonize fly ash in order to make full use of resources while simultaneously lowering the amount of carbon that is contained in fly ash. The flotation method can typically be used in conjunction with the decarbonization method.

The difference in the hydrophilic properties of the surface of fly ash and coal core is exploited by the flotation method, which separates the two types of material. When a collector is added to the mortar (such as diesel oil, for example), the hydrophobic coal particles are infiltrated by the collector and then adsorbed on the air bubbles that are generated by stirring. Finally, the coal particles rise to the surface of the liquid to form a mineralized foam layer, which is carbon concentrate. Fly ash particles that are hydrophilic are not used in the tailings process. It is necessary to add an agent, known as a foaming agent, to the mortar in order to reduce the surface tension of the water. This is done in order to maintain the stability of the air bubbles.

Fly ash is used in the electric separation method because it has a higher electrical conductivity than carbon particles, which allows it to separate more easily under the influence of a high-voltage electric field. This is the fundamental idea behind the electric separation method. Fly ash is a material that does not conduct electricity, whereas carbon particles are materials that are excellent conductors. In a circular corona electric field, when the fly ash acquires an electric charge, the carbon particles, which have excellent electrical conductivity, remove the charge as quickly as possible through the cylinder. This is because the carbon is positively charged. It is dislodged from the surface of the cylinder by the combined effects of gravity and the centrifugal force caused by its own inertia, and it is then deposited into the conductor product groove. The charge that was generated by the non-conducting fly ash is slowly dissipated on the surface, and as a result, the cylinder is able to take in that charge because of the action of the electric field force. In order to separate the ash from the carbon, it is first brought to the back of the surface by the rotating cylinder, and then it is discharged into the non-conductor product trough by the discharge brush. This is done so that the ash and carbon can be separated.

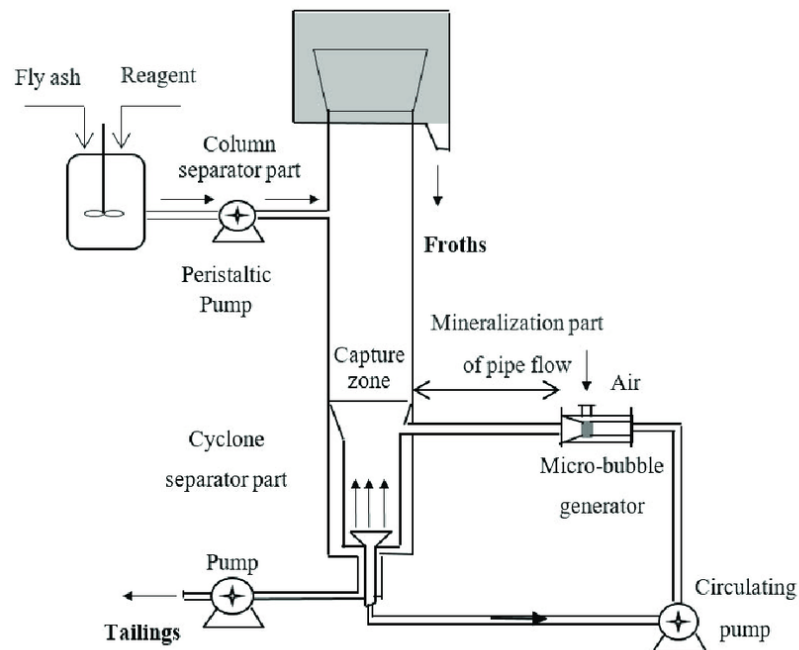


Fig 1.3 Schematic of the cyclonic-static micro-bubble flotation column (FCSMC) system [5]

As a result of research into the physicochemical properties of fly ash and carbon particles, we now know that the majority of the unburned carbon in fly ash is present in the form of monomer, the surface is hydrophobic and lipophilic, and it possesses good surface activity. This information was obtained through the study of the aforementioned properties. Make use of the carbon particles as well as the other fly ash particles.

Through the use of froth flotation, it is possible to separate carbon particles from fly ash by utilizing the differences in the surface's physical and chemical properties (wettability). As a result of the high loss on ignition of the raw material fly ash, which can reach up to 13 percent, and the target that was determined by the experiment, the flotation method will be used to decarbonize the fly ash in this study.

Flotation is a method for separating coal and other particles from one another based on the differences in the surface properties of the material in terms of both its physical and chemical composition. The first step in the flotation process is to thoroughly mix a predetermined amount of coal slurry with a predetermined amount of flotation agent in a mixing tank before introducing the mixture into the flotation machine. The coal particles run into the air bubbles and cling to them, quickly rising to the surface of the ore slurry to form a mineralized foam layer, which is then scraped off by the foam scraper to produce carbon concentrate; the hydrophilic particles that are unable to cling to the air bubbles remain in the water, and this is then discharged out of the machine as tail ash. This accomplishes the goal of sorting by separating the hydrophilic particles from the hydrophobic particles. Flotation occurs at the two and three interfaces of solid-liquid, solid-gas, and liquid-gas phases, and it is carried out under the interaction of solid, liquid, and gas three-phase interfaces.

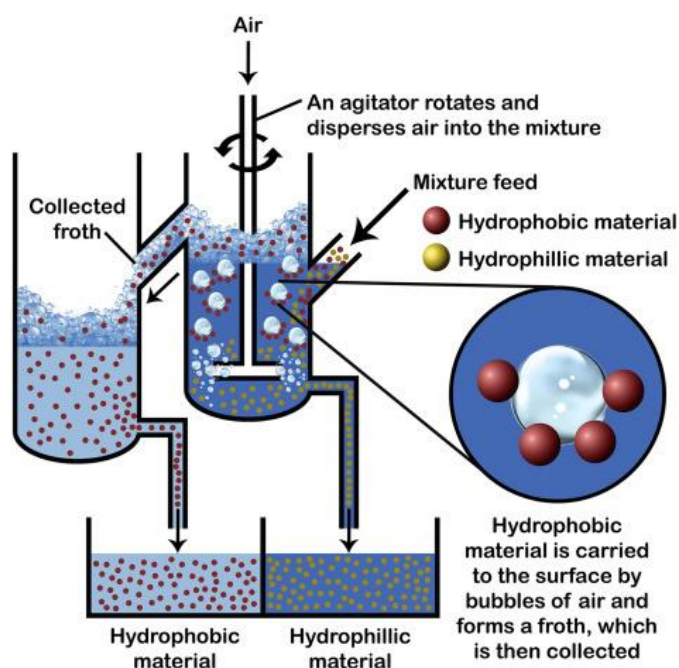


Fig 1.4 The process of froth flotation.[6]

Because of this, the flotation process is a very complicated physicochemical and hydrodynamic process, and the disparity in the degree to which the surfaces of coal and other particles can be wetted is a significant factor in the outcome of this process. Carbon particles in fly ash have a surface wettability and floatability that are comparable to those of coal. Additionally, the contact angle of the carbon particles is between 60 and 70 degrees, whereas the contact angle of the other particles is only about 10 degrees. Because other particles have smaller contact angles, the carbon particles used in the froth flotation process are the ones that are able to adhere to the surface of the bubbles and float to the top of the mortar, while the other particles are ineffective at doing either.

The surface that is unable to adhere to the air bubbles is left in the mortar, and thanks to the action of the flotation agent, the wettability between the carbon particles can be increased. As a result, the carbon particles can be separated from other particles in an efficient manner.

The surface properties of unburned charcoal in fly ash have become more complicated as a result of high temperature combustion and sudden water cooling. Although the surface wettability of unburned charcoal in fly ash is comparable to that of coal, the surface properties of unburned charcoal in fly ash have become more complex. It has undergone significant oxidation, which has increased the hydrophilicity of its surface. However, its flotation activity is lower than that of coal, which makes the recovery of its unburned carbon through flotation somewhat challenging. Therefore, in order to maximize the recovery rate when using foam flotation to flotote unburned carbon particles in fly ash, it is necessary to select excellent flotation reagents in order to improve and strengthen the physical and chemical properties of the flotation fly ash and its carbon particles. These improvements and strengthenings can be accomplished by selecting excellent flotation reagents. Experiments are used as a means of determining the various flotation processes and chemical systems in use during the flotation process.

1.1.3 Research significance of fly ash concrete

Fly ash has been the subject of both scientific inquiry and exploration ever since the turn of the

previous century. In 1914, the research conducted by Anon on the properties shared by fly ash and volcanic ash was presented in a paper that was published in the journal *Engineering News* in the United States. R. E. Davis was a pioneer in the research on the application of fly ash in concrete in 1937. As a result, this research ushered in a new era for the application of fly ash in concrete.

Fly ash was only used in large-scale projects back then, and it was used in large-volume coagulation because technology and people's ideas had not yet advanced to the point where they could support such an endeavor. It has seen widespread application in the building of residential structures. After some time, it was eventually used in the engineering of structures and pavements. People have, over time, gradually realized that a significant quantity of fly ash can be utilized in this manner. It has been proven useful over the course of time as well. It has been discovered that adding fly ash to concrete can improve some of the properties of the concrete, and that turning fly ash into treasure can save some of the raw materials used to make concrete. This time period marks a pivotal point in the dissemination of concrete technologies with a diverse range of applications. In the same vein, water conservation projects in Europe, Asia, and other parts of the world frequently make use of fly ash concrete in their construction.

People gained a better understanding of the characteristics of fly ash as time went on, particularly from the 1950s through the 1960s, and came to recognize it as a unique pozzolanic material during this period of time. The majority of researchers and specialists have devoted themselves to examining how fly ash is involved in the coagulation process. The action of the hydration reaction process. In later years, fly ash concrete gradually became more cost-effective, and academics working in the field of concrete increased their investigation into and testing of new fly ash concrete technologies.

Throughout each stage of development, the theory of using fly ash in concrete practical technology was never articulated in a way that was clear. However, it does so in a way that serves as a point of reference for the thinking and development of later stages. Following the transition that took place in the 1960s and 1990s, members of the general public, in addition to concrete professionals and academics, started to gradually accept this novel material, fly ash concrete. At this point in time, the concrete technology that has been used in the construction of highway pavements has been initially qualitative, in addition to a reduction in water content. The theoretical development of fly ash as an additive to concrete has been significantly sped up as a result of the widespread application of the agent. The percentage of fly ash that is added to road concrete can reach up to about sixty percent, which is a significant amount of fly ash concrete right from the start. Some characteristics of the potential of fly ash

Now let's take a look at the applications and benefits of fly ash, which mainly include the following:

(1) As a cement substitute material to reduce the project cost; in project construction, the form of fly ash, pozzolanic activity, and micro-aggregate effect are typically used as a cementitious material to partially or excessively replace cement. In other words, fly ash, pozzolanic activity, and micro-aggregate effect are used as a cement substitute (generally less than 30 percent). Normal or everyday coagulation. When compared with regular concrete of the same strength, studies have shown that CO₂ emissions can be reduced by 10-15 percent when the cement replacement rate is 20 percent. This is the case even when the strength of the concrete remains the same. However, the expansion and utilization of this aspect is restricted due to the influence of the requirements placed on the quality of fly ash, the output, and the process of transporting it.

(2) Increase the early strength as well as the later strength after 90 days of age in order to meet the design strength; when used as a concrete admixture, silicon and aluminum are precipitated from the fly ash particles, and a hydration reaction takes place. This reaction promotes the increase in the long-term strength of the concrete. The air separation method was used to obtain fine fly ash with a particle size of 45 nm in order to improve the working performance of the material; Naik [7] et al. improved the early increase in strength of fly ash concrete by changing the components, adding activators, and using other methods.

(3) As a cement substitute material to inhibit the effect of coagulation temperature; research shows that only ten percent of the hydration reaction of fly ash coagulation is completed in twenty-eight days, and practically no effect occurs at the beginning of the aging process. The generation of hydration heat can be seen to be suppressed by replacing cement with fly ash, and as a result, the large seepage amount of fly ash is frequently used in large-volume coagulation engineering in order to reduce the possibility of temperature cracks.

(4) Because of the properties of fly ash fines on their own, the workability of concrete can be significantly improved.

(5) The incorporation of fly ash into concrete has the potential to increase the material's resistance to deterioration. In a later stage, it will act as part of the cementitious material to undergo hydration reaction, and part of it will play the role of micro-aggregate filling; both of these roles, when combined, increase the integrity of the interior of the concrete. In the earlier stage, it will act as part of the cementitious material to undergo hydration reaction, as well as its compactness, reduce the strength of the capillary channels present in the concrete, and block the passage of other substances. The addition of fly ash to concrete can improve its ability to resist the penetration of external substances, effectively increasing its durability. This effect can be achieved by improving concrete's ability to resist the penetration of external substances.

The majority of the aforementioned research relies on the pozzolanic activity of fly ash as a cementitious material to replace cement; however, there is very little published research on fly ash as an independent material component that can be researched and analyzed. The results of the research have been analyzed, and the findings show that the strength properties of fly ash can vary, even when the conditions are the same, including the type of material and the ratio of ingredients. The proposed calculation methods and results of fly ash strength are primarily restricted by the conditions under which they were tested, and as a result, they are not widely used in practical projects.

1.1.4 Effect of fly ash on properties of recycled concrete

Mechanical properties: At this time, there are a great number of studies that have been conducted on the topic of the mechanical properties of recycled concrete made with fly ash, and a great number of conclusions have been drawn. The outcomes of the tests, on the other hand, varied quite a bit depending on aspects such as the manner in which fly ash was mixed, the locations from which recycled aggregates were obtained, and the percentage of recycled aggregates that were used to replace virgin aggregates.

Researchers Kurda [8] et al. investigated the effects that varying amounts of fly ash had on the mechanical qualities of recycled concrete made with a hundred percent replacement rate of recycled coarse aggregate. According to the findings, the percentage of recycled concrete that is composed of fly ash contributes positively to the compressive strength of the material. The splitting tensile strength

decreases with an increase in the content of fly ash, and the decrease range is not very large. The strength reaches its maximum when the percentage of fly ash in the material is 10 percent; after that, the strength begins to decrease. The primary purpose of fly ash is to strengthen the interfaces of recycled concrete, which ultimately results in increased compressive strength.

Pore was able to realize. Because of this chemical action, the bond between cement hydration products and aggregates can be strengthened, the occurrence and development of interfacial bond cracks can be prevented, and the performance of recycled concrete can be enhanced as a result. However, the amount of cementitious materials that are present in recycled concrete decreases as the quantity of fly ash that is used as a substitute for cement increases.

The strength of recycled concrete starts to decrease once the percentage of fly ash used in replacement exceeds 10 percent, which is an indication that fly ash should be avoided. There is a limit to the modification of mechanical properties. Another group of researchers, B et al., arrived at the same verdict: the compressive strength of recycled concrete with 10 percent fly ash substitution is 11 percent higher than that of recycled concrete without fly ash, and the compressive strength of recycled concrete with 20 percent fly ash is significantly higher still. When compared to recycled concrete without fly ash, recycled concrete with 10 and 30 percent fly ash has a compressive strength that is marginally inferior to that of recycled concrete without fly ash.

Because the "pozzolanic effect" of fly ash can only be stimulated by the alkaline substances produced by the cement hydration reaction, the rate of strength development in recycled concrete mixed with fly ash is significantly slower than that of unmixed concrete. The authors B et al. utilized the fly ash excess substitution method in order to make a direct comparison between the 28-day strength of recycled concrete without fly ash and the 90-day strength of recycled concrete mixed with fly ash. The results of the test demonstrated that the compressive strength and split tensile strength of recycled concrete experience a slight decrease when the percentage of fly ash in the mixture increases.

Kou [9] et al. conducted research to investigate how the mechanical properties of recycled concrete are affected by the replacement rate of recycled coarse aggregate as well as the replacement rate of fly ash. According to the findings of the study, the flexural strength of recycled concrete is impacted when the replacement rate of fly ash is lower than 35 percent. Specifically, the study found that the replacement rate of fly ash has a bearing on the issue when it is less than 35 percent. There is not much of an impact from the changes. In addition to this, the incorporation of fly ash into concrete has been shown to have some bearing, to a certain extent, on both the concrete's shrinkage performance and its fatigue performance.

The amount of dry shrinkage that concrete experiences when different grades and quantities of fly ash are incorporated into the mix was investigated. The findings indicate that: fly ash containing a significant amount of substitution has a good inhibitory effect on the shrinkage of concrete; the inhibitory effect of grade I fly ash is obviously superior to that of grade II fly ash; and the results indicate that the shrinkage of concrete can be reduced by using fly ash with a higher grade. By performing a bending fatigue test on recycled concrete mixed with fly ash, and then comparing the results to those of an ordinary cement concrete test as well as an ordinary cement concrete test mixed with fly ash. It has been discovered that the fatigue performance of recycled concrete that has been mixed with fly ash is not significantly different from the performance of regular cement concrete. When there is less stress, there is not much of a difference. The recycled concrete that has been

combined with fly ash is completely resistant to the application of repeated loads.

The incorporation of fly ash into recycled concrete will, in addition to having an effect on the concrete's mechanical properties, have the potential to enhance the microscopic pore structure of the concrete, increase the concrete's compactness, and improve the recycled concrete's ability to resist permeation. The researchers Guo [10] et al. utilized the chloride ion penetration test in order to investigate the impact that fly ash content has on the resistance of recycled concrete to chloride ion penetration. According to the findings, the chloride ion penetration resistance of recycled concrete gradually improves along with an increase in the amount of fly ash that is included in the mix. When there is only a small amount of fly ash present, recycled concrete has a high level of resistance to the penetration of chloride ions.

The chloride ion natural diffusion test was used to investigate how much of an impact fly ash has on the level of resistance offered by recycled concrete to chloride ion penetration. It has been demonstrated that the incorporation of fly ash into a material can significantly enhance its resistance to the invasion of chloride ions; however, there is a maximum value of fly ash that can be incorporated into the material before its effectiveness begins to deteriorate. This maximum value falls somewhere between 10 and 30 percent.

The resistance of recycled concrete to sulfate attack is improved by the incorporation of fly ash, which also has beneficial effects. They [11] believed that the ability of recycled concrete to resist sulfate corrosion was at its best when the replacement amount of fly ash was 15 percent, and the mass loss rate after corrosion resistance was not obvious. This was the case when the fly ash replacement amount was 15 percent. The structure of the interfacial transition layer in recycled concrete is an important factor that plays a role in the sulfate corrosion resistance of the material. When the appropriate amount of fly ash is added to recycled concrete, it is possible to uniformly disperse the $\text{Ca}(\text{OH})_2$ crystal structure, improve the microstructure of the cement-aggregate interface transition zone, improve the internal compactness of the recycled concrete, and effectively prevent the infiltration of sulfate. All of these benefits can be achieved through the addition of fly ash. Although adding fly ash to recycled concrete can improve its anti-chloride and anti-sulfate properties, this does not improve the recycled concrete's ability to withstand freezing temperatures.

The frost resistance of recycled concrete was investigated by Li [12] and colleagues, who looked at how recycled aggregate replacement rate and fly ash content impacted the material. The findings revealed that the frost resistance of recycled concrete significantly decreased as the amount of fly ash used as a substitute for cement increased. In order to investigate the impact that fly ash has on the ability of recycled concrete to resist carbonation, recycled concrete was created using waste concrete as recycled coarse aggregate, and mineral admixture was also mixed in. After that, the carbonation resistance of the recycled concrete was analyzed.

It is possible to significantly enhance the carbonation resistance of concrete that has been recycled. They also brought up the fact that the optimal improvement effect occurs at a fly ash content of twenty percent. The addition of fly ash to recycled concrete has the potential to lower the amount of heat released during the hydration process. On the one hand, fly ash can replace some of the cement, which lowers both the amount of cement required per unit volume and the amount of heat that is released during the hydration process. On the other hand, the secondary hydration reaction that fly ash undergoes has the properties of releasing less heat and taking a longer amount of time. As a result, the

amount of heat that is released by recycled concrete gets lower as the percentage of fly ash in the mix gets higher.

1.1.5 The elastic modulus of fly ash concrete

The Modulus of Elasticity, also referred to as Young's Modulus or simply E , is defined as "the ratio of the axial stress to the axial strain for a material that is being subjected to uni-axial load [13]." Concrete's Young's Modulus is one of the most important material properties because it is used throughout the entire process of structural design. This makes it one of the most important material properties overall. It is common for building specifications to demand that a certain value of E be attained in order to guarantee that the structural integrity of the building is satisfactory and to forestall deformations that are not satisfactory. One building in the United States that exemplifies this is the Two Union Square Building, which can be found in Seattle, Washington. The architect of the structure stipulated that the concrete's Modulus of Elasticity had to be at least 50 GPa [13].

When analyzing the deflection of a structure, Young's Modulus is always required to be calculated. The concrete structural members need to have an appropriate design in order to avoid lateral and longitudinal deformations and to guarantee that the applied loads do not go beyond the capacity of the concrete structural members. When concrete structures have already been built, it can be difficult to determine the in-situ properties of the concrete without causing damage to the structure. When trying to determine the compressive strength of a structure, it is common practice to load companion core samples to the point of failure before drilling them out. Despite the fact that there is an empirical relationship between the compressive strength and the modulus of elasticity of the concrete, the formula produces results that are excessively conservative. Choosing concrete with a strength that is significantly higher than the required strength can lead to increased costs associated with the material.

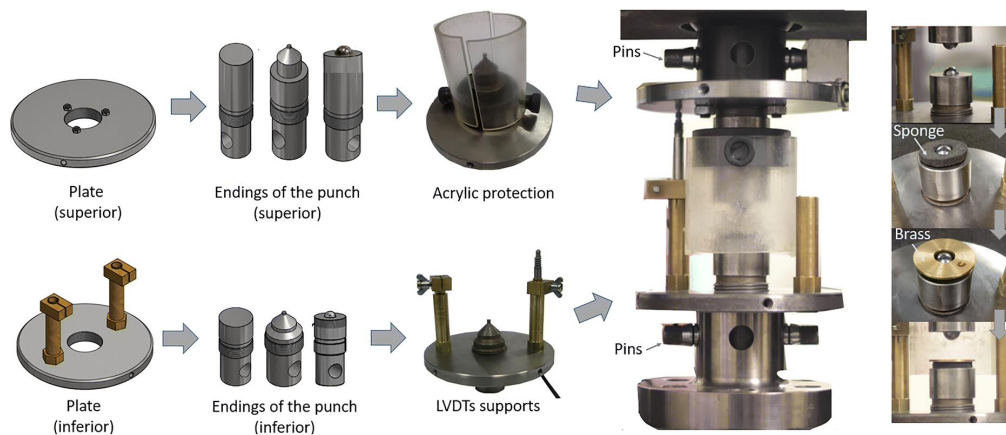


Fig 1.5 Static elastic modulus [14]

Estimating the Young's Modulus of structures that are already present in their environments can be accomplished with the help of a wide variety of dynamic non-destructive testing (NDT) methods. Methods such as ultrasonic pulse velocity methods, methods based on resonance frequency, and other wave propagation techniques are included here. The fact that the value of this dynamic modulus, E_d , is frequently discovered to be greater than that of the static modulus, E , is the source of the issue that arises when attempting to calculate E_d . Concrete's stress-strain relationship can be complicated due to the behavior of its gel structure and the way that water is held in concrete [16]. This can make the relationship more difficult to understand. By loading the concrete and determining the slope of the

stress-strain curve, one can calculate the static modulus of the material. When compared to the static loading, the methods of dynamic testing apply a very small amount of force. The concrete will not experience any further deformations as a consequence of the utilization of dynamic testing methods. This is considered to be the fundamental reason behind why the dynamic modulus almost always demonstrates itself to be greater than the static modulus.

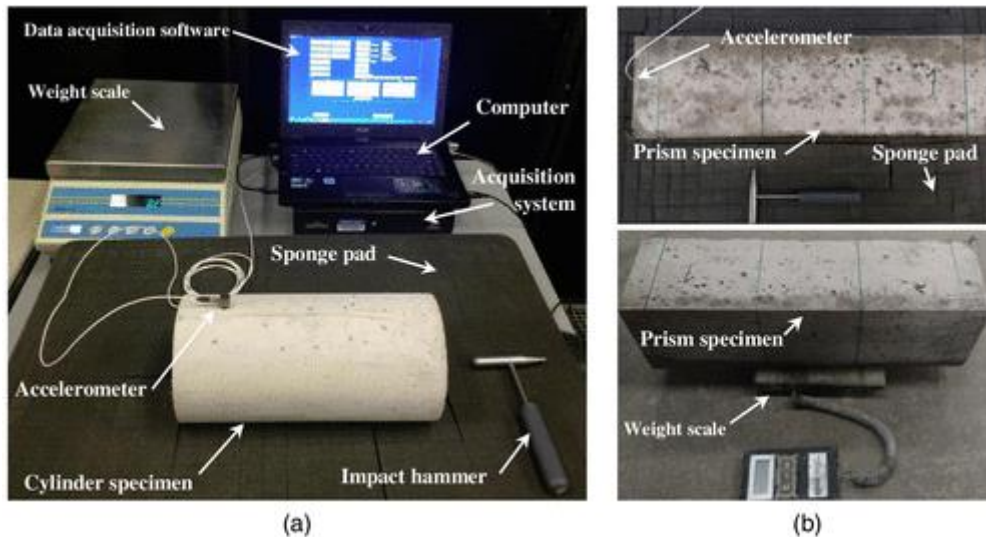


Fig 1.6 Static elastic modulus [15]

As was previously mentioned, there are a variety of non-destructive approaches that can be utilized in the process of computing E_d . The non-destructive testing (NDT) methods that are utilized most frequently to ascertain E_d are the vibration resonance techniques and the pulse wave propagation techniques. It has been demonstrated that the ultrasonic pulse velocity method produces higher E_d values than the vibration resonance methods do, which are used to obtain the same information. It is also important to keep in mind that the shape of the specimen can have some bearing on the value of the dynamic modulus. In general, prismatic beams that go through the process of vibration resonance produce a higher dynamic modulus than cylinders that are cast from the same batch of concrete [16]. It turns out that the relationship between the Static Young's Modulus and the Dynamic Young's Modulus is quite complicated, and its nature shifts depending on a number of different aspects. There are a number of factors that can affect the correlation between E_d and E , including the type of concrete used, the size and shape of the specimens, and the testing procedures.

As was stated earlier, E_d 's identity can be established through the use of a variety of different dynamic-based tests. Pulse wave propagation and vibration resonance methods are the two most common forms of non-destructive testing (NDT) that are utilized in the process of determining E_d in concrete specimens. In this particular investigation, each of these methods will be put to use. An additional non-destructive testing (NDT) method that is widely utilized to compute the static modulus, E , involves computing the compressive strength of concrete and applying loads to cylindrical concrete specimens that are up to 35 percent of the strength. As a result of advancements in technology, non-destructive testing (NDT) and evaluation methods are becoming more popular and simpler to employ. The utilization of these non-destructive testing (NDT) techniques can be used to determine Young's Modulus, as well as the uniformity of the concrete, voids, discontinuities, and other concrete properties, in addition to determining Young's Modulus. Testing that is not destructive is utilized quite frequently

in a variety of contexts and with a wide range of materials, including steel, timber, and composite elements.

1.2 Purpose of this study

As part of this investigation, we developed a prototype of an unburned carbon removal device that utilizes the flotation method to separate unburned carbon from fly ash. The first goal is to develop a simple floatation separation apparatus that is capable of efficiently separating materials that need to be treated. The second goal is to develop a simple floatation separation method that is capable of efficiently separating unburnt carbon that is contained in fly ash. Both of these goals will be accomplished if we are successful. The third goal is to devise an easy manufacturing method for efficiently producing a cement mixture by making use of high-quality fly ash that has a reduced amount of unburnt carbon content. We investigated the conditions of operation as well as the size of bubbles that were appropriate for removal. We investigated how the environmental factors impacted the rate of carbon removal and made adjustments to the system accordingly. Since the amount of unburnt carbon in the fly ash slurry that was obtained in this manner was reduced to an adequate degree, unburnt carbon-related issues almost never occur, even when a large amount is used. Therefore, it is worthwhile to investigate whether or not such fly ash slurry can be used as various raw materials in large quantities. As a result, the mechanical and physical properties of concrete containing 15 or 30 percent fly ash, as well as modified fly ash slurry (MFAS) with unburned carbon removed using our apparatus, were evaluated and compared. The challenge of implementing sustainable development while also protecting the environment in the immediate area is a common one. The construction of a large number of homes, roads, and other structures is a necessary part of both industrial and urban development. This has a significant negative impact on the surrounding environment. It is possible to lessen environmental deprivation and increase the use of renewable resources if natural gravel and cement are mixed into the concrete that is used in building projects. There has been a significant amount of research carried out in which each of these materials has been replaced by itself; however, there is still a need for investigation into the physical and mechanical properties of concrete produced using both RFA and FA. This study makes a contribution to the ongoing conversation on the subject by concentrating on the compressive strength and drying shrinkage of concrete mixtures that include both RFA and FA. Following an investigation into the characteristics of RAC, a straightforward linear regression was carried out with the gathered data. To determine the optimal interval division for the correlation, the correlation coefficients that exist between the cumulative pore volume of the concrete at varying pore diameters and the compressive strength or drying shrinkage of the concrete were calculated. This allowed for the determination of the optimal division of the interval. The objective of this research project is to establish empirical relationships between the Static Young's Modulus, E , and the Dynamic Young's Modulus, E_d , for a variety of concrete mixes that are typically put to use. In order to develop this relationship, it is essential to make use of a variety of different dynamic Non-Destructive Testing techniques, such as ultrasonic pulse velocity and impact resonance frequency. In addition, a connection needs to be established between the E_d values obtained from the UPV and the E_d values obtained from the frequency analysis of the Impact Resonance. In-house castings will be done with four distinct types of concrete mixes (slag, flyash, ordinary Portland cement, and self-consolidating concrete) in order to ascertain the aforementioned characteristics of the finished product. The accuracy and validity of

CHAPTER 1: RESEARCH BACKGROUND AND PURPOSE OF THE STUDY

the analysis will then be determined based on a comparison of these empirical relationships to other, similar analyses that have been carried out by a variety of researchers. These values will be compared to the ones obtained from the Static Modulus Test, and the compressive strength will be used to estimate the Young's Modulus using the ACI equations.

1.3 Research structure

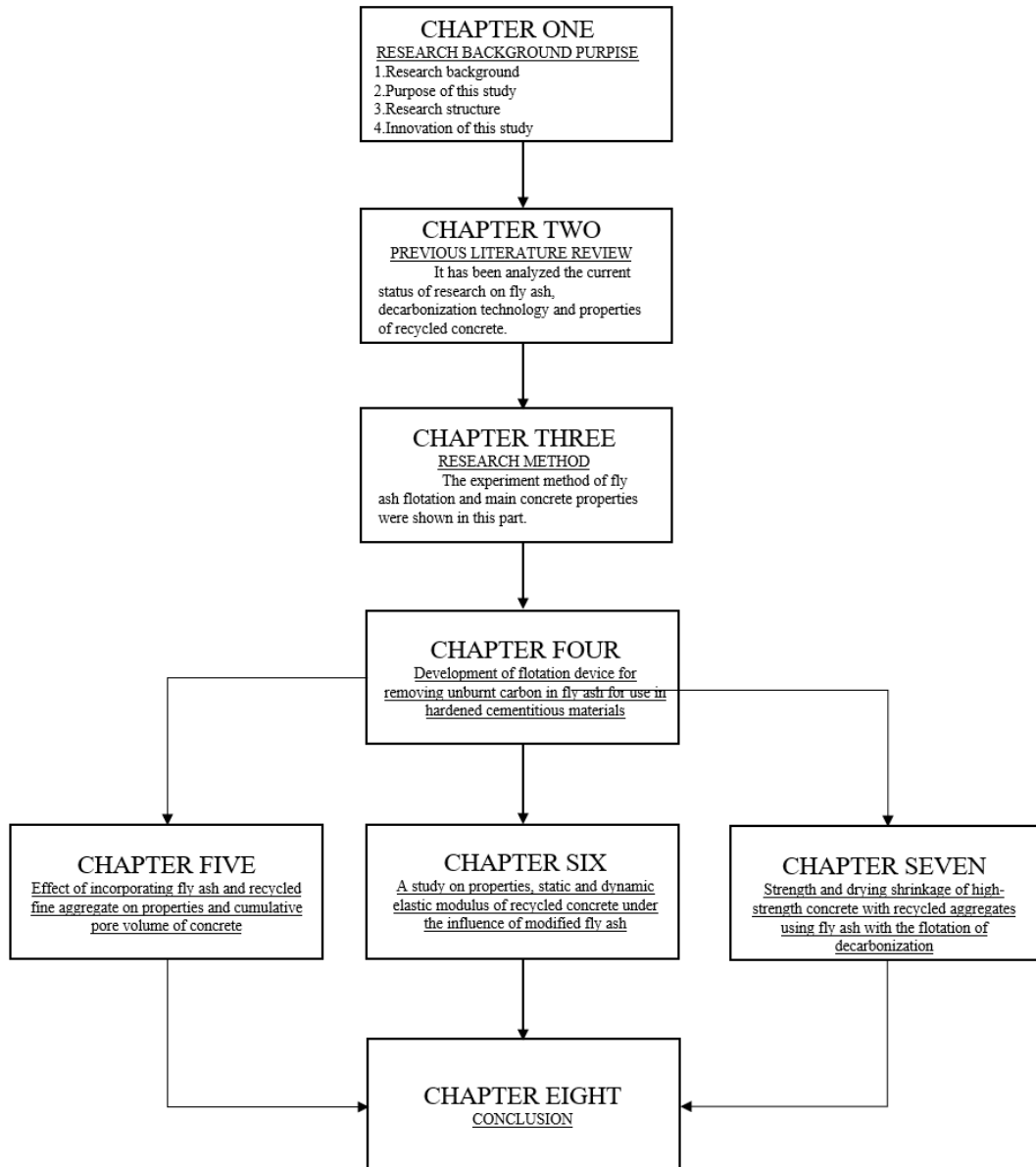


Figure 1.7. Research flow chart of the thesis

1.4 Innovation of this study

This paper presents the development and application of an innovative flotation machine for the removal of carbon from fly ash. In place of the conventional froth flotation process, micro-bubble technology is used. This results in an increase in the flotation efficiency of fly ash and a decrease in the carbon content of tail ash. As a result, the modified fly ash that is obtained from this process is

able to satisfy the requirements of Japanese industrial standards regarding its chemical and physical properties. At the same time, the carbon that is produced during the flotation process is collected, which not only helps to save energy but also makes the utilization of carbon a more environmentally responsible and efficient process. In order to demonstrate the viability of using modified fly ash in construction projects, modified fly ash was mixed in with recycled aggregate and Portland cement was substituted for it in the concrete. Experiments on mechanical properties and durability properties were carried out to compare the effect of ordinary fly ash, and experiments on porosity were carried out to study the relationship between porosity, compressive strength, and drying shrinkage in order to explain the effect of fly ash on recycled concrete. At the same time, the static elastic modulus and the dynamic elastic modulus of this concrete were measured and compared with the norms and standards of a number of different countries in an effort to come up with an empirical formula that is appropriate for modified fly ash recycled concrete. At the same time, an effort is made to make a prediction regarding the development of the concrete's strength using the concrete's static and dynamic elastic moduli as the basis. In conclusion, use the porosity of the material as a link in your search for the connection between the elastic modulus and the drying shrinkage. In a nutshell, the purpose of the experiments was to validate the utilization of the modified fly ash that was generated by the latest iteration of the fly ash flotation machine in recycled concrete.

References

- [1] <https://www.civilengineeringforum.me/production-fly-ash/>
- [2] Ye, Penghao & Xia, Senmao & Xiong, Yu & Liu, Chaoyang & Li, Fei & Liang, Jiamin & Zhang, Huarong. (2020). Did an Ultra-Low Emissions Policy on Coal-Fueled Thermal Power Reduce the Harmful Emissions? Evidence from Three Typical Air Pollutants Abatement in China. *International Journal of Environmental Research and Public Health*, 17, 8555. 10.3390/ijerph17228555.
- [3] Basu, Manisha & Pande, Manish & Bhadoria, P. & Mahapatra, S.C.. (2009). Potential fly-ash utilization in agriculture: A global review. *Progress in Natural Science - PROG NAT SCI*, 19, 10.1016/j.pnsc.2008.12.006.
- [4] Shearer, Christopher. (2014). The productive reuse of coal, biomass and co-fired fly ash. Wei, Guoxia & Liu, Hanqiao & Liu, Fang & Zeng, Tongtong & Liu, Guisheng & Zhou, Jianhua. (2018). Experimental Investigation of the Decarburization Behavior of Medical Waste Incinerator Fly Ash (MWIFA). *Processes*, 6, 186. 10.3390/pr6100186.
- [5] Cao, Y.J., Li, G.S., Liu, J.T., Zhang, H.J., & Zhai, X.. (2012). Removal of unburned carbon from fly ash using a cyclonic-static microbubble flotation column. *Journal of the Southern African Institute of Mining and Metallurgy*, 112(10), 891-896. Retrieved May 17, 2022, from http://www.scielo.org.za/scielo.php?script=sci_arttext&pid=S2225-62532012001000010&lng=en&tlng=en.
- [6] Crawford, C. B., & Quinn, B. (2017). 9 - Microplastic separation techniques. In C. B. Crawford & B. Quinn (Eds.), *Microplastic Pollutants* (pp.203–218). Elsevier. <https://doi.org/https://doi.org/10.1016/B978-0-12-809406-8.00009-8>
- [7] Naik, T. R., & Ramme, B. W. (1989). High early strength concrete containing large quantities of fly ash. *ACI Mater. J*, 86(2), 111-116.
- [8] Kurda, R., de Brito, J., & Silvestre, J. D. (2017). Combined influence of recycled concrete aggregates and high contents of fly ash on concrete properties. *Construction and Building Materials*, 157, 554-572.
- [9] Kou, S. C., & Poon, C. S. (2013). Long-term mechanical and durability properties of recycled aggregate concrete prepared with the incorporation of fly ash. *Cement and Concrete Composites*, 37, 12-19.
- [10] Guo, Z., Jiang, T., Zhang, J., Kong, X., Chen, C., & Lehman, D. E. (2020). Mechanical and durability properties of sustainable self-compacting concrete with recycled concrete aggregate and fly ash, slag and silica fume. *Construction and Building Materials*, 231, 117115.
- [11] Berndt, M. L. (2009). Properties of sustainable concrete containing fly ash, slag and recycled concrete aggregate. *Construction and building materials*, 23(7), 2606-2613.
- [12] Li, Y., Wang, R., Li, S., Zhao, Y., & Qin, Y. (2018). Resistance of recycled aggregate concrete containing low-and high-volume fly ash against the combined action of freeze–thaw cycles and sulfate attack. *Construction and Building Materials*, 166, 23-34.
- [13] Popovics, J. (2008). A Study of Static and Dynamic Modulus of Elasticity of Concrete. American Concrete Institute - Concrete Research Council, Urbana, IL.
- [14] Silva, N. v, Angulo, S. C., da Silva Ramos Barboza, A., Lange, D. A., & Tavares, L. M. (2019). Improved method to measure the strength and elastic modulus of single aggregate particles. *Materials and Structures*, 52(4), 77. <https://doi.org/10.1617/s11527-019-1380-7>

[15] Bassim, R., & Issa, M. (2020). Dynamic-and static-elastic moduli and strength properties of early-age Portland cement concrete pavement mixtures. *Journal of Materials in Civil Engineering*, 32(5), 04020066.

[16] Chavhan, P. and Vyawahare, M. (2015). Correlation of Static and Dynamic modulus of Elasticity for Different SCC Mixes. *International Journal on Recent and Innovation Trends in Computing and Communication*.

CHAPTER 1: RESEARCH BACKGROUND AND PURPOSE OF THE STUDY

Chapter 2

PREVIOUS LITERATURE REVIEW

CHAPTER 2: PREVIOUS LITERATURE REVIEW

2.1 Research status of Fly ash flotation method

2.1.1 Research status of Fly ash

In 2016, the global fly ash was about 1.143 billion tons, with an average utilization rate of 60%: of which China was about 600 million tons, with a utilization rate of 68% to 70% (comprehensive utilization was 408 million tons); the United States was about 400 million tons. 4 million t, the utilization rate is 54% (23.76 million t comprehensive utilization); Japan 12 million t, the utilization rate is close to 100%; EU 40 million t (all coal-fired solid waste in EU 15), the utilization rate is 90% (The comprehensive utilization is 36 million tons); India is 169 million tons, the utilization rate is 63% (the comprehensive utilization is 106 million tons).[1-2]

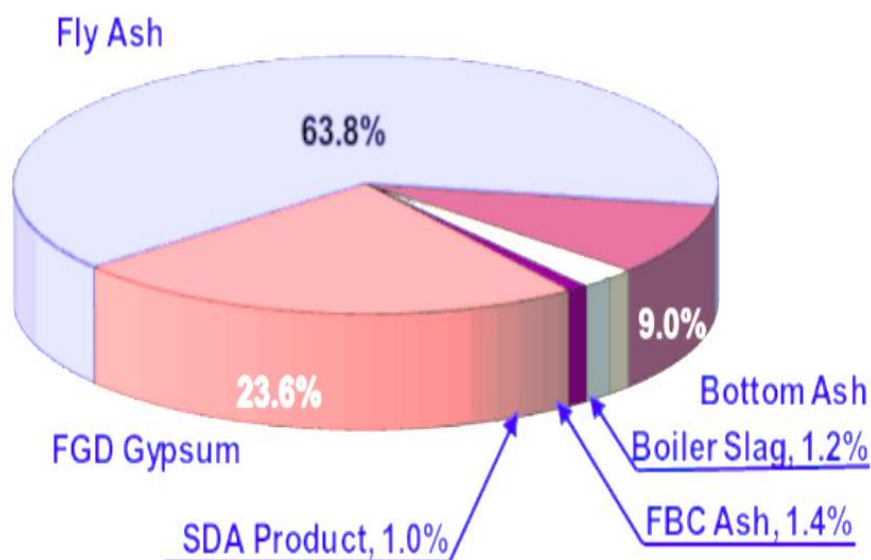


Fig 2.1 Production of fly ash in EU [2]

The change of fly ash production and utilization rate in Japan in recent ten years is shown in the figure. The growth trend of solid waste output of coal-fired power plants has eased, but the comprehensive utilization of solid waste has not increased significantly and has basically remained at the original level. This is mainly because: On the one hand, with the increase in the proportion of new energy power generation, the traditional coal-fired power generation is constrained; on the other hand, many "high value-added" comprehensive utilization of fly ash at home and abroad has not been industrialized and popularized at this stage.

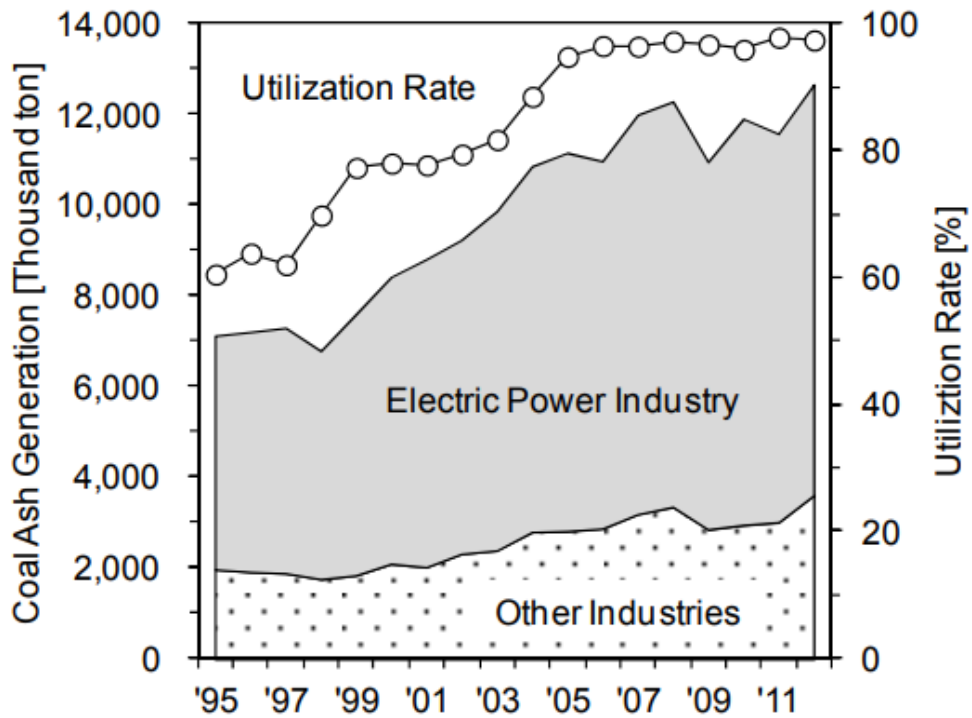
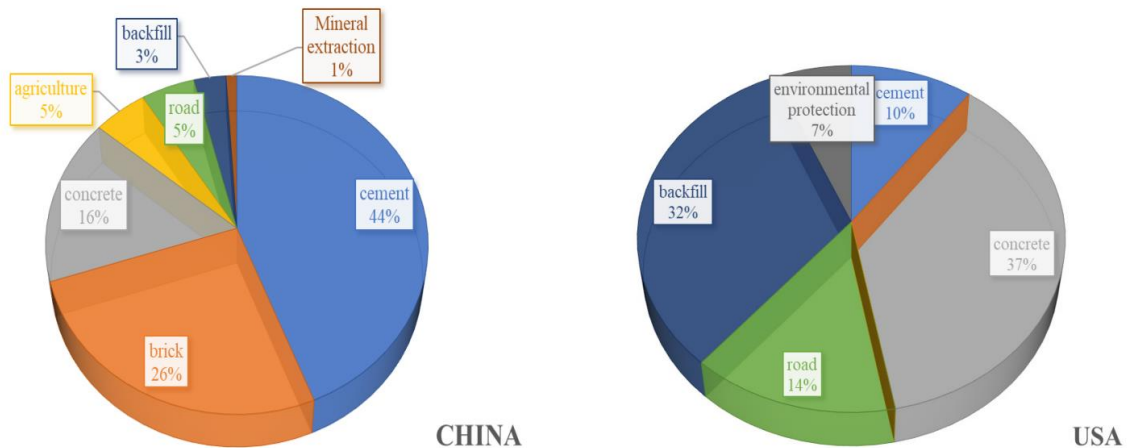


Fig 2.2 Generation of coal ash in Japan [3]

The comprehensive utilization of fly ash in each country depends on the output of fly ash in each country, the development of process technology, environmental protection requirements, scarcity of raw materials, industrial structure and other factors. The comparison of the main comprehensive utilization methods of fly ash in major countries and regions is shown in Table 1 [4-6].

Countries basically focus on the application of building materials, while the application choices in other ways are affected by the policies and industries of various countries; in terms of high value-added utilization, only Japan has a relatively large proportion of the utilization rate [7], which is due to the fact that Japan’s own raw materials Due to the constraints, fly ash has been developed into various materials to replace raw materials.



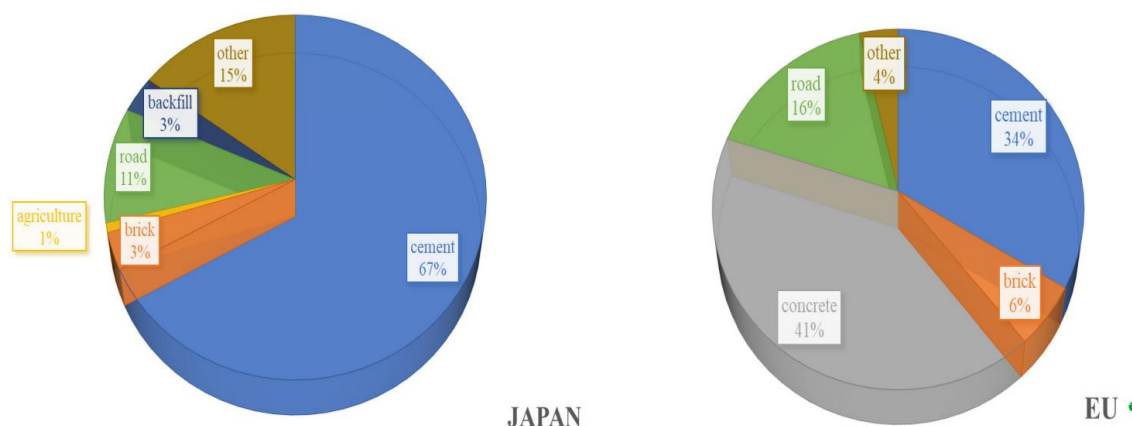


Fig 2.3 Main utilization ways of fly ash in various countries [7]

Japan's main utilization method is cement, accounting for 67.12% of Japan's comprehensive utilization of fly ash. Although Japan's comprehensive utilization of solid waste is rich and advanced, due to the large shortage of various raw materials in Japan, and due to residents It is opposed to the accumulation of fly ash in landfills, so the comprehensive utilization rate of various solid wastes is high, and it is basically used to supplement building materials, and the rest is used as road subgrade materials, fertilizers, and foundation improvers [8].

In the field of high value-added utilization, Japan applies fly ash in the manufacture of anti-corrosion additives [9], sludge curing agents [10], materials for iron-making industry [11], polymer material fillers, etc. [12]. The U.S. Environmental Protection Agency (EPA) divides the utilization of fly ash into two aspects: Encapsulated beneficial use (mainly building materials) and Unencapsulated beneficial use (structural filling and embankment). EPA has released the feasibility assessment methods for the utilization of solid waste in coal-fired power plants in the above two application fields, "Methodology for evaluating encapsulated beneficial uses of coal combustion Residuals" and "Coal combustion residual beneficial use evaluation: Fly ash concrete and FGD gypsum" wallboard", which is used to better guide the application of fly ash in these two fields [13-14]. Europe mainly focuses on two factors in solid waste policy and utilization: environmental protection and resource utilization. Due to the low solid waste production in the EU and the lack of building materials raw materials, more than 95% of fly ash is used in the field of building materials and infrastructure [15].

1) The Japanese government and banks will give special concessions with high financing rate (40%) and low interest rate (1.9%) to the general industries that use fly ash processing equipment, which will economically improve the comprehensive utilization of ash-producing units. China and other countries have no preferential policies in this regard [16].

2) Developed countries have significant flexibility in both policy adjustment and standard formulation, which can be adjusted in time according to market and technical conditions in order to better promote the comprehensive utilization and use of fly ash and gypsum.

3) In the promotion of comprehensive utilization of fly ash abroad, the participation of private institutions is relatively high, such as the American Ash and Slag Association and the American Electric Power Research Institute. In China, the government takes the lead, and the research units and research institutes of enterprises in various industries are the technical research units to promote the

comprehensive utilization of solid waste [17].

4) In China, especially in the western region, policy guidance has a huge impact on the comprehensive utilization rate of solid waste, which can significantly increase or reduce the comprehensive utilization rate of solid waste, reflecting the singleness of comprehensive utilization of solid waste in my country and the high degree of policy dependence [18].

2.1.2 Decarbonization technology of fly ash

Unburned carbon extraction techniques from coal fly ash. A number of technologies (both wet and dry) for recovering unburned carbon from coal fly ash have been developed, and there are several possibilities for beneficiating coal fly ash to lower the LOI value. Sieving, gravity separation, electrostatic separation, froth flotation, and oil agglomeration are some of the current technologies for separating unburned carbon from fly ash. The next sections will go over the main techniques for separating unburned carbon from fly ash.

In view of the limitations of dry decarbonization technology and the difference in surface properties between unburned carbon and ash particles, flotation is still the most widely used technical approach for the removal of unburned carbon from fly ash. A lot of work has also been done in this regard.

(1) Electro-separation decarbonization technology

The basic principle of electro-separation decarbonization is to realize the separation according to the difference of the charged properties between the unburned carbon particles and the ash particles in the fly ash. The current triboelectric separation decarbonization devices have different forms, but they have a consistent working principle, which can be described as follows: first, the dispersion of fly ash particle groups is usually carried out by means of strong air flow; the second is the electrification of the particles

The process is mainly realized through the collision between particles and triboelectric plates or between particles, so that unburned carbon particles and ash particles are charged with different charges; finally, the charged fly ash particles are passed through a certain The particles are transported to the electrostatic separation chamber with two different polar plates, and the particles with different charge signs are adsorbed to different polar plates in the electrostatic field, so as to realize the separation. American Separation Technology Corporation (STI) has developed a fly ash triboelectric separation decarbonization device with a processing capacity of 20t/h [61].

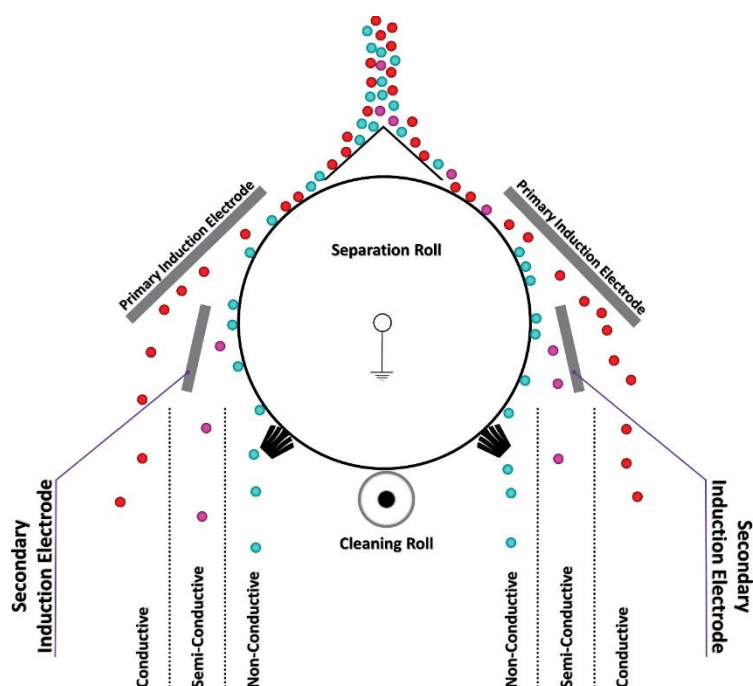


Fig.2.9 Electro-separation

Its core components are two electrode plates arranged in parallel and an open belt made of polymer material. When the unburned carbon particles and the gray matter particles carry different charges through the parallel electrode plates, the strong agitation of the belt and its Under the cleaning action of the plate, particles with different electrical properties are collected at both ends. Using this equipment to treat raw ash with a loss on ignition of 6.59% from a power plant in southern Italy, three products can be obtained: low carbon ash yield of 86.56%, loss on ignition of 3.12%; medium mineral yield of 7.52%, loss on ignition of 13.48 %; the yield of refined carbon is 5.92%, and the loss on ignition is 48.90%.

R. Ciccu et al. [63] used the process of classification and electrostatic separation of coarse-grained products to treat unburned carbon in fly ash. The development of this process is closely related to the particle size distribution characteristics of unburned carbon. The unburned carbon content of the high-grade fly ash product is low, which can meet the requirements of direct utilization.

(2) Flotation and decarburization technology

O. Sahbaz et al. [19] used Jameson flotation column to conduct a sorting test study on the fly ash of a power plant in Turkey for the purpose of carbon extraction. Through the optimization test of process parameters, the equipment can achieve a loss on ignition from about 10%. The refined carbon product with ash content of 44% is extracted from the original ash product, and the carbon recovery rate is 67.5%.

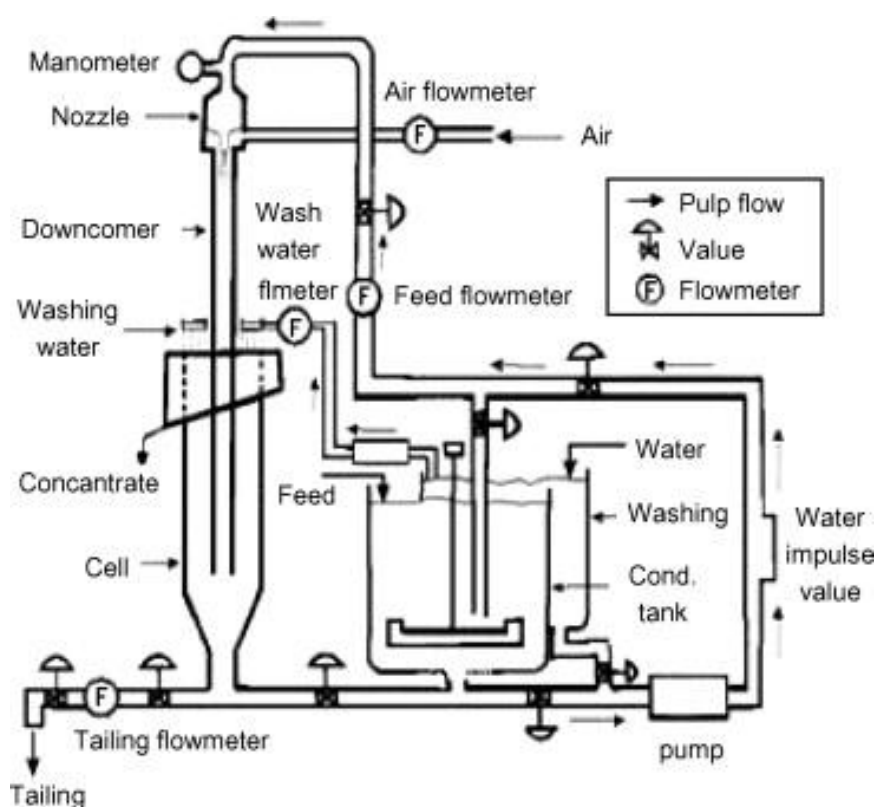


Fig 2.4 A schematics of the laboratory scale Jameson cell unit.[19]

U. Demir et al. [20] used a traditional gas-filled countercurrent flotation column to study the flotation carbon extraction of raw ash products with a loss on ignition of 22.4%. Under the optimized test conditions, refined carbon with a calorific value of 3840kcal/kg could be obtained. product, the carbon recovery rate reached 53.8%.

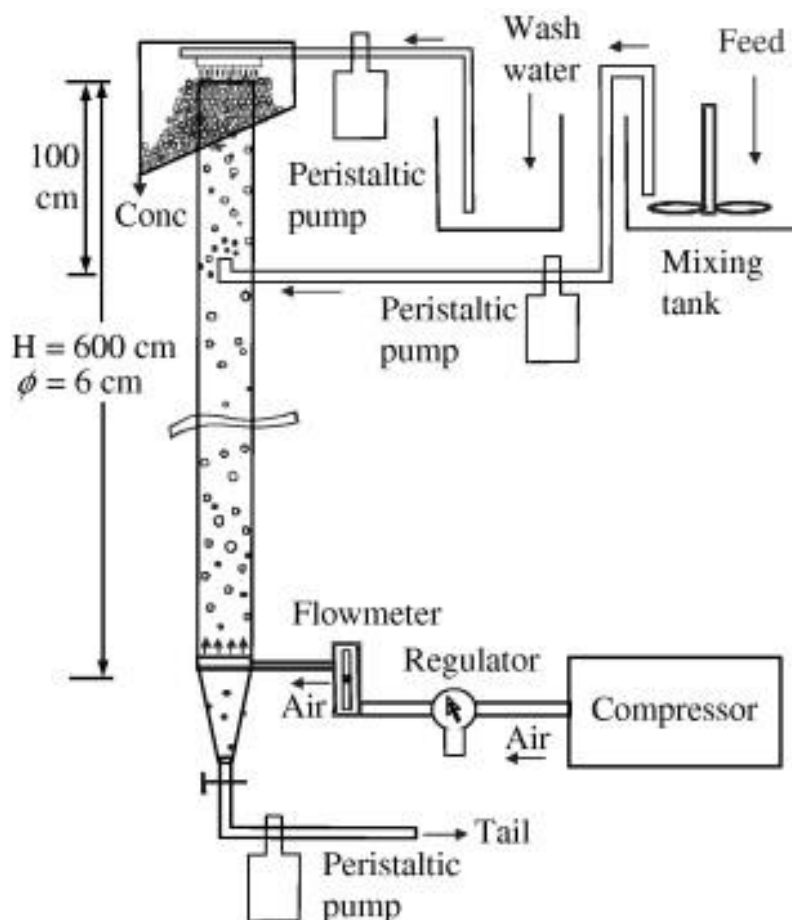


Fig. 2.5 Schematic diagram of flotation column [20]

E. Emre Altun et al. [21] conducted an experimental study of fly ash flotation decarbonization by using a new type of downstream flotation column from the perspective of equipment application, which is characterized by the use of static mixer-type bubble generation device.

Under the optimized test conditions, the equipment can recover nearly 95% of the unburned carbon in the fly ash, and the loss on ignition of the low carbon ash is reduced from 5.9% of the original ash to less than 1%, realizing the efficient removal of the unburned carbon.

M. Niewiadomski [22] et al. used an air jet cyclone flotation device to recover fine unburned carbon from power plant fly ash in Gdansk, Poland. The research shows that the refined carbon product with ash content of 35% can be extracted from raw ash with loss on ignition of 15.5% by using this equipment, and the recovery rate of combustibles is 54.3%.

The above researches on fly ash flotation decarbonization are mostly carried out for the purpose of resource development or application of new equipment. So far, no one has been found in the literature to study the characteristics of fly ash flotation system. The common characteristics of fly ash flotation decarbonization process are also the basis for the problems and research ideas of this paper.

In the mineral processing and coal preparation industries, froth flotation is now the most extensively utilized separation technology [23]. In a lab setting, a typical Denver flotation cell was employed to remove unburned carbon from fly ash [24].

Increased fuel consumption was caused by the existence of many pores. The most important impacts on carbon recovery were shown to be diesel doses and impeller speeds during conditioning. Huang et al. [25] removed unburned carbon using a conventional contemporaneous flotation column. The impact of gas flow rate, pH, collector kerosene dose, and different kinds of fly ash on separation performance was studied in detail. The removal of unburned carbon by column flotation was proven to be successful.

Mount Isa Mines and Prof. G.J. Jameson of the University of Newcastle, Australia, collaborated on the Jameson cell [26,27].

Figure 12 [28] shows a schematic illustration of the Jameson flotation cell.

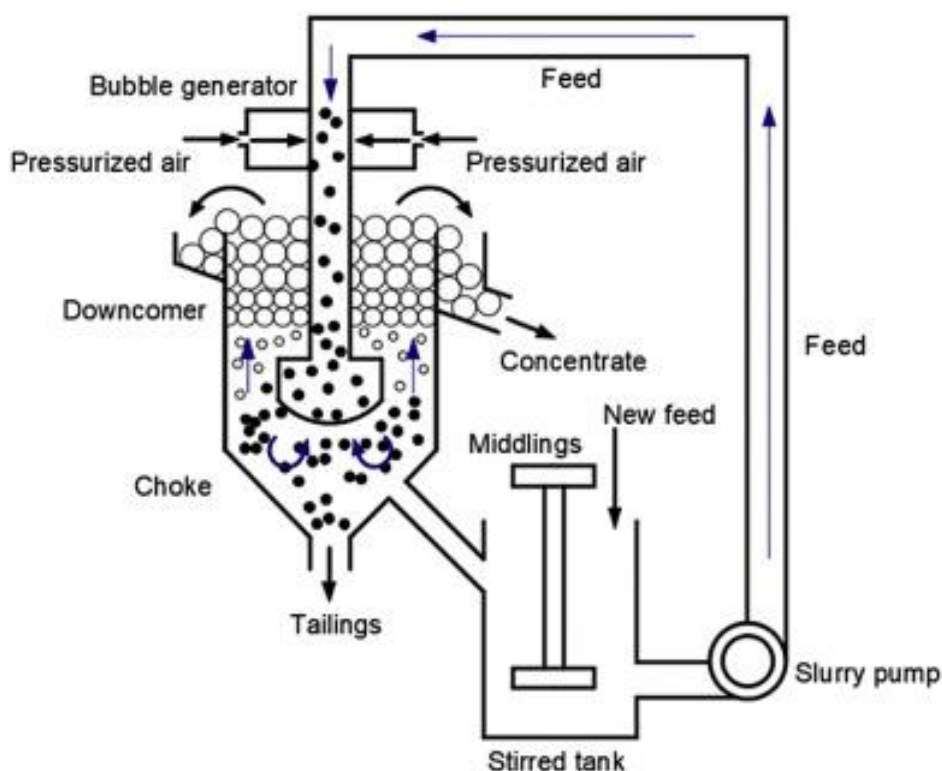


Fig.2.6. Schematic diagram of the Jameson flotation cell revised from [28].

Jameson cell has been proven to be an effective flotation equipment with high recovery capacity for micro fine particles. The effect of Jameson flotation operation variables on the recovery and kinetics of unburned carbon was studied by Uçurum [29].

Within the ranges studied, the optimal conditions were a pulp density of 15%, a wash water rate of 0.17 cm s^{-1} , and a downcomer immersion depth of 50 cm, indicating the Jameson flotation technique was effective for removing unburned carbon. It was also found that the classical first-order flotation kinetic model fits the test data very well. The Jameson cell was also used by Şahbaz et al. [30] to separate unburned carbon from bottom ash. The effect of superficial gas velocity, bias factor, percent solids, dosage of reagents, and conditioning time, on the recovery of unburned carbon were investigated. Unburned carbon recovery was shown to be highly sensitive to the frother dosage at unusually high levels. The differences in physical and chemical properties of particle surface provide a possibility for foam separation. At the same time, the turbulent environment of the flotation machine promotes particle-bubble attachment and improves the recovery ability.

It was challenging to achieve a satisfactory carbon recovery using a standard flotation cell due to the low floatability and micro fine feed of fly ash. A variety of flotation devices have been developed in recent years to increase the flotation recovery of unburned carbon. Niewiadomski et al. [31] employed an air-sparged hydrocyclone to remove the unburned carbon. Air was injected into the hydrocyclone through a porous wall and sheared into little bubbles, comparable to flotation. The air-sparged hydrocyclone produced 35 percent coke, which was discovered in the flotation concentrate. The presence of a cyclone field is advantageous for fine particle separation.

Altun et al. [32] created a novel concurrent flotation column system. As illustrated in Fig. 2.7, a static mixer in the feeder was paired with a froth separator and an extra bubble generator to promote bubble production. The static mixer (S1) was responsible for creating significant turbulence and efficient bubble–particle collision. The extra bubble generator (S2) was built to generate enough air bubbles to allow recapture of unattached or free carbon particles leaving the froth phase, resulting in increased ultimate recovery. Using this innovative concurrent flotation column technique, unburned carbon flotation tests were conducted with and without the extra bubble generator.

With and without the extra bubble generator, the carbon concentrations of the ash product were 2.53 percent and 1%, respectively. Flotation columns, in comparison to flotation machines, enhance the contact duration between bubble and particle, making them ideal for fine unburned carbon separation.

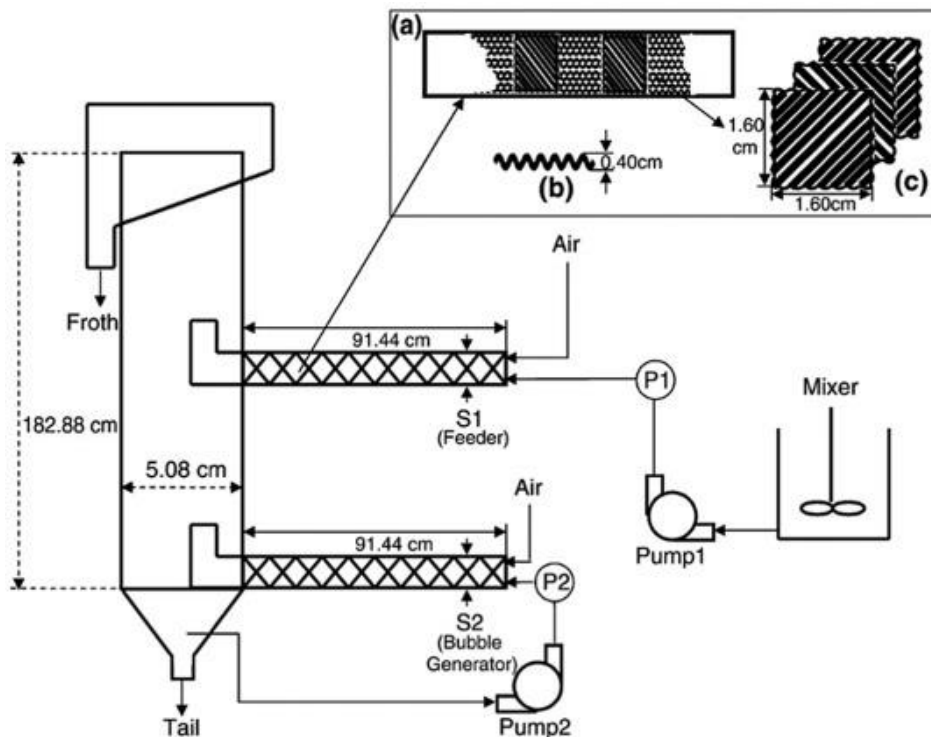


Fig. 2.7 Schematic diagram of a concurrent flotation column and packing units: a) packing arrangement in static mixers, b) side view of the packing arrangement, and c) top view of the packing arrangement [33].

Liu at the China University of Mining and Technology has created a novel flotation device called the cyclonic-static microbubble flotation column (FCSMC) [34]. As illustrated in Fig. 14, one FCSMC had a flotation column unit, a cyclone separation unit, and a pipe flow unit. The following is

a description of FCSMC's working process: To generate a high-quality concentrate, the pulp is first fed to the column unit for typical countercurrent mineralization.

A cyclone separation technique involving density separation and flotation is used in the second separation stage to create high-quality tailings. With high Reynolds numbers, the pipe flow mineralization unit is linked perpendicularly to the cyclone separation zone in the tangential direction [34].

In the pipe flow mineralization zone, an external bubble generator based on the idea of a venture cavitation tube, similar to the Jameson cell, is mounted to create microbubbles, which can improve ultrafine particle flotation performance. Overall, countercurrent collision mineralization, cyclone mineralization, and pipe flow mineralization are combined in a single FCSMC to provide an optimum mineralization response mechanism, particularly for microfine particles [34].

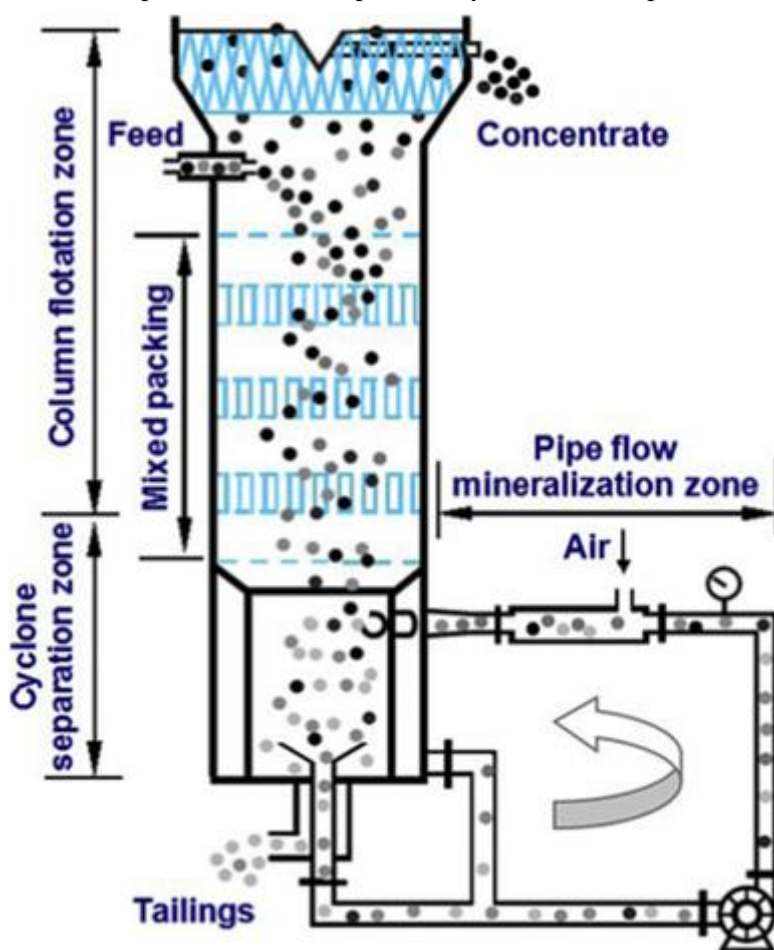


Fig. 2.8. Schematic diagram of a cyclonic-static microbubble flotation column [34].

At an industrial scale, FCSMCs have been employed to extract unburned carbon from high-carbon fly ash [35]. A column flotation system capable of processing 110 tons of coal fly ash per hour (dry basis) was employed. Tailings ash was recovered with a LOI of 3.08 percent, an unburned carbon removal rate of 80.41 percent, and a calorific value of 3534 cal/g for the unburned carbon products.

The findings showed that when the circulation pulp pressure is increased, the LOI of clean ash decreases, implying that raising the circulation pulp pressure improves the FCSMC's mineralization

efficiency and recovery capacity. Xu et al. [36] examined unburned carbon flotation from fly ash using the FCSMC with a standard mechanical flotation cell.

The FCSMC recovered 89.69 percent of unburned carbon, which was 6.5 percent greater than typical mechanical flotation. Furthermore, the FCSMC's LOI of 1.99 percent for flotation tailings was 1.11 percent lower than the standard flotation cell. Two significant elements in the FCSMC's superior recovery are pipe flow mineralization and cyclonic mineralization.

The bubble size in the FCSMC is much smaller than that in a typical flotation cell. Furthermore, the bubble generator's strong shear force can enhance collisions between bubbles and micro-fine particles. This strengthening mechanism is similar to that of the Jameson flotation cell explained above. The FCSMC [37] was used to investigate the flotation behavior of unburned carbon from coal ash and came to the same findings.

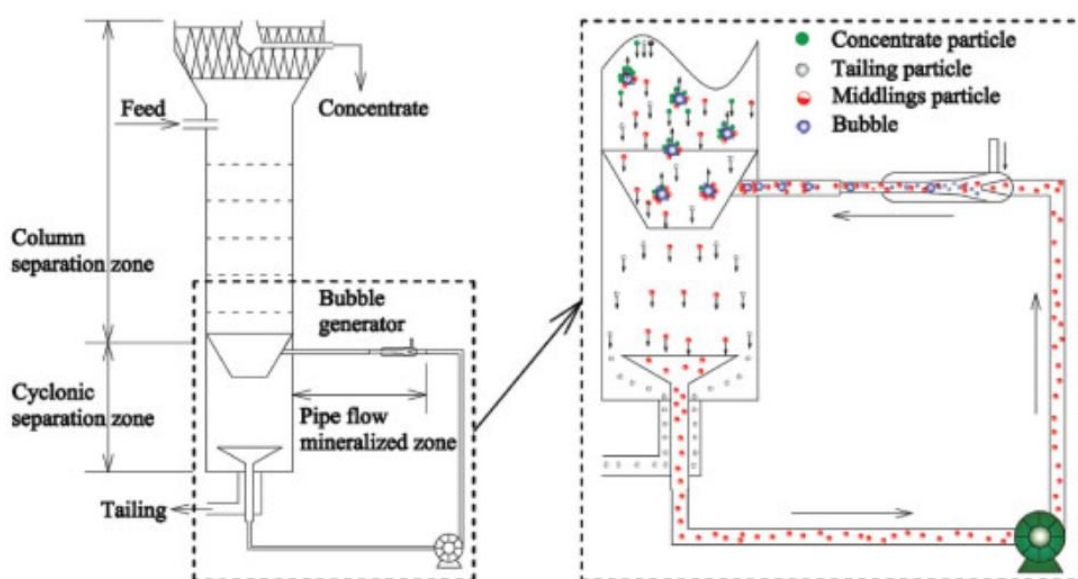


Fig 2.10 Schematic view of FCSMC separator

The FCSMC flotation device provides diverse flow fields, which minimize the particle size lower limit, increase particle selective adhesion, and allow sufficient time for particle-bubble attachment [38,39]. The flotation column, which is based on numerous flow fields and force fields, will be an essential technical technique for treating fine fly ash in the future.

However, there are still technical issues in the unburned carbon removal process, such as low floatability, micro fine feed particles, and a lack of adequate foam stability, as compared to the flotation of ores [40,41]. The creation of multiporous and highly oxidized surfaces, as well as the deposition of certain hard-to-float minerals fused in the combustion process on the surfaces of unburned carbon, are all effects of coal combustion at high temperatures.

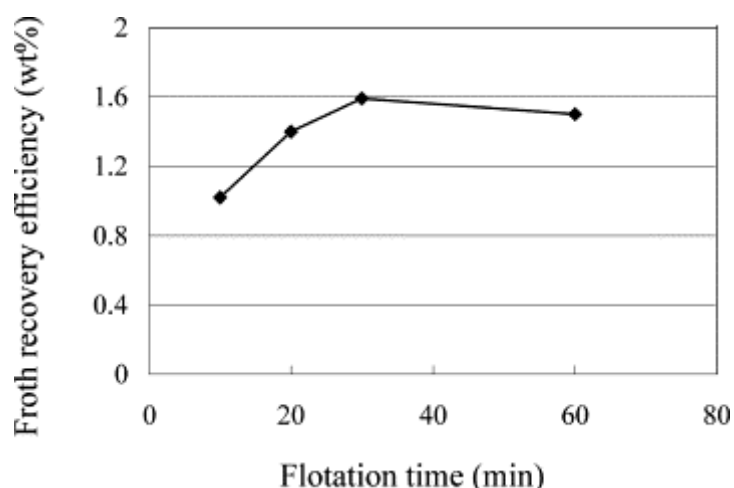


Fig 2.11 Influence of flotation time on the recovery efficiency of the froth

Special polar collectors employed in oxidized coal flotation, such as carboxylic acid, ammonium salt, and ester, may be promising in coal fly ash flotation. In unburned carbon flotation, a combination of polar reagent and oil has been shown to be efficient collectors [42]. Furthermore, the pulp solution chemistry in flotation systems has a variety of features. Because of these modifications, froth flotation systems are unstable, and flotation removal of unburned carbon is challenging.

It should be emphasized that following flotation, the flotation products must be dewatered, which is a major issue. The clean coal was previously dewatered using a pressure filter, but throughout the manufacturing process, it was discovered that the moisture content of the filter cake was greater, affecting the quality of the flotation product, increasing transportation costs, and reducing the economic advantage.

Filtration and dewatering of flotation foam products is a complex process that is influenced by a variety of factors including feed qualities, operating conditions, and equipment stability. Reducing the moisture content of flotation coal is a subject worth investigating since it is linked to the method's application.

2.1.3 Flotation reagents for separating unburned carbon

Conventional flotation reagents (kerosene, diesel) are ineffective due to the presence of oxygen-containing groups on unburned carbon surfaces as well as the wide microporous structures. Because low-rank coal, oxidized coal, and unburned carbon have comparable surface features, such as porosity and oxygen-containing functional groups, many heuristics have been created utilizing polar reagents designed for oxidized coals and low-rank coals [43,44].

As a result, collectors that work well with oxidized and low rank coals may also work well with unburned carbon particles. The carbon floatability was improved by forming hydrogen bonds between novel polar reagents and oxygen-containing groups on the unburned carbon surface. Nonylphenol and either hexadecane or fuel oil [45], 4-dodecylphenol (DDP) and hexadecane (HXD), oleic acid and #2 fuel oil [46], and diesel oil, acetic acid, and a proprietary alkanolamine [46] have all been shown to be helpful in increasing unburned carbon recovery.

Zhou et al. [47] examined four different surfactants (sodium dodecyl sulfate, sodium dodecyl benzene sulfonate, Tween-80, and Triton X-100) coupled with collectors (kerosene) to improve

collector dispersion efficiency on the carbon surface. The flotation findings demonstrated a substantial correlation between the product's LOI, and the surfactant type utilized. The best flotation index was found when Triton X-100 was combined with the collectors, with a 79.58 percent combustible recovery and 54.43 percent LOI.

The tail length of the surfactants has a considerable impact on kerosene adsorption, according to removal mechanism studies. Frothers, in addition to collectors, play a critical part in unburned carbon flotation. One of the challenges with unburned carbon flotation is the absence of sufficient foam stability. In the future, more research on high efficiency frothers should be conducted.

2.1.4 Research progress on the structure and dynamics of foam

The research on foam physics in academia has a long history, and it is also an important branch of modern mechanics. As early as the mid-to-late nineteenth century, Plateau and Kelvin gave a detailed description of the structural statics of bubbles and foams, which became the theoretical basis for subsequent research on foams. After entering the 20th century, with the development of microscopic technology, fluid mechanics and computer science, the research on the physical structure of foam has entered a new era.

The application has also been further developed. The classical statics theory of foam structure was founded by Belgian physicist Plateau in the 1830s and 1840s. He described the thermodynamically unstable foam system as follows: The foam is composed of liquid film, Plateau channel and node three. A dynamic system composed of structural elements according to certain internal structural laws. For more than 100 years, the above-mentioned law of equilibrium of foam structure has been used, and the mathematical proof of this law has never stopped.

Until 1973, the American mathematicians Taylor J. and Almgren F. mathematically deduced the law, and it was clear that when the liquid film area is the smallest, when three liquid films are combined at an angle of 120° ; four liquid films are at an angle of 109.47° . Angles are connected together. This is consistent with Plateau's description, but there are still incomplete and unclear parts of the proof, which require further scientific testing.

Foam systems have typical thermodynamic instability, so the spontaneous reduction of system energy has become a basic physical and chemical law. For foams in the process of dynamic decay, the spontaneous reduction of the energy of this system is manifested as the continuous reduction of the liquid film area in the foam structure. Under the premise of the minimum contact area between objects, if a three-dimensional space is filled, what shape do these physical objects have?"

The above problem is known as the "Kelvin problem" in the physics world. Shortly after Kelvin himself posed the question, he gave his own answer to the question in connection with the structure of the foam: the bubbles in the foam take the shape of a tetrahedron with 6 squares and 8 regular hexagons, when the bubbles The contact area between them, that is, the liquid film area is the smallest, as shown in Figure 1-8. Such tetrahedral structural units are called Kelvin cells. For the next hundred years or so, Kelvin cells have been considered the optimal structure for foams.

With the development of computer simulation technology, in 1993, Denis Weaire and Robert Phelan of Ireland used numerical simulation to find a more reasonable basic structural unit of foam than Kelvin unit: foam is composed of two kinds of bubbles of the same volume, one is each Each face is a regular pentagon and a regular dodecahedron; the other is a tetrahedron consisting of 2 regular hexagons and 12 regular pentagons, and 6 tetrahedrons and 2 regular dodecahedrons.

This structure is also referred to as a Weaire-Phelan foam cell. After the 1870s, the study of foam dynamics has gradually been paid more attention. The research on the dynamics of liquid foam in the chemical, mining, washing and other industries is particularly important. Whether it is foam stabilization or defoaming, the research on the foam stabilization mechanism and its stability regulation are the keys. The foam dynamics is also in the process of related research and practice. gradually developed.

As a non-equilibrium system, the structure of liquid foam evolves with time, and the research content of foam dynamics mainly includes the following aspects

- ① Foam drainage: The liquid in the foam structural elements seeps out under the action of gravity, resulting in the gas phase of the foam and the liquid phase separation;
- ② Rupture of the liquid film: The thinning of the liquid film in the foam causes it to rupture, which in turn causes the adjacent bubbles to merge;
- ③ Bubble coarsening: The bubble merging phenomenon caused by the diffusion of gas molecules from small bubbles to large bubbles through the liquid film under the action of Laplace pressure.

For the above three kinetic processes, the gas diffusion process is relatively slow, the liquid film rupture can be slowed down by suitable surfactants, and the gravity-driven foam drainage can be controlled by the regulation of liquid phase viscosity, but the above mechanisms can only be determined from the time to slow down the decay of the foam, but not prevent it.

These three dynamic processes interact with each other during the evolution of the foam structure: when the liquid drain occurs, the flow of a small amount of liquid in the liquid film will affect the gas diffusion between the bubbles; at the same time, the bubble merger and gas diffusion caused by the rupture of the liquid film. The resulting coarsening of the bubbles can lead to an increase in the average diameter of the bubbles, which in turn accelerates the drainage process. At present, the research on the mechanism of foam decay mainly focuses on these aspects.

It is well known that the adhesion of solid particles to the surface of the bubble can improve the mechanical strength of the bubble liquid film. The stabilizing effect of particles on foam is also widely used in various industrial production and daily life. Especially for the mineral flotation system, the adhesion of hydrophobic particles, the non-selective entrainment of fine particles, and the effect of bubble armor all make the flotation three-phase foam more stable to a certain extent. Theoretical studies are mostly concentrated in the field of colloid and surface chemistry, and only a few literatures have reported the effect of particles in flotation systems on foam stability.

(1) The field of colloid and interface chemistry

British surface physicist B.P. Binks [64-66] first proposed the concept of solid surfactant and compared the similarities and differences between solid particles and traditional surfactants when they are used as foam stabilizers. He believed that in the O/W (W/O) type emulsion system, when the contact angle of the solid particles at the oil-water interface is less than 90° , the O/W type emulsion can be more stable; When the contact angle of the interface is greater than 90° , the W/O

emulsion can be more stable. In the research on the mechanism of foam stabilization of liquid film, Horozov [67] et al. studied the stabilizing effect and mechanism of 3 μm quartz particles on the liquid film in emulsion under the condition of no surfactant. He believed that solid particles play a role in the liquid film.

A bridging effect is reached, which makes the foam more stable. In recent years, some researchers have expanded this bridging mechanism [68-71], and established the single-row particle bridging mechanism, the backrest-type double-row particle bridging mechanism and the mesh structure bridging mechanism. related models. In recent years, related studies have also been carried out from the perspective of the effect of particle properties on foam stability.

S.I. Karakasheva [72] used spherical silica particles with a particle size d_{90} of 38 μm and fibrous sepiolite as the research objects, and investigated the effects of solid particles of the same size and hydrophobicity on foam formation and stability. Studies have shown that fibrous sepiolite is better than spherical silica particles in stabilizing foam.

Liu Qian of Shandong University [73-76] studied the foam stabilized by n-hexylamine and hydrophilic hectorite particles (30nm) synergistically and the foam stabilized by the mixed aqueous dispersion system of cationic surfactant and hectorite. The research shows that: solid The adsorption of particles at the air-water interface can improve the expansion viscoelasticity of the interface, that is, a gel-like layer is formed on the interface to slow down the drainage and coalescence of the foam.

A. Britana [77] studied the effect of fine particle fly ash on foam drainage and merger, using a particle diameter of 10 μm . The study showed that when there are fly ash particles in the system, the foam drainage and merger rate Significantly slowed down, and this phenomenon is not only due to the increase in slurry viscosity, he may explain that the presence of solid particles blocks the route of liquid discharge.

(2) flotation field

In the field of flotation, some researchers have also studied the influence mechanism of mineral particles with different particle sizes and hydrophobic degrees on the foam stability. A study of the merger behavior between bubbles. He believed that smooth spherical particles with a contact angle greater than 90 degrees, if able to form a bridge between two bubbles, would bring the two bubbles together and destabilize the foam.

On this basis, Johansson G.[79] obtained quartz particles with different degrees of hydrophobicity through special treatment in 1992, and the particle size was between 26 and 44 μm . His research showed that the stability of the quartz particles with $\theta < 40^\circ$ to the foam was The effect is not large; $\theta \approx 65^\circ$ has the smallest bubble merger phenomenon, and the foam is the most stable; $\theta > 80^\circ$ quartz particles promote the bubble merger and rupture, making the foam unstable. This is consistent with Dippenaar's findings

T.V. Subrahmanyam [80] summarized previous studies on foam stability, particle entrainment and drainage in flotation. Properties are the three major factors affecting the foam stability, and it is pointed out that the mineral particles affect the foam stability by adjusting the surface wettability of the collector, and the fine particle entrainment in the flotation slows down the flotation foam to a certain extent. Liquid process, enhanced foam stability.

In recent years, some studies have also analyzed the relationship between mineral particles and foam stability for actual flotation systems. Z. Aktas[81,82] used platinum ore from a mine in South

Africa, and obtained materials with different fineness (30-70 μ m) through grinding. A dithiophosphate and DF-200 were used as collectors and DF-200, respectively. Foaming agent, tested for flotation operation and froth stability in a common Denver flotation cell. Studies have shown that foam stability is largely dependent on particle size, and that finer particles increase the foaming power and foam stability of the pulp.

N. Barbian [83,84] established a system for testing dynamic froth stability on laboratory and industrial flotation machines, and established a relationship between the foamability index and flotation behavior, i.e., through the detection and adjustment of froth stability To guide the flotation production process, this is a very meaningful attempt.

2.2 Research status of fly ash recycled aggregate concrete

2.2.1 Recycled aggregate

The word "recycled aggregate" refers to the aggregate for concrete that is formed by breaking up concrete lumps or other similar materials as the raw material and then putting them through various processing steps such as crushing, grinding, sorting, and so on. Additionally, the quality of the recycled aggregate is taken into consideration while classifying the material. High quality recycled aggregate class H species, medium quality recycled aggregate class M species, and low quality recycled aggregate class L species are the three categories that result.

The JIS standard system requires a certain grade of recycled aggregate, although the requirements of the standard change based on the type of recycled aggregate. In the case of recycled aggregate class H species, the JIS A 5021 standard for recycled aggregate H for concrete has been set up as an independent product standard. This is similar to how crushed stone and crushed aggregate as well as slag aggregate have their own standards. On the other hand, recycled aggregate class M species and recycled aggregate class L species cannot be used for ready mixed concrete prescribed in JIS A 5308. Because of this, the product specifications of concrete [JIS A 5022, JIS 5023] have been established, and the quality of recycled aggregate is specified in the appendix of both of these documents. The quality of the recycled aggregate is detailed in table 2.1. [48]

Table 2.1. The quality of recycled aggregate [48]

Test items	Recycled aggregate class H species		Recycled aggregate class M species		Recycled aggregate class L species	
	Coarse aggregates	Fine aggregates	Coarse aggregates	Fine aggregates	Coarse aggregates	Fine aggregates
	Absolute drying density [g / cm ³]	over 2.5	over 2.5	over 2.3	over 2.3	-
Water absorption rate [%]	under 3.0	under 3.5	under 5.0	under 7.0	under 7.0	under 13.0
Abrasion loss [%]	under 35	-	-	-	-	-
Particle content [%]	under 1.0	under 7.0	under 1.5	under 7.0	under 2.0	under 10.0



Photo 2.1. Recycled coarse aggregate and recycled fine aggregate [2]

(1) Heating pad method

A heating mechanism in the form of a rotary kiln is used to get the temperature of the concrete mass up to around 300 degrees Celsius. This causes a dehydration reaction in the cement paste, which in turn weakens the bonding between the individual pieces of concrete. The aggregate and the cement paste are then separated after the agglomerates that were heated by the grating device are rotated by a spinning rotor. This ensures that the aggregate does not become crushed during the process. In addition, the product is marketed using a vibrating screen to sort the product sizes. The manufacturing process as depicted by the heated rub mill method can be seen in Photo 2.2.

By heating the raw material used to manufacture the concrete block, it is possible to weaken the cement paste so that it can be readily peeled off. This also makes it simpler to separate the aggregate from the cement paste, which results in a reduction in the amount of energy required. In addition, it is possible to keep the quality of the aggregate consistent while simultaneously lowering the amount of devastation caused by dust. Additionally, the term "cement filler" refers to the fine powder that is produced during the process of creating recycled aggregate. This cement filler has the same degree of fineness as cement, a small hydraulic property, and the ability to be used for improving soil and other similar purposes.

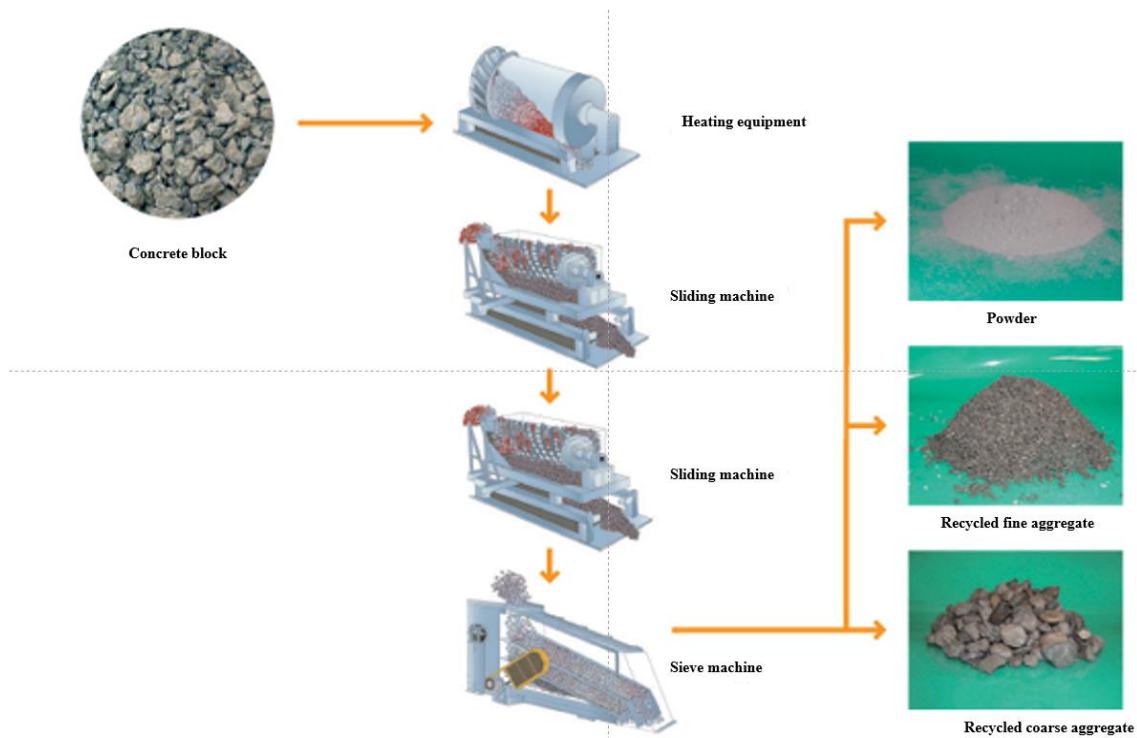


Photo 2.2. Recycled Aggregate Production Process by Heating Rake Cake Method[49]
 (2) Screw grinding method

By frequently rubbing concrete that has been crushed to 40 mm or less and then throwing it into the screw grinding apparatus, peeling and grinding the mortar portion of the surface part, and doing all of this without crushing the aggregate, the screw grinding method can produce a high-quality product. Consequently, recyclable aggregate will be produced. The production apparatus for the screw grinding process can be seen in Photo 2.3.

The advantages of using a screw grinding process are as follows: The generation of by-product fine particles from high-quality recycled aggregate that satisfies JIS standards is too low to medium for the conventional recycled aggregate production methods, but can be reduced by changing the number of treatments used in the screw grinding method, which distinguishes it from those methods. It is a process that has the potential to manufacture recycled aggregate of high quality..



Photo 2.3 Screw grinding method manufacturing equipment [49]

The aggregate that is produced by reducing demolished concrete through the process of comminution is referred to as recycled concrete aggregate (RCA). Up until this point, the most common applications for RCA have been in roadway pavements and in non-structural concrete. Yet, there is little doubt that the structural application of RCA will rise in the future; however, caution is necessary. RCA is considered an artificial aggregate by the ASTM C 294-05 standard. When employing recycled concrete as aggregate in the production of fresh concrete, the following special considerations need to be given priority. The unit weight (density) of concrete manufactured with recycled construction aggregate (RCA) is lower than that of concrete made with conventional aggregate. This is due to the fact that RCA contains a portion of old mortar. Porosity and absorption are both increased in concrete that was produced with RCA for the same reason. If the RCA is soaked before it is mixed, you can take advantage of its higher absorption rate and achieve internal curing thanks to the water that was absorbed. In particular, this is the case with RCA that consists of a significant quantity of brick.

If the fine aggregate is crushed rock or natural sand of enough quality, the potential compressive strength of the new concrete is primarily constrained by the strength of the old concrete. This is the case provided that the fine aggregate is of sufficient quality. It is possible that the conventional fine aggregate's compressive strength will decrease significantly if the fine aggregate from the old concrete is used to replace some or all of the conventional fine aggregate. Anything that is smaller than 2 millimeters in size should be eliminated. When RCA is used, the workability of fresh concrete drops at a given water content, the amount of water needed to achieve a certain consistency increases, drying shrinkage increases at a given water content, and the modulus of elasticity decreases at a given water-to-cement ratio. When the old concrete is used for both the coarse and the fine aggregate, these effects are amplified to their full potential. Freezing and strength of the old concrete, together with the features of the new concrete that match to those characteristics.

transform the characteristics of the existing concrete. On the other hand, if there are a lot of chloride ions in the old concrete, they could speed up the corrosion of any steel that is embedded in the new concrete. Possible sources of old concrete may not be suitable for use if they have been damaged by an aggressive chemical attack or leaching, have been subjected to service at high temperatures, or have been damaged in any other way.

It is important to conduct an analysis of the relevance of pollutants in the old concrete, such as noxious, poisonous, or radioactive compounds, in relation to the projected service of the new concrete. despite the fact that there are steel embedments in the freshly mixed concrete. Possible sources of old concrete may not be suitable for use if they have been damaged by an aggressive chemical attack or leaching, have been subjected to service at high temperatures, or have been damaged in any other way.

It is important to conduct an analysis of the relevance of pollutants in the old concrete, such as noxious, poisonous, or radioactive compounds, in relation to the projected service of the new concrete. Although the presence of bituminous materials may make it more difficult for air to become entrained, significant concentrations of organic materials may result in an excessive amount of air becoming entrained. Metallic inclusions may result in rust discoloration or surface blistering, and glass shards may create an alkali-aggregate reaction. Both of these issues can be caused by alkali-aggregate reaction.

The document known as BS 8500-2:2002 provides a method for determining the composition of RCA.

The essential treatment of trash is not a straightforward process, and the utilization of aggregate produced from waste calls for the application of specialized knowledge due to the lack of standardization among the materials. In instance, the debris left behind by building demolition may include harmful quantities of brick, glass, gypsum, or chlorides. [50-52]

The processing of waste from demolition in order to transform it into aggregate that can be used in adequate amounts and is free of contaminants is still in the process of being developed. Gonzalez et al. have demonstrated and validated that the use of recycled aggregate in concrete results in a reduction in the amount of aggregate interlock. [53] Regan discusses the impact that the type of aggregate has on the interlocking process. [54]

After the removal of ferrous and non-ferrous metals, the ash from the incinerator can be crushed into a fine powder, combined with clay, pelletized, and then burnt in a kiln to generate artificial aggregate. This method is applicable in the context of the recycling of household waste.

After 28 days, concrete made with this material has the potential to achieve compressive strengths of up to 50 MPa, which is equivalent to 7000 psi. There will, of course, be issues with fluctuations in the composition of the raw ash, and the features of the material that contribute to its long-term durability have not yet been discovered, despite the fact that the findings obtained to this point look good.

These subjects are outside the focus of this book; however, readers should be aware of the new and expanding possibilities of using processed waste as aggregate.[55]

Some of the ancient mortars have a propensity to attach to the surfaces of the original aggregate, and as a result, they end up being included in the RCA. Due to the nature of mortar, which is to be less dense and porous than the aggregate matrix, this old mortar makes for a lighter system in the RCA.

Because of the presence of these ancient mortars, the absorption capacity of RCA was significantly improved, and the specific gravity was significantly reduced when compared to that of most NA. As can be seen in Figure 2.8, the use of RCA in conjunction with a surface that contains attached mortar layers produces two distinct varieties of ITZ in the concrete system: the old and the new. It was discovered that the initial moisture state of the RCA as well as the strength of the RCA source concrete had a significant impact on the porosity distribution of the new ITZ. [56]

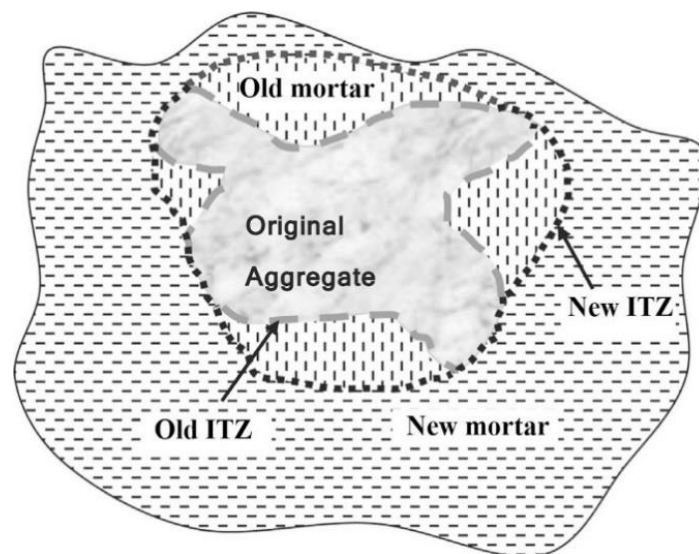


Fig 2.8 Schematic of old and new ITZ in RCA concrete—adapted from isku et al. [56]

Researchers named Verian, Verian, and Verian analyzed the cross-section of epoxy-embedded RCA particles with the use of an optical microscope in order to determine the percentage of mortar that was adhered to their surfaces. The specimens that were looked at are shown in figure 2.9. The research concluded that there is a possibility of up to 28.9 percent of finding ancient mortars clinging to the surfaces of RCA.

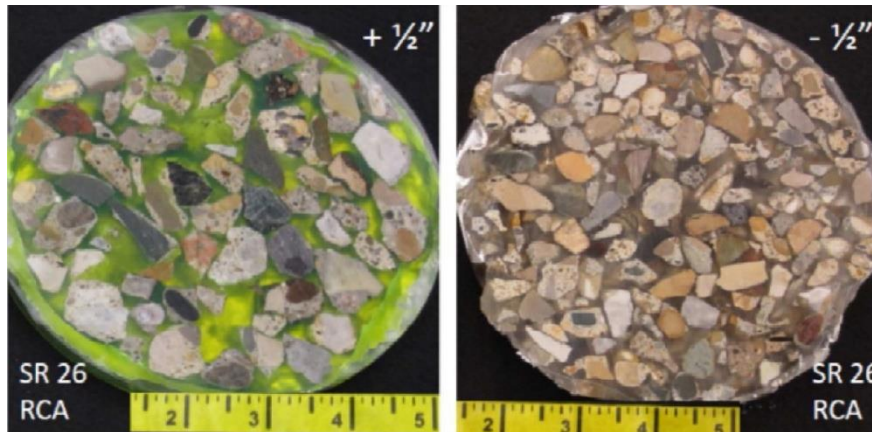


Fig 2.9. Cross sections of the sawn surface test specimens made from RCA embedded in epoxy—
adapted from Verian, Verian et al. [56]

According to Etxeberria et al., the amount of old mortar pollutants in the RCA aggregates that were used in their experiment ranged between approximately 20 and 40 percent for two distinct RCA fractions (10 and 25 millimeters). Li's research demonstrated that the adhering mortar can take up as much as 20–30 percent of the volume of the RCA, which is in line with the findings of Etxeberria et al. Afroughsabet et al. estimated that there was as much as 24 percent and 38 percent of connected mortar on the two different types of RCA that were used in the researcher's investigation.

In Section 7, we explore more into the ways in which these RCA elements affect the properties of the concrete. Roesler et al. reported the amount of recovered mortar content of the coarse RCA at a range of different diameters. As may be shown in Figure 2.10, the RMC of the finer fractions of RCA (4.75 and 9.5 mm) was higher than that of the coarser fractions (>9.5 mm). During the course of their experiment, Liu and colleagues measured the amount of old mortar that was found in RAs taken from concrete with strength grades of 20 MPa and 30 MPa (termed as RA20 and RA30, respectively). The percentages of old mortar found in RA20 and RA30 are, respectively, 42.22 and 46.51 percent.

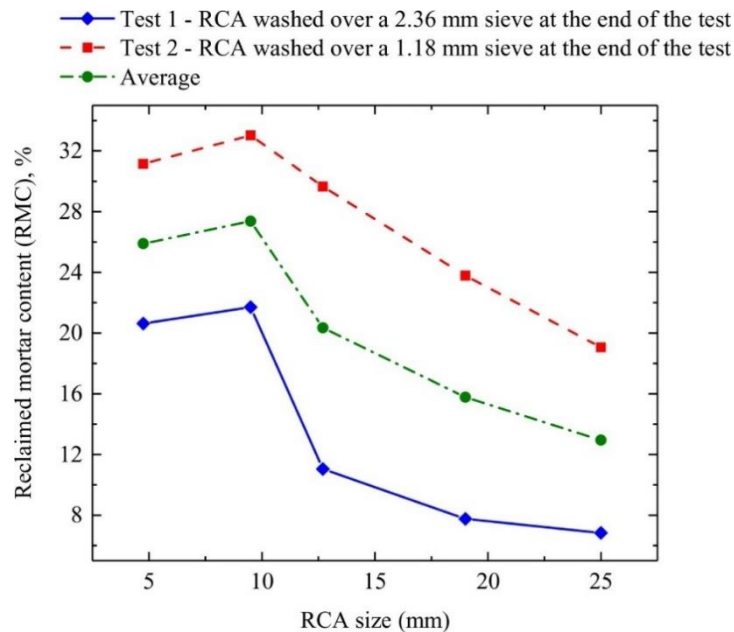


Fig 2. 10. RMC of different sizes of RCA—adapted from Roesler et al. [56]

2.2.2 Research state of workability

When compared to NC concrete, RCA concrete has a more manageable slump at the same w/cm. Concrete that contains RCA is less workable than concrete that does not contain RCA due to the higher capacity of the RCA to absorb water, the rougher surfaces, and the more irregular forms. To achieve the same level of workability as NC when employing RCA in a drying state, approximately 5 to 15 percent more mixing water must be included in the mixture than is required when using NC. It is common practice to raise the apparent water to binder ratio (w/b) in concrete mixes that contain RCA. This is done to account for the increased water content caused by the addition of the RCA.

If the RCA is controlled properly, and the concrete composition is created in the appropriate manner, then it may be possible to avoid employing this method in some scenarios. Prior to mixing, the RCA should be at or slightly below SSD state in order to provide a workability that is comparable to that of NC. The use of admixtures, such as fly ash (FA), or a combination of the two, improves the workability of concrete that contains RCA and is commonly utilized to cut down on the amount of water required for production. [56]

The decreased density of RCA concrete can be attributed to the greater quantity of RCA present in the concrete. The combination of RCA's lower specific gravity and the old mortar that is connected to it causes the concrete that contains RCA to have a lower density. The density of concretes with increasing amounts of coarse RCA is illustrated in Figure 2.6.

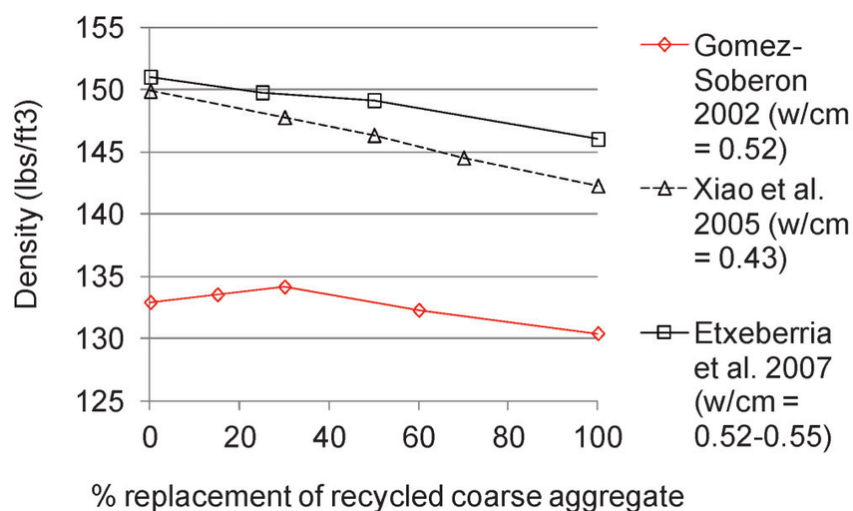


Fig. 2.6. Density of concrete containing different amount of coarse RCA [57]

The variation in density of concrete that contains RCA is caused by a combination of factors, including the amount of RCA used in the concrete mixes, the specific gravity of RCA in relation to NA, and other variables. According to Xiao et al. and Verian, the density of concrete that contains 100 percent coarse RCA is approximately 5 percent lower than that of concrete that contains 100 percent NAs. This was determined by comparing the two types of concrete's respective coarse RCA contents.

According to Etxeberria and colleagues' research, the density of concrete can be reduced by 3.3 percent when all coarse NA is substituted with coarse RCA. According to Dong et al findings, 's the density of concrete is unaffected when coarse RCA is replaced with fine RCA for up to fifty percent of the mix (0.8 percent drop). Marinkovi et al. used three distinct fractions of RCA to replace 65 percent of NA at various w/cm. The end result was a density that was 4.7 percent–4.9 percent lower than the density of the control concrete.

2.2.3 Research state of compressive strength

The compressive strength of various different concretes that were made with variable amounts of RCA is displayed in Figure 2.7. According to the findings of a number of research, the strength growth rate of RCA concrete is higher than that of NC concrete, particularly at later ages (e.g. 28 days). This is because non-hydrated old cement is present on the surfaces of RCA particles, which reacts with water to speed up the process of strength growth. As a result, this phenomenon is observed.

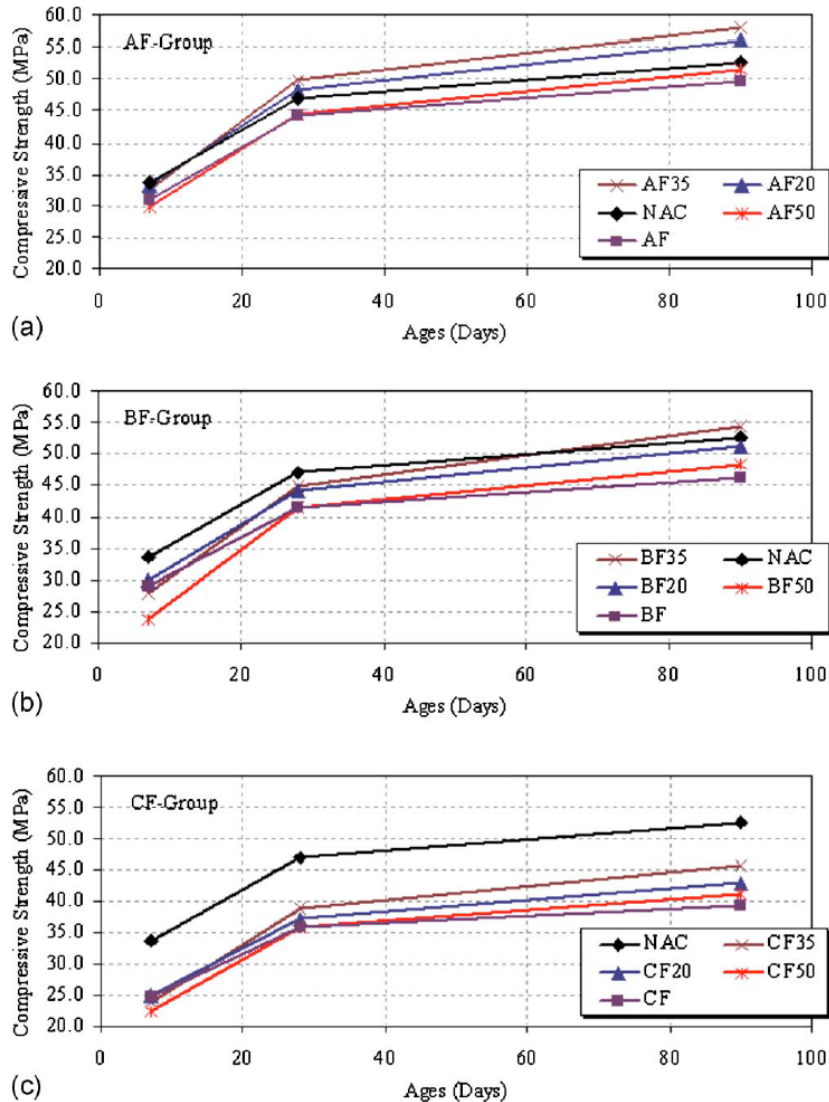


Fig. 2.7. Compressive strength values of various concretes made with different levels of RCA [58]

After conducting statistical analysis on the data found in the literature, Silva et al. came to the conclusion that a model could be constructed to predict the strength decrease that occurs in concrete that contains RCA at varying levels of replacement. This is in agreement with the results shown in Fig. 2.7(A) and (B), which demonstrate that the compressive strength of the material reduces as the amount of RCA present in it increases.

In spite of this, Poon et al. discovered that the initial moisture state of RCA has a significant bearing on the influence of RCA replacement level on the compressive strength of concrete. When 100% aggregate is replaced with RCA, the compressive strength can either be decreased by up to 30 percent or increased by up to 20 percent, depending on the moisture levels (see Fig. 2.8).

The lower compressive strength of RCA concrete is due to the existence of two different kinds of interfacial transition zones (ITZ) in the matrix. In most cases, the ITZ is a weaker binding than either the aggregate or the hydrated cement paste. This is because the ITZ is responsible for holding the paste

to the aggregate. In normal aggregate concrete (NA), the ITZ is found between the aggregate and the mortar, whereas in recycled aggregate concrete (RCA), the ITZ is found between the original aggregate, the old mortar, and the new mortar.

In addition, the decreased compressive strength can be attributed to the fact that in many instances, additional water is added to the mixture of RCA concrete in order to guarantee that it is as workable as possible. The presence of aged mortar on the surfaces of RCA concrete contributes to the material's decreased compressive strength. This is because RCA concrete has a lower density in contrast to the density of the aggregate.

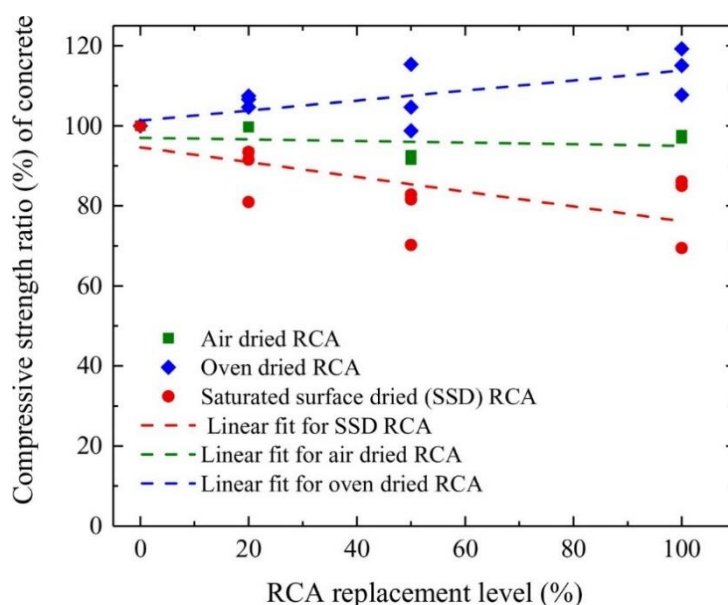


Fig. 2.8. Compressive strength variation of concrete with RCA replacement levels for different initial moisture conditions. [59]

When compared to the compressive strengths of concretes generated with oven-dried and SSD aggregates, the compressive strength of concretes produced with air-drying aggregates had a higher value (for normal and RCA concrete). The compressive strength of both RCA and NC concrete is increased when the w/cm is decreased (see Figure 2.7(B)). In Fig. 2.7(B), the integration of RCA into concrete mixture has a bigger impact on diminishing the compressive strength of concrete made with low w/c than concrete manufactured with high w/cm. This can be seen by comparing the two types of concrete in the figure.

The reason for this is that the quality of new cement paste that is created with a high w/cm is closer to that of ancient mortar than the quality of paste that is prepared with a low w/cm. These findings are consistent with those of Kurad et al., who conducted their investigation using high-quality RCA.

As can be seen in Fig. 2.7(C), the benefits of the TSMA, which was developed by Tam and Tam, allow for the production of concrete with a higher compressive strength than that which is achieved via the use of the conventional mixing method (NMA). Brand et al. combined the usage of TSMA with the application of saturated RCA in order to boost the compressive strength of RCA concrete.

The recycling of used concrete is considered to be of utmost importance in Japan. As early as 1977, the Japanese government established "Specifications for the Use of Recycled Aggregate and Recycled

Concrete" and recycling processing plants, the primary focus of which was on waste concrete. These plants were designed to produce recycled aggregate and recycled concrete. The "Resource Reuse Promotion Law" was enacted by the Japanese government in 1991. This law requires that wastes generated during construction, including muck, concrete blocks, asphalt concrete blocks, wood, and metals, be taken to "recycling facilities" for disposal.

The Japanese Ministry of Construction came up with a five-year plan to "control the discharge of construction by-products and develop technologies for the reuse of construction by-products" in the year 1992. The plan was proposed. The "Renewable Resources Law"[85] was signed into law in October of 2008 to encourage the reusing of construction by-products and to provide institutional protections. There are plants that produce recycled aggregate in various locations throughout Japan including Tokyo, Chiba, Nagoya, Osaka, and Kyoto. The utilization rate of construction waste in Japan in 1995 reached 58 percent, and the utilization rate of waste concrete was 65 percent, according to reports (86). In Tokyo, the reuse rate of construction waste reached 56 percent in 1988, and in Japan as a whole, the utilization rate of construction waste reached 58 percent in 1995. The recycling rate in Japan reached 98 percent in 2003, while the utilization rate of waste concrete in Japan reached 96 percent in 2000 [86]. In 1990, the utilization rate of waste concrete in Japan was only 48 percent, but it increased to 96 percent in 2000.

The majority of the waste concrete is recycled into foundation underlayment for use in the construction of roads. The most recent information indicates that Japanese researchers have developed a machine that combines a pulverizer and a mixer into a single unit. This new machine has the capability of recycling the waste concrete that is produced when buildings are demolished and producing recycled concrete on the spot. The recycled coarse aggregates used in non-load-bearing structures in Japan are separated into three categories, while the recycled fine aggregates are separated into two categories. In the same time period, the Japanese Industrial Standards (JIS) promulgated recycled aggregates used in load-bearing structures. and recycled concrete standards, and in 2005 and 2006, respectively, promulgated the "Specifications for the use of advanced recycled aggregates" and the "Specifications for the use of low-grade recycled aggregates" [87]. This was done in order to encourage the use of recycled aggregates. recycled aggregates used in load-bearing structures. and recycled concrete standards.

It is estimated that the EU had a recycling rate of approximately 28 percent for its construction waste in the early 1990s. In the years that followed, the majority of EU countries developed concrete plans to raise the rate of construction waste utilization to between 50 and 90 percent. Germany was the first nation in the world to introduce a system for the labeling of products based on their impact on the environment. Every region in Germany contains large complexes for the reprocessing of construction waste; in Berlin alone, there are more than 20 of these facilities. At the moment, recycled concrete is utilized primarily for the paving of roads.

The German Reinforced Concrete Committee published "Application Guidelines for the Use of Recycled Aggregate in Concrete" in August of 1998. These guidelines stipulate that concrete that has been prepared using recycled aggregate needs to fully comply with the national standard for ordinary concrete [88]. The United States was one of the first nations to propose the use of environmental labels. According to the data provided by the Federal Highway Administration, more than twenty states in the United States have made the decision to incorporate recycled aggregates into the construction of

state highways, 26 states permit the use of recycled aggregates as base materials, and four states permit the use of recycled aggregates as base materials.

Fifteen of the state-level agencies that use recycled aggregates as subbase materials have regulations on recycled aggregates that apply them to both the base and the subbase. This makes the total number of state-level agencies that use recycled aggregates for subbase materials 28. The "Super Fund Act" that was drafted by the US government offers legal protection for the growth of recycled concrete production. It states that "Any enterprise that produces industrial waste must dispose of it on their own and shall not dump it without authorization."

At the moment, the United States makes use of approximately 2.7 billion tons of waste concrete aggregates, of which 10–15 percent are used for the construction and maintenance of sidewalks, 20–30 percent are used for the construction of highways, and the remaining 60–70 percent are used for concrete structures. constitutes both the basis and the infrastructure. The International Federation of Materials and Structure Research Institutes (RILEM) published the "Regulations on Recycled Aggregate Concrete" in 1993. These regulations classify recycled coarse aggregate into one of three categories based on the source of the material, and they define recycled concrete based on the two indicators of strength and environmental grade. application spectrum [89].

An investigation conducted in 2004 revealed that the total amount of recycled aggregate that had been utilized in the United States had reached 2.7 billion tons, of which sixty percent to seventy percent were utilized in the production of recycled concrete [90,91]. Certain nations, such as the Netherlands and Denmark, which have a limited supply of stone materials and are highly reliant on natural aggregates imported from other countries, place a significant amount of importance on the recycling of waste from construction projects. The Netherlands was one of the first countries in the world to conduct research on recycled concrete and use it in construction projects.

In the 1980s, the Netherlands formulated the specifications for the use of recycled concrete aggregates to prepare plain concrete, reinforced concrete, and prestressed reinforced concrete. Additionally, the Netherlands put forward clear requirements for the use of recycled aggregates in the aforementioned types of concrete. And pointed out that if the mass content of recycled aggregate in the aggregate does not exceed 20 percent, then the production of concrete can be completely and completely carried out in accordance with the design and preparation method of ordinary natural aggregate concrete. This is because recycled aggregate does not have the same physical properties as natural aggregate, so it can be used interchangeably.

According to the plan for environmental policy developed by the Dutch cabinet in 2000, the rate of recycling of construction waste was as high as 90 percent (approximately 14 million tons) [86]. In 1990, Denmark was responsible for the generation of 12.2 million tons of waste from construction and demolition, of which 8.2 million tons were recycled. At the moment, the rate of recycling of waste from construction in Denmark has reached an impressive 80 percent [88].

To summarize, beginning in the late 1970s, developed nations such as Japan, the Netherlands, Belgium, Denmark, Germany, and the United States have been very active in the research and development of recycled concrete. These nations have achieved a number of successes, and they have actively promoted and utilized these successes in actual engineering.

Overall, foreign research focuses primarily on the preparation technology of recycled aggregates, finds solutions to the technical problems of recycling, and works to broaden the application scope of

recycled aggregates; the impact of concrete performance, the formulation of technical specifications for recycled aggregate and recycled concrete, to provide a technical basis for its application; research and formulation of supporting laws and regulations to encourage the application of recycled aggregates; and research and formulation of supporting laws and regulations to encourage the application of recycled concrete.

2.2.4 Research state of drying shrinkage

Drying shrinkage is the term used to describe the reduction in volume and the deformation that occurs in concrete when it is exposed to air that is not saturated with moisture [92]. The water in the concrete capillary evaporates gradually from the outside to the inside when the internal humidity of the concrete is higher than the external environmental humidity. This results in a reduction in the macroscopic volume of the concrete. When the internal humidity of the concrete is higher than the external environmental humidity.

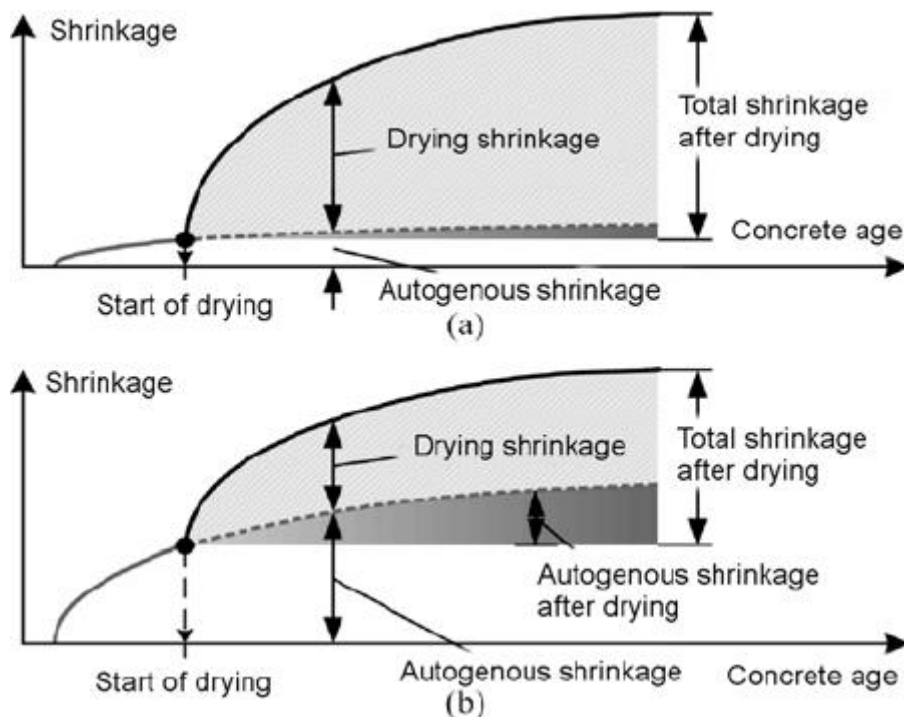


Fig. 2.9 Shrinkage strain components in normal (a) and high-strength (b) concrete [95]

In addition, if the relative humidity is right, the CO in the air will react with the products of the cement's hydration to produce calcium carbonate, silica gel, iron oxide gel, and water, which will lead to carbonization shrinkage in the cement. In most cases, carbonization and drying each contribute to the overall shrinkage of the material. Because of this, the value for drying shrinkage takes into account the carbon shrinkage as well.

At the moment, the most important mechanisms responsible for concrete drying shrinkage are the theories of capillary stress, disassembly stress, surface energy change of gel particles, and interlayer water migration [93]. These theories are broken down as follows:

The capillary tension theory postulates [94,95] that the meniscus of capillary water is connected to drying contractions. [Capillary water] shrinks as it dries. The evaporation of the free water in the capillary causes the formation of a meniscus, which generates tensile stress, which causes the concrete

skeleton to be subject to negative compressive stress, which ultimately results in a reduction in the volume of the concrete [96]. The capillary pressure, denoted by the symbol P , for cylindrical capillaries. The capillary meniscus is no longer stable when the relative humidity is lower than about 40 percent, and the absence of capillary stress is immediately noticeable after this threshold is reached. As a result, the application of this theory is restricted to situations in which the pore humidity is greater than 40 percent [97].

According to the disintegration pressure theory, the drying shrinkage is connected to the evaporation of the water that has been adsorbed on the surface of the concrete. When the distance between the gels is less than or equal to the thickness of 10 water molecules, a molecular attraction is generated between the particles. This attraction is balanced by the tension of the water molecules that are adsorbed onto the particles. As the water evaporates, the gel particles start to move closer to one another, which is caused by the interaction of van der Waals forces. This hypothesis can be used in situations in which the relative humidity contained within the concrete is greater than fifty percent. [93]

According to the theory of surface energy change, the change in surface tension between gel molecules is related to the drying process's ability to cause shrinkage. When compared to the surface energy of solids, water's value is significantly higher. The theory of thermodynamics states that substances with a high surface energy are unable to spread evenly on the surface of substances with a low surface energy. Because of this, water will contract into the shape of a sphere, which has the lowest possible contact rate with the solid surface. The volume of the solid particles is decreased as a result of compression caused by the action of the spherical surface tension of the water film on the film's surface. The relative humidity range that this theory can accommodate is from 5% to 50% [98].

According to the interlayer water migration theory, the shrinkage that occurs during the drying process is connected to the movement of water between the layers of the gel. C-S-H gel crystals have a layered structure, and water molecules are able to enter between the layers, which causes the crystal to expand. When the water is lost, however, the crystal will shrink as a result of the lack of water. This theory is applicable to situations in which the relative humidity is lower than 35 or 40 percent [97].

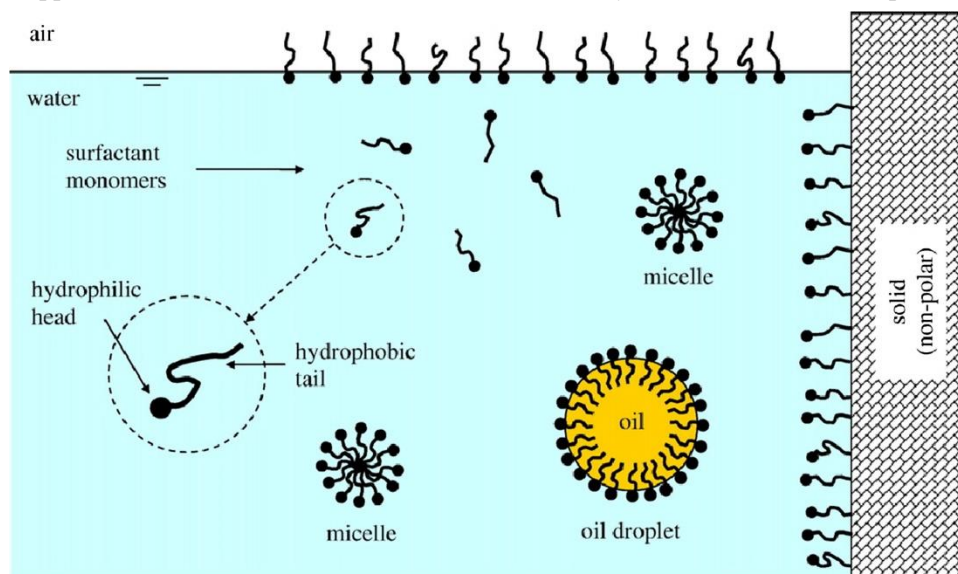


Fig. 2.10. Interactions of surfactant (amphiphilic) molecules with a polar solvent (e.g., water) [100].

The four aforementioned mechanisms each have their own specific humidity ranges that they are effective in. Concrete's drying shrinkage is frequently the result of a confluence of several different shrinkage theories, but only under certain conditions. In the references [99, 100], the nonlinear diffusion equation of Fick's law and the humidity diffusion coefficient are both utilized to provide a description of the movement of moisture through concrete as well as the volume change that results from this movement.

(1) Factors that contribute to drying shrinkage and its effects

In concrete, the cement mortar shrinks and deforms; however, aggregate slows down both processes by acting as a barrier between the cement mortar and the outside environment. It is clear that the factors that hasten the rate at which water in the concrete evaporates or that reduce the inhibitory effect of aggregate shrinkage will result in an increase in the drying shrinkage value of the concrete. This is because both of these effects will have the effect of increasing the drying shrinkage value. The aggregate, mineral admixture, water-binder ratio, and other factors are the most significant contributors to drying shrinkage.

The recycled aggregate contains old mortar, and because old mortar is porous, it will contract and change shape when it comes into contact with water. In addition to this, the crushing process will result in the formation of microscopic cracks in the recycled aggregate. Because of these initial defects, recycled aggregate will have a higher porosity, permeability, and water absorption rate than natural aggregate. As a result, the water diffusion coefficient of concrete made with recycled aggregate will be higher than that of concrete made with ordinary aggregate. Concrete Large [101,102]. In most cases, the drying shrinkage value of recycled concrete is going to be significantly higher than that of regular concrete.

Studies conducted by Domingo-Cabo A. [103] and others have shown that the drying shrinkage of recycled aggregate concrete is greater than that of ordinary concrete. Furthermore, the studies have shown that the relationship between the replacement rate of recycled coarse aggregate and the drying shrinkage value is as follows: the higher the replacement rate, the higher the drying shrinkage value. There are some variations in the experimental findings that can be attributed to the various researchers' utilization of recycled coarse aggregate of varying degrees of quality. The drying shrinkage value of recycled concrete is 12 percent to 66 percent higher than that of ordinary concrete when the replacement rate of recycled coarse aggregate is 50 percent; when the replacement rate of recycled coarse aggregate is increased to 100 percent, the drying shrinkage value of recycled concrete is 12 percent smaller than that of ordinary concrete: d: 180d. The range of possible improvements is from twenty to one hundred thirty six percent.

The results of experiments conducted by Khatib [104] and others demonstrate that the addition of recycled fine aggregate will also result in an increase in the drying shrinkage strain of recycled concrete. Furthermore, these results show that this increase is proportional to the replacement rate of recycled fine aggregate. Because recycled fine aggregate not only contains old mortar and initial cracks, but also fine powder with high water absorption, it is not recommended for use in new construction. Because of this, using recycled fine aggregate of poor quality with an excessively high percentage of fines will significantly increase the drying shrinkage of concrete.

The technique of improving the drying shrinkage properties of concrete by adding mineral admixtures is one that is utilized frequently by academics [105,106]. The drying shrinkage of recycled

aggregate concrete can be reduced by adding fly ash, ultra-fine mineral powder with an average particle size of 6 μ m, and silica fume if the proper dosage ratio is used. However, different types of recycled aggregate concrete have varying degrees of drying shrinkage. Mineral admixtures each have their own unique effect on quality improvement. The early shrinkage of recycled concrete can be effectively reduced by using fly ash, while ultrafine mineral powder and silica fume have obvious effects on the reduction of late shrinkage. However, the early shrinkage performance of recycled concrete can be negatively impacted by using silica fume. Fly ash is the best option.

To summarize, fly ash, slag, and silica fume are the types of mineral admixtures that are most frequently used. The drying shrinkage of concrete will be affected by the fineness, water demand ratio, activity effect, and other indicators of the three, and the difference in concrete mix ratio will also have an effect on the shrinkage reduction effect of mineral admixtures. Other indicators include the fineness, water demand ratio, and activity effect of the three. It is imperative that the impact of various mineral admixtures on the drying shrinkage performance of recycled aggregate concrete be thoroughly researched, and that an efficient method of controlling the drying shrinkage of recycled aggregate concrete be identified and developed.

In contrast to the effect of autogenous shrinkage, in general, the drying shrinkage of concrete will be greater when the water-binder ratio is higher. This is because a higher water-binder ratio will result in a greater increase in the amount of free water that is available for evaporation, as well as a smaller amount of cementitious material being used. raise the count to [107].

(2) Test method for drying shrinkage

When compared to autogenous shrinkage, the drying shrinkage test piece does not require being sealed, and the method of testing drying shrinkage is relatively straightforward. Autogenous shrinkage is measured by comparing the original size to the new size after it has been dried. When it comes to data collection, the most common methods include computerized automatic collection or dial gauges.

Drying shrinkage specimens do not require any kind of sealing treatment; however, autogenous shrinkage within the concrete is something that cannot be avoided. To be more precise, the drying shrinkage should be calculated as the measured deformation of the concrete when it is subjected to dry conditions minus the autogenous shrinkage deformation of the specimen that has been sealed. On the other hand, autogenous shrinkage is typically measured right after the concrete is poured, whereas drying shrinkage is measured two or three days after molding [92], which means that the time dimension of the starting point of the two tests is inconsistent.

When it comes to the early stages of the process, autogenous shrinkage develops more quickly, and by the time drying shrinkage is measured, some autogenous shrinkage will have already taken place. According to the "superposition principle," which states that total shrinkage is equal to drying shrinkage plus autogenous shrinkage, there are those in the academic community who believe that drying shrinkage and autogenous shrinkage are not dependent on one another. The literature [108] also pointed out that the water loss of concrete during the drying process affects the hydration process, as well as the pore structure and autogenous shrinkage of concrete, which will also be affected. This was mentioned in the context of the process of drying the concrete.

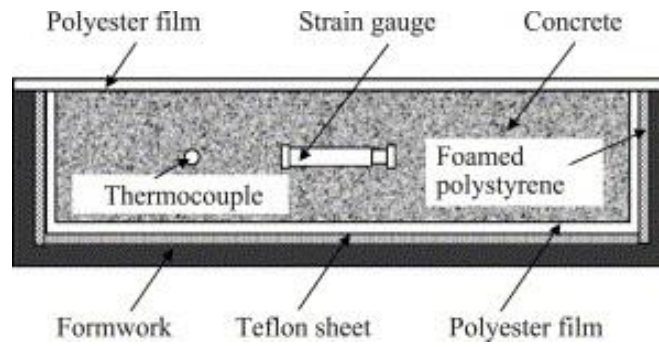


Fig 2.11 Outline of specimen for shrinkage test.[108]

It is clear that the drying shrinkage and autogenous shrinkage of concrete may have interactive effects, and the concept of "superposition principle" as it is currently understood is not fully developed. The drying shrinkage test results are not separated from the autogenous shrinkage for the sake of convenience. Instead, the drying shrinkage test results and the autogenous shrinkage test results are combined for comprehensive consideration. This is because the drying shrinkage deformation and the autogenous shrinkage deformation both have similar effects on engineering..

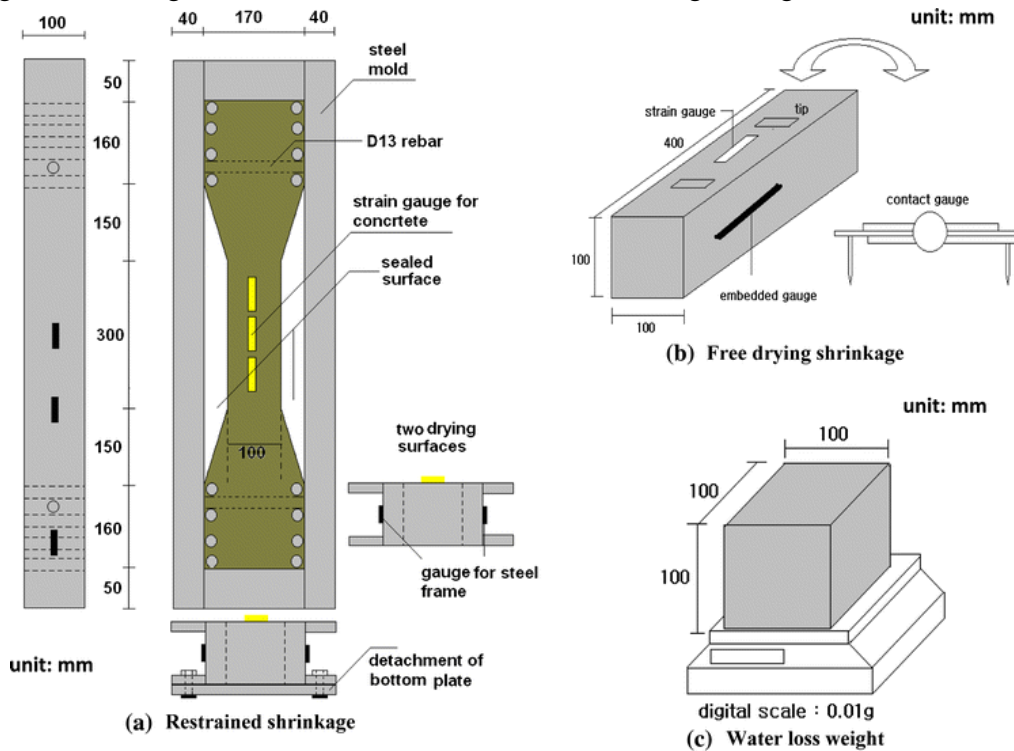


Fig 2.12 Test equipment for shrinkage [109]

(3) Drying shrinkage calculation model

Currently, the empirical models of drying shrinkage are rich in variety, come in a variety of forms, and involve many different factors. These models are based on experiments. Among these models, the CEB series model, the ACI model, and the Wang Tiemeng model, among others, express concrete drying shrinkage as the product of several sub-items. These models primarily take into consideration the influence of factors such as compressive strength, cement type, relative humidity, component size, maintenance situation, relative humidity, reinforcement, and so on.

The Bazant-Panula model takes the form of adding several terms and focuses on the analysis of the

effects of compressive strength, relative humidity, concrete composition, and member size. This model was developed in the 1970s. The product and sum models are combined in the GL2000 model as well as in the Sakata model, and the model is finally expressed as the final shrinkage multiplied by the time function. In terms of the mechanism model, the calculation methods of the theoretical model of concrete shrinkage include the Mori-Tanaka method, the self-consistent method, the Neville formula value method, the sparse method, and so on [103]. These methods are based on the meso-mechanical method of composite materials and the Eshelby equivalent inclusion theory. [103] Other calculation methods include the sparse method.

The drying shrinkage model presented earlier is most commonly used for standard concrete or high-performance concrete. In most cases, the amount of drying shrinkage caused by recycled concrete will increase when recycled aggregate is added to the mix. On the basis of the empirical model for drying shrinkage, the influence of characteristic parameters such as the replacement rate of recycled aggregate should be taken into consideration, and the fitting is appropriate for the drying of recycled aggregate concrete. A contracted computational model.

Comparatively speaking, the structure of naturally occurring aggregate is simpler than that of recycled aggregate. Concrete made from recycled aggregate is a multi-component material that typically consists of new cement paste, sand, and recycled mortar. Not only will the old mortar produce drying shrinkage due to its own water absorption, but also its lower elastic modulus will weaken the overall shrinkage constraint of recycled aggregate. This is because the old mortar has a lower water absorption rate. As a result, it is necessary to combine the performance characteristics of recycled aggregates, further investigate the mechanism of action of recycled aggregates, and improve the theoretical research on drying shrinkage of recycled concrete. These three steps are all necessary.

2.3 Research state of static and dynamic modulus in concrete

As was mentioned in the introduction, the Static Modulus of Elasticity and the Dynamic Modulus of Elasticity are not identical to one another. In a study that was conducted in 2008 by John S. Popovics [110] from the University of Illinois, a number of empirical correlations were discovered between the Static Modulus, E , and the Dynamic Modulus, E_d . Based on a large sample of concrete specimens ranging in compressive strengths from 24 to 161 MPa, he devised the following equation to describe the relationship between the two variables.

In addition to determining a connection between E and E_d , Popovics looked into the possibility of a connection between the E_d that is generated by UPV and the E_d that is generated by the resonant frequency approach. Figure 2-1 presents a comparison of the outcomes of these tests on paste cylinders and concrete cylinders. The paste specimens were found to have higher Poisson's Ratio values than the concrete ones.

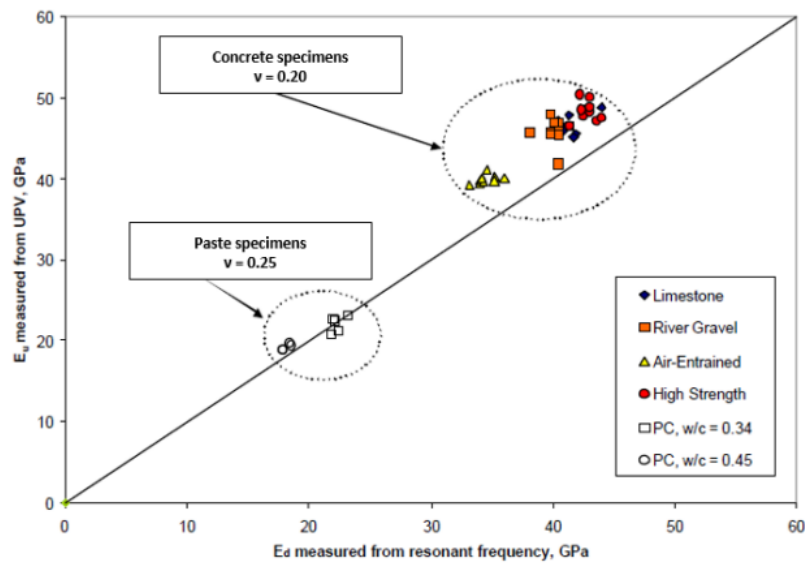


Fig 2.13 Comparison of UPV and resonant frequency analysis [110]

The preceding graph demonstrates that the E_d value obtained by calculating it with UPV yielded a larger value than the E_d value obtained by calculating it with the resonant frequency approach. According to Popovics, the longitudinal resonant frequency approach, when applied to cylindrical concrete specimens, produced the findings that were the least accurate of all the resonant frequency methods.

The difference between the dynamic and static moduli of concrete may be attributable, in part, to the composite composition of concrete. According to Popovics, the static and dynamic moduli in composite components each have their own unique mixing behaviors. This explains why the dynamic modulus is invariably greater than the static modulus in any given situation. According to Popovics, the difference between these moduli values could not be found in any of the specimen samples that were taken from paste because it is a significantly more homogeneous substance.

Chavhan and Vyawahare [111] from the B.N. College of Engineering in Maharashtra, India, used both the UPV approach and the resonant frequency method to illustrate the link between E and E_d for a variety of Self-Compacting Concrete mixtures in 2015. They did this by using the UPV approach to calculate the resonant frequency and the resonant frequency method to calculate the UPV. By contrasting the outcomes of the static modulus tests, they found a correlation between the two variables as follows:

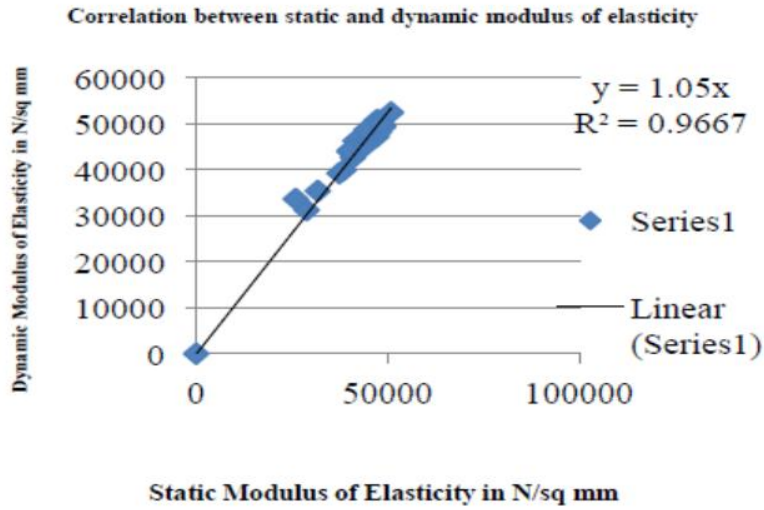


Fig 2.14 Correlation of dynamic and static modulus [111]

According to Chavhan and Vyawahare's [111] research, the difference between the Static Modulus E and the Dynamic Modulus E_d was approximately five percent. In addition to this, they found that there is a linear connection between E and E_d , which can be seen in Figure. This was found to be the case for high-strength SCC.

In the research that Salman and Al-Amawee presented in 2010, they discovered that there is a linear association between E and E_d in concrete mixtures of both standard and high strength. The transverse impact resonance method was utilized in the analysis in order to compute the Dynamic Modulus. In addition to the correlation that was found between E and E_d , another link, this one between E_d and the compressive strength, f_c , was discovered. This connection is depicted graphically for concrete with normal strength in figure [112]. The various mixtures that were utilized for the investigation are detailed in the caption.

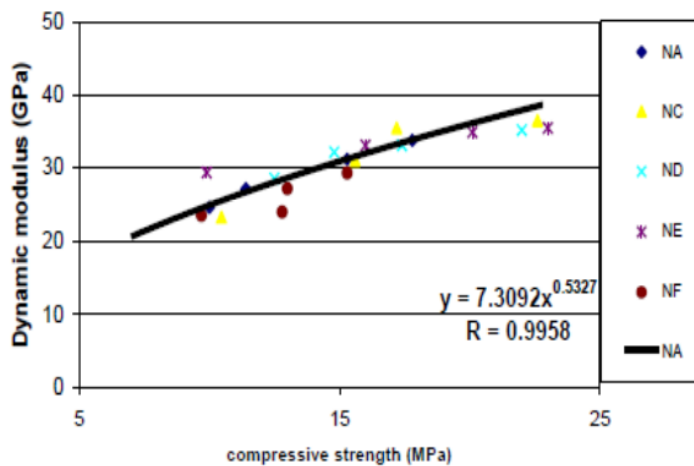


Fig 2.15 Relationship of dynamic and compressive strength [112]

According to investigations that were conducted in the past, the relationship that exists between the Static Modulus of Elasticity and the Dynamic Modulus of Elasticity is linear; however, the slope of

the linear relationship can change. Because concrete with larger particles has a higher strength, the linear connection between E and E_d could potentially be altered as a result. The type of concrete mix used is another factor that can affect this relationship. Self-compacting concrete, in comparison to other standard concrete mixes, produced a variety of empirical connections between E and E_d .

In order to ensure the reliability of Dynamic Modulus tests like UPV and resonant frequency wave techniques, it is necessary to have an understanding of this linear connection. These methods, as opposed to the Static Modulus test, can save both time and money, and they will continue to play an important role in non-destructive testing of concrete structures as long as the connection between the two is understood.

In this particular research endeavor, the Dynamic Modulus was determined by conducting resonance frequency analysis. The non-destructive testing method that utilizes resonance frequencies to evaluate the properties of the material is a technology that was developed relatively recently. The resonant frequencies of vibration are influenced, in part, by the density of the material as well as its dynamic modulus of elasticity. In order to determine the frequencies at which concrete specimens exhibit resonance, the specimens must first be stimulated in either the longitudinal, transverse, or torsional modes, and then the free vibrations that result must be detected [113].

The frequencies known as resonant frequencies are those at which waves combine constructively after reflecting off the ends of specimens [114]. The impulse force and acceleration are initially measured in the time domain, and then the Fast Fourier Transform is used to convert the values to the frequency domain (FFT). After that, the system that collects the data generates and shows the frequency response functions (FRF). After that, the FRFs can be plugged into a formula to determine the resonant frequency [115].

The flexural resonant frequencies are determined, in part, by the boundary conditions of the specimen as well as the size of the specimens. These parameters need to be maintained at a constant level throughout the entirety of the experimental method in order to reduce error and bias. ASTM identifies two techniques for determining resonant frequencies: the forced resonance technique and the impact resonance method. Both of these techniques use a resonance that is induced by an external force. The impact resonance methodology was utilized for this study.

The size of the specimens and the location of the impact point on the specimen both play a role in the accuracy of the measurement of the fundamental resonance frequency [115]. This frequency can be measured using transverse, longitudinal, or torsional vibrations in the impact, or impulse resonance frequency technique. It's possible that the boundary conditions of the specimens will change depending on which direction you go. The different boundary conditions that apply to each of these orientations are depicted in the figure.

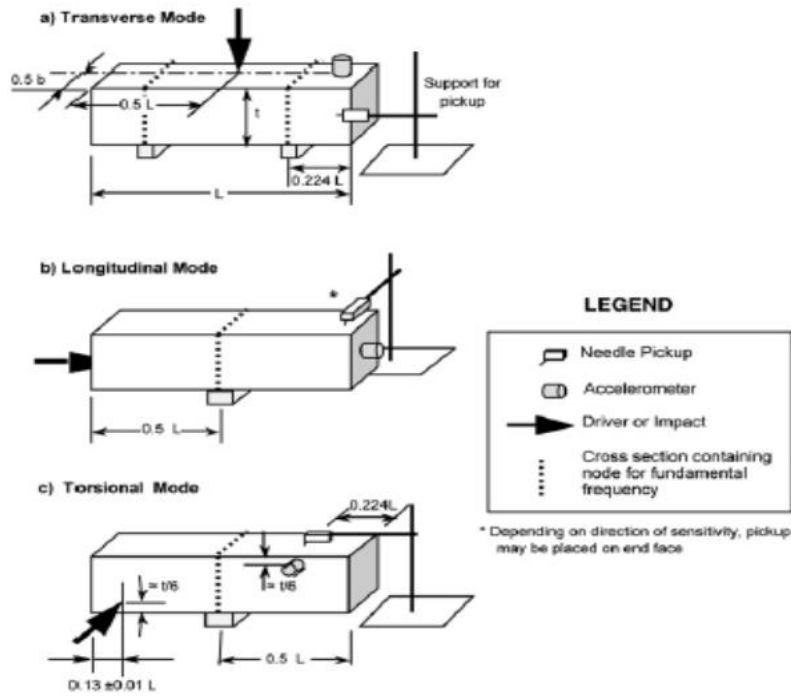


Fig 2.16 Boundary conditions for impact resonance [116]

The fundamental arrangement and configuration of the impact resonance test consists of coupling both an impact hammer and an accelerometer to a signal conditioner. This is done in order to measure the impact resonance. The data acquisition hardware is connected to the signal conditioner, which is responsible for converting the analog signals into their digital equivalents. The measuring signals can have their strength increased by the signal conditioner if that turns out to be necessary [113]. The impact resonance test's fundamental setup and configuration are depicted in the figure below.

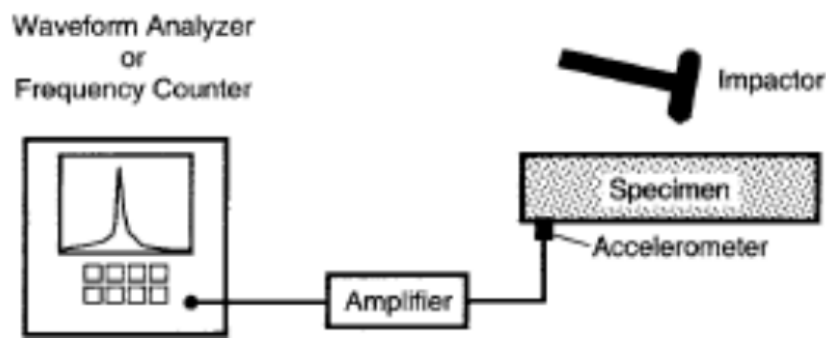


Fig 2.17 Impact resonance equipment and configuration [116]

The position of the impact hammer and the direction in which it will impact the specimen are determined by the boundary conditions and mode directions of the specimen.

In this particular research endeavor, the Dynamic Modulus was determined by employing transverse resonant frequencies in the calculation. The equation that must be used to determine E_d based on transverse fundamental resonant frequencies is provided by JIS.

The Impact Resonance Frequency Method has been shown to be a reliable method for determining various characteristics in concrete specimens. [Case in point:] [Case in point:] However, there are a variety of factors that could potentially distort or otherwise affect the results of the test. In order to obtain results from the experiment that can be relied upon, the ASTM Standard for Resonant Frequencies of Concrete Specimens must be adhered to.

According to a study that was published in the KSCE Journal of Engineering, the conditions under which concrete was cured had very little impact on the frequencies that were generated by resonance. It was found that the fundamental resonant frequency of specimens that were cured in wet conditions was slightly higher than that of specimens that were cured in air dry conditions at any given time. As a direct consequence of this, the Dynamic Modulus of the specimens increased [114].

The amounts of each component in the mixture have the potential to have an effect on both the fundamental resonance frequency and the subsequent dynamic modulus. The findings are also susceptible to being impacted by the characteristics of the aggregate. The size of the specimen is another important factor to take into consideration [117].

However, despite its many advantages and the ease with which it can be applied to concrete samples, the Impact Resonant Frequency Method does have a few significant limitations. In the impact test, it is common practice to use miniature cylinders or prisms made of concrete. The frequency findings that were obtained on these specimens may have significant differences from those that were obtained from in situ structures in the field. This is because of the boundary conditions. Even though efforts are made to lessen the impact of these boundary conditions, it is inevitable that they will have some kind of effect on the fundamental resonant frequencies that are discovered [117].

The second major drawback of the technique is that it does not provide the necessary equations to calculate the dynamic modulus. Formulas include correction variables that are dependant on the shape of the specimen being measured. These shape factors are only available for cylinders and prisms; they cannot be used for any other complicated form and do not require any complex correction factor calculation.

The Impact Resonance Frequency Method is a reliable method for calculating the Dynamic Young's Modulus, in addition to other concrete characteristics, despite the drawbacks that are associated with the method. This method can also be utilized to investigate the deterioration of concrete that has been subjected to alternating periods of freezing and thawing. In some of the research that has been done on the topic, this method has also been utilized to identify concrete damage and degradation caused by fire.

3.4 The Current State of Research Regarding Cement Porosity

Porosity, pore gradation, fractal dimension, and pore morphology are the primary components that make up the pore structure of cement-based materials. Other components include pore volume. Pore sizes in cement-based composites can range from a few angstroms (A), tens of angstroms (A), hundreds of angstroms (A), to several um or even tens um. These include air bubbles that are brought on by insufficient vibration during the molding process, capillary pores and gel pores in the cement paste, pores at the contact, and micro-cracks that are brought on by drying shrinkage and temperature changes in the cement paste. A significant component of the microscopic structure. According to where they are located in concrete, pores are classified into one of three categories: those that are found in the cement stone, those that are found in the aggregate, and contact pores that are found at the interface

between the cement stone and the aggregate. Every variety of pore has its own distinct characteristics, as well as unique factors that contribute to its development. Additionally, pores of varying sizes each serve a unique purpose in the materials that are based on cement.

Porosity, pore morphology, pore size distribution, pore state, and their testing and evaluation have all become important contents of scientific research on concrete materials in recent years. Pore size distribution has also become increasingly important. At the sixth International Conference on Cement Chemistry, Kondo Renichi and Daemon Masaki presented a proposal to classify the pores in cement stone into the following four categories:

(1) The inner pores of gel microcrystals have a pore radius of less than 0.6 nm, and the pores are interlayer water. Interlayer water pores are the smallest pores possible and have the highest energy level. This pore is in the same category as Brunauer's ultra-micropore (as determined by the water-saturated method test), Mikhail's small inner pore (as determined by the water-saturated method test), and Feldman's interlayer pore (as determined by the water-saturated method test) (water adsorption and helium adsorption method test).

(2) The gel intercrystallite pores have a pore radius of approximately 0.6-1.6 nm, according to the results of tests using nitrogen and methanol adsorption methods.

(3) Pores between gel particles: The mercury intrusion method was used to test, and the pore radius was approximately 1.6-100 nm, which can also be referred to as transition pores. These pores had an effect on the reversible dry shrinkage. This pore is of the same type as Brunauer's submicron pore, and Mikhail employs the same testing method and utilizes the same definition for it.

(4) Capillary pores: all of these pores were tested using the mercury intrusion method, and the pore radius was found to be greater than 100 nm.

In 1973, Wu Zhongwei proposed the concept of pore class division and sub-porosity in concrete, along with the factors that influence these characteristics. It is possible to classify the pores in concrete as either harmless (less than 20 nanometers in diameter) or less harmful (greater than 20 nanometers in diameter) depending on the effect that the different pore diameters have on the performance of the concrete. 20-50 nm), harmful pore level (50-200 nm), and harmful pore level (>200 nm), and proposed that the performance of concrete can be significantly improved by increasing the macropores below 50 nm and reducing the pores above 100 nm.

Mehta P.K. and colleagues demonstrated in 1997 that pores smaller than 132 nm had little impact on the strength and impermeability of concrete. Based on this research, Mehta classified pores into four grades: 4.5 nm, 4.5-50 nm, 50-100 nm, and >100 nm. Mehta also categorized pores according to their size.

In the field of civil engineering, one of the most important design parameters to consider is the compressive strength of concrete. Pore structure is one of the important components in the microstructure of concrete, and it has a significant impact on the macroscopic properties of concrete, such as its permeability and its strength. Pore structure is one of the important components in the microstructure of concrete. The connection between pore structure and strength has been the subject of a significant amount of investigation in a number of studies.

At first, many researchers believed that porosity was the only factor that should be taken into account when determining the strength uniformity of cement-based materials.

It has been known for a very long time that decreasing the porosity of a solid material typically

results in an increase in that material's strength, particularly the strength of cement-based materials. The frost resistance of concrete is significantly impacted by the presence of porosity. In addition, porosity exerts some influence on the relationship between the compressive strength and the elastic modulus of concrete, in addition to other mechanical properties of the material.

Researchers have learned a great deal more about the relationship between the pore structure of concrete and frost resistance than they have about the relationship between strength and porosity. This is because the practical importance of the durability of cement-based materials has sparked a surge in research activity. However, this does not imply that researchers have not extensively studied the quantitative relationship between strength and porosity; however, the results of the research are not satisfying.

As the investigation continued, it was discovered that the pore size distribution also had a significant impact on the material's overall strength. At the 7th International Conference on Cement Chemistry, Wittmann presented the "concept of porosity," which broadened the research scope of pore structure in concrete to include pore size distribution (also known as pore gradation) and pore morphology. This was accomplished by extending the research scope of pore structure in concrete. It has also been suggested by authorities within the United States that the pore structure is more significant on the macroscopic behavior of concrete than the porosity is.

The experimental determination of porosity parameters has proven to be extremely difficult due to the unique nature of hydration products in cement-based materials, despite the fact that considerable experimental studies have been conducted to characterize the relationship between pore structure characteristics and strength. However, few systematic models of the relationship between pore structure characterization parameters and strength are currently able to go beyond simple expressions. The results of the experiments demonstrate that these models of strength are not accurate enough to be used for strength prediction.

Regarding the connection between the pore volume fractal dimension and the compressive strength of cement-based materials, there is not one single definitive conclusion that can be drawn. Although quite a few experts and academics have carried out a large number of experimental studies on the connection between the fractal dimension of the pore structure of cement-based materials and the compressive strength, the conclusions that have been drawn by these individuals vary, and in some cases, they are even contradictory to one another. It demonstrates that the research on the relationship between the pore volume fractal dimension and the compressive strength of cement-based materials is still in the exploratory stage, and that additional analysis and research are still required at this point. [118-121]

References

- [1] SU Wu. Application analysis of fly ash in building material field [J]. Henan Building Material, 2017(1) : 12 - 13
- [2] European Coal Combustion Products Association . EU statistics: estimate on production [EB/OL]. [2016 - 12 - 31]. <http://www.ecoba.com/ecobaccpprod.html>
- [3] Sato, K., & Fujikawa, T. (2015). Effective use of coal ash as ground materials in Japan. Japanese Geotechnical Society Special Publication, 3(2), 65-70.
- [4] European Coal Combustion Products Association . Utilisation of fly ash in the construction industry and underground mining in Europe(EU 15) in 2016 [EB/OL] . [2016 - 12 - 31] . <http://www.ecoba.com/ecobaccputil.html>.
- [5] ISHIKAWA Y, WU C N, YAJIMAN. Current state and future prospect of CCPs utilization technology in Japan [J]. Journal of the Chinese Ceramic Society, 2010, 38(9) : 1746 - 1752.
- [6] GOLLAKOTAA R K, VOLLI V, SHU C M. Progressiveutilization prospects of coal fly ash: A review [J]. Science of the Total Environment, 2019, 672: 951 - 989.
- [7] Jin, S., Zhao, Z., Jiang, S., Sun, J., Pan, H., & Jiang, L. (2021). Comparison and summary of relevant standards for comprehensive utilization of fly ash at home and abroad. In IOP Conference Series: Earth and Environmental Science (Vol. 621, No. 1, p. 012006). IOP Publishing.
- [8] HUANG Dingguo, WU Yumin, WANG Wenhua. The comprehensive utilization of fly ash in Japan [J]. Clean Coal Technology, 2006, 12(2) : 92 - 95.
- [9] Kimitaka, U. (2005). Roller compacted concrete dam and utilization of fly ash in Japan. k.uji@ecomp.metro-u.ac.jp.
- [10] HUANG Dingguo, WANG Wenhua, WU Yumin. Research and development status of practical fly ash utilization technology in Japan [J]. Coal Processing & Comprehensive Utilization, 2006 (3) : 48 - 49
- [11] Japan Coal Energy Center. Coal ash generation process and application fields [DB/OL]. [2005 - 07 - 01]. http://www.jcoal.or.jp/cctinjapan_en.html.
- [12] TANG Yuxiang, CHEN Wenen. Comparative research on comprehensive utilization of fly ash between China and Japan [J]. Journal of Anhui Agricultural Sciences, 2010, 38(36) : 20852 - 20854.
- [13] United States Environmental Protection Agency. Methodology for evaluating encapsulated beneficial uses of coal combustion residuals [EB/OL]. [2013 - 09 - 30]. <https://www.epa.gov/coalash/methodology-evaluating-encapsulated-beneficial-uses-coal-combustion-residuals>.
- [14] United States Environmental Protection Agency. Coal combustion residual beneficial use evaluation: Fly ash concrete and FGD gypsum wallboard [EB/OL]. [2014 - 02 - 28]. <https://www.epa.gov/coalash/coal-combustion-residual-beneficial-use-evaluation-fly-ash-concrete-and-fgd-gypsum-wallboard>.
- [15] Standardization Administration. Fly ash used for cement and concrete: GB /T 1596—2017 [S]. Beijing: Standards Press of China, 2017.
- [16] LI Wenxin, ZHU Lin. Enlightenment of comprehensive utilization of fly ash in Japan to China [J]. Comprehensive Utilization of Fly Ash, 2010(3) : 52 - 56.
- [17] HUANG Qian. Analysis of development prospects and status quo of comprehensive utilization of fly ash at home and abroad [J]. China Well and Rock Salt, 2011, 42(4) : 41 - 43

- [18] SU Yu, FANG Huafeng. Research on fly ash policy in China [J]. *Clean Coal Technology*, 2016, 22(4): 52 - 55
- [19] Sahbaz O., Oteyaka B., Kelebek S., et al. Separation of unburned carbonaceous matter in bottom ash using Jameson cell [J]. *Separation and Purification Technology*, 2008, 62(1): 103–109.
- [20] Demir U., Yamik A., Kelebek S., et al. Characterization and column flotation of bottom ashes from Tuncbilek power plant [J]. *Fuel*, 2008, 87(6):666-672.
- [21] Emre Altun E., Xiao C., Hwang J.Y., et al. Separation of unburned carbon from fly ash using a concurrent flotation column[J]. *Fuel Processing Technology*, 2009, 90(12):1464-1470.
- [22] Niewiadomska M., Hupka J., Bokotko R., et al. Recovery of coke fines from fly ash by air sparged hydrocyclone flotation[J]. *Fuel*, 1999, 78(2):161-168.
- [23] Y. Xia, Z. Yang, R. Zhang, et al., Enhancement of the surface hydrophobicity of low-rank coal by adsorbing DTAB: an experimental and molecular dynamics simulation study, *Fuel*, 239 (2019), pp. 145-152
- [24] W. Zhang, R. Honaker, Studies on carbon flotation from fly ash, *Fuel Process. Technol.*, 139 (2015), pp. 236-241
- [25] Y. Huang, M. Takaoka, N. Takeda, Removal of unburned carbon from municipal solid waste fly ash by column flotation, *Waste Manag.*, 23 (4) (2003), pp. 307-313
- [26] R. Clayton, G.J. Jameson, E.V. Manlapig, The development and application of the Jameson cell, *Miner. Eng.*, 4 (7–11) (1991), pp. 925-933
- [27] Y. Yan, G.J. Jameson, Application of the Jameson cell technology for algae and phosphorus removal from maturation ponds, *Int. J. Miner. Process.*, 73 (1) (2004), pp. 23-28
- [28] S. Li, D. Lu, X. Chen, et al., Industrial application of a modified pilot-scale Jameson cell for the flotation of spodumene ore in high altitude area, *Powder Technol.*, 320 (2017), pp. 358-361
- [29] M. Uçurum, Influences of Jameson flotation operation variables on the kinetics and recovery of unburned carbon, *Powder Technol.*, 191 (2009), pp. 240-246
- [30] O. Şahbaz, B. Öteyaka, Ş. Kelebek, A. Uçar, U. Demir, Separation of unburned carbonaceous matter in bottom ash using Jameson cell, *Sep. Purif. Technol.*, 62 (2008), pp. 103-109
- [31] G. Li, L. Deng, J. Liu, Y. Cao, H. Zhang, J. Ran, A new technique for removing unburned carbon from coal Fly ash at an industrial scale, *Int. J. Coal Prep. Utilization*, 35 (2015), pp. 273-279
- [32] N.E. Altun, C. Xiao, J.Y. Hwang, Separation of unburned carbon from fly ash using a concurrent flotation column, *Fuel Process. Technol.*, 90 (12) (2009), pp. 1464-1470
- [33] Emre Altun E., Xiao C., Hwang J.Y., et al. Separation of unburned carbon from fly ash using a concurrent flotation column[J]. *Fuel Processing Technology*, 2009, 90(12):1464-1470.
- [34] H. Zhang, J. Liu, Y. Wang, Y. Cao, Z. Ma, X. Li, Cyclonic-static micro-bubble flotation column, *Miner. Eng.*, 45 (2013), pp. 1-3
- [35] G. Li, L. Deng, J. Liu, Y. Cao, H. Zhang, J. Ran, A new technique for removing unburned carbon from coal Fly ash at an industrial scale, *Int. J. Coal Prep. Utilization*, 35 (2015), pp. 273-279
- [36] M. Xu, H. Zhang, C. Liu, Y. Ru, G. Li, Y. Cao, A comparison of removal of unburned carbon from coal fly ash using a traditional flotation cell and a new flotation column, *Physicochem. Prob. Min. Proces.*, 51 (2017), pp. 628-643

- [37] Y.J. Cao, G.S. Li, J.T. Liu, et al., Removal of unburned carbon from fly ash using a cyclonic-static microbubble flotation column, *J. South. Afr. Inst. Min. Metall.*, 112 (10) (2012), pp. 891-896
- [38] Y. Xing, X. Gui, L. Pan, B.E. Pinchasik, Y. Cao, J. Liu, M. Kappl, H.J. Butt, Recent experimental advances for understanding bubble-particle attachment in flotation, *Adv. Colloid Interf. Sci.*, 246 (2017), pp. 105-132
- [39] Y. Xing, M. Xu, X. Gui, Y. Cao, B. Babel, M. Rudolph, S. Weber, M. Kappl, H.J. Butt, The application of atomic force microscopy in mineral flotation, *Adv. Colloid Interf. Sci.*, 256 (2018), pp. 373-392
- [40] J. Drzymala, J.T. Gorke, T.D. Wheelock, A flotation collector for the separation of unburned carbon from Fly ash, *Coal Prep.*, 25 (2005), pp. 67-80
- [41] Y. Huang, M. Takaoka, N. Takeda, Removal of unburned carbon from municipal solid waste fly ash by column flotation, *Waste Manag.*, 23 (4) (2003), pp. 307-313
- [42] A. Walker, T.D. Wheelock, Separation of carbon from fly ash using froth flotation, *Coal Prep.*, 26 (2006), pp. 235-250
- [43] S. Dey, Enhancement in hydrophobicity of low rank coal by surfactants — a critical overview, *Fuel Process. Technol.*, 94 (1) (2012), pp. 151-158
- [44] X. Gui, Y. Xing, T. Wang, et al., Intensification mechanism of oxidized coal flotation by using oxygen-containing collector α -furanacrylic acid, *Powder Technol.*, 305 (2017), pp. 109-116
- [45] T. Harris, T.D. Wheelock, Process conditions for the separation of carbon from Fly ash by froth flotation, *Int. J. Coal Prep. Utilization*, 28 (2008), pp. 133-152
- [46] T.C. Eisele, S.K. Kawatra, Use of froth flotation to remove unburned carbon from fly ash, *Miner. Process. Extr. Metall. Rev.*, 23 (2002), pp. 1-10
- [47] F. Zhou, C. Yan, H. Wang, S. Zhou, H. Liang, The result of surfactants on froth flotation of unburned carbon from coal fly ash, *Fuel*, 190 (2017), pp. 182-188
- [48] Japan Concrete Engineering Association: Symposium on Promotion of Recycled Aggregate for Concrete, pp 102 - 170, Japan Concrete Engineering Association (2005)
- [49] Environmental Business Line <http://www.kankyo-business.jp/>
- [50] A. M. Neville, *Concrete: Neville's Insights and Issues* (London, ICE, 2006).
- [51] E. K. Lauritzen, Ed., *Demolition and reuse of concrete and masonry*, Proc. Third Int. RILEM Symp. on demolition and Reuse of Concrete and Masonry, Odense, Denmark, 534 pp. (London, E & FN Spon, 1994).
- [52] ACI 221R-89, Guide for use of normal weight aggregates in concrete, *ACI Manual of Concrete Practice, Part 1: Material and General Properties of Concrete*, 23 pp. (Detroit, Michigan, 1994).
- [53] B. Gonzalesn Fonteboa et al., Shear friction capacity of recycled concretes, *Materiales de Construcción*, 60, No. 299, pp. 53-67.
- [54] P. E. Regan et al., The influence of aggregate type on the shear resistance of reinforced concrete, *The structural Engineer*, 6 Dec., pp. 27-32(2005).
- [55] A. Peyvandi et al.; Recycled glass concrete, *Concrete International*, 35, January 2013, pp. 29-32.
- [56] Kho Pin Verian, Warda Ashraf, Yizheng Cao. Properties of recycled concrete aggregate and their influence in new concrete production. *Resources, Conservation and Recycling*. Volume 133, June 2018, Pages 30-49.

- [57] Verian, Kho & Jain, Jitendra & Whiting, Nancy & Olek, Jan & Snyder, Mark. (2013). Using Recycled Concrete as Aggregate in Concrete Pavements to Reduce Materials Cost. 10.5703/1288284315220.
- [58] Tangchirapat, W., Buranasing, R., & Jaturapitakkul, C. (2010). Use of high fineness of fly ash to improve properties of recycled aggregate concrete. *Journal of Materials in Civil Engineering*, 22(6), 565-571.
- [59] C.S. Poon, Z.H. Shui, L. Lam, H. Fok, S.C. Kou, Influence of moisture states of natural and recycled aggregates on the slump and compressive strength of concrete, *Cem. Concr. Res.*, 34 (no. 1) (2004), pp. 31-36
- [60] M.G. Beltrán, A. Barbudo, F. Agrela, A.P. Galvin, J.R. Jimenez, Effect of cement addition on the properties of recycled concretes to reach control concretes strengths, *J. Clean Prod.*, 79 (2014), pp. 124-133
- [61] Tondur, E., Thompson, W. G., Whitlock, D. R., Bittner, J. D., & Vasiliauskas, A. (1996). Commercial separation of unburned carbon from fly ash. *Mining engineering*, 48.
- [62] Chelgani, S. C., & Asimi Neisiani, A. (2022). Electrostatic Separation. In S. C. Chelgani & A. Asimi Neisiani (Eds.), *Dry Mineral Processing* (pp. 91–123). Springer International Publishing. https://doi.org/10.1007/978-3-030-93750-8_4
- [63] Ciccu, R., Ghiani, M., Muntoni, A., Serici, A., Peretti, R., Zucca, A., ... & Quattroni, G. (1999, October). The Italian approach to the problem of fly ash. In *Proceedings of the International Ash Utilization Symposium* (pp. 18-20).
- [64] Binks B. P. Particles as surfactants similarities and differences[J]. *Current Opinion in Colloid & Interface Science*, 2002, 7(1):21-41.
- [65] Xu Q. Y., Nakajima M., Binks B. P. Preparation of particle-stabilized oil-in-water emulsions with the microchannel emulsification method[J]. *Colloids and Surfaces A: Physicochemical and Engineering Aspects*, 2005, 262(1-3):94-100.
- [66] Binks B. P., Dong J. Emulsions and equilibrium phase behaviour in silicone oil + water + nonionic surfactant mixtures[J]. *Colloids and Surfaces A: Physicochemical and Engineering Aspects*, 1998, 132(2): 289-301.
- [67] Horozov T. S., Aveyard R., Clint J. H., et al. Particle zips: vertical emulsion films with particle monolayers at their surfaces[J]. *Langmuir*, 2005, 21(6):2330-2341. [68] Nushtaeva A. V., Kruglyakov P. M. Capillary pressure in a thinning emulsion film stabilised by spherical solid particles[J]. *Mendelev Communications*, 2001, 11(6):235-236.
- [69] Kaptay G. Interfacial criteria for stabilization of liquid foams by solid particles[J]. *Colloids Surface A*, 2003, 230(1-3): 67-80.
- [70] Kruglyakov P. M., Nushtayeva A. V. Phase inversion in emulsions stabilized by solid particles[J]. *Advances Colloid Interface Science*, 2004, 108-109:151-158.
- [71] Kaptay G. On the equation of the maximum capillary pressure induced by solid particles to stabilize emulsions and foams and on the emulsion stability diagrams[J]. *Colloids Surface A*, 2006, 282-283:387-401.
- [72] Karakasheva S. I., Ozdemirb O., Hamptonc M. A. Formation and stability of foams stabilized by fine particles with similar size, contact angle and different shapes[J]. *Colloids and Surfaces A: Physicochemical and Engineering Aspects*, 2011, 382(1-3):132-138

- [73] Liu Q., Zhang S., Sun D. Aqueous foams stabilized by Hexylamine-modified Laponite particles[J]. *Colloid Surface A*, 2009, 338(1-3):40-46.
- [74] Li C., Liu Q., Mei Z. Pickering emulsions stabilized by paraffin wax and Laponite clay particles[J]. *Journal of Colloid and Interface Science*, 2009, 336(1):314-321.
- [75] Liu Q., Luan L., Sun D. Aqueous foam stabilized by plate-like particles in the presence of sodium butyrate[J]. *Journal of Colloid and Interface Science*, 2010, 343(1):87-93.
- [76] Liu Q., Zhang S., Sun D. Foams stabilized by Laponite nanoparticles and alkylammonium bromides with different alkyl chain lengths[J]. *Colloid Surface A*, 2010, 355(1-3):151-157.
- [77] Britan A., Liverts M., Ben-Dor G., et al. The effect of fine particles on the drainage and coarsening of foam[J]. *Colloids and Surfaces A: Physicochemical and Engineering Aspects*, 2009, 344(1):15-23.
- [78] Dippenaar A. The destabilization of froth by solids. I. The mechanism of film rupture [J]. *International Journal of Mineral Processing*, 1982, 9(1): 1-14.
- [79] Johansson G., Pugh R. J. The influence of particle size and hydrophobicity on the stability of mineralized froth [J]. *International Journal of Mineral Processing*, 1992, 34(1):1-21.
- [80] Subrahmanyam T. V., Forssberg E. Froth stability, particle entrainment and drainage in flotation — A review[J]. *International Journal of Mineral Processing*, 1988, 23(1): 33-53.
- [81] Ata S., Ahmed N., Jameson G. J. A study of bubble coalescence in flotation froths[J]. *International Journal of Mineral Processing*, 2003, 72(1-4):255-266.
- [82] Aktas Z., Cilliers J. J., Banford A. W. Dynamic froth stability: Particle size, airflow rate and conditioning time effects[J]. *International Journal of Mineral Processing*, 2008, 87(1):65-71.
- [83] Barbian N., Ventura-Medina E., Cilliers J. J. Dynamic froth stability in froth flotation[J]. *Mineral Engineering*, 2003, 16(11): 1111-1116.
- [84] Barbian N., Hadler K., Ventura-Medina E., et al. Froth stability column: linking froth stability and flotation performance[J]. *Mineral Engineering*, 2005, 18(3): 317-324.
- [85] Takahashi Taiichi, Abe Michihiko. Current status and future of application of waste concrete aggregates.
- [86] Japanese Government-Ministry of Land Infrastructure and Transport. Japan environment white paper. Ministry of Land Infrastructure and Transport, Japanese Government, 2006
- [87] Vivian. W Y Tam. Comparing the implementation of concrete recycling in the Australian and Japanese construction industries. *J Cleaner Production*, 2009: 688
- [88] C.F. Hendriks, H.S. Pietersen. Sustainable raw materials: construction and demolition waste. Cachan Cedex France: RILEM Publication, 2000
- [89] RILEM TC 121-DRG. Specifications for concrete with recycled aggregates. *Mater Struct*, 1994, 27: 557
- [90] Gilpin Robinson Jr R, Menzie D W, Hyun H. Recycling of construction debris as aggregate in the Mid-Atlantic Region, USA. *Resource Conserv Recycl*, 2004, 42(3): 275
- [91] Akash Rao, Kumar N Jha, Sudhir Mishra. Use of aggregates from recycled construction and demolition waste in concrete. *Resources Conserv Recycl*, 2007, 50(1): 71
- [92] Huang Guoxing, Hui Rongyan, Wang Xiujun Creep and shrinkage of concrete [M]. Beijing: China Electric Power Press, 2012.
- [93] KOVLER K, ZHUTOvsKY s. Overview and future trends of shrinkage research [J]. *ACI* [94]

Materials Journal,2006,39:827-847.

[95] Gribniak, Viktor & Kaklauskas, Gintaris & Bacinskas, Darius. (2008). Shrinkage in reinforced concrete structures: A computational aspect. JOURNAL OF CIVIL ENGINEERING AND MANAGEMENT. 14. 49-60. 10.3846/1392-3730.2008.14.49-60.

[96] Weng Jiarui. Experimental research on drying shrinkage and autogenous shrinkage of high performance concrete [D]. Fuzhou: Fuzhou University Master's Thesis, 2006.

[97] ISHAI O. The time-dependent deformational behavior of cement paste[C mortar and concrete. Proceedings of conference on structure of concrete and its behavior under load.Cement and Concrete Association,London:1968:345-364.

[98] WITTMANN F H.Surface tension, shrinkage and strength of hardened cement paste. Materials & Structures,1968(6):547-552.

[99] JLUZIO G D, CUSATIS G Hygro-thermo-chemical modeling of high performance concrete. Theory[J]. Cement & Concrete Composites, 2009,31: 301-308.

[100] R. Zana Introduction to surfactants and surfactant self-assemblies R. Zana (Ed.), Dynamics of Surfactant Self-Assemblies, Taylor and Francis, Boca Raton, Florida (2005), pp. 1-35

[101] Sakata K. A Study on Moisture Diffusion in Drying and Drying Shrinkage of Concrete[J]. Cem. Con cr.Res,1983,13(3): 164-170.

[102] Wong s F, Wee T H . Study of Water Movement in Concrete[J].Magazine of ConcreteResearch ,2001,53(3): 205-220.

[103] DOMINGO C A.Creep and shrinkage of recycled aggregate concrete[J].Construction andBuilding Materials, 2009,23:2545-2553.

[104] KHATIB J M.Properties of concrete incorporating fine recycled aggregate [JJ.Cement andConcrete Research,2005,35(4):763-769.

[105] Gao Xiaojian, Yang Yingzi, Deng Hongwei.Influence of Mineral Admixtures on Shrinkage Distribution of High Performance Concrete[J].Journal of Harbin Engineering University.2010,31(09):1185-1190.

[106] Zhang Jian, Du. Hui, Zhang Cai, etc. Effects of mineral admixtures and recycled aggregates on the shrinkage properties of concrete[J.Qingdao Science.Journal of University of Technology,2009(30):145-153.

[107] Cao Yong, Liu Bingkang, Xia Qin.Recycled Concrete: Experimental Research on Drying Shrinkage[J].Testing and Testing,2009,(01):47-49

[108] YANG Y,RYOICHI S, KENJI K.Autogenous shrinkage of high-strength concrete containing silica fume under drying at early ages[J]. Cement and Concrete Research, 2005,35:449-456.

[109] Park, S. S., Kwon, S.-J., & Song, H.-W. (2011). Analysis technique for restrained shrinkage of concrete containing chlorides. Materials and Structures, 44(2), 475–486. <https://doi.org/10.1617/s11527-010-9642-4>

[110] Popovics, J. (2008). A Study of Static and Dynamic Modulus of Elasticity of Concrete. American Concrete Institute - Concrete Research Council, Urbana, IL

[111] Chavhan, P. and Vyawahare, M. (2015). Correlation of Static and Dynamic modulus of Elasticity for Different SCC Mixes. International Journal on Recent and Innovation Trends in Computing and Communication.

- [112] Salman, M. and Al-Amawee, A. (2006). The Ratio between Static and Dynamic Modulus of Elasticity in Normal and High Strength Concrete. *Journal of Engineering and Development*.
- [113] Gudmarsson, A. (2014). Resonance Testing of Asphalt Concrete.
- [114] Lee, K., Kim, D., and Kim, J. (1997). Determination of dynamic Young's modulus of concrete at early ages by impact resonance test. *KSCE Journal of Civil Engineering*.
- [115] Plachy, T., Padevet, P., and Polak, M. (n.d.). Comparison of Two Experimental Techniques for Determination of Young's Modulus of Concrete Specimens. *Recent Advances in Applied and Theoretical Mechanics*.
- [116] ASTM C215-14, Standard Test Method for Fundamental Transverse, Longitudinal, and Torsional Resonant Frequencies of Concrete Specimens, ASTM International, West Conshohocken, PA, 2014, www.astm.org
- [117] Lamond, J. F., & Klieger, P. (1994). Making and Curing Concrete Specimens. *ASTM SPECIAL TECHNICAL PUBLICATION*, 169, 71-76.
- [118] Gonzalez-Corominas, Andreu, Miren Etxeberria, and Chi Sun Poon. "Influence of steam curing on the pore structures and mechanical properties of fly-ash high performance concrete prepared with recycled aggregates." *Cement and Concrete Composites* 71 (2016): 77-84.
- [119] Mehta, P. Kumar, and Paulo JM Monteiro. *Concrete microstructure, properties and materials*. 2017.
- [120] WU ZW, LIAN H. Z. "High Performance Concrete." Beijing: China Railway Publication House (1999).
- [121] Ho, Hsin-Lung, et al. "Pore-structures and durability of concrete containing pre-coated fine recycled mixed aggregates using pozzolan and polyvinyl alcohol materials." *Construction and Building Materials* 160 (2018): 278-292.

CHAPTER 2: PREVIOUS LITERATURE REVIEW

Chapter 3

RESEARCH METHOD

3.1 Flotation Method Experiment

In the first experiment, which was conducted in order to design a base model for an unburned coal removal device, we investigated the effects of bubble diameter and the circumstances on the removal of unburned carbon. The subsequent experiments were carried out in a step-by-step manner, progressing from device I to device III.

Table 3.1 displays the various physicochemical characteristics of fly ash generated by two different thermal power plants.

Fly ash types a-2, a-3, a-5, and a-6 were matched to JIS A 6201 type II; types a-4, b-1, b-2, and b-3 were matched to type III; type a-1 was matched to type IV; and type b-4 was matched to no stated type due to its high LOI.

Table 3.1. Physical characteristics of fly ash.

Fly Ash	LOI (%)	Density (g/cm ³)	Specific Surface Area(cm ² /g)
a-1	0.72	2.30	1510
a-2	0.42	2.27	2970
a-3	1.30	2.29	2790
a-4	6.99	2.30	4640
a-5	3.86	2.24	4250
a-6	2.22	2.25	4200
b-a	5.87	2.12	4590
b-2	7.39	2.27	4890
b-3	7.85	2.37	4620
b-4	12.92	2.24	4890
c	7.25	2.3	5560
d	9.85	2.11	6060
e	2.81	2.11	3470
f	3.36	2.26	3280

Experiment I was designed to determine the extent to which bubble diameter has an effect on the results. Fly ashes from the 'a' series were used in device I, which had a capacity of 80 liters, and two general-purpose air diffusers measuring 70 mm by L200 mm were mounted to the flotation device at the bottom. Device I had a capacity of 80 liters (Figure 3.1 is based on the equipment used for coal flotation). The air was moved about at a rotation speed of 19 revolutions per minute, and the air diffuser discharged 165 liters of air per minute worth of air into the room.

The bubbles typically had a diameter of two hundred micrometers. The foaming agent consisted of 0.3 percent pine oil and included 5.0 percent kerosene. The unburned carbon collector was kerosene. The system used aeration from the air diffuser to float fly ash that had a significant amount of unburned carbon close to the water's surface. Next, the material that was floating (foam ash) was removed, and the fly ash that sunk to the bottom after standing (tail ash) was collected. The experiment was carried out in the manner that is described below.

After adding the additives and the tap water to the apparatus and giving it a swirl for five minutes, the fly ash was added to create a slurry with a weight percentage of twenty percent and the foam ash was recovered after an additional five minutes of stirring. Before the tail ash could be evaluated for its LOI, it had to be collected from the bottom of the device and then dried in an electric furnace at 105

degrees Celsius for twenty-four hours. The LOI was measured by JIS A6201 [1], and using that value, we were able to compute the unburned carbon removal rates for each kind of ash..



Figure 3.1. The flotation device of the air diffuser.

In Experiment II, the impact of bubble diameter was investigated using 'b' series fly ashes, which had a larger LOI than 'a' series fly ashes. Additionally, 'b' series fly ashes were used. In device II, the fly ash was put into a plastic container that held 2 liters (Figure 3.2). In order to forestall the formation of precipitation, we made use of a miniature mixer with a rotation speed of 250 rpm as well as a high-speed rotary blade microbubble generator.

On average, the diameter of the microbubbles was around 40 meters. Because of the significant improvement in the separation performance of unburned carbon from coal fly ash, a slurry consisting of 60 weight percent fly ash and the collector was pre-stirred in a 0.6 liter high-speed mixer before to the flotation process in device II.

The pretreatment step is quite important for the flotation process. The kinetic energy that is lost in the stirred tank due to the absence of preconditioning has the potential to enhance the contact process between mineral particles and flotation chemicals, hence increasing the efficiency of the flotation process [3]. Yu et al. [4] observed that in the process of flotation of coal, high-intensity agitation (greater than 1200 rpm) decreases the kaolinite coating, which results in a higher combustibles recovery rate.

After combining the collection agent and the tap water in the mixer with a rotation speed of 10,000 rpm, swirling the mixture for one minute, adding the foaming agent, and bringing the slurry concentration up to 20 percent by weight, the concentration was increased. After that, the ventilation system was activated, and the floss ash was gathered for a period of ten minutes. In experiment I, the rates of additive addition were exactly the same as they were here. The apparatus was allowed to stand, the tail ash from the bottom of the apparatus was collected and dried, and the LOI was calculated in the same way as it had been in the first experiment.



Figure 3.2. Microbubble generator.

Experiment III was carried out in order to acquire data for the purpose of constructing a device for use in the real world and testing the effectiveness of preprocessing based on the results of device II. The chemical in question was the same fly ash that was used in the device II. In Device III, the fly ash slurry was cycled using a roller pump that had an aperture microbubble generator built right in. This was done to prevent the ash from settling and did not need the use of a stirrer (Figure 3.3). The methodology was the same as in experiment II; the only difference was that the outcomes were evaluated both with and without any prior stirring.





Figure 3.3. Microbubble circulation device.

3.1.1 Concrete Specimen Fabrication

A sample of concrete was made using MFAS in addition to type II fly ash. We used regular Portland cement, crushed stone for the coarse aggregate, and sea sand for the natural fine aggregate. Cement was purchased from a local supplier. The features of raw ash as well as MFA were looked into (Table 3.2). Fly ash was used in lieu of some of the cement in the construction. It was ensured that both the JIS R 5210 [5] and the JIS A 6201 [1] standards were met.

Table 3.2. Properties of FA and MFA.

Type	MFA	Raw Ash
LOI (%)	1.75	13
Density (g/cm ³)	2.33	2.32
Blaine (cm ² /g)	3220	4830

Table 3.1 outlines the quantities of the combination to be used. After mixing the fine aggregate, cement, and fly ash for 30 seconds, water was added and mixed for 60 seconds, followed by the addition of coarse aggregate and further mixing for 60 seconds.

3.1.2 concrete mix

The physicochemical characteristics of the materials used in this investigation are detailed in Table 3.2. Crushed stone was utilized for the coarse aggregate, and ordinary Portland cement was utilized for the production of the cement. Sea sand and recycled fine aggregate were utilized for the production of the fine aggregate (M standard of JIS A 5022), and crushed stone was utilized for the production of the coarse aggregate.

Table 3.2 Materials

Cement	Ordinary Portland	Density 3.16 [g/cm]		C
Water	Tap water	-		W
	Sea sand	Density in oven-dry condition 2.56% [g/cm]	Water absorption 0.76%	S
Fine aggregate	Recycled fine aggregate class M species	Density in oven-dry condition 2.23% [g/cm] Fineness modulus 4.3	Water absorption 7.38%	R
			Solid volume percentage 60.9%	S
Coarse aggregate	Crushed stone	Density in oven-dry condition 2.69% [g/cm] Fineness modulus 6.9	Water absorption 1.41%	G
			Solid volume percentage 56.6%	

3.1.3 Formulation

The formulation is shown in Table 3.3 and Table 3.4. The formulation calls for a unit water amount of 180 kilograms per cubic meter, a unit cement amount of 327 kilograms per cubic meter, a water cement ratio that remains constant at 55 percent and 44 percent, and a replacement rate of regenerated fine aggregate that varies between two levels of 50 and 100 percent. In this experiment, recycled aggregate was exclusively used for fine aggregate, while natural aggregate crushed stone was utilized for coarse aggregate in all of the formulations. The experiment was designed to test the effectiveness of using recycled aggregate for fine aggregate. In terms of the compounding symbols, the formulation denoted by the letter N is the one in which natural aggregate is used for both the coarse and the fine components of the aggregate. This order indicates the replacement rate of the recycled fine aggregate. For example, M50 is a formulation that consists of fifty percent recycled fine aggregate Class M and fifty percent sea sand. The percentage of cement that is being replaced by fly ash is given in this sequence. For example, the N-FA10 formulation consists of replacing cement with 10% fly ash. The compressive strength test was performed in accordance with JIS A 1108, which is known as the "Compressive strength test technique of concrete."

Table 3.3 Mix proportions and compressive strength

W/C (%)	W/B (%)	Unit mass(kg/m ³)							Compressive strength (MPa)		
		Water	Cement	Fly Ash	Fine aggregate	Recycled fine aggregate	Coarse aggregate	7day	28day	91day	
M0-FA0	55	55	180	327	0	832	0	945	16.4	22.25	26.46

						2		
M50-FA0	55		327	0	398	398	15.78	23.03 24.94
M100-FA0	55		327	0	0	765	12.53	18.83 22.97
N-FA10	61		295	33	826	0	15.73	20.79 28.15
M50-FA10	61		295	33	396	396	13.71	18.89 25.19
M100-FA10	61		295	33	0	759	13.62	19.33 25.70
M0-FA20	69		262	65	820	0	12.43	17.97 25.04
M50-FA20	69		262	65	392	392	9.87	15.25 22.55
M100-FA20	69		262	65	0	754	8.21	12.70 17.91
M-FA0	40		450	0	731	0	30.49	37.80 41.67
M50-FA0	40		450	0	350	350	26.67	34.17 40.48
M100-FA0	40		450	0	0	672	25.26	33.91 40.92
M0-FA10	44		405	45	723	0	31.84	41.37 50.42
M50-FA10	44	40	405	45	346	346	27.78	36.71 45.03
M100-FA10	44		405	45	0	665	27.09	34.11 40.40
M0-FA20	50		360	90	716	0	27.63	36.65 46.20
M50-FA20	50		360	90	342	342	25.14	34.09 44.43
M100-FA20	50		360	90	0	658	26.09	34.54 41.43

Table 3.4 Mix proportions.

Type	W/C				Unit (kg/m ³)				
	(%)	C	FA	MFA	S	RSM	RSL	G	RG
N	55	327	-	0	857	-	-	945	-
F15	65	278	49		840	-	-	945	-
F30	79	229	98		824	-	-	945	-
M15	65	278	-	49	842	-	-	945	-
M30	79	229	-	98	828	-	-	945	-
F50M15	65	278	-	49	421	386	-	945	-
F50M30	79	229	-	98	414	380	-	945	-
FL50M15	65	278	-	49	421	-	363	945	-
FL50M30	79	229	-	98	414	-	357	945	-
F100M15	65	278	-	49	0	773	-	945	-
F100M30	79	229	-	98	0	759	-	945	-
FL100M15	65	278	-	49	0	-	727	945	-
FL100M30	79	229	-	98	0	-	714	945	-
C100M15	65	278	-	49	842	-	-	-	885
C100M30	79	229	-	98	828	-	-	-	885

3.2 Fly ash recycled concrete experiment

3.2.1 Mixing of concrete

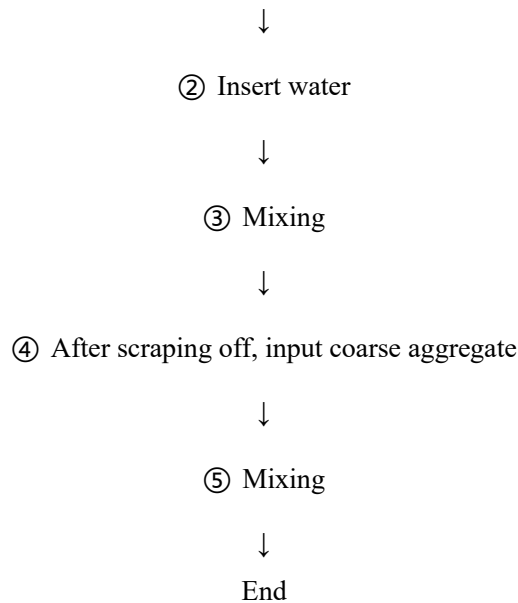
As can be seen in Photo 3.1, the kneading of the concrete was accomplished with the assistance of a mixer machine with a capacity of 60 liters. The following diagram illustrates the mixing conditions:



Photo 3.1 Mixer machine

The mixture was in a 60liter mixer machine, and the mixing amount per time was set to 40 liters. The mixing procedure is shown below.

- ① Fine aggregate and cement are put in,



Test of Slump: The usual Slump test for Hydraulic-Cement Concrete was carried out on the batch that included 50 percent slag, the batch that had 30 percent flyash, and the OPC batch. Due to the very flowable nature of the SCC batch, a slightly modified version of this test was carried out on it. The slump test is an experimental test that is often performed in the field to measure the overall consistency of the new concrete mix as well as the workability of the fresh concrete mixture.

In order to get the most precise findings, it is normally carried out right after the concrete has been mixed. The ASTM Standard for Slump Test was adhered to for each of the individual batches of concrete (ASTM C143, 2010). The newly mixed concrete is pressed into the conventional slump cone (seen in Figure 3.4). The cone is then removed carefully (an interval of 5-7 seconds should pass), and the difference in height is recorded as soon as possible to establish the slump value.

The typical range for measuring slump is anywhere from 2 in. to 7 in., with the lower end of the range resulting in less workability and the higher end of the range resulting in better workability.

The OPC had a drop of 8.25 inches, which suggests that the batch may have been 35 too flowable. This might have led to a drop in the strength of the batch as a whole. An excessive amount of air entraining agent was added to the mixture, which was the primary cause of this significant slump.

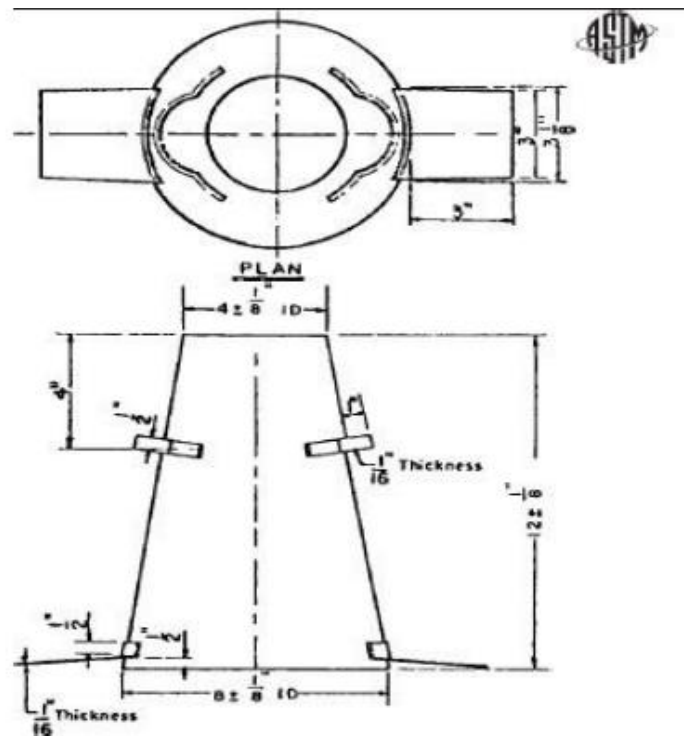


Fig 3.4 Standard slump cone mold (ASTM C143, 2010)

Test for Air Content: The purpose of the air content test is to determine the percentage of air that is contained in freshly mixed concrete, excluding any air that may exist inside voids of aggregate. This is done so that the test can determine how much air is actually present in freshly mixed concrete. The air content that is measured may be affected by a variety of factors, including consolidation methods, exposure, and the homogeneity of air bubbles, amongst others (ASTM C231, 2003). The amount of air present in concrete is significant because it may have a direct bearing on the material's strength and its capacity to withstand the effects of freezing and thawing. Concrete with a smaller amount of air in it often has a greater strength than concrete with a larger amount of air in it, and vice versa.

Type A meters and Type B meters are the two kinds of air content instruments that are often used in the process of determining the air content in newly mixed concrete. A Type B Meter was used in order to accomplish the objectives of this research endeavor. Figure 3.5 provides a schematic representation of the equipment, and Figure 3.6 provides visual representation of the actual apparatus that was used in each of the castings.

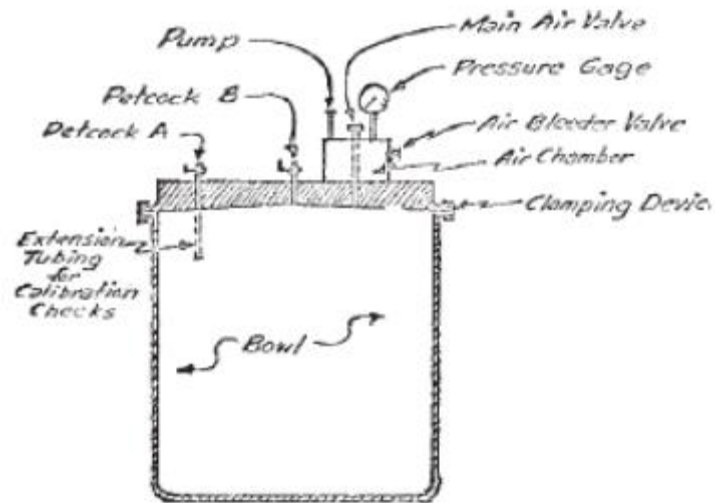


Fig 3.5 Type B air content apparatus (ASTM C231, 2003)

The instrument for measuring the air content was properly calibrated in accordance with the standards of ASTM C231 (ASTM C231, 2003). After that, the newly mixed concrete was poured into the apparatus bowl, and it was rodded and completed in the appropriate manner.

3.2.2 Compression Strength test

For the purpose of establishing the loading load, the compressive strength test was carried out. After curing in water at 20 degrees Celsius for seven days, the test specimen was then cured in air in a thermostatically controlled room before being used in a compressive strength test utilizing a cylinder frame of 100 millimeters in diameter and 200 millimeters in length. After 28 and 91 days of curing, the material's compressive strength was evaluated using the Compressive Strength Test Method for Concrete specified in JIS Standard A 1108.

In order to determine the loading load, the compressive strength of the material at the age of 28 days was determined. Subsequently, the compressive strength of the material at the age of 91 days was measured to determine whether or not there was an increase in the compressive strength of the aged aggregate concrete of long-term age.



Photo 3.2 State of compressive strength test

3.2.3 Drying shrinkage test

On the material that had been aged for 181 days, the drying shrinkage was measured using JIS A 1129 [Methods of measurement for length change of mortar and concrete Part 3: Method using dial gauge]. A test specimen consisting of a cuboid measuring 100 mm on a side, 100 mm on the opposite side, and 400 mm in height was created. The number of specimens needed for each test will be the number that is decided for that test, and there will be a minimum of two specimens needed for tests that evaluate the same condition. During the course of the test, the specimen is to be maintained at the temperature and humidity levels that have been designated for that particular test. In particular, in cases when the temperature and humidity cannot be precisely measured, the temperature must be maintained at 20 degrees Celsius, give or take, and the relative humidity must be maintained at 60 percent, give or take.



Photo 3.3 State of drying specimen in curing room

Method of measurement: the base length is the distance between the inner end faces of the gauge plug. This distance is referred to as the base length. Instructions for putting in the gauge plug. After attaching the gauge plug to the form in advance in order to position it at the center of both end faces of the specimen, the concrete test specimen is created. Alternatively, a tiny hole may be bored into the cured specimen using a drill or something similar.



Photo 3.4 The gauge plug in the specimen

The following is the approach that is used to measure:

- a) At the time of the measurement, the temperature that has been prescribed for each test should be applied to the specimen, the standard scale, and the measuring equipment. The temperature is often set at 20 degrees Celsius, plus or minus 2 degrees, especially when it is not fixed.
- b) Before measuring the length of the specimen, be sure that any foreign matter that has adhered to the gauge plug has been thoroughly removed.
- c) The measuring frame is brought back to the same position it was in when the specimen was being measured.
- d) The contact point of the measuring frame is brought into contact with one of the gauge plugs of the standard ruler. This causes the tip of the spindle of the dial gauge to move along the axis connecting the gauge plugs, the spindle to gradually come out of the dial gauge, and the other gauge plug to become engaged. And make sure you're familiar with the dial gauge's scale. In this instance, you should handle the spindle with care and check to see if the contact portion is comfortable and familiar.
- e) Remove the spindle and carry out step
- d) once again. Next, determine the value that is representative of an average of the second and subsequent measurements, and label this number X_{i1} .
- g) If required, measure the mass of the specimen.
- f) Replace the standard scale with a specimen, perform the same process as in d), e), and take the

average value from the reading of the scale on the dial gauge. Let this value be X_{i2} . In the case of mortar, the weight must be less than 1 kilogram, and the eye size must be less than 0.2 grams or less; in the case of concrete, the weight must be greater than 15 kilograms, and the eye size must be less than 2 grams or less.



Photo 3.5 Drying shrinkage test equipment

The following equation is used to compute the drying shrinkage, and the results are rounded to three significant digits by rounding off.

$$\varepsilon = \frac{(X_{01} - X_{02}) - (X_{i1} - X_{i2})}{L_0} \quad (\text{Eq 3.1})$$

ε : Drying shrinkage ($\times 10^{-6}$)

L_0 : Original length

$X_{01} - X_{02}$: Measurement values of the standard scale and specimen at the reference time point

$X_{i1} - X_{i2}$: Measurements of the standard scale and specimen at time i

The unit of the length of L_0 , X_{01} , X_{02} , X_{i1} , X_{i2} is the same.

3.3 Modulus of Elasticity Experiment

3.3.1 Static Modulus of Elasticity test

Using the "Standard Test Method for Static Modulus of Elasticity and Poisson's Ratio of Concrete in Compression," two cylindrical concrete specimens measuring 6 inches by 12 inches were tested at 1, 3, 7, 14, and 28 days after the concrete was mixed. These tests were performed on each of the concrete batches (ASTM C469, 2002). In accordance with the standard established by the ASTM, the equipment that was connected to each specimen comprised of an extensometer and a compressometer.

The compressometer is used in order to measure the axial deformation of the specimen in relation to the load that is being applied. The Static Modulus may then be estimated after these variables have been determined. The extensometer is used to determine the transverse strain that the applied force has caused on the specimen. The Poisson's Ratio of the concrete may then be calculated based on the transverse stresses that were measured. Compressometer and extensometer, two pieces of equipment that were used during the course of this technique, are shown in Figure 3.6.

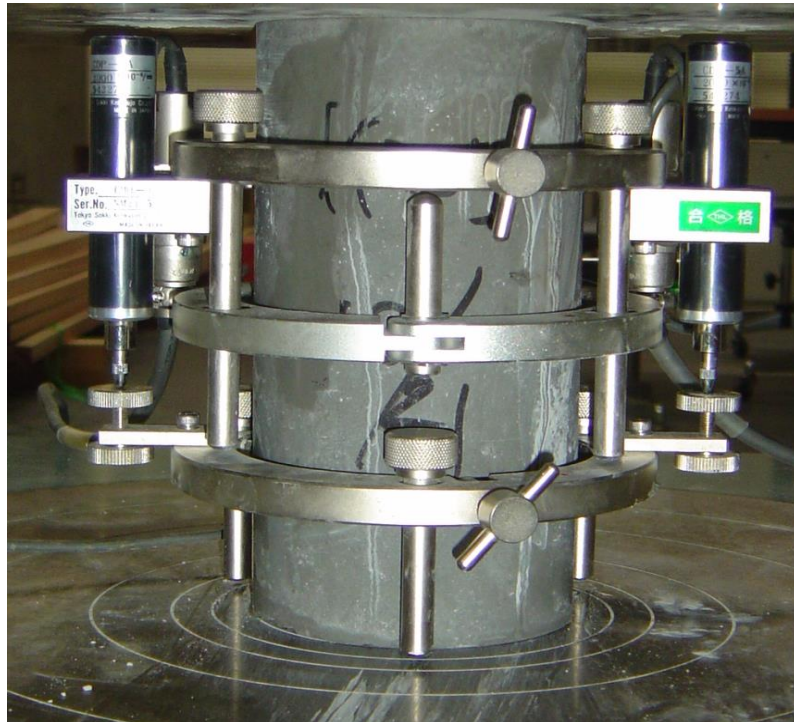


Fig 3.6 Static Modulus Apparatus Consisting of Compressometer Gage (Dial Gage) and Extensometer Gage (Digital Gage)

1) The process of preparing the specimen

After the prescribed amount of time has passed for the specimen to cure, it should be immediately ready for testing in the state in which it contains water. In order to secure strain gauges to the surface of a specimen that has been cured in water or wet-cured, it is possible to wait for the surface to dry out on its own.

2) The measurement of the dimensions of the specimen

For cylindrical specimens prepared in accordance with bullet 4 of JIS A 1132, take the dimensions of the specimen and measure them in accordance with JIS A 1108; for cylindrical core specimens, measure them in accordance with JIS A 1107.

3) The installation of equipment for measuring strain in the material.

The instrument for measuring strain is attached to two lines that are parallel to the axis of the specimen and symmetrical to each other. The instrument is centered at half the height of the specimen.

4) Get everything ready for loading.

The following shall constitute preparation for loading: a) The tests need to be carried out in a room that has consistent temperature and humidity levels. b) The specimen is positioned so that the center axis of the specimen coincides with the center of the pressure plate with an error that is no greater than one percent of the specimen's diameter.

5) Type of loading procedure

The following is the prescribed loading procedure: a) The loading should be done at a constant speed so that the specimen is not subjected to sudden accelerations or decelerations. It is important to keep in mind that the initial strain cannot be measured if a load is applied to the specimen at an excessive speed in the beginning stage of the loading process. b) The rate of loading should be adjusted

so that the increase in compressive stress is within the range of 0.6–0.4 N/mm² per second. c) The specimen's longitudinal strain should be measured up to approximately half of the maximum load, and a minimum of ten points should be recorded at equally spaced intervals in order to get an accurate reading. d) Once the specimen starts to deform quickly, you should stop adjusting the rate at which the load is being applied but you should keep applying the load. e) Before the specimen breaks, read the maximum load that the compression tester indicates to three significant digits before reading the result.

6) The process of computing the results

The following formula is to be used in the computation of the test results: a) Using the results from step 6.5, construct a stress-strain curve for each of the specimens. b) The static modulus of elasticity of each specimen needs to be calculated using the following formula, and the results need to be rounded off to three significant digits.

$$E_c = \frac{S_1 - S_2}{\epsilon_1 - \epsilon_2} \times 10^{-3}$$

Ec: Static modulus of elasticity of each specimen (kN/mm²)

S1: Stress equivalent to 1/3 of the maximum load (N/mm²)

S2: Stress at 50 x 10⁻⁶ longitudinal strain of the specimen (N/mm²)

ε1: Longitudinal strain of the specimen caused by the stress of S1 50×10⁻⁶

3.3.2 Dynamic elastic modulus Test

The resonance method is one that can be used to determine the dynamic modulus of elasticity of concrete in a way that does not involve breaking the concrete in any way. On the other hand, the resonance method and the ultrasonic pulse method are frequently used in conjunction with one another. The ultrasonic pulse method has the benefit of being able to test virtually any shape of specimen, making it a very versatile testing technique.

a) Resonance vibration

One of the most common methods of measuring the intrinsic vibration frequency of a specimen is to excite a longitudinal vibration in the specimen in a tensile and compressive waveform. For this purpose, a vibration transmitter (shaker) E should be set up on the end face of the prismatic specimen, the axis of the shaker should be parallel to the axis of the specimen, and the frequency should be able to change. The test piece is generated by the shaker E to the receiver R (pickup) propagation of the stretching a compressional wave type of vibration (pickup should be set at the opposite end).

To avoid bending of the test piece, the test piece should be supported in the center. Due to the change in vibration frequency of the shaker, it is possible to produce a wavelength into the specimen length l approximately the same vibration. In this case, the sound waves can be propagated until the test piece is forced to vibrate with the intrinsic frequency due to interference and the formation of standing wave system. This is where resonance can be observed, i.e., the interference force frequency is the same as the fundamental intrinsic frequency of the rod.

Calculating the Mass and Dimensions of an Object It is required that the mass of the specimen be measured with an accuracy of within 0.5 percent. The length of the specimen is to be measured multiple times with an accuracy of 0.5 percent, and the average of these measurements is to be recorded as the length of the specimen. For the purpose of determining the cross-sectional dimension, the cross-sectional dimension must first be measured with an accuracy of 1 percent at a number of

different locations. The average of these measurements must then be used to determine the cross-sectional dimension.

During a continuous test using the same specimen, measurements need to be taken at each iteration if there is a change in either the mass or the cross-sectional dimensions of the specimen.

In the event of deflection vibration, determination of the resonance number is required. In the event that deflection vibration is present, the resonance number should be calculated as follows: a) The EUT is mounted on a support in the same manner in order to permit free deflection and vibration at both ends without a great deal of constraint. Applying the driving force in the direction that causes the specimen to deflect is the correct way to do it.



Photo 3.6 Dynamic elastic modulus test machine.

It is important that the driving force be applied in a location that is remote from the nodes of the vibration (usually in the center of the EUT). It is necessary for the pickup to make contact with the opposite end face of the EUT in order for it to function in the same direction as the vibration of the EUT.

Adjust the frequency of the oscillator while monitoring the voltage at the output of the amplified pickup. Do this while simultaneously applying a driving force to ensure that the EOT vibrates in the appropriate manner. When the indicator has a definite maximum oscillation and the measurement of the nodes of the oscillation confirms that it is a first-order resonant deflection vibration, the frequency in such a case should be the first-order resonant frequency of the deflection vibration.

This is because the indicator has a definite maximum oscillation and the measurement of the nodes of the oscillation confirms that it is a first-order resonant deflection vibration. In the case of first-order deflection vibration, the node of vibration is situated one-fourth of the way (or, more precisely, 0.224 of the way) of the way away from the edge of the specimen.

As a consequence of this, the indicator runout demonstrates a maximum value at both ends of the specimen and a minimum value at the nodes. In this instance, the location of the nodes and belly of the vibration can be verified by moving the pickup in the direction of the length of the specimen and

measuring the runout of the indicator. Alternatively, the location of the nodes and belly of the vibration can be inferred from the fact that there is a vibration. The indicator ought to display the lowest possible runout at the node, whereas it ought to display the highest possible value at the belly. It is possible to check the phase of the Lissajous figure both before and after the node using an oscilloscope if the apparatus in question is fitted with a cathode-ray oscilloscope.

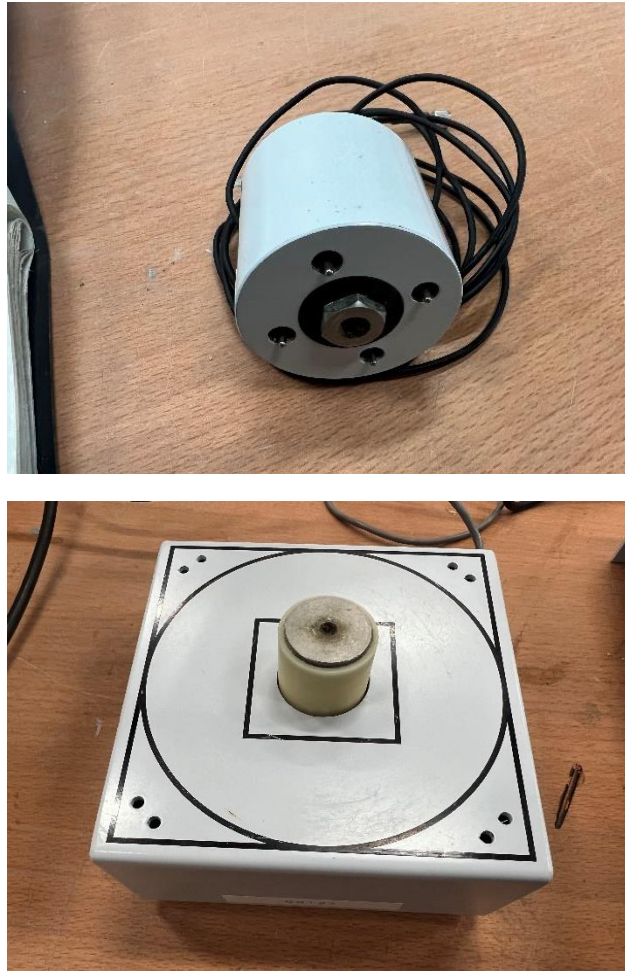


Photo 3.7 Resonance vibration machine

In the case of longitudinal vibration, a determination of the resonance number is required. a) The specimen should be placed on a support in the same manner, so that it is able to vibrate freely at both ends and without much constraint. The specimen's end face is the location where the driving force is applied, and it is applied at a right angle to the end face. It is necessary for the pickup to make contact with the opposite end face of the EUT in order for it to function in the same direction as the vibrations produced by the EUT.

During the process of varying the frequency of the oscillator and applying a driving force so that the EUT vibrates in response, observe the output voltage of the amplified pickup. The frequency at which the indicator has a clear maximum runout is the first-order resonance frequency of longitudinal vibration. This frequency can then be used to determine the second-order resonance frequency of the longitudinal vibration.

In the event that it is necessary to do so, move the pickup in the direction of the length of the EUT,

and then measure the runout of the indicator to confirm the nodes of vibration. Note When the longitudinal vibration is occurring at its first-order resonant frequency, there is only one node in the center of the specimen, and the vibration is bellying out at both ends of the specimen, which results in the largest possible amplitude.

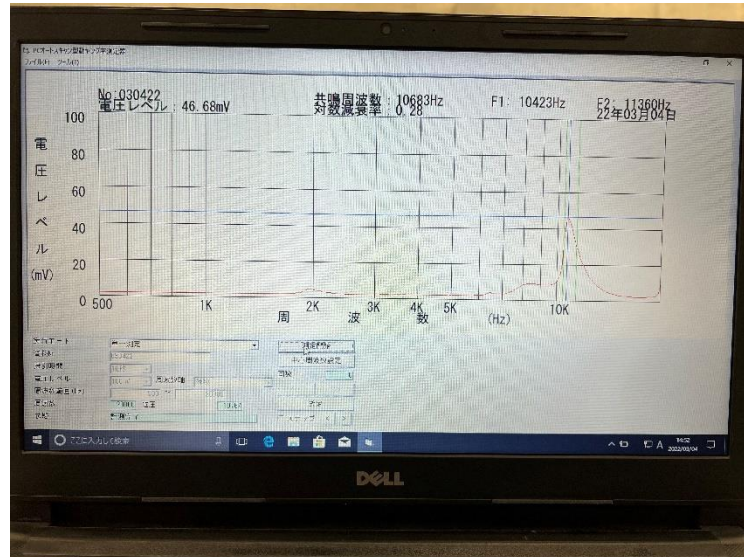


Photo 3.8 Resonance frequency output image

The process of determining the frequency of resonance in the event of torsional vibration a) The specimen is mounted on a support in the same way that it was done in step 3.3 so that free torsional vibration can occur at both ends without a great deal of constraint. In order to generate torsional vibration in the specimen, the driving force needs to be applied relatively close to one end of the component.

It is important that the driving force be applied in a location that is remote from the nodes of the vibration (usually near the end). It is important that the pickup be brought into contact with the opposite end face of the specimen so that it can function in the same direction as the specimen's vibration. It is recommended that the drive terminal be positioned 0.10 to 0.12 L away from the end of the EUT, and that the pickup be positioned 0.224 L away from the opposite end. These adjustments will help to mitigate the effects of deflection vibration.

Observe the output voltage of the amplified pickup while simultaneously altering the oscillator frequency and applying a driving force in order to ensure that the specimen vibrates in the appropriate manner. When the indicator has a definite maximum oscillation and the measurement of the nodes of the oscillation confirms that it is a first-order resonant torsional vibration, the frequency in such a case should be the first-order resonant frequency of the torsional vibration.

If the indicator does not have a definite maximum oscillation, the frequency should be the same as the fundamental frequency of the torsional vibration. Note There is only one node in the center of the vibration that occurs during first-order torsional vibration. This node transforms into a belly at both ends of the specimen and displays the highest possible amplitude.

b) Ultrasonic pulse method

The establishment of ultrasonic pulses, which are mechanical vibrations that last for only a brief period of time, is the foundation of the ultrasonic pulse method. However, the frequency should also

be low enough so that the pulse can propagate over a considerable distance in the concrete. The vibration frequency should be high enough so that the wave crest is steep enough to allow accurate measurements; however, the frequency should also be low enough so that the pulse can propagate over a considerable distance in the concrete.

Attenuation caused by scattering frequently takes place when the wavelength is comparable to the size of the aggregate particle. For concrete with an aggregate particle size of 30 millimeters or less, the relationship is accurate when the frequency is 150 kilohertz. If the ultrasonic frequency that is being used is too high, there is a possibility that there will be attenuation caused by scattering.

Based on this information, it is possible to deduce that the ultrasonic frequency range that should be used to test concrete should be anywhere between 20 and 200 kilohertz. The frequencies between 40 and 100 kHz are the most useful ones to consider when working within the two parameters outlined above.

Because the pulse is transferred to the concrete via the mechanical contact method, a coupling agent needs to be used, and a reliable contact is required, in order for the energy that is emitted by the transmitting transducer to be fully transferred to the concrete.

While the longitudinal wave that is perpendicular to the direction of the excitation plane is going to be able to transmit the majority of the energy to the concrete, there will be a certain frequency of the pulse that will be transmitted through the concrete that will be propagated in all directions. As a result, it is feasible to position the receiving transducer along the longitudinal axis in a direction that is both perpendicular to the plane on which the exciter is positioned and parallel to the plane.

Following its journey through the concrete, the ultrasonic vibration pulse eventually arrives at the receiving transducer. The spectral composition of the transducer is altered so that it more closely resembles its prototype as a result of the frequency of the pulse being filtered out by the concrete. Since a number of similar conditions need to be established before the pulse can be transmitted from the transmitting transducer to the concrete and transformed into a mechanical vibration, the question of how the mechanical energy can be transmitted from the concrete to the receiving transducer presents itself as a challenge.

It is not possible to measure the propagation time in this manner if the observation is based on the propagation of a pulse with a continuation time of a few tenths or a few percent of microseconds. In this case, it is necessary to send multiple pulses at a high enough repetition frequency to establish a constant image on the fluorescent screen of the oscilloscope. On the other hand, the repetition frequency shouldn't be too high in order to have enough time to completely attenuate the most recent pulse. This can only be accomplished with more time. Under these circumstances, the sending frequency of the pulse ought to range anywhere from 1 to 50 Hz.

The method of using an ultrasonic pulse that is currently in use is predicated on the measurement of the amount of time that it takes for ultrasound to propagate and the amount that the pulse is attenuated by the concrete.

Pulses can be produced in three different ways: (1) through the use of the blasting method; (2) through the use of the hammering method; and (3) through the utilization of electroacoustic transducers [6]. Methods such as blasting and hammering produce pulses that are significantly more intense than those produced by electroacoustic transducers. However, because the pulses that are produced in this manner have a broad spectrum and a very shallow steepness of the wave front, it is

not possible to measure them at close ranges (below 30 cm). Because the hammering method, and especially the blasting method, can cause damage to the concrete structure, the blasting method is typically not used for testing concrete. Additionally, the blasting method can cause damage to the concrete structure.

There are three distinct manifestations of the vibration that results when an impulse excites an energy-stable vibration at the surface of a semi-infinite medium. When the mass of the material moves only in the longitudinal direction, that is to say along the direction that its wave propagation is taking place, the vibration travels at its quickest speed. A longitudinal wave or a compressional wave is the name given to this type of wave.

The transverse wave, also known as an S-wave when applied to seismology, is the next fastest type of wave in the order of wave speed. Similar to longitudinal waves, transverse waves are able to propagate in all solids; however, their velocity, v_y , is significantly lower. When transverse waves are present, the material's mass system moves in a direction that is perpendicular to the direction in which the wave is traveling.

There is a third kind of wave that can travel along the surface of a solid, and it is called surface waves. Surface waves, also known as Rayleigh waves, are another name for this type of wave. When the value of the material's Poisson's coefficient is between 0.2 and 0.3, the speed of surface wave propagation is between 0.91 and 0.93 of the speed of the transverse wave.

Utilizing an electroacoustic transducer will yield the best results if the test parameters call for a relatively short distance to be specified between the transmitting and receiving transducers. This advantage also keeps the directionality of the emitted energy better because of the high frequency and large diameter transmitter transducer, so that the energy is highly concentrated. Although the amount of energy generated by the electroacoustic transducer is not very high in comparison to the hammering method, this advantage allows it to produce a fixed optimal frequency of vibration, which allows the wavefront to obtain a steep enough pulse value.

The primary portion of the pulse's energy, as it travels through the null space, is dispersed within a cone that has a diffusion angle of zero. This occurs because the wavelengths that were used. There is a certain interval around the object that is being investigated in which the sound pressure of ultrasonic waves drops in a manner that is inversely proportional to the square of the distance between them.

In spite of this common misconception, the angle of 0 in concrete testing is never less than 90 degrees. When testing concrete components, it can be seen from the information presented above that the use of an electroacoustic transducer is the best option if the transducer coefficient is measured at a short distance (less than 1 m); however, if the test distance is greater than 1 m, then the use of an exciter that is similar to hammering is the best option.

The application of the ultrasonic pulse method in the examination of concrete is predicated on the observation and measurement of the time required for the propagation of the longitudinal wave (other wave types are utilized infrequently at this time), as well as the amplitude of the signal (the method of measuring the pulse frequency is rarely used).

The effect of the non-homogeneity of the concrete [7-9] is also evaluated based on the measured amplitude of the signal and the time it took for the signal to propagate. For the purpose of making the investigation more manageable, concrete can be broken down into its two primary components: an

inert part that is made up of aggregates and an active part that is a mortar that contains air-filled or moisture-filled voids or micropores within it.

If you have a constant v , the volume V of the aggregate will increase proportionately with the velocity v , but the aggregate's propagation velocity will decrease as the volume increases. Because of this, the speed at which ultrasonic waves travel through concrete is contingent not only on the kind and the strength of the mortar, but also on the amount and the kind of the aggregate.

The inhomogeneity of the composition of the concrete also has an impact on the velocity measurements taken over relatively short distances (distances less than 3 to 4 times the maximum particle size of the aggregate). Due to the different composition of the concrete at different points along the direction of pulse propagation, this velocity varies greatly from one point to the next. Due to the fact that the size of the concrete non-homogeneity of the phenomenon, which is determined by the base distance (the distance between the transmitting and receiving transducers), will gradually disappear as its size increases (roughly equal to 10 times the maximum size of the aggregate).

H. Kolski (H. Kolski) [10] has studied the effect of material viscoelasticity [11-13] on the propagation velocity of the pulse. He points out that: theoretically, the propagation velocity of the pulse system and the same propagation velocity in elastic materials, but due to the scattering and attenuation effect, the wave shape has changed. [H. Kolski] [10] [11-13] The wave front will be flattened and the measurement accuracy of the pulse that reaches the specimen will be reduced if the conditions are as they have been described. It is possible that the effect of viscoelasticity of the material has a greater magnitude than the effect of non-homogeneity, and this effect is related to the testing method that was used.

The effect of the anisotropy of concrete is particularly pronounced close to the surface at which the concrete is being poured. In this range, the anisotropy of concrete along the pouring direction will increase due to the use of mechanical methods of vibrating, which will separate a layer of concrete in which the content of fine particles in cement, water, and aggregates, compared to other parts of the concrete. This layer will have a greater degree of anisotropy than the other parts of the concrete. When measured at or near the surface layer, the pulse propagation velocity is extremely sensitive to variations of this kind. As a result, the characteristic values that were measured within this range are not suitable for use as a representation of the component as a whole.

It is important to note, as a final point of discussion, that geometric dispersion of ultrasonic pulses can be caused by concrete, just as it can be caused by any other solid elastic material. This phenomenon, which is a variation of the waveform that is propagating in the material, is typically seen when the section size of the specimen is relatively close to the wavelength produced by the transmitting transducer. The longitudinal wave that was moving through what was thought to be an infinitely solid block has gradually transformed into an elastic stretching wave that is moving through a rod. In this particular instance, the speed of the longitudinal wave's propagation is about to start slowing down.

3.4 Mercury intrusion porosimetry test for porosity

Studies that are currently being conducted on recycled concrete (RC) promise a feasible path for its application, thereby satisfying a need, saving energy, improving environmental conditions, and providing a solution for waste construction. This is made possible through the partial substitution of natural aggregate (NA) with recycled aggregate (RA). [14-20]

Recycled concrete may be seen as a kind of porous concrete since it has permeability values that

are twice as high as those of regular concrete. As the fraction of coarse NA that is replaced by fine RA grows, their overall behavior demonstrates a reduction in the mechanical and physical qualities they possess. It is also generally acknowledged that there is an inverse correlation between the volume of pores and the levels of stress to which the concrete can be subjected. In addition, it is recommended that this relationship take into account the distribution of the sizes of the pores as well as the interconnection between them. [21-24]

This paper presents eighteen various kinds of concrete with varying fine RA and fly ash (FA) levels, together with the behavior of the concrete, using tests of mercury intrusion porosimetry (MIP). The experiments were carried out using the mercury intrusion porosimetry (MIP) method.

The AutoPore V is equipped with two high pressure ports in addition to its four low pressure ports. The low pressure port is used most often for the process of loading mercury into the penetrometer. The vast bulk of the data is gathered via the high pressure port.



Photo 3.9 AutoPore V

Make a note of the event in the log book that corresponds to the tool. Using the switch located at the rear of the system, activate the porosimeter if doing so is required. Determine the mass of the sample material that will be examined. Aim for less than 1000 mg if at all feasible; nonetheless, the substance and the experience level of the user will ultimately decide this figure.



Photo 4.2 [25]

Place the penetrometer in the holder and use the wrench to release the locking ring.

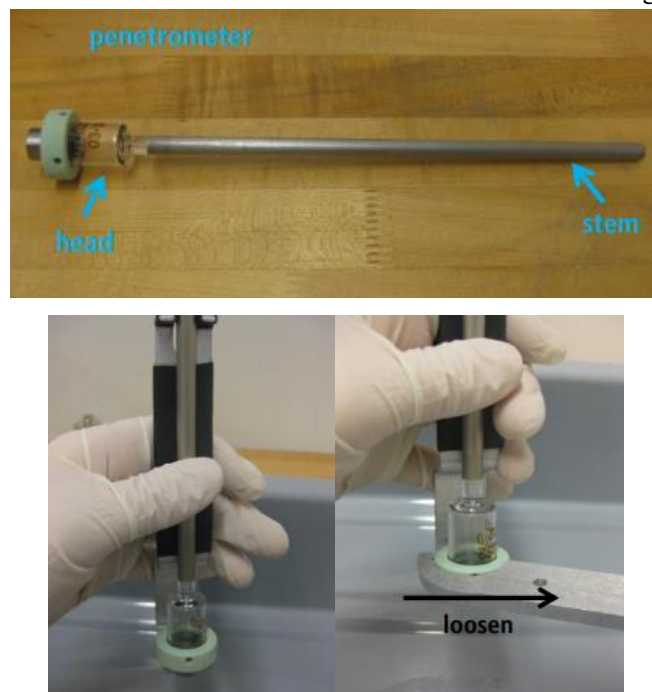


Photo 4.3 [25]

Turn on the penetrometer and then put the sample inside it. Make use of a very little quantity of vacuum grease, and then apply it all the way around the penetrometer's rim. Put the cap back on the penetrometer, put it in the holder, and then turn the ring that secures it.

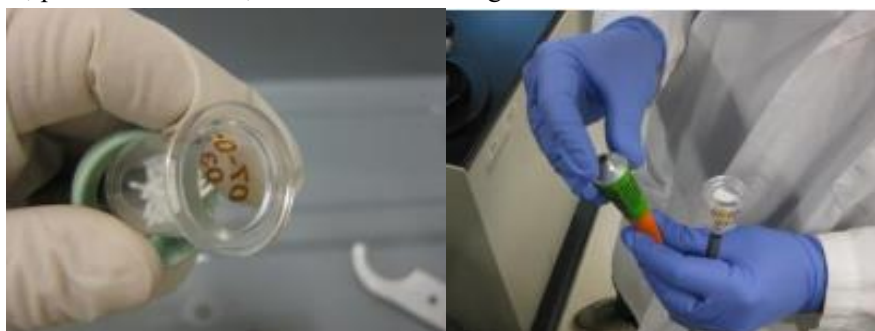




Photo 4.4 [25]

Measure the weight of the penetrometer, sample, and mercury. Use the black weighing support.



Photo 4.5[25]

Take the metal rod out of the low pressure port and place it on top of the porosimeter on a paper towel. Put the penetrometer into the low pressure port, then make sure it's secure by turning the screw on top of the port clockwise.



Photo 4.6 [25]

Launch the Autopore V. To generate a new file, go to File, give the sample a new name, and then pick Open from the drop-down menu. Enter the details, as well as the weight of the assembled product, into the Sample Description field. Choose to save it.

Choose Unit 1's examination of low pressure to continue. Choose the file you want to launch based

on the appropriate port. When you are ready, press "start."

The system will wait for five minutes after evacuating the penetrometer to a pressure of 50 umHg. The whole procedure of evacuating the building might take up to half an hour. The user must click the "Skip" button in order to go to the subsequent stage if the pressure has not reached 50 umHg after one hour but is lower than 100.

The machine will then begin the analysis when it has finished pouring mercury into the penetrometer. The system will take a measurement of the incursion volume at each pressure that is specified in the analysis conditions while the analysis is being performed.

When the tool's status changes back to "Idle," the analysis is considered to be finished.

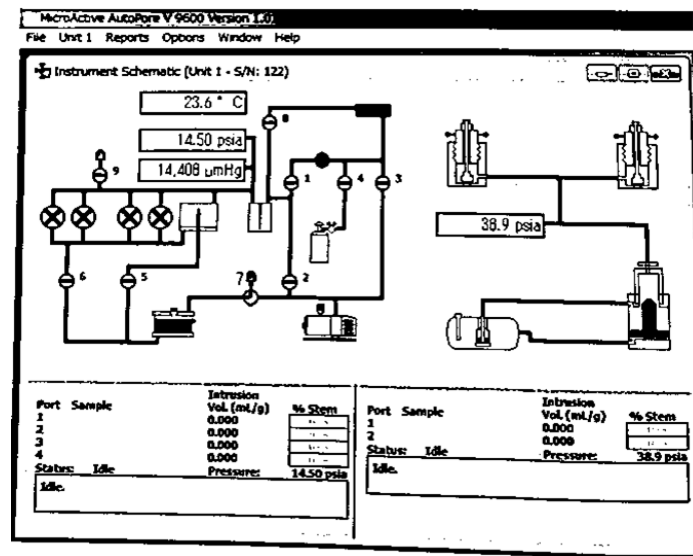


Photo 4.9

After the procedure is finished, take the penetrometer out of the low-pressure port and put it in the Rubbermaid container. The sample should be loaded into the high-pressure port. (don't forget to use protective gear like gloves, goggles, and a lab coat)

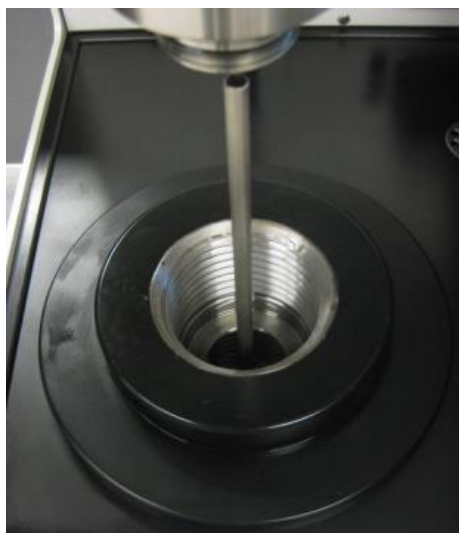


Photo 4.10

When the screw is being tightened, the vent valve needs to be open. To eliminate air bubbles, labor

gently and alternate between forward and backward motion.

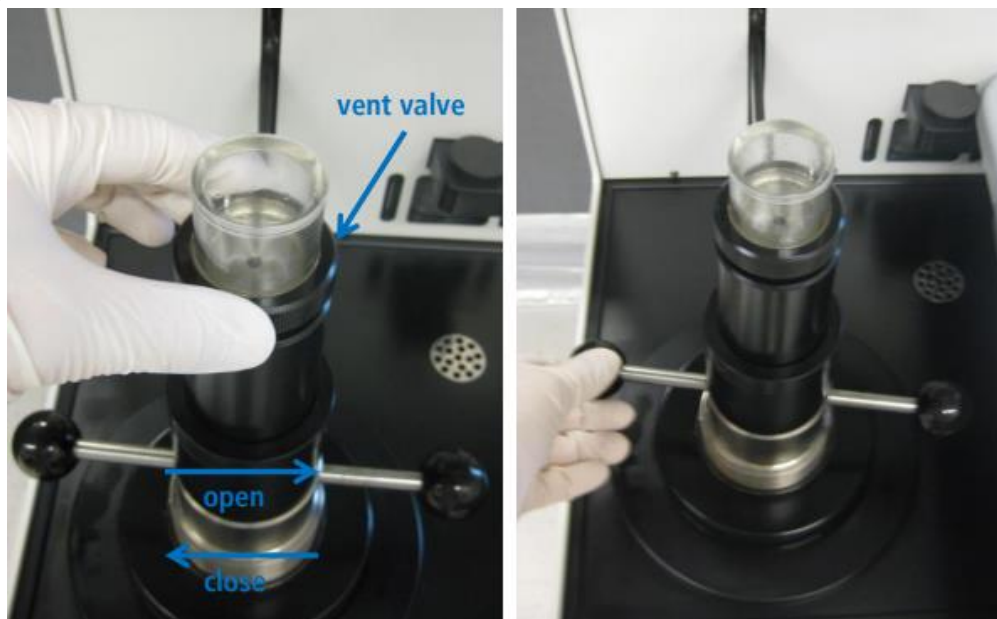


Photo 4.11[25]

Select Unit 1 for the analysis of high pressure. Choose the file you want to execute. When instructed, open the vent valve, and when instructed again, seal the vent valve. In order to finish the report, the system will perform analysis on samples while subjected to the pressures specified in the Analysis Conditions. Wait until the system state changes back to Idle and the red light labeled "Pressurized" goes off before proceeding.



Photo 4.14

Open the vent valve. Release the pressure on the high pressure port. Put the grey tray down on the top of the deck. Take out the penetrometer and turn it upside down so that the majority of the oil may run down the penetrometer's exterior and into the high pressure port. It is very important to make sure that the stem of the penetrometer is pointed in the UP direction at all times.

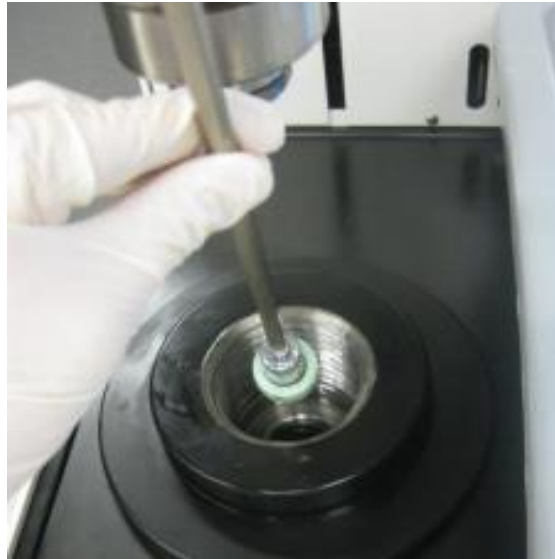


Photo 4.15

Wipe the majority of the oil off using paper towels. Dispose of the paper towels in the mercury waste bag.

References

- [1] JIS A 6201, 2015. Fly Ash for Use in Concrete. Japanese Industrial Standard Committee, Japan, 2015. Available online: www.jisc.go.jp (15/7/2021accessed on).
- [2] Yang, L.; Li, D.; Zhu, Z.; Xu, M.; Yan, X.; Zhang, H. Effect of the intensification of preconditioning on the separation of unburned carbon from coal fly ash. *Fuel* 2019, 242, 174–183, <https://doi.org/10.1016/j.fuel.2019.01.038>.
- [3] Yang, L.; Zhu, Z.; Qi, X.; Yan, X.; Zhang, H. The process of the intensification of coal fly ash flotation using a stirred tank. *Minerals* 2018, 8, 597, <https://doi.org/10.3390/min8120597>.
- [4] Yu, Y.; Cheng, G.; Ma, L.; Huang, G.; Wu, L.; Xu, H. Effect of agitation on the interaction of coal and kaolinite in flotation. *Powder Technol.* 2017, 313, 122–128, <https://doi.org/10.1016/j.powtec.2017.03.002>.
- [5] JIS R 5201, 2015. Physical Testing Methods for Cement. Japanese Industrial Standard Committee, Japan, 2015. Available online: www.jisc.go.jp (21/7/2021accessed on).
- [6] Jones R. Non-Destructive Testing of Roads and Structures. Inst. of Mun. Eng. and RRL, London, 1965.
- [7] Zhu Xiaolin, Yang Jialin, eds. *Soil Engineering*. Tongji University Press, 1996.
- [8] Chen Yuzhu. Nonlinear vibration, bifurcation and chaos theory and its applications. *Journal of Vibration Engineering*, 1992.

- [9] Zheng YL, Xi DaoYing. Study of strain rate effect on Young's modulus of rock. Chinese Young Scholars Symposium on Geotechnical and Engineering Applications, 1994.
- [10] Kolski H. The propagation of longitudinal elastic waves along cylindrical bars, *Phil. Mag. Rev.*, 1954.
- [11] Wu Rui Feng. Dynamic analysis of viscoelastic beams. *Earthquake Engineering and Engineering Vibration*, 1983.
- [12] Properties of concrete. China Construction Industry Press, 1983.
- [13] Zheng YL. Study of dynamic modulus of elasticity of geotechnical materials. *Journal of Geotechnical Engineering*.
- [14] J. Bjørn-Jakobsen, M. Elle, E.K. Lauritzen, On-site use of regenerated demolition debris, in: Y. Kasai (Ed.), *Demolition and Reuse of Concrete and Masonry, Reuse of Demolition Waste*, vol. 2, E&FN SPON, London, 1988, pp. 537–546.
- [15] W. Grubl, Environmentally Friendly Construction Technology-Interaction Between Construction and Environment (1999) (<http://www.b-i-m-de/public/Tudmassiv/dacon98gruebl.htm>).
- [16] T.C. Hansen, Recycled of demolished concrete and masonry, Report of Technical Committee 37-DRC Demolition and Reuse of Concrete, Part 1, E&FN SPON, London, 1992, pp. 1. 160.
- [17] T.C. Hansen, E. Bøegh, Elasticity and drying shrinkage of recycle aggregate, *ACI J.* (5) (1995) 648.652.
- [18] T.C. Hansen, M. Marga, Strength of recycle made from coarse and fine recycled concrete aggregates, in: Y. Kasai (Ed.), *Demolition and Reuse of Concrete and Masonry, Reuse of Demolition Waste*, vol. 2, Chapman & Hall, London, 1988, pp. 605.612.
- [19] M. Kakizaki, M. Harada, T. Soshiroda, S. Kubota, T. Ikeda, Y. Kasai, Strength and elastic modulus of recycled aggregate concrete, in: Y. Kasai (Ed.), *Demolition and Reuse of Concrete and Masonry, Reuse of Demolition Waste*, vol. 2, Chapman & Hall, London, 1988, pp. 565. 574.
- [20] E.K. Lauritzen, M. Jannerup, Guidelines and experience from the demolition of houses in connection with the resound Link between Denmark and Sweden, *Demolition and Reuse of Concrete and Masonry*, in: E.K. Lauritzen (Ed.), *Guidelines for Demolition and Reuse of Concrete and Masonry*, E&FN SPON, Denmark, 1993, pp. 35. 46.
- [21] P.J. Wainwright, A. Trevorrow, Y. Yu, Y. Wang, Modifying the performance of concrete made with coarse and fine recycled concrete aggregates, in: E.K. Lauritzen (Ed.), *Demolition and Reuse of Concrete and Masonry, Guidelines for Demolition and Reuse of Concrete and Masonry*, E&FN SPON, Denmark, 1993, pp. 319. 330.
- [22] A. Mueller, A. Winkler, Characteristics of processed concrete rubble, in: K.R. Dhir, N.A. Henderson, M.C. Limbachiya (Eds.), *Uses of Recycled Concrete Aggregate. Sustainable Construction*, Tomas Telford, London, 1998, pp. 1109. 1119.
- [23] P.J. Wainwright, J.G. Cabrera, Use of demolition concrete to produce durable structural concrete, in: J.J.J.M. Goumans, H.A. Van Der Sloot, T.G. Aalbers (Eds.), *Environmental Aspects of Construction with Waste Materials*, Elsevier, The Netherlands, 1994, pp. 553.562.
- [24] B. Zhang, Relationship between pore structure and mechanical properties of ordinary concrete under bending fatigue, *Cem. Concr. Res.* 28 (5) (1998) 699. 711.
- [25] Mercury Porosimeter, Standard Operating Procedure. Revision: 3.0. Last Updated: Mar.31/2015, Revised by Nathanael Sieb.

Chapter 4

***DEVELOPMENT OF FLOTATION DEVICE FOR
REMOVING UNBURNT CARBON IN FLY ASH FOR
USE IN HARDENED CEMENTITIOUS MATERIALS***

CHAPTER 4: DEVELOPMENT OF FLOTATION DEVICE FOR REMOVING UNBURNT
CARBON IN FLY ASH FOR USE IN HARDENED CEMENTITIOUS MATERIALS

4.1 Introduction

In Japan, the power supply includes renewable [1], thermal [2], and nuclear energy [3]; however, global environmental issues and the recent power supply situation mean that renewable energy is expected to expand substantially. Nevertheless, increasing the proportion of renewable energy in the energy mix will take time, and thermal power generation will still be required.

Coal-fired power generation has the second-highest utilization rate worldwide after liquefied natural gas power generation, but the treatment of the coal ash generated is a major problem. Fly ash is the fine residue generated by the combustion of ground or powdered coal and is transported through flue gasses. Global fly ash production is estimated to be 400–500 million tons per year and the utilization rate in cement and concrete components is about 30% [4–5]. The total amount of coal ash generated by Japan's electric power industry and general industry exceeded 10 million tons and 97.4% of the coal ash was used, and 96.3% of the total was used in the cement industry as a raw material.

The properties of recycled aggregate concrete (RAC) cause major problems globally and improving the properties of RAC is expected to increase the use of RAC in structures. Recycled aggregates generally increase the water absorption and drying shrinkage and reduce the modulus of elasticity, workability and compressive strength of RAC compared with concrete containing natural aggregate [6]. However, fly ash has a shrinkage-reducing effect on both ordinary concrete and RAC and can mitigate the increase in shrinkage caused by recycled aggregates [7]. For concrete with a water:cement ratio of 0.55, the dry shrinkage of concrete prepared with 0%, 20%, 50%, and 100% recycled aggregate is reduced by 14%, 13%, 10%, and 7%, respectively [8]. When 35 wt% of cement is replaced with fly ash, the shrinkage strain of all types of concrete is decreased by 55×10^{-6} on average, and the shrinkage strain of concrete without fly ash is 15–20% higher than that with fly ash at an age of 112 days [9]. Using fly ash as an alternative to cement or as an additive that can improve the durability and workability of the concrete is the recommended approach and helps to protect the environment and reduce water consumption. The strength of concrete in which a percentage of cement is replaced by fly ash is lower at an early age, although its strength is higher than or similar to concrete without fly ash later on [10–12]. In general, concrete containing fly ash as an additive or to replace cement has improved durability. The higher compressive strength of concretes containing fly ash is related to the improved bonding between aggregates and slurry and the denser microstructure obtained by changing the pore size distribution [13].

Fly ash is classified into types I to IV according to Japanese Industrial Standard (JIS), and the quality of fly ash must be considered when it is used as an admixture for concrete. According to the Architectural Institute of Japan, type I or JASS5M-401 [14] fly ash is suitable for replacing cement, and types II or IV are suitable for replacing a proportion of fine aggregate. In other words, fly ash used as an admixture for concrete requires a loss on ignition (LOI) of 5.0% or less. This is because fly ash with an unburned carbon content of 5.0% or more may cause poor coagulation of cement, and that with an unburned carbon content of 3.0% or more, adsorbs admixtures and decreases the fluidity and workability of concrete, which prevents entrainment and adversely affects the concrete's quality [15]. Some fly ash discharged from coal-fired power plants has a LOI of more than 5.0%, but other qualities mainly conform to JIS standard. Even for fly ash with a LOI of less than 5.0%, the smaller the amount of unburned carbon, the smaller the effect on the fresh properties of concrete. Therefore, methods of separating unburned carbon from fly ash will help increase the use of fly ash as an admixture for

CHAPTER 4: DEVELOPMENT OF FLOTATION DEVICE FOR REMOVING UNBURNT CARBON IN FLY ASH FOR USE IN HARDENED CEMENTITIOUS MATERIALS

concrete and the reuse of the fine un-burned carbon, achieving more efficient use of waste fly ash and greater economic and environmental benefits compared with landfill disposal or storage. Methods for separating unburned carbon particles from fly ash and the effect of the method on the unburned carbon properties have been investigated.

In general, high-carbon fly ash can be beneficiated using dry and wet separation processes, such as froth flotation, electrostatic separation, fluidized bed reactors, oil agglomeration, density separation, and sieving [16–19]. Each separation method has disadvantages and advantages and can be adapted for different types of coal fly ash. For improved separation efficiency and higher purities of unburned carbon, a combination of several techniques is typically needed. For example, Bittner et al. [20] developed a processing system based on triboelectric charging and electrostatic separation, and Parallel and louvered plate separators were used for the beneficiation of fine coal fly ash particles by Soong et al. [21].

The flotation method is a conventional technique that is mainly used for coal beneficiation, ore beneficiation, and the deinking of used paper [22,23]. Hydrophobic particles are attached to the surface of bubbles and floated in the water, allowing for hydrophilic particles to be collected from the bottom. To improve the separation, a foaming agent and a collecting agent that improves particle adhesion to bubbles are often added [24,25]. Froth flotation is widely used in mineral processing and coal preparation industry [26]. The traditional Denver flotation cell has been used for the separation of unburned carbon in laboratory scale fly ash [16]. The existence of a large number of pores increases the consumption of diesel. During the adjustment process, the amount of diesel and the speed of the impeller have the greatest impact on the carbon recovery rate. Altun et al. [27] used a concurrent flotation column. Unburned carbon was separated from fly ash, and the effects of gas flow, pH value, the amount of collected kerosene and different types of fly ash on the separation performance were investigated. It was concluded that column flotation was an effective method. Li et al. [28] developed a flotation method, which is a novel device with the characteristics of an internal recycling process and multiple mineralization steps. Uçurum et al. [29] found that in trials of a flotation method, unburned carbon was removed from the fly ash, but they did not determine the effectiveness of the removal effect. With the technique disclosed in past research, since separation cannot be performed efficiently, treatment requires a long time period, thus preventing sufficient productivity from being obtained and the floatation machine then becomes complicated and large, requiring extremely large installation space and a high facility cost. It is therefore impossible for small to medium fresh concrete factories to install such facilities.

In floating ore and coal beneficiation equipment, air bubbles are discharged from the bottom of a cylindrical container by an air diffuser and push the carbon over the top of the container. To use this equipment to remove unburned carbon from fly ash, the following factors must be studied: the effect of the bubble size; the methods for recovering fly ash from which the unburned carbon has been removed and for recovering the fly ash containing a large amount of unburned carbon; the method of recovering the fly ash from the fly ash slurry; the stirring method; the operating conditions of the device; and the types of device that can remove unburned carbon efficiently.

In this research, we prototyped an unburned carbon removal device for separating unburned carbon from fly ash by the flotation method. The first objective is to provide a floatation separation apparatus in a simple structure capable of efficiently separating materials to be treated, and the second objective

CHAPTER 4: DEVELOPMENT OF FLOTATION DEVICE FOR REMOVING UNBURNT
CARBON IN FLY ASH FOR USE IN HARDENED CEMENTITIOUS MATERIALS

is to provide a simple floatation separation method for efficiently separating unburnt carbon contained in fly ash. The third objective is to provide a simple manufacturing method for efficiently manufacturing a cement mixture using high-quality fly ash with a reduced unburnt carbon content. We investigated the size of bubbles suitable for removal and the operating conditions. We measured the effect of the conditions on the carbon removal and optimized the device design. Since the unburnt carbon content of the fly ash slurry thus obtained was decreased sufficiently, unburnt carbon-related problems hardly occur, even if a large amount is used, and whether such fly ash slurry can be used as various raw materials in large amounts is worthy of investigation. Therefore, the mechanical and physical properties of concrete containing 15% or 30% fly ash and modified fly ash slurry (MFAS) with unburned carbon removed with our device were measured.

4.2 Materials and Methods

4.2.1 Flotation Method Experiment

In the initial experiment, we examined the effects of the bubble diameter and the conditions on the unburned carbon removal to develop a base model of an unburned coal removal device, and the experiments described later were carried out step-by-step from devices I to III.

Table 4.1 shows the physical characteristics of the fly ash, which was generated from two thermal power plants. Fly ash a-2, a-3, a-5, and a-6 corresponded to JIS A 6201 [30] type II; a-4, b-1, b-2, and b-3 corresponded to type III; a-1 corresponded to type IV; and b-4 did not correspond to a defined type due to its high LOI.

Table 4.1 Mix proportion

Fly Ash	LOI (%)	Density (g/cm ³)	Specific Surface Area(cm ² /g)
a-1	0.72	2.30	1510
a-2	0.42	2.27	2970
a-3	1.30	2.29	2790
a-4	6.99	2.30	4640
a-5	3.86	2.24	4250
a-6	2.22	2.25	4200
b-a	5.87	2.12	4590
b-2	7.39	2.27	4890
b-3	7.85	2.37	4620
b-4	12.92	2.24	4890
c	7.25	2.3	5560
d	9.85	2.11	6060
e	2.81	2.11	3470
f	3.36	2.26	3280

Experiment I was performed to examine the effect of bubble diameter. In device I, which had a capacity of 80 L, fly ashes from the ‘a’ series were used, and two general-purpose air diffusers Ø 70 mm × L200 mm in size were attached to the flotation device near the bottom (Figure 4.1 is based on the equipment used for coal flotation). The air was agitated at a rotation speed of 19 rpm, and the amount of air discharged from the air diffuser was 165 L/min. The most frequent bubble diameter was about 200 µm. The foaming agent was 0.3% pine oil and the unburned carbon collector was 5.0% kerosene. The device floated fly ash containing a large amount of unburned carbon near the water surface through aeration with the air diffuser, and then the floating material (foam ash) was removed and the fly ash that settled on the bottom after standing (tail ash) was collected. The experiment was performed as follows. The additives and tap water were inserted into the device and stirred for 5 min, fly ash was

CHAPTER 4: DEVELOPMENT OF FLOTATION DEVICE FOR REMOVING UNBURNT CARBON IN FLY ASH FOR USE IN HARDENED CEMENTITIOUS MATERIALS

added to make a 20 wt% fly ash slurry and was stirred for 5 min, and then the mixture was aerated for 10 min before the foam ash was recovered. The tail ash was collected from the bottom of the device and dried in an electric furnace at 105 °C for 24 h and its LOI was measured. The unburned carbon removal rates of the ash types were determined based on the LOI measured by JIS A6201 [30].



Figure 4.1. The flotation device of the air diffuser.

Experiment II examined the effect of the bubble diameter and used fly ashes from the ‘b’ series, which had a larger LOI than fly ashes from the ‘a’ series. In device II, the fly ash was put into a 2 L plastic container (Figure 4.2). To prevent precipitation, a small mixer with a rotation speed of 250 rpm was used for mixing, and a high-speed rotary blade microbubble generator was used. The mode of the microbubble diameter was about 40 μm . In addition, in device II, a 60 wt% fly ash slurry and the collector were pre-stirred in a 0.6 L high-speed mixer before flotation due to the significant improvement in the separation performance of unburned carbon from coal fly ash [31]. Pretreatment has great importance for the flotation method. The kinetic energy that is dissipated in the stirred tank could strengthen the interaction process between mineral particles and flotation reagents to improve the flotation efficiency in the presence of preconditioning [32]. Yu et al. [33] found in the flotation of coal that high intensity agitation, greater than 1200 rpm, reduces the kaolinite coating, which will lead to a higher combustibles recovery rate. The collecting agent and tap water were placed in the mixer (rotation speed 10,000 rpm), stirred for 1 min, the foaming agent was added, and the slurry concentration was increased to 20 wt%. Then, the air rotation was started and the floss ash was collected for 10 min. The additive addition rates were the same as those for experiment I. The device was left to stand, the tail ash was collected from the bottom of the device and dried, and then the LOI was measured in the same way as in experiment I.

CHAPTER 4: DEVELOPMENT OF FLOTATION DEVICE FOR REMOVING UNBURNT CARBON IN FLY ASH FOR USE IN HARDENED CEMENTITIOUS MATERIALS



Figure 4.2. Microbubble generator.

Experiment III was conducted to collect data for designing the actual device used in the industry and confirming the effectiveness of preprocessing based on the results of de-vice II. The same fly ash as for device II was used as the material. Device III consisted of a 5 L metal container (Figure 4.3) and the fly ash slurry was circulated by a roller pump with a built-in orifice microbubble generator to prevent the ash from settling without using a stirrer. The experimental procedure was the same as that of experiment II, but the results with and without pre-stirring were compared.



Figure 4.3. Microbubble circulation device.

4.2.2. Concrete Specimen Fabrication

Concrete specimens were fabricated using MFAS and type II fly ash. Ordinary Port-land cement was used, with sea sand as a natural fine aggregate, and crushed stone was used as a coarse aggregate. The properties of raw ash and MFA were tested (Table 4.2). Fly ash was used to partially replace cement. The JIS R 5210 [34] and JIS A 6201 [30] standards were followed.

Table 4.2 Properties of raw ash and MFA

Type	MFA	Raw Ash
LOI (%)	1.75	13
Density (g/cm ³)	2.33	2.32
Blaine (cm ² /g)	3220	4830

4.2.3. Concrete Specimen Tests

The compressive strength test was conducted using cylindrical specimens ($\varnothing = 100$ mm, $h = 200$ mm) according to JIS A 1108 [35]. For each mix, 12 cylinders were cast in a mold and kept in a chamber at 20 °C and 60% relative humidity for 24 h, after which they were demolded. The ages of the tested specimens were 1, 4, and 13 weeks. In addition, a specimen was tested immediately after the curing was complete. The load was applied at a uniform rate to avoid subjecting the specimen to impact loading; the loading rate was such that the compressive stress increased by 0.6 ± 0.4 N/mm² per second. During each test, the static elastic modulus specimens stored at the temperature and humidity specified for the test were tested (JIS A 1149 [36]).

The drying shrinkage test was conducted using a cuboid ($100 \times 100 \times 400$ mm³) according to JIS A 1129-3 [37]. For each mix, three cuboids were cast in a steel mold and kept in a chamber at 20 °C and 60% relative humidity for 24 h until demolded. After demolding, the concrete specimens were immersed in water at 20 ± 2 °C and cured for 7 days. During the drying period, the specimens were kept at least 25 mm apart so as not to impede drying from the bottom of the specimen. Measurements were taken when a specimen was 7 days old, and this time was taken as the reference.

Dynamic elastic modulus tests were conducted using a cylinder or cuboid placed on a support base so that both ends could vibrate freely without being restrained. The output voltage of the amplified pickup was observed, and the frequency at which the indicator had a clear maximum vibration was defined as the primary resonance frequency of the longitudinal vibration according to JIS A 1127 [38].

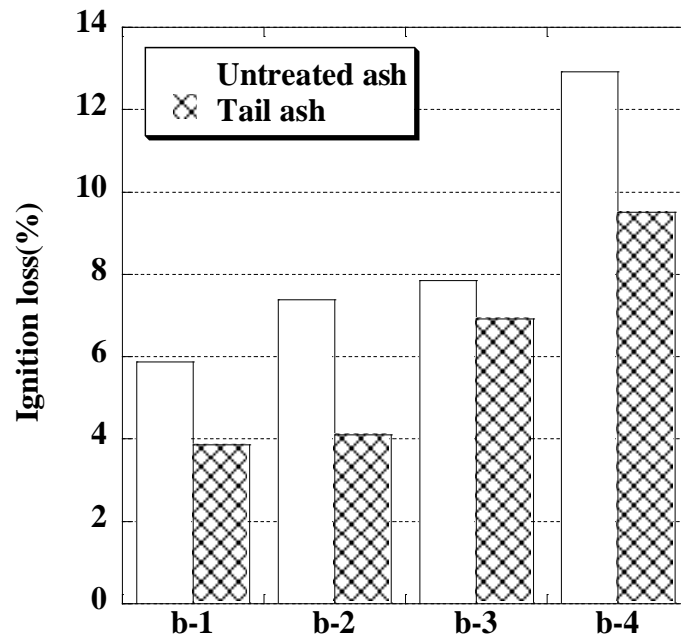
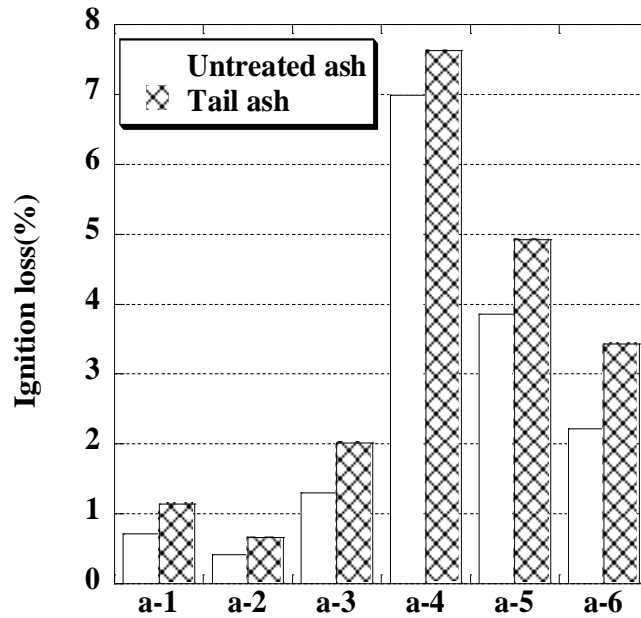
4.3. Results and Discussion

4.3.1. Removal of Unburned Carbon by the Flotation Method

Figure 4. shows the LOI of untreated ash and tail ash for each device. When a diffuser tube was used in experiment I (Figure 4.4a), the LOI of the tail ash for all fly ash was slightly larger than that of the untreated ash in the range of this experiment, showing that the re-moval method had no effect. However, in experiment II (Figure 4.4b), the microbubble gen-erator reduced the LOI and removed unburned carbon from the fly ash. In experiments I and II, it was not possible to compare samples from the same discharge source, but the decrease in LOI was due to the difference in equipment rather than the fly ash characteris-tics. One reason for the larger LOI in experiment I was that the mode of the bubble diame-ter generated from the air diffuser was about 200 μ m, which was about 10 times larger than that of the fly ash particles, and thus it was difficult to collect or raise the unburned carbon

CHAPTER 4: DEVELOPMENT OF FLOTATION DEVICE FOR REMOVING UNBURNT CARBON IN FLY ASH FOR USE IN HARDENED CEMENTITIOUS MATERIALS

to the surface. In contrast, in experiment II, the mode of the microbubble diameter was 40 μm , which was about twice as large as that of the fly ash particles, allowing the unburned carbon to be efficiently collected and raised to the surface. There-fore, microbubbles were effective in removing unburned carbon in fly ash by the flotation method.



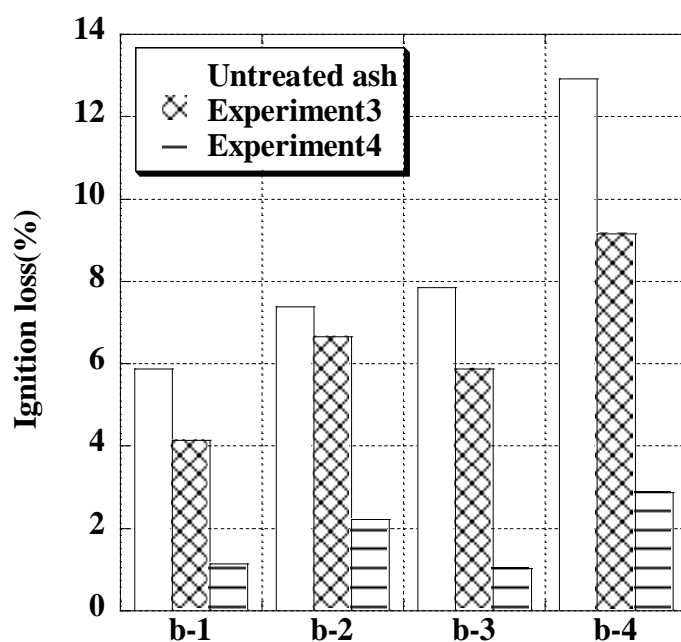


Figure 4.4. LOI of untreated ash and tail ash in experiment I (a), experiment II (b) and experiment III (c)

Next, we compare the results of experiment II, in which pre-stirring was performed, with those of experiment III. For fly ashes b-1 to b-4, the LOI was lower in experiment III than in experiment II. In particular, in experiment II, the LOI was reduced to 3.0% or less by using the circulating microbubble generator in device II, and the fly ash was modified to the equivalent of JIS type I. The circulating microbubble generator prevented the fly ash from settling without a stirrer, and the microbubbles were in uniform contact with the fly ash particles, and so the microbubbles enclosed the unburned carbon collected by the collector, which increased the effectiveness of the device. The effect of pre-stirring in the circulating microbubble generator was examined in experiment III. In the absence of pre-stirring, the LOIs of the tail ash of all types of fly ash were slightly lower than those of the untreated ash (Figure 4.4c). In contrast, when pre-stirring was performed, the LOIs of the tail ash were 3.0% or less for all types of fly ash, and the LOI could be decreased by up to 82%. Especially for fly ash b-4, the untreated ash did not correspond to a JIS type, but the tail ash had an LOI equivalent to JIS type I. Figure 4.5 shows scanning electron microscope images of untreated ash and tail ash of b-1. Unburned carbon and other deposits were attached to the untreated fly ash particles, whereas the unburned carbon was physically removed from the surface of the tail ash particles. Pre-stirring most likely removed the unburned carbon from the fly ash particles and explained why pre-stirring decreased LOI substantially. Therefore, these results showed that for the flotation method using a microbubble generator, unburned carbon in the fly ash was effectively removed by pre-stirring using a mixer. The LOI of the foam ash was in the range of 55 to 70 wt%, indicating that it contained a large amount of unburned carbon and could be used as an auxiliary fuel after drying.

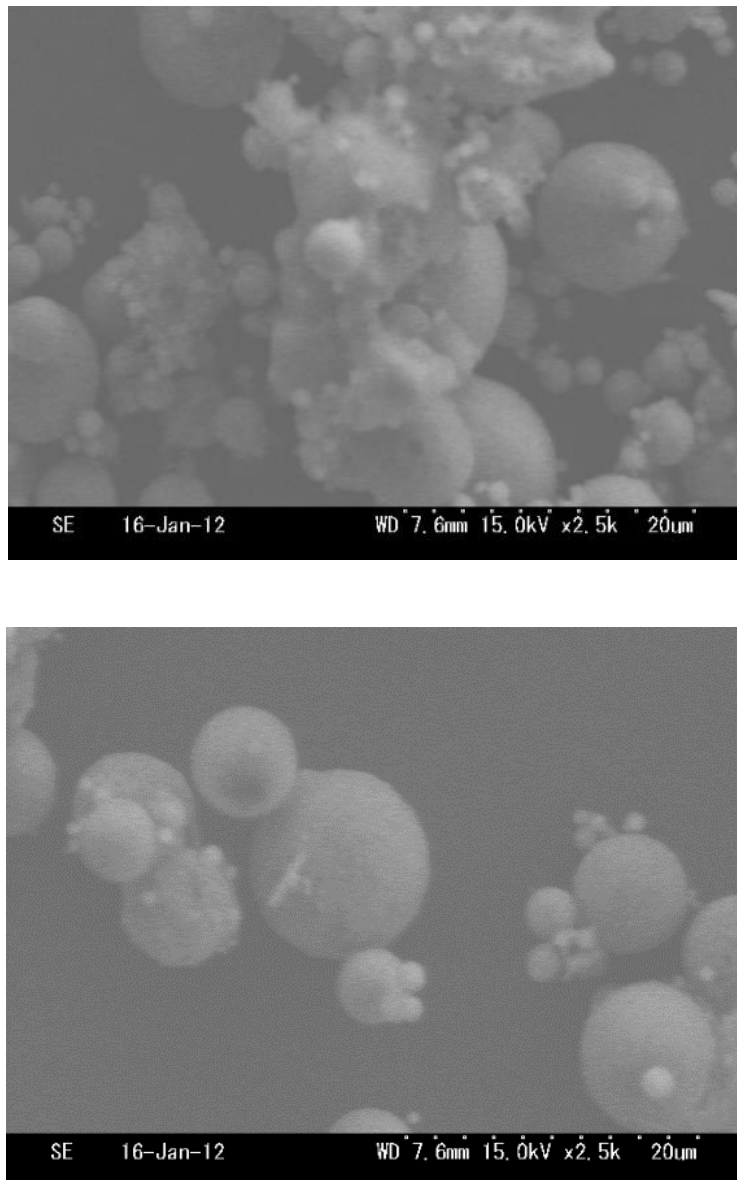


Figure 4.5. SEM images of raw ash and tail ash of b ash-1.

4.3.2. Base Model Development and Performance Verification

Based on the results of experiments I–III, we developed a base model of an unburned coal removal device that used the flotation method. Figure 6 shows the base model of the device, the spiral circulation pump, and the removal of foam ash. Figure 4.7 shows the draw of the base model of the device. The capacity of the device was 130 L. In experimental de-vices I–III, a roller pump was used to circulate the fly ash slurry, but in the base model, a spiral circulation pump with a higher circulation capacity was used. This type of pump can be used in an actual plant with a capacity of 10 m³ or more. In the base model, the mi-crobubble generator was placed eccentrically at the bottom of the side surface of the device to generate a vortex, and the top of the device was conical. This vortex attracts the foam ash to the center and causes the foam ash to flow from the upper part of the device so that it

CHAPTER 4: DEVELOPMENT OF FLOTATION DEVICE FOR REMOVING UNBURNT CARBON IN FLY ASH FOR USE IN HARDENED CEMENTITIOUS MATERIALS

can be automatically discharged. The microbubble diameter was $40\ \mu\text{m}$, the pump out-put was 0.4 kW, the pump flow rate was 30 L/min, and the maximum air supply was 10 L/min. Compared with the traditional flotation technology, it does not need mechanical agitation and has the advantages of a more compact design and lower capital cost.



CHAPTER 4: DEVELOPMENT OF FLOTATION DEVICE FOR REMOVING UNBURNT
CARBON IN FLY ASH FOR USE IN HARDENED CEMENTITIOUS MATERIALS



Figure 4.6. The medium unburned carbon removal device.

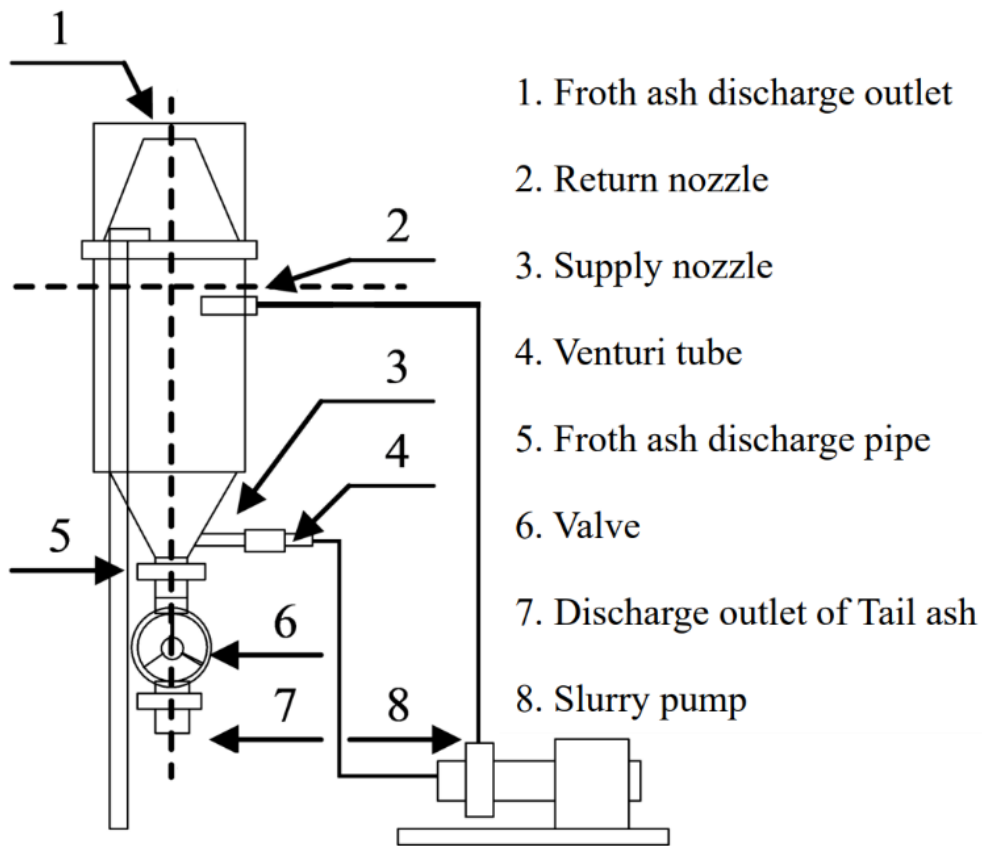


Figure 4.7. The draw of medium unburned carbon removal device.

Figure 4.8 shows the process of the flotation method using this device. The device is composed of the flotation tank, the circulating pump, and the microbubble generator. Fly ash, kerosene, and water are mixed as a prior process, and it is supplied to the flotation tank. The circulating pump is operated, and microbubbles are blown in from the lower side of the flotation tank. The froth ash that contains most of the unburned carbon accumulates and is expelled from the upper part of the flotation tank. The tail ash from which unburned carbon is removed accumulates below and is expelled from the lower side of the flotation tank.

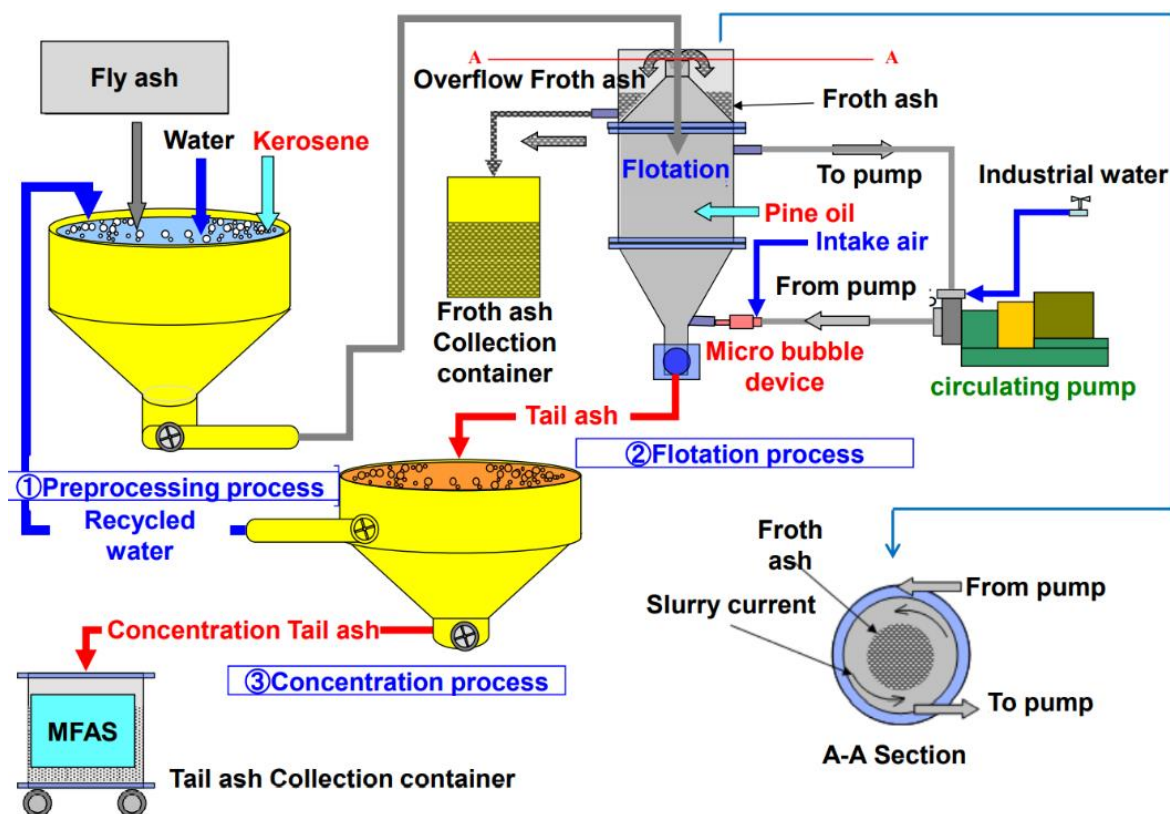


Figure 4.8. The flotation process of using medium unburned carbon removal device.

Fly ashes c and d generated from the two thermal power plants from Japan were used (Table 4.1). Fly ash c was equivalent to JIS type III, and fly ash d did not conform to JIS standards. The experimental procedure was the same as for experiment III with pre-stirring, but because the device capacity was 130 L and the number of input samples was large, pre-mixing was performed with a 50 L concrete mixer which from MARUI & CO., LTD in Japan (speed 50 rpm) to eliminate the effect of the rotation speed caused by the insufficient capacity of the 0.6 L high-speed mixer. However, the rotation speed of the pre-stirring was 1/200th of that in experiment III. To make the total rotation speed of the mixer approximately the same as that in experiment III, the flotation beneficiation time was set to 30 min to consider the increased capacity of the device. The additive addition rate was the same as in experiment III.

Table 4.4 shows the physical characteristics of untreated ash and tail ash for fly ashes c and d. In all ashes, the LOI of the tail ash decreased to 3.0% or less compared with the un-treated ash, the specific surface area decreased, and the density increased due to the re-moval of unburnt carbon, which is porous and amorphous. Fly ash that is usable as various materials, preferably the fly ash with an unburnt carbon content as low as 5 wt%, and more preferably the fly ash with an unburnt carbon content as low as 3 wt%, can be obtained efficiently with a simple structure.

Table 4.4 Physical characteristics of untreated ash and tail ash

Type	LOI (%)	Density (g/cm ³)	Specific Surface Area(cm ² /g)	
C-ash	Untreated ash	7.25	2.30	5560

CHAPTER 4: DEVELOPMENT OF FLOTATION DEVICE FOR REMOVING UNBURNT CARBON IN FLY ASH FOR USE IN HARDENED CEMENTITIOUS MATERIALS

	Tail ash	2.31	2.31	4660
D-ash	Untreated ash	9.85	2.11	6060
	Tail ash	2.88	2.20	4520

Figure 4.9 shows the chemical composition of untreated ash and tail ash obtained by fluorescence X-ray analysis. The chemical composition was analyzed to measure the chemical effects of removing unburned carbon. Some components of the tail ash increased slightly when the LOI decreased, although none of the components changed substantially. Therefore, the unburned carbon removal device did not affect the chemical composition of the fly ash, other than removing the unburned carbon.

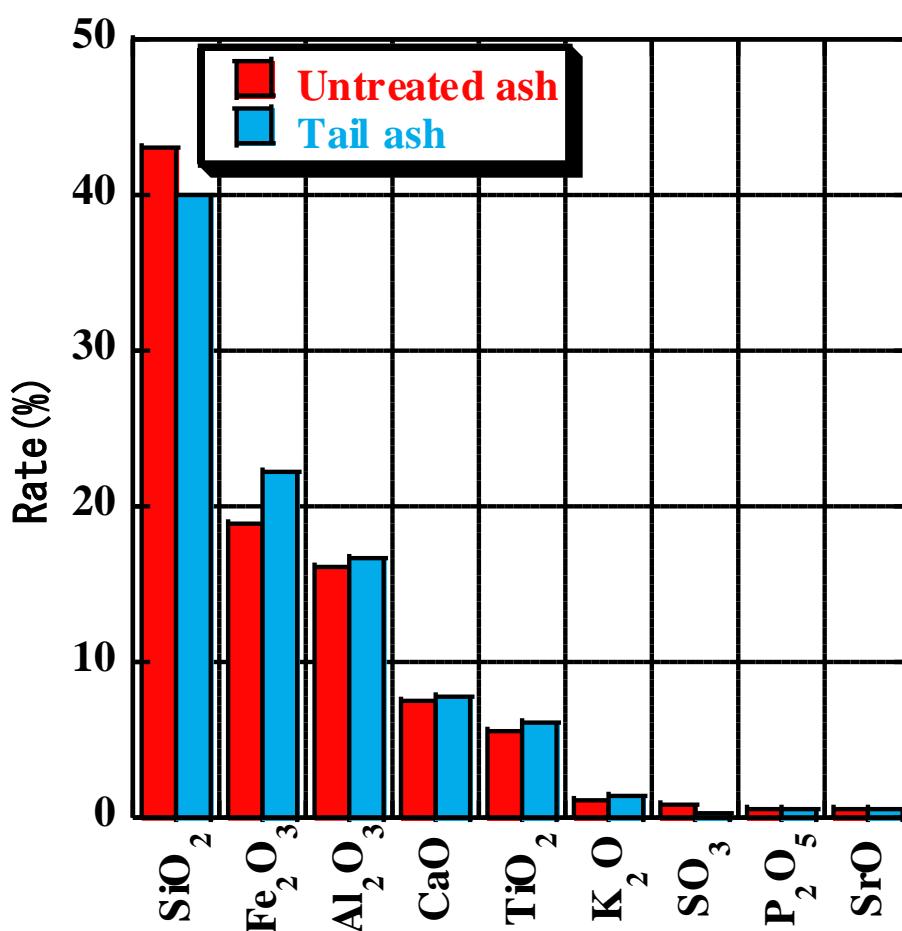


Figure 4.9. Chemical components of untreated ash and tail ash

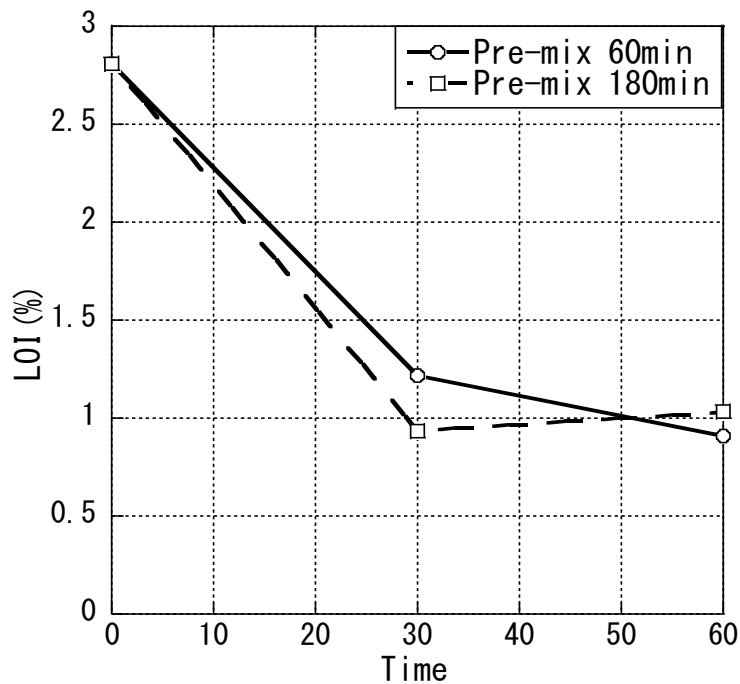
4.3.3. Treatment Conditions

Pre-stirring enhances the interaction between the collector and the fly ash. However, too much energy input from the stirring tank cannot improve the flotation efficiency. Flotation process factors of pre-stirring greatly affect the flotation capacity and efficiency. We examined the effect of the pre-stirring time, fly ash slurry concentration during flotation treatment, flotation processing time, and chemicals, and the optimum treatment conditions, such as the addition rate, in device III. Fly ash e was used in the tests (Table 4.1). Ash e was equivalent to JIS type II, but because the conditions strongly affect the

CHAPTER 4: DEVELOPMENT OF FLOTATION DEVICE FOR REMOVING UNBURNT CARBON IN FLY ASH FOR USE IN HARDENED CEMENTITIOUS MATERIALS

removal of un-burned carbon, untreated ash with a low LOI was selected. First, the pre-stirring time and flotation processing time were examined. The concentration of the fly-ash slurry was set to 60%, and the slurry was pre-stirred using a concrete pan mixer (rotation speed 50 rpm). Then, the slurry concentration was adjusted to 6.6 wt%, and flotation was performed. The chemical addition rate was the same as for experiments I–III (collecting agent 5.0% and foaming agent 0.3% with respect to the fly ash mass). After determining the appropriate treatment time, the slurry concentration during the flotation treatment was changed to examine the treatment efficiency, and finally the chemical addition rate was changed. The microbubble diameter was 40 μm , the pump output was 0.4 kW, the pump flow rate was 30 L/min, and the maximum air supply was 10 L/min.

Figure 10a shows the LOI after 60 min of flotation treatment with 60 or 180 min of pre-stirring. The LOI was measured during the flotation treatment by sampling the tail ash from the tail ash outlet at 30 and 60 min without stopping the equipment. At 60 min, LOI was 0.12% lower for a pre-stirring time of 180 min; thus, the effect of the pre-stirring time on the reduction in LOI was small. After 30 min, there was a large reduction in LOI, and a smaller change after 60 min, which suggested that the flotation treatment time could be shortened to 30 min or less.



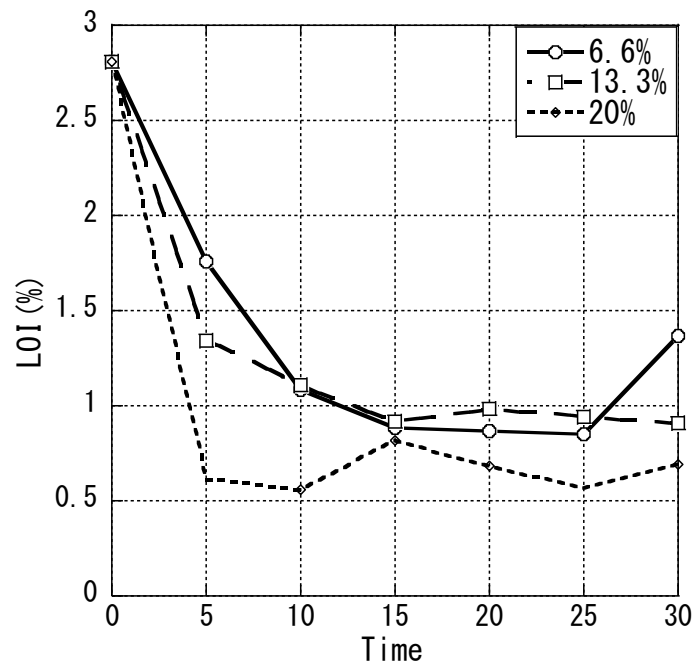
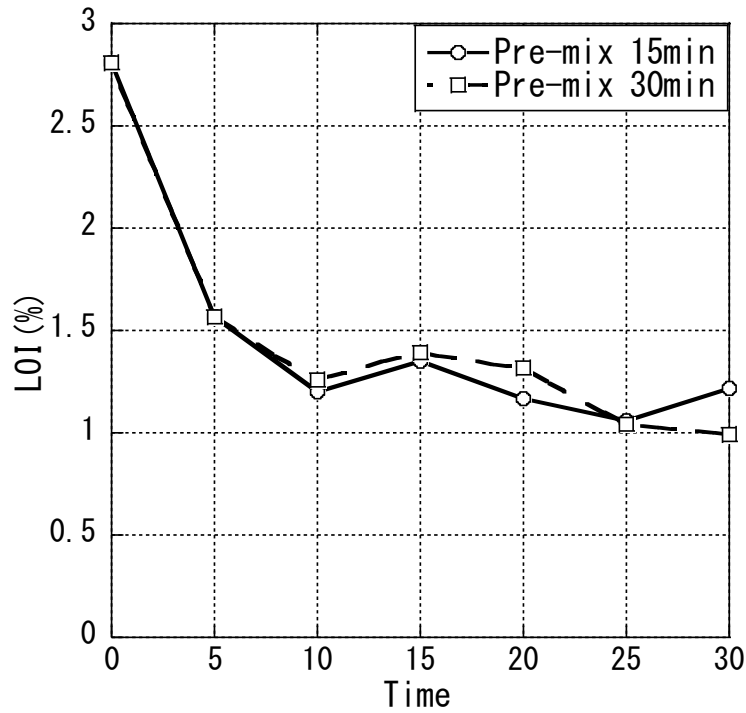


Figure 4.10. LOI of the flotation treatment with 60 or 180 min (a) and 15 or 30 min (b) pre-stirring, and at slurry concentrations of 6.6, 13.3, and 20.0 wt% (c).

Figure 4.10b shows the time course of the tail ash LOI sampled every 5 min up to a flotation time of 30 min with a pre-stirring time of 15 or 30 min. LOI was greatly reduced within 10 min. Because decreasing the pre-stirring time from 60 min to 15 min reduced the LOI, and there was almost no

CHAPTER 4: DEVELOPMENT OF FLOTATION DEVICE FOR REMOVING UNBURNED CARBON IN FLY ASH FOR USE IN HARDENED CEMENTITIOUS MATERIALS

difference in LOI between pre-stirring times of 15 and 30 min, in the subsequent experiments the pre-stirring time and flotation treatment time were each set to 30 min for safety considerations.

In the flotation treatment, the efficiency of one treatment increased when the fly ash slurry concentration was increased. Therefore, we investigated the change over time in LOI at slurry concentrations of 6.6, 13.3, and 20.0 wt% (Figure 10c). At all fly ash slurry concentrations, the reduction in LOI was large within 10 min, and the smallest reduction was for a fly ash slurry concentration of 20.0 wt%. A preliminary experiment with a slurry concentration of 25.0 wt% showed that the reduction rate of LOI was lower than that at 20.0 wt% (data not shown). Therefore, the floating beneficiation method was efficient at a slurry concentration of 20.0 wt%.

The addition rates of the collecting agent and foaming agent were examined because they affect the processing cost. Flotation treatment was performed under a total of nine conditions at different mixing ratios. Here, we set the fly ash slurry concentration to 6.6 wt%. Figure 11 shows the relationship between the additive cost ratio and LOI under each condition, where the additive cost for treatment with 5.0% collecting agent and 0.3% foaming agent is 1.0. The additive cost is the unit price when 18 L of the collecting agent and 18 L of the foaming agent are purchased as laboratory chemicals, and the LOI was measured after 30 min treatment by the flotation method. Assuming that the LOI control value was 1.0% or less, the best mixing ratio was 3.0% for the collecting agent and 0.2% for the foaming agent, which was a reduction of about 40% for the collector and about 33% for the foaming agent compared with the initial conditions. However, because the additive addition rate depends on the control value of LOI, the rate must be set at the operation stage, and the optimum mixing ratio can be determined by conducting the same experiment. In addition, the results show that the removal of unburned carbon was high for a ratio of 3.0% for the collecting agent and 0.3% for the foaming agent. The unburned carbon removal did not increase with the collection agent addition rate, whereas it did increase with the foaming agent addition rate. It is considered that there may be an optimum addition rate. Furthermore, the optimum additive addition rate is expected to depend on the type of fly ash and thus requires further study.

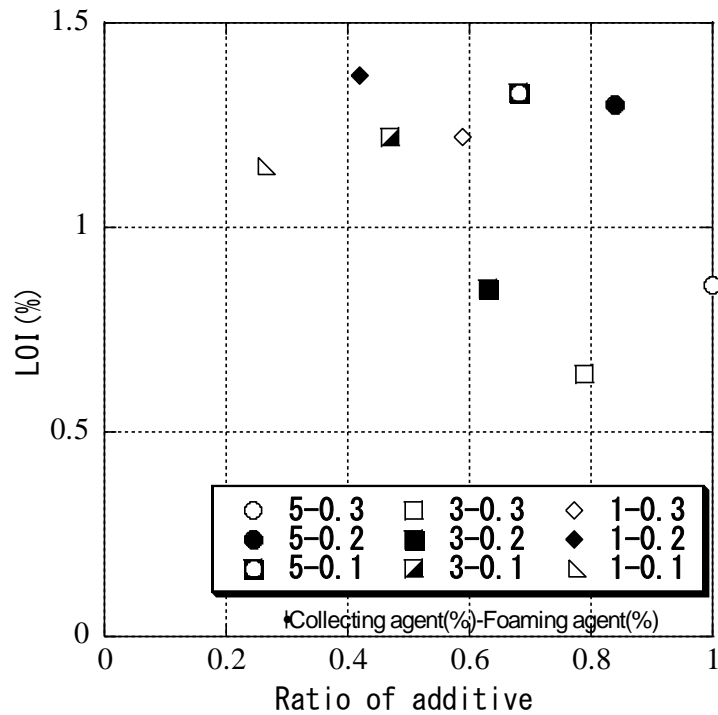


Figure 4.11. Relationship between the agent ratio and LOI under each condition

4.3.4. Properties of Concrete with MFAS

The mechanical and physical properties of concrete with fly ash replacement ratios of 15% and 30% and different amounts of MFAS were measured.

Figure 4.12a shows the compressive strength of concrete containing recycled aggregate and fly ash or modified fly ash at 7–91 days. Using fly ash reduced the compressive strength of concrete at 7–91 days, and a 30% replacement ratio decreased the compressive strength with more than a 15% replacement ratio. For a replacement ratio of 15%, although the strength for modified fly ash concrete was lower than that for normal fly ash concrete, the modified fly ash concrete strength increased faster. At 7, 28, and 91 days, the strengths of F15 (15% fly ash) were 81.1%, 84.7%, and 97.5%, whereas the strengths of M15 (15% modified fly ash concrete) were 71.2%, 79.1%, and 92.5%, respectively. For the re-placement ratio of 30%, the growth rate of the strength of fly ash and modified fly ash concrete was the same. At 7, 28, and 91 days, the strengths of F30 (30% fly ash) were 60.7%, 72.5%, and 86.6%, whereas the strengths of M30 (30% modified fly ash concrete) were 60.0%, 68.5%, and 82.5%, respectively.

CHAPTER 4: DEVELOPMENT OF FLOTATION DEVICE FOR REMOVING UNBURNT CARBON IN FLY ASH FOR USE IN HARDENED CEMENTITIOUS MATERIALS

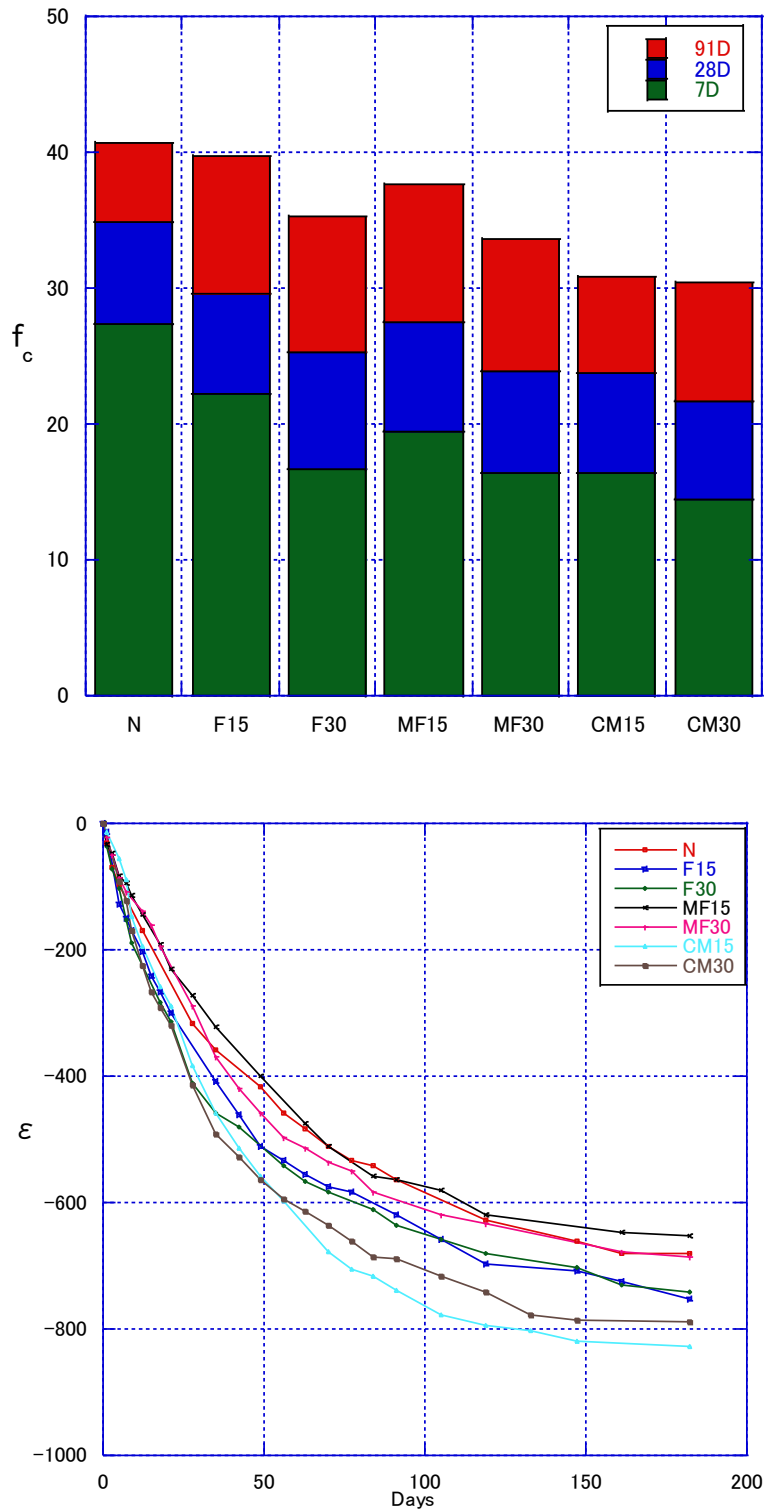


Figure 4.12. Compressive strength (a) and drying shrinkage (b) of concrete with modified fly ash slurry.

The use of MFA had little effect on the strength of concrete. This is because the chemical characteristics of fly ash have a large effect on pozzolanic reactivity [39], and as discussed above, the

flotation does not change the chemical characteristics of FA. Adding 30% of MFA or FA had a greater impact on the strength of concrete, increasing it by more than 15%. However, for recycled concrete, the two different mixing amounts of MFA or FA showed a very minor difference in strength. In words, the impact on the strength of recycled concrete was very minor.

Figure 12b shows the drying shrinkage of concrete specimens containing recycled aggregate and fly ash or modified fly ash up to 118 days—see the F15 line and F30 line in the figure, which are both below the red line. Fly ash increased the drying shrinkage of concrete compared with the control. The distance between these two lines is small. At fly ash replacement ratios of 15–30%, the replacement ratio did not affect the drying shrinkage—see the C100M15 line and C100M30 line, which are both below the red line. The distance between these two lines is small. At fly ash replacement ratios of 15–30%, and a recycled aggregate replacement ratio of 100%, the fly ash replacement ratio did not affect the drying shrinkage. The distance between the two lines is small. This suggests that within a certain range (15–30%), for non-mixed aggregates, the influence of fly ash on drying shrinkage is constant. Therefore, the carbon content of FA is different, and the effect on the drying shrinkage of concrete is different. However, the amount of FA mixed does not have a huge impact on the drying shrinkage.

Figure 4.13 shows the static elastic modulus and dynamic elastic modulus of concrete containing MFAS. The measurement of the static elastic modulus destroys the concrete test block, whereas the measurement of the dynamic elastic modulus does not; thus, measuring the dynamic elastic modulus is more convenient. Both measure the same characteristic of concrete, and thus showed consistent results. The effect of fly ash content on both moduli decreased as the fly ash content increased. The trend of the elastic modulus is consistent with the performance of the concrete's compressive strength, indicating that there is a certain correlation between the static elastic modulus and the compressive strength, and the trend of the dynamic elastic modulus is also consistent, meaning that when predicting the compressive strength of concrete, the dynamic elasticity modulus can also be used as an important factor, and is not limited to ordinary concrete. For example, when Farooq et al. [40] predicted self-compacting concrete, the dynamic elastic modulus was considered as a factor.

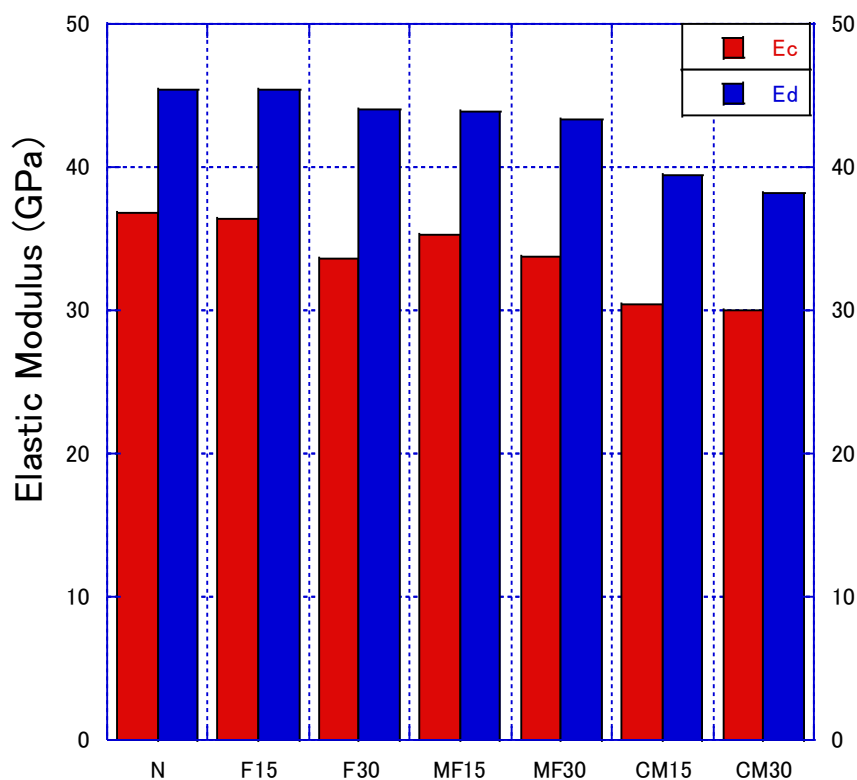


Figure 4.13 Static elastic modulus and dynamic elastic modulus of concrete

4.4. Conclusions

We developed a prototype device for removing unburned carbon from fly ash by means of the flotation method and examined the operating conditions of the device experimentally. The fly ash was used in Portland cement concrete and the concrete properties were measured. Our findings are summarized as follows.

The base model, which used a circulating microbubble generator with a spiral pump, removed unburned carbon from fly ash by means of the froth flotation method without affecting the chemical composition of the fly ash. The removal efficiency was increased by adding a collecting agent to 60 wt% fly ash slurry and pre-stirring with a concrete mixer for 30 min. The LOI was greatly reduced within 10 min, and a treatment time of 30 min was sufficient. Flotation was improved by pre-stirring the sample and adding water to form a slurry with a concentration of 20 wt%.

MFAS was used in the mortar, and its properties were better than those of dry fly ash. MFAS reduced the compressive strength of concrete at 7–91 days. The drying shrinkage of concrete containing fly ash was greater than that of ordinary concrete; however, at fly ash replacement ratios of 15–30%, the replacement ratio did not affect the drying shrinkage.

Our results demonstrate that it is feasible to use modified fly ash prepared using the flotation method in concrete.

References

1. Furubayashi, T. Design and analysis of a 100% renewable energy system for Akita prefecture, Japan. *Smart Energy* 2021, 2, 100012. <https://doi.org/10.1016/j.segy.2021.100012>.
2. Matsumoto, K.I. Economic Analysis of Introducing Renewable Energy in a Remote Island: A Case Study of Tsushima Island, Japan. 2021. <https://ssrn.com/abstract=3880819>. (3/9/2021) <http://dx.doi.org/10.2139/ssrn.3880819>.
3. Kikuchi, M. Changing dynamics of the nuclear energy policy-making process in Japan. *Environ. Policy Gov.* 2020, 31, 116–124, <https://doi.org/10.1002/eet.1922>.
4. Gollakota, A.R.; Volli, V.; Shu, C.-M. Progressive utilisation prospects of coal fly ash: A review. *Sci. Total. Environ.* 2019, 672, 951–989, <https://doi.org/10.1016/j.scitotenv.2019.03.337>.
5. Sancho, I.; Licon, E.; Valderrama, C.; de Arespacochaga, N.; López-Palau, S.; Cortina, J.L. Recovery of ammonia from domestic wastewater effluents as liquid fertilizers by integration of natural zeolites and hollow fibre membrane contactors. *Sci. Total. Environ.* 2017, 584-585, 244–251, <https://doi.org/10.1016/j.scitotenv.2017.01.123>.
6. Xiao, J.; Li, W.; Poon, C.S. Recent studies on mechanical properties of recycled aggregate concrete in China—A review. *Sci. China Ser. E Technol. Sci.* 2012, 55, 1463–1480, <https://doi.org/10.1007/s11431-012-4786>
7. Guo, H.; Shi, C.; Guan, X.; Zhu, J.; Ding, Y.; Ling, T.-C.; Zhang, H.; Wang, Y. Durability of recycled aggregate concrete—A review. *Cem. Concr. Compos.* 2018, 89, 251–259, <https://doi.org/10.1016/j.cemconcomp.2018.03.008>.
8. Kou, S.C.; Poon, C.S.; Chan, D. Influence of fly ash as a cement addition on the hardened properties of recycled aggregate concrete. *Mater. Struct.* 2007, 41, 1191–1201, <https://doi.org/10.1617/s11527-007-9317-y>.
9. Kou, S.C.; Poon, C.S.; Chan, D. Influence of fly ash as cement replacement on the properties of recycled aggregate concrete. *J. Mater. Civ. Eng.* 2007, 19, 709–717, [https://doi.org/10.1061/\(asce\)0899-1561\(2007\)19:9\(709\)](https://doi.org/10.1061/(asce)0899-1561(2007)19:9(709)).
10. Katar, I.; Ibrahim, Y.; Malik, M.A.; Khahro, S. Mechanical Properties of Concrete with Recycled Concrete Aggregate and Fly Ash. *Recycling* 2021, 6, 23, <https://doi.org/10.3390/recycling6020023>.
11. Shariati, M.; Mafipour, M.S.; Mehrabi, P.; Ahmadi, M.; Wakil, K.; Trung, N.T.; Toghroli, A.J.S.S. Systems, Prediction of concrete strength in presence of furnace slag and fly ash using Hybrid ANN-GA (Artificial Neural Network-Genetic Algorithm). *Smart Struct. Syst.* 2020, 25, 183–195. <https://doi.org/10.12989/sss.2020.25.2.183>.
12. Oner, A.; Akyuz, S.; Yildiz, R. An experimental study on strength development of concrete containing fly ash and optimum usage of fly ash in concrete. *Cem. Concr. Res.* 2005, 35, 1165–1171, <https://doi.org/10.1016/j.cemconres.2004.09.031>.
13. Wang, Q.; Wang, D.; Chen, H. The role of fly ash microsphere in the microstructure and macroscopic properties of high-strength concrete. *Cem. Concr. Compos.* 2017, 83, 125–137, <https://doi.org/10.1016/j.cemconcomp.2017.07.021>.
14. Architectural Institute of Japan, Japanese Architectural Standard Specification JASS 5 Reinforced Concrete Work; Architectural Institute of Japan, Tokyo, Japan, 2009; pp.187, 672.
15. Feng, X.; Clark, B. In Evaluation of the physical and chemical properties of fly ash products for

CHAPTER 4: DEVELOPMENT OF FLOTATION DEVICE FOR REMOVING UNBURNT CARBON IN FLY ASH FOR USE IN HARDENED CEMENTITIOUS MATERIALS

use in Portland cement concrete. In Proceedings of the World of Coal Ash (WOCA) Conference, Denver, CO, USA, 9–12 May 2011; pp. 1–8.

16. Zhang, W.; Honaker, R. Studies on carbon flotation from fly ash. *Fuel Process. Technol.* 2015, 139, 236–241, <https://doi.org/10.1016/j.fuproc.2015.06.045>.
17. Yang, L.; Zhu, Z.; Li, D.; Yan, X.; Zhang, H. Effects of particle size on the flotation behavior of coal fly ash. *Waste Manag.* 2019, 85, 490–497, <https://doi.org/10.1016/j.wasman.2019.01.017>.
18. Walker, A.; Wheelock, T.D. Separation of Carbon from Fly Ash Using Froth Flotation. *Coal Prep.* 2006, 26, 235–250, <https://doi.org/10.1080/07349340601104883>.
19. Temuujin, J.; Surenjav, E.; Ruescher, C.H.; Vahlbruch, J.J.C. Processing and uses of fly ash addressing radioactivity (critical review). *Chemosphere* 2019, 216, 866–882. <https://doi.org/10.1016/j.powtec.2019.05.037>.
20. Bittner, J.; Hrach, F.; Gasiorowski, S.; Canellopoulos, L.; Guicherd, H. Triboelectric belt separator for beneficiation of fine minerals. *Procedia Eng.* 2014, 83, 122–129, <https://doi.org/10.1016/j.proeng.2014.09.021>.
21. Soong, Y.; Schoffstall, M.; Link, T. Triboelectrostatic beneficiation of fly ash. *Fuel* 2001, 80, 879–884, [https://doi.org/10.1016/s0016-2361\(00\)00150-2](https://doi.org/10.1016/s0016-2361(00)00150-2).
22. Ejtemaei, M.; Gharabaghi, M.; Irannajad, M. A review of zinc oxide mineral beneficiation using flotation method. *Adv. Colloid Interface Sci.* 2014, 206, 68–78, <https://doi.org/10.1016/j.cis.2013.02.003>.
23. Ayhan, F.D.; Abakay, A.H.; Saydut, A. Desulfurization and Deashing of Hazro Coal via a Flotation Method. *Energy Fuels* 2005, 19, 1003–1007, <https://doi.org/10.1021/ef049747r>.
24. Yang, L.; Li, D.; Zhang, L.; Yan, X.; Ran, J.; Wang, Y.; Zhang, H. On the utilization of waste fried oil as flotation collector to remove carbon from coal fly ash. *Waste Manag.* 2020, 113, 62–69, <https://doi.org/10.1016/j.wasman.2020.05.045>.
25. Drzymala, J.; Gorke, J.T.; Wheelock, T.D. A flotation collector for the separation of unburned carbon from fly ash. *Coal Prep.* 2005, 25, 67–80, <https://doi.org/10.1080/07349340590927404>.
26. Xia, Y.; Yang, Z.; Zhang, R.; Xing, Y.; Gui, X. Enhancement of the surface hydrophobicity of low-rank coal by adsorbing DTAB: An experimental and molecular dynamics simulation study. *Fuel* 2018, 239, 145–152, <https://doi.org/10.1016/j.fuel.2018.10.156>.
27. Altun, N.E.; Xiao, C.; Hwang, J.-Y. Separation of unburned carbon from fly ash using a concurrent flotation column. *Fuel Process. Technol.* 2009, 90, 1464–1470, <https://doi.org/10.1016/j.fuproc.2009.06.029>.
28. Li, G.; Deng, L.; Liu, J.; Cao, Y.; Zhang, H.; Ran, J. A new technique for removing unburned carbon from coal fly ash at an industrial scale. *Int. J. Coal Prep. Util.* 2014, 35, 273–279, <https://doi.org/10.1080/19392699.2015.1008098>.
29. Uçurum, M. Influences of Jameson flotation operation variables on the kinetics and recovery of unburned carbon. *Powder Technol.* 2009, 191, 240–246, <https://doi.org/10.1016/j.powtec.2008.10.014>.
30. JIS A 6201, 2015. Fly Ash for Use in Concrete. Japanese Industrial Standard Committee, Japan, 2015. Available online: www.jisc.go.jp (15/7/2021).
31. Yang, L.; Li, D.; Zhu, Z.; Xu, M.; Yan, X.; Zhang, H. Effect of the intensification of preconditioning on the separation of unburned carbon from coal fly ash. *Fuel* 2019, 242, 174–183,

CHAPTER 4: DEVELOPMENT OF FLOTATION DEVICE FOR REMOVING UNBURNT
CARBON IN FLY ASH FOR USE IN HARDENED CEMENTITIOUS MATERIALS

<https://doi.org/10.1016/j.fuel.2019.01.038>.

32. Yang, L.; Zhu, Z.; Qi, X.; Yan, X.; Zhang, H. The process of the intensification of coal fly ash flotation using a stirred tank. *Minerals* 2018, 8, 597, <https://doi.org/10.3390/min8120597>.
33. Yu, Y.; Cheng, G.; Ma, L.; Huang, G.; Wu, L.; Xu, H. Effect of agitation on the interaction of coal and kaolinite in flotation. *Powder Technol.* 2017, 313, 122–128, <https://doi.org/10.1016/j.powtec.2017.03.002>.
34. JIS R 5201, 2015. Physical Testing Methods for Cement. Japanese Industrial Standard Committee, Japan, 2015. Available online: www.jisc.go.jp (21/7/2021).
35. JIS A 1108, 2018. Method of Test for Compressive Strength of Concrete. Japanese Industrial Standard Committee, Japan, 2018. Available online: www.jisc.go.jp (28/7/2021).
36. JIS A 1149, 2017. Method of Test for Static Modulus of Elasticity of Concrete. Japanese Industrial Standard Committee, Japan, 2017. Available online: www.jisc.go.jp (1/8/2021).
37. JIS A 1129-3, 2010. Methods of Measurement for Length Change of Mortar and Concrete–Part 3: Method with Dial Gauge. Japanese Industrial Standard Committee, Japan, 2010. Available online: www.jisc.go.jp (3/8/2021).
38. JIS A 1127, 2010. Methods of Test for Dynamic Modulus of Elasticity, Rigidity and Poisson's Ratio of Concrete by Resonance Vibration. Japanese Industrial Standard Committee, Japan, 2010. Available online: www.jisc.go.jp (6/8/2021).
39. Cho, Y.K.; Jung, S.H.; Choi, Y.C. Effects of chemical composition of fly ash on compressive strength of fly ash cement mortar. *Constr. Build. Mater.* 2019, 204, 255–264, <https://doi.org/10.1016/j.conbuildmat.2019.01.208>.
40. Farooq, F.; Czarnecki, S.; Niewiadomski, P.; Aslam, F.; Alabduljabbar, H.; Ostrowski, K.A.; Śliwa-Wieczorek, K.; Nowobilski, T.; Malazdrewicz, S. A Comparative Study for the Prediction of the Compressive Strength of Self-Compacting Concrete Modified with Fly Ash. *Materials* 2021, 14, 4934, <https://doi.org/10.3390/ma14174934>.

Chapter 5

***EFFECT OF INCORPORATING FLY ASH AND
RECYCLED FINE AGGREGATE ON PROPERTIES
AND CUMULATIVE PORE VOLUME OF
CONCRETE***

CHAPTER 5: EFFECT OF INCORPORATING FLY ASH AND RECYCLED FINE AGGREGATE
ON PROPERTIES AND CUMULATIVE PORE VOLUME OF CONCRETE

5.1. Introduction

It is well known that natural gravel used in concrete production will lead to the renewable resource reduction and environment poverty. The mass of aggregate in concrete accounts for a large proportion, resulting in the properties of the aggregate has a significant impact on the engineering performance of the concrete product [1]. Therefore, to achieve sustainable development and construction, the use of recycled fine aggregate (RFA) and maximize it in concrete manufacturing is a promising approach [2,3]. Ordinary concrete has half the permeability value of recycled aggregate concrete (RAC) which is a porous concrete [4]. When ordinary aggregates are largely replaced by recycled aggregates which can have a significant impact on the properties of RAC, it shows a decrease in mechanical properties. [5].

The durability properties of RAC are major problems that is continuously concerned all over the world and enhancing the durability properties for RAC are common research in the world, and it is considered that managing these will lead to an increase in the use of RAC to building structures. The behavior of recycled aggregate generally shows increases in the water absorption and drying shrinkage and reduces the modulus of elasticity, workability and compressive strength of RAC compared to the concrete using natural aggregate [6,7]. Hansen thought that, compared with the RAC, the shrinkage of control concrete was decreased by 37% [8]. Domingo-Cabo thought that the shrinkage of reference concrete was, after a period of 180 days, about 40% lower than that of the RAC using 100% recycled aggregate [9]. And Pacheco thought that for 100% recycled aggregate incorporation ratios, compressive strength of RAC decreased about 10% on 28 days [10]. The impact of recycled aggregate on the physical properties and workability of RAC is related to the amount and quality of adhered mortar which affects the particle density and the porosity of the recycled aggregate and enhance their water absorption capacity [11].

In past research, main studies focused on the RAC which use coarse recycled aggregates, while the properties of RAC which use RFA is still poorly investigated, as it can have significant impact on certain properties of RAC [12,13]. However, RAC using RFAs also has great international interest, mainly due to the economic impact and environmental considerations associated with the reduction of natural sand used in producing ordinal concrete [14]. Cement and aggregate-based concretes are, now and in the nearest future, a basic building material [15]. The cement used in concrete production will also lead to the natural resources reduction and impact the ecological conditions, and it stimulate the studies aiming at the decrease of use of cement in concrete components. Generally, fly ash (FA) can be used to replace the cement used in the production of concrete and it is one of the effective methods and meets the environmental protection and sustainable development of society.

FA is the fine residue that generated by the combustion of ground or powered coal and that is transported through flue gasses. Global FA production is estimated to be around 900-1000 million tons and the utilization rate of cement and concrete components is about 30% [16]. Concrete shows a decrease in their early age when there is percentage of replacement of ordinary cement by FA. But concrete with the addition of FA has a higher or similar strength in later period than the concrete without FA. In general, the concrete using FA as an additive or replace cement is characterized by improved durability [17,18]. Higher compressive strength of concretes when adding FA is related to improved bonding between aggregates and slurry and the denser microstructure obtained by changing the pore size distribution [19]. FA has a reducing effect on both ordinary concrete and RAC and the

CHAPTER 5: EFFECT OF INCORPORATING FLY ASH AND RECYCLED FINE AGGREGATE ON PROPERTIES AND CUMULATIVE PORE VOLUME OF CONCRETE

use of FA can improve the increase in shrinkage caused by recycled aggregate. When using FA, the shrinkage of concrete, incorporating 100% RFA, is 17% lower than that of concrete without FA [20,21]. Researchers reported that when 35% (by weight) of cement is replaced by FA, the shrinkage strain of all concrete will decrease by 55×10^{-6} , in average, and the shrinkage strain of concrete without FA will be 18-25% higher than that with FA at the age of 112 days. Using FA as an alternative cement or as an additive which can improve the durability and workability of the concrete is the recommended approach, for protecting the environment and reducing the consumption of water resources. [22-24] Since recycled aggregate often present old adhered mortar which makes the RAC microstructure more fragile, the porosity of RAC is usually higher than that of ordinary concrete [25]. There are two most important characteristics of the pore system of concrete: porosity and pore size distribution, which will help to evaluate the properties of the RAC. [26].

Implementing sustainable development while preserving the local environment is a common challenge. Industrial and urban development require the construction of large numbers of houses, roads, and other structures, resulting in substantial environmental impacts. Incorporating natural gravel and cement into the concrete used in construction work has the potential increase the use of renewable resources and reduce environmental poverty. Much research has been conducted in which these materials are substituted individually, but the physical and mechanical properties of concrete produced using both RFA and FA remains to be investigated. This research is a contribution to this topic and focusing on the compressive strength and drying shrinkage of concrete containing both RFA and FA. The properties of RAC were investigated and the results were used to perform simple linear regression. The correlation coefficients between the cumulative pore volume at different pore diameters and the compressive strength or drying shrinkage of the concrete were calculated to determine the optimal interval division of the correlation.

5.2. Experimental outlines

Ordinary Portland cement was used, with sea sand as a natural fine aggregate and as a RFA, and crushed stone was used as a coarse aggregate. The physical properties of natural aggregate and RFA are shown in Table 5.1. FA was used to partially replace cement. in this study. Following JIS R 5210 and JIS A 6201 standards, ordinary Portland cement and class II FA were considered. The chemical composition and physical properties of FA are listed in Tables 5.2.

Table 5.1 Characteristics of natural aggregate and RFA

Property	Coarse aggregate	Fine aggregate	RFA
Partical oven-dried density (g/cm ³)	2.69	2.59	2.23
Fineness modulus	6.9	2.58	4.3
Water absorption (%)	1.14	1.04	7.38
Solid content (%)	62.1	60.9	56.6

Table 5.2 Chemical composition and physical properties of FA

SiO ₂ (%)	53.8
Al ₂ O ₃ (%)	13.5
Fe ₂ O ₃ (%)	13

CHAPTER 5: EFFECT OF INCORPORATING FLY ASH AND RECYCLED FINE AGGREGATE
ON PROPERTIES AND CUMULATIVE PORE VOLUME OF CONCRETE

CaO (%)	8.99
SO ₃ (%)	0.489
MgO (%)	1.48
Loss on ignition (%)	2.1
Density (g/cm ³)	2.2
Blaine specific area (cm ² /g)	3270

Table 5.3 gives the mix proportions and compressive strength of the concrete. For the mix proportions, the unit water amount was 180 kg/m³, the unit cement amount was 327 kg/m³, the water-to-binder ratio was either 55% or 40%, and the replacement ratio of the RFA was either 50% or 100%. RFA replaces natural aggregate by volume and FA replaces Ordinary Portland cement by weight. In these experiments, only the fine aggregate was recycled; natural crushed stone was used as coarse aggregate in all mix proportions. The symbol M0 is the mix proportions of natural aggregate including both coarse aggregate and fine aggregate. As an example of how the replacement ratio of the RFA is indicated, M50 is the mix that uses 50% class-M RFA and 50% sea sand. As an example of how the replacement ratio of the FA is indicated, FA10 is the mix in which cement is replaced with 10% FA. The mixing procedure is shown below: Fine aggregate and cement are putted in and mix for 30s; Insert water and mix for 60s; Input coarse aggregate and mix for 60

CHAPTER 5: EFFECT OF INCORPORATING FLY ASH AND RECYCLED FINE AGGREGATE ON PROPERTIES AND CUMULATIVE PORE VOLUME OF CONCRETE

Table 5.3 Mix proportions and compressive strength

	W/ C (%)	W/ B (%)	Unit mass(kg/m ³)						Compressive strength (MPa)			
			Water	Cement	F A	Fine aggreg ate	Recycl ed fine aggreg ate	Coarse aggreg ate	7day s	28day s	91day s	
M0-FA0	55			327	0	832	0			16.4 2	22.25	26.46
M50-FA0	55			327	0	398	398			15.7 8	23.03	24.94
M100-FA0	55			327	0	0	765			12.5 3	18.83	22.97
N-FA10	61			295	3 3	826	0			15.7 3	20.79	28.15
M50-FA10	61	55		295	3 3	396	396			13.7 1	18.89	25.19
M100-FA10	61			295	3 3	0	759			13.6 2	19.33	25.70
M0-FA20	69			262	6 5	820	0			12.4 3	17.97	25.04
M50-FA20	69			262	6 5	392	392			9.87	15.25	22.55
M100-FA20	69		180	262	6 5	0	754	945		8.21	12.70	17.91
M-FA0	40			450	0	731	0			30.4 9	37.80	41.67
M50-FA0	40			450	0	350	350			26.6 7	34.17	40.48
M100-FA0	40			450	0	0	672			25.2 6	33.91	40.92
M0-FA10	44	40		405	4 5	723	0			31.8 4	41.37	50.42
M50-FA10	44			405	4 5	346	346			27.7 8	36.71	45.03
M100-FA10	44			405	4 5	0	665			27.0 9	34.11	40.40
M0-FA20	50			360	9 0	716	0			27.6 3	36.65	46.20
M50-	50			360	9	342	342			25.1	34.09	44.43

CHAPTER 5: EFFECT OF INCORPORATING FLY ASH AND RECYCLED FINE AGGREGATE
ON PROPERTIES AND CUMULATIVE PORE VOLUME OF CONCRETE

FA20			0			4		
M100-FA20	50	360	9	0	658	26.0	34.54	41.43
			0			9		

The compressive strength test was conducted using a cylinder ($\varnothing=100\text{ mm} \times h=200\text{ mm}$) in accordance with JIS A 1108. For each mix, 12 cylinders were cast in a mold and kept in a chamber at $20\text{ }^{\circ}\text{C}$ and 60% RH for 24 hours until demolded. The ages of the tested specimens were 1, 4, and 13 weeks. In addition, a specimen was tested immediately after the prescribed curing was completed. The load was applied at a uniform rate to avoid subjecting the specimen to impact loading; the loading rate was such that the compressive stress increased by $0.6\pm 0.4\text{ N/mm}^2$ per second. During each test, the specimens were stored at the temperature and humidity specified for that test.

The drying shrinkage test was conducted using a cuboid ($100 \times 100 \times 400\text{ mm}$) in accordance with JIS A 1129-3. For each mix, 3 cuboids were cast in a steel mold and kept in a chamber at $20\text{ }^{\circ}\text{C}$ and 60% RH for 24 hours until demolded. After demolding, the concrete specimens were immersed in water at $20\pm 2\text{ }^{\circ}\text{C}$ and cured until the age of 7 days. During the drying period, the specimens were kept at least 25 mm apart so as not to impede drying from the bottom of the specimen. Measurements were taken when a specimen was 7 days old, and this time is taken as the reference.

The samples for mercury intrusion porosimetry (MIP) were extracted from the center of a cylinder that had dried in a curing room for either 28 or 91 days. Three specimens were tested under each set of conditions. The cylinder was then cut with a vise to obtain particles of 2–5 mm in diameter. The samples were dehydrated by submerging them in acetone for 2 h, after which they were dried in an oven at $105\text{ }^{\circ}\text{C}$ for 1 h and then put under a vacuum pump for 48 h. The MIP tests were done on AutoPore V, which subjected the samples to a maximum pressure of 60,000 psia and could measure pore diameters of 0.003–1100 μm . With MIP, numerous sample properties could be calculated, such as total pore surface area, median pore diameter, pore size distributions, total pore volume, and sample densities.

5.3. Experimental results and discussion

5.3.1 Influence of RFA and FA on the compressive strength of concrete

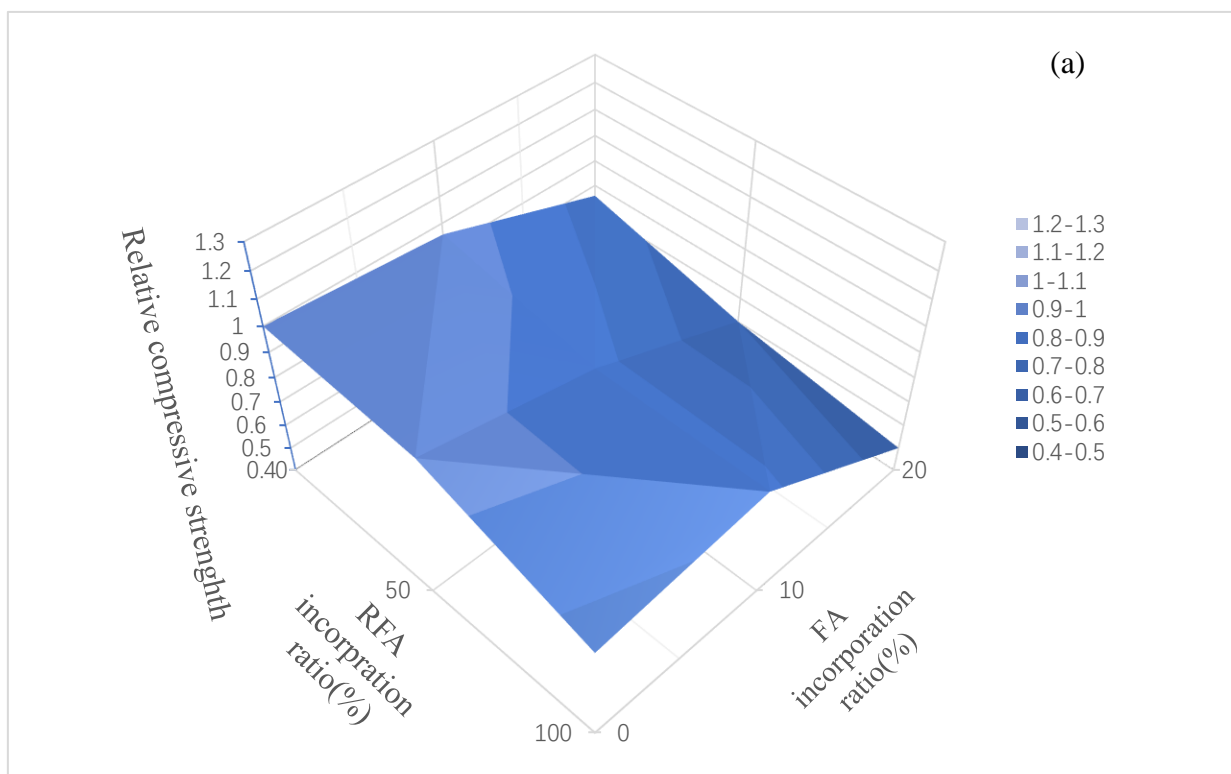
Table 3 shows the compressive strength of all mixes. Fig. 1 shows the compressive strength of water-to-binder ratio (W/B) 0.55 and 0.40 mixes relative to that of reference concrete (M0-FA0) in a 3D surface on 7, 28 and 91 days, separately.

The relative changes the compressive strength was between 0.50 and 0.96 shown in Fig. 1a. The relative values of compressive strength for M50-FA0 and M100-FA0 are 0.96 and 0.76, respectively, and the relative values for M0-FA10 and M0-FA20 are nearly to those of the first two groups. Fig. 1b shows the compressive strength of concrete at 28 days, where the relative values of M100-FA0 and M0-FA20 are about 0.85 and 0.81, which is similar to the situation shown in Fig. 1a, meaning that the use of low amount of FA or RFA reduced the compressive strength of concrete at 7 and 28 days. The results for the incorporation of RFA are consistent with previous studies [27,28,29]. Incorporation of a certain amount of FA reduces the early strength of cement paste [30] and concrete [31]. However, concrete in which an appropriate ratio of fly ash is used was stronger after 28 days compared with concrete in which fly ash was not used.

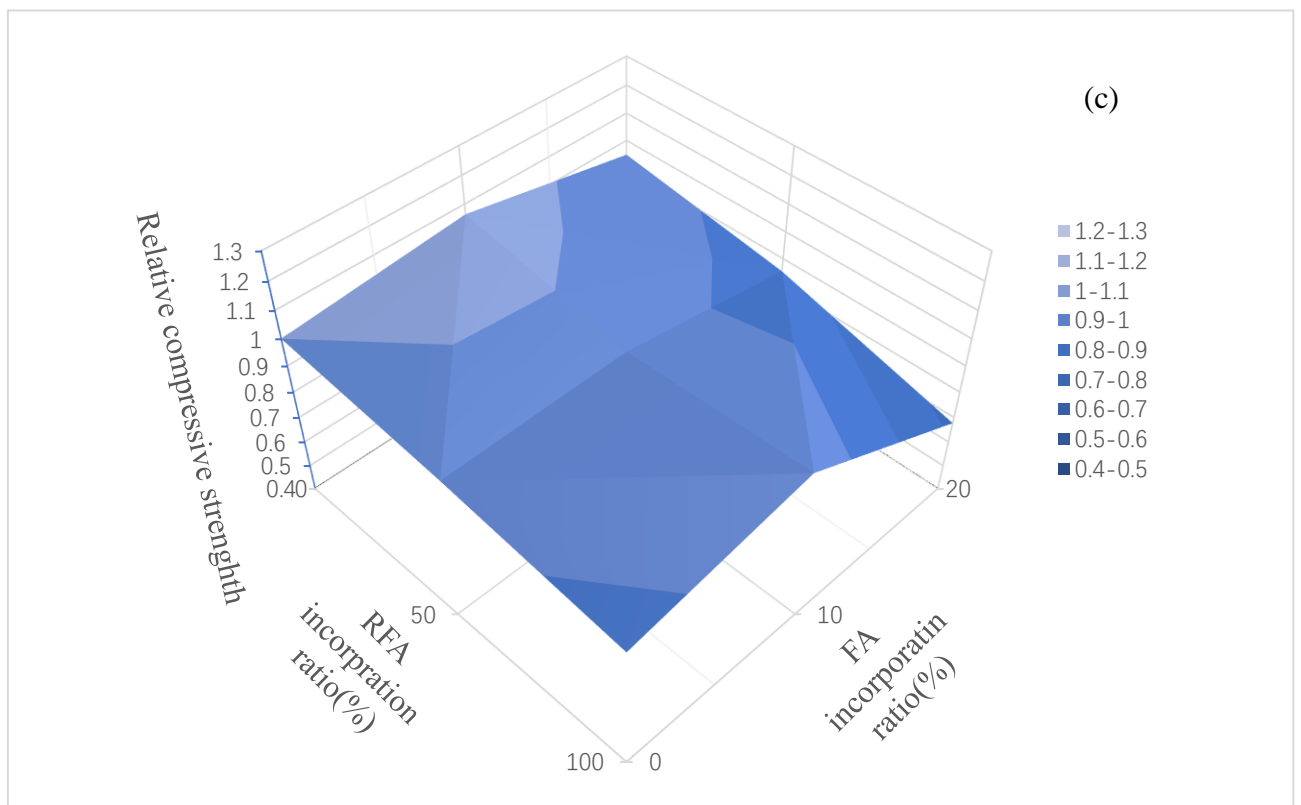
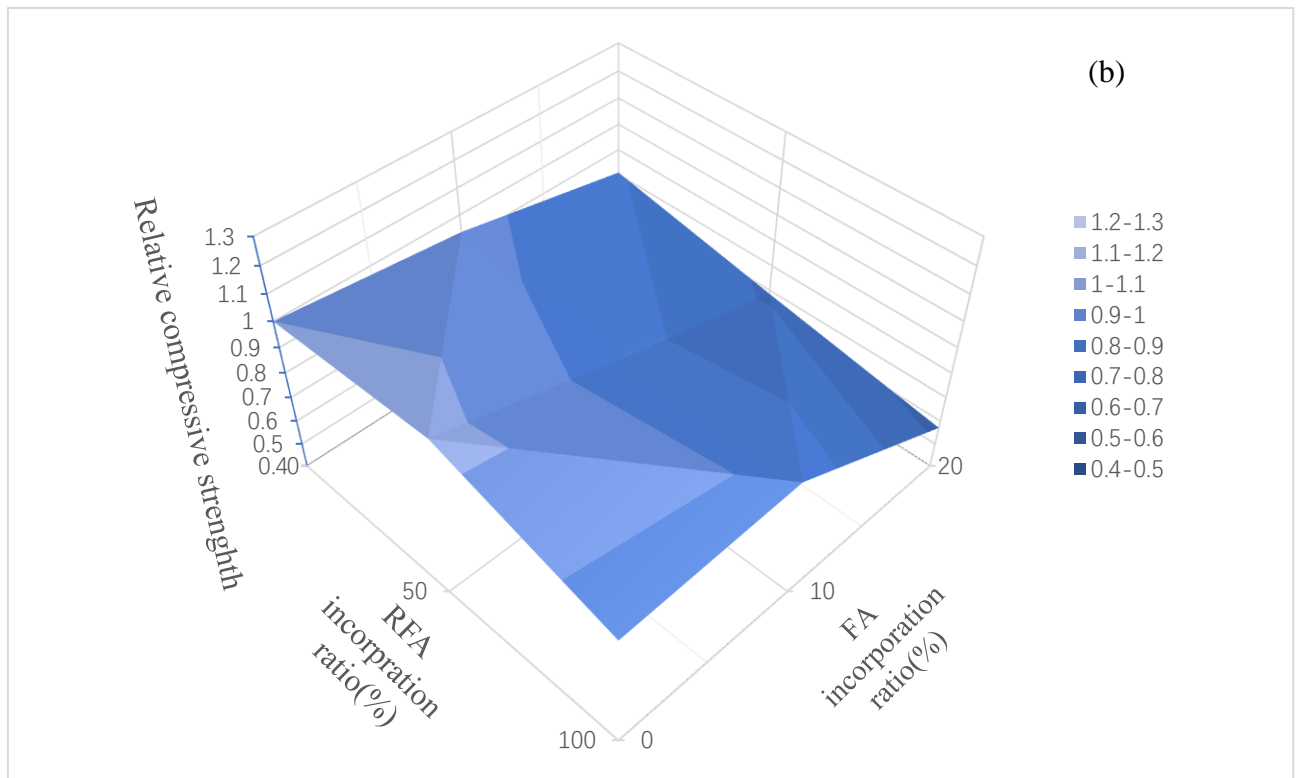
As shown in Fig. 1c, the relative value of the compressive strength of M0-FA10 was 1.06, whereas the

others were not greater than 1. This result is due to the physical ‘packing’ effect of FA, which makes the cement paste more homogeneous or denser [32]. Moreover, as the pozzolanic reaction between FA and cement progresses, C-S-H and C-A-H might be produced making the structure more hence [33], but this benefit will take some time to manifest because the reaction is slow [34]. The relative values of the compressive strength of M50-FA10 and M100-FA20 are respectively 0.83 and 0.5 at 7 days, 0.85 and 0.57 at 28 days, and 0.95 and 0.68 at 91 days. This shows that when FA and RFA are used as a substitute for concrete at a W/B of 0.55, the effect on compressive strength is greater than when they are used separately. Kurda reported that [35] when FA and RFA are both used, the strength of concrete decreases with the amount used, which is similar to the effect of FA and recycled coarse aggregate on concrete. This suggests that FA might fill the micropores in the interface transition area around RFA, similar to recycled coarse aggregate, and improve the particle size distribution [36].

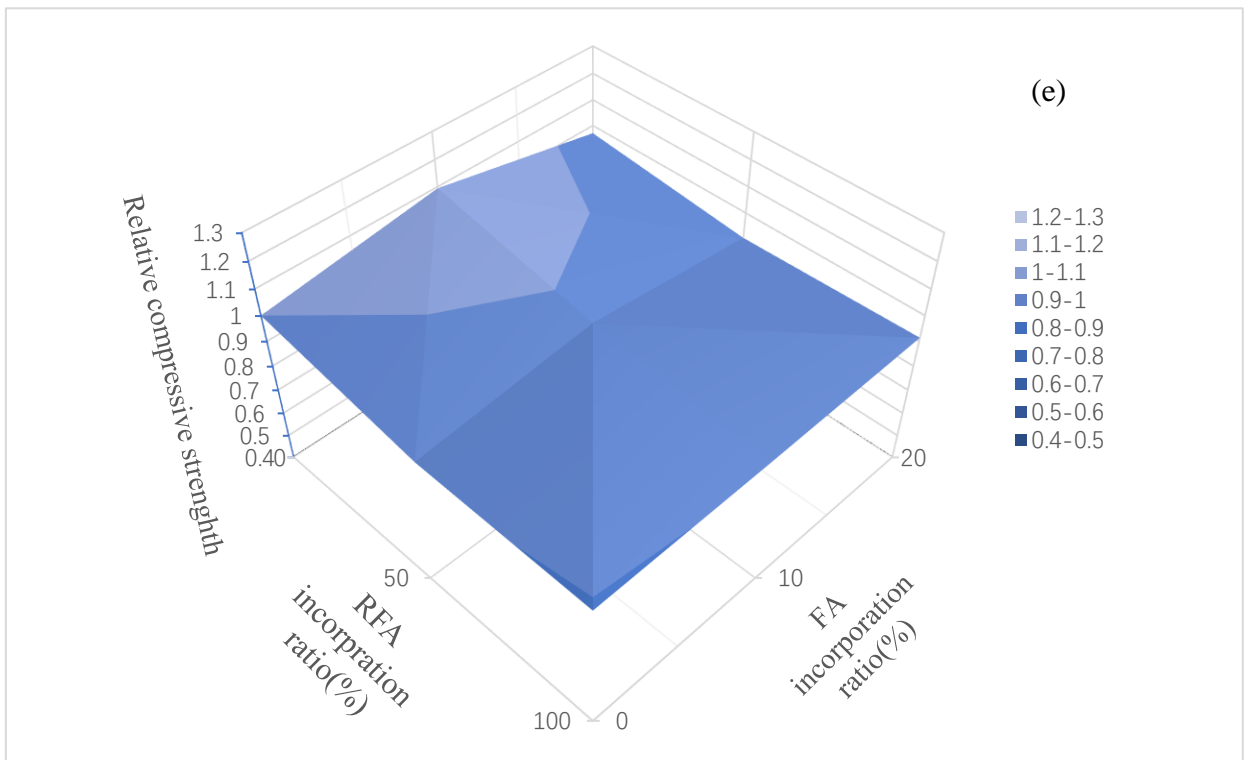
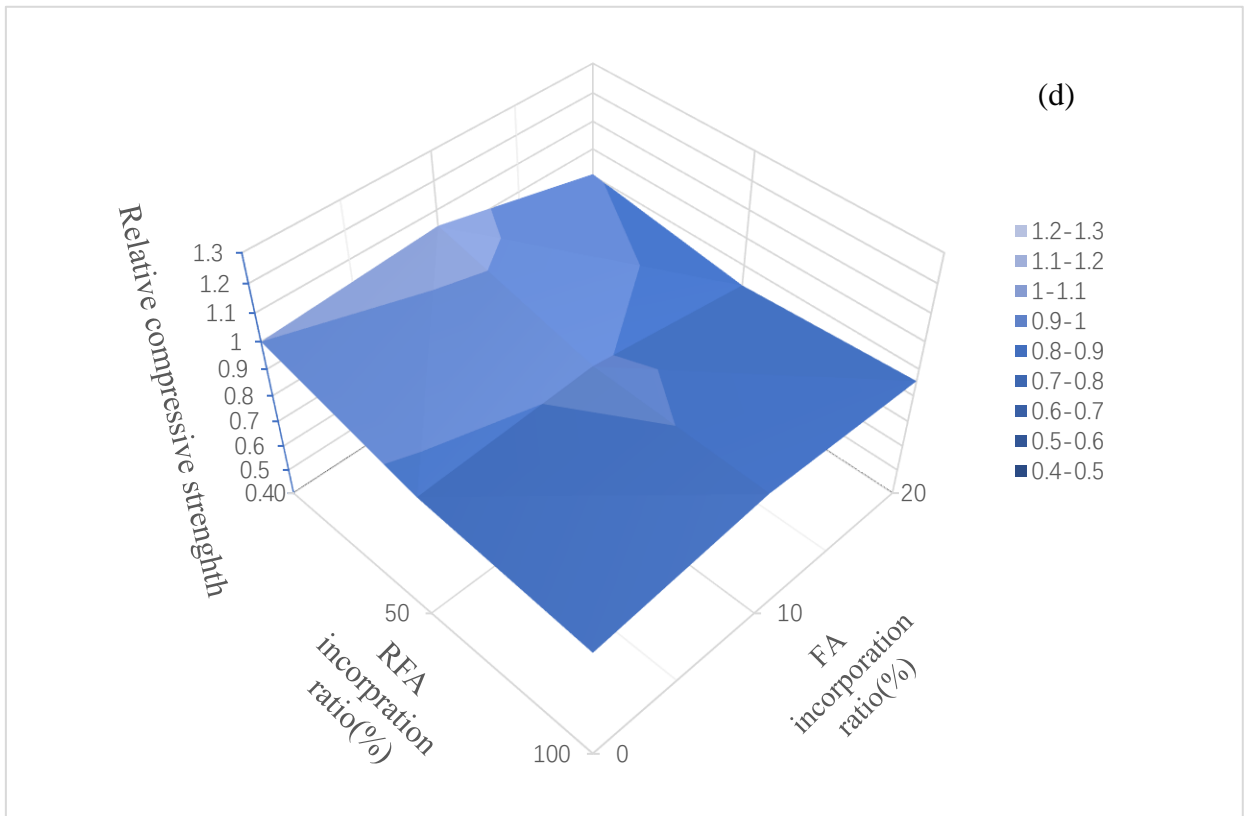
Figs. 5.1d, e and f show the compressive strength of W/B 0.40 mixes relative to that of reference concrete (M0-FA0) on a 3D surface at 7, 28 and 91 days, respectively. As shown in Fig. 1e, the relative value of the compressive strength of only group M0-FA10 (relative value is 1.09) is greater than 1. When a certain amount of FA was used, the early strength of the concrete still reached a level similar to that of the reference concrete. Poon [37] reported that in a low W/B condition, the compressive strength of the concrete at 28 days was 6%–9% higher than that of the original concrete when the ratio of FA in the concrete was 25%. As shown in Fig. 1f, the relative values of the compressive strength of M0-FA10, M0-FA20, M50-FA10, and M50-FA20 were 1.21, 1.11, 1.08, and 1.07, respectively, whereas those of M100-FA10 and M100-FA20 were less than 1. At 91 days, the contribution of FA to compressive strength of concrete was greater than that of RFA.



CHAPTER 5: EFFECT OF INCORPORATING FLY ASH AND RECYCLED FINE AGGREGATE ON PROPERTIES AND CUMULATIVE PORE VOLUME OF CONCRETE



CHAPTER 5: EFFECT OF INCORPORATING FLY ASH AND RECYCLED FINE AGGREGATE ON PROPERTIES AND CUMULATIVE PORE VOLUME OF CONCRETE



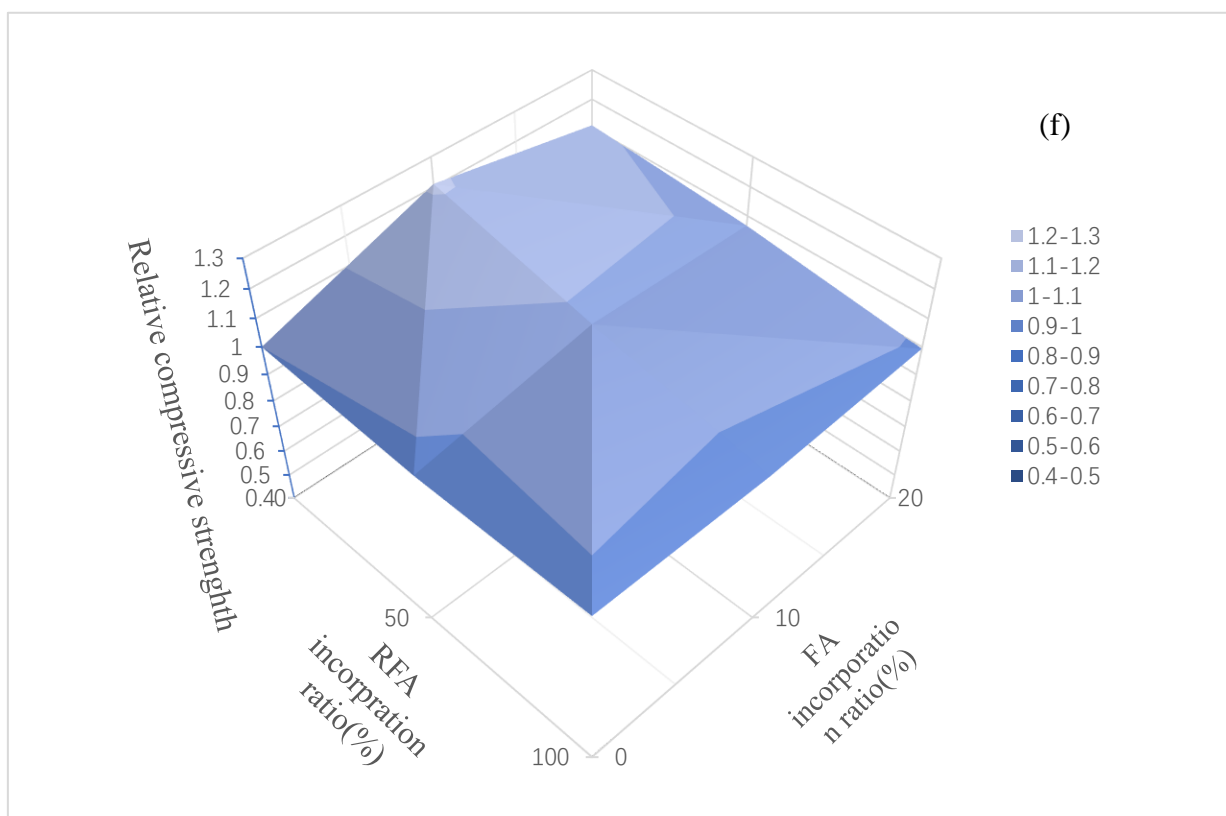


Fig.5.1. Influence of incorporating FA and RFA on the compressive strength of concrete at different days and W/B: (a) 7days, 0.55; (b) 28days, 0.55; (c) 91days, 0.55; (d) 7days, 0.40; (e) 28days, 0.40; (f) 91days, 0.40.

5.3.2 Influence of RFA and FA on the drying shrinkage of concrete

Fig. 5.2 shows the drying shrinkage at 182 days for a series of concrete mixes with various proportions of RFA and FA. Each presented value is the average of three measurements. The results show that incorporating RFA in the concrete mixes increased the drying shrinkage of the concrete. The mortar adhering to the recycled aggregate helped to increase the volume of the paste, thus increasing the drying shrinkage of the resulting concrete [38]. For this series, compared with the concrete containing no RFA, the maximum increase in drying shrinkage was 18.2%, 9.4%, and 24.8% with an FA content of 0%, 10%, and 20%, respectively. Incorporating FA in the concrete decreased the drying shrinkage and FA can inhibit the increase of drying shrinkage of concretes by RFA. Atis reported that [39], dilution effect of the FA particles will lead to the reduction in the drying shrinkage. In this series, the 10% FA replacement ratio decreased the drying shrinkage to a greater extent than the 20% FA replacement ratio. For this series, compared with the concrete with no FA content, the maximum decrease in drying shrinkage was 13.4%, 21.1%, and 18.8% with RFA replacement ratios of 0%, 50%, and 100%, respectively.

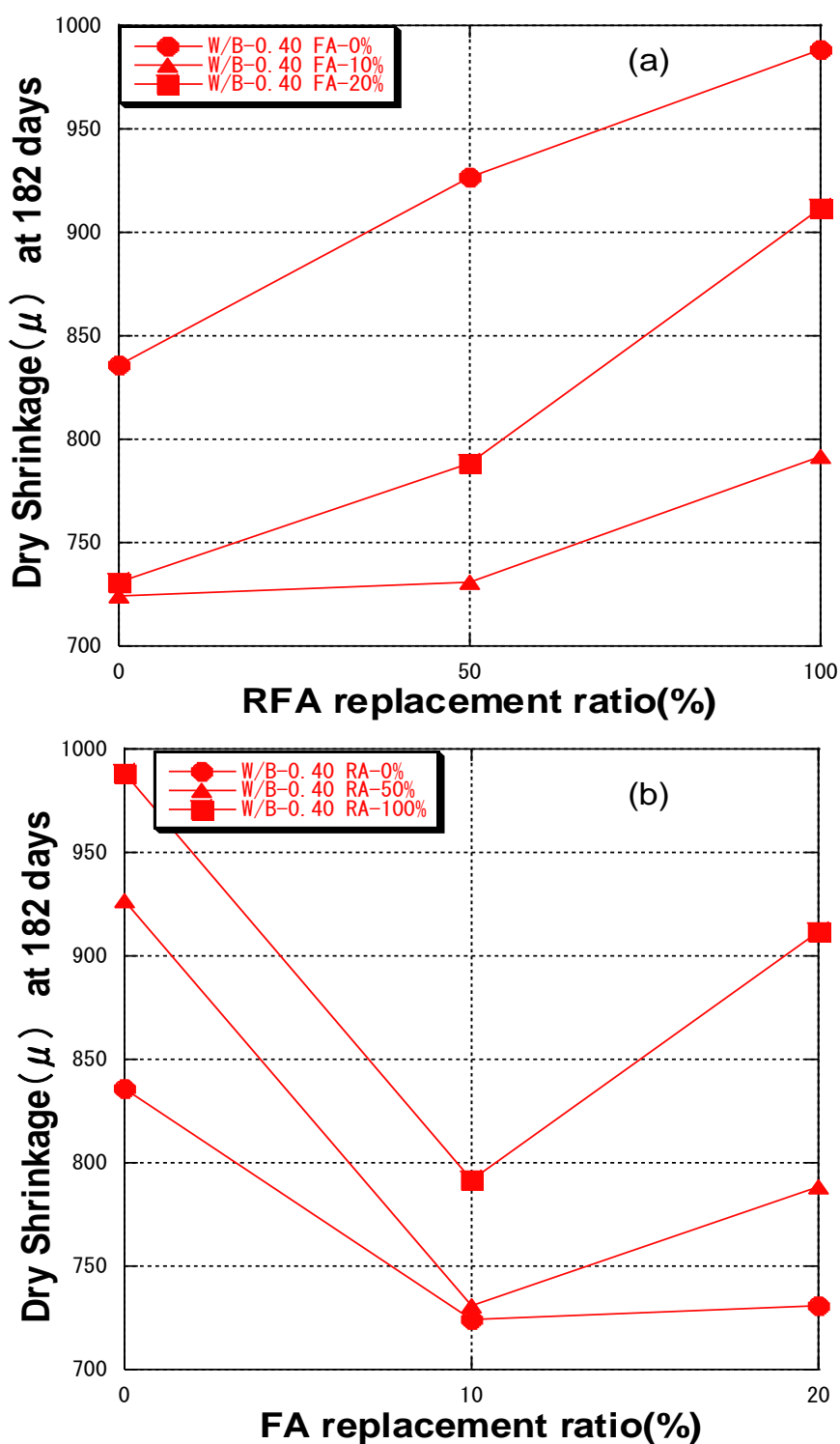


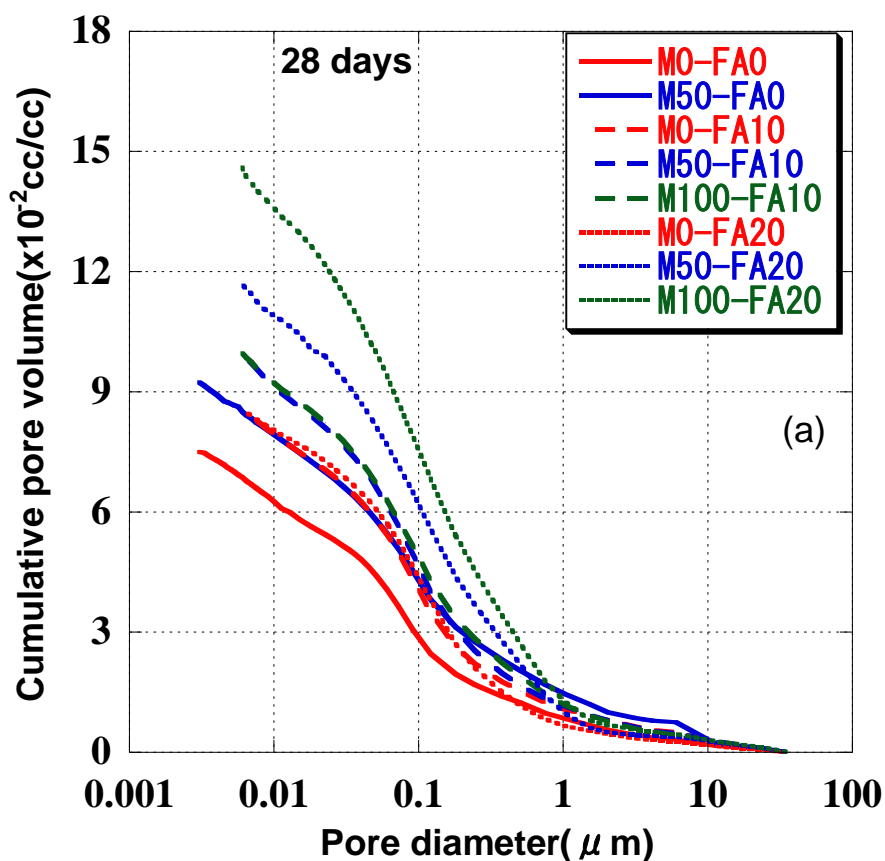
Fig.5.2. Effect of RFA and FA on the dry shrinkage

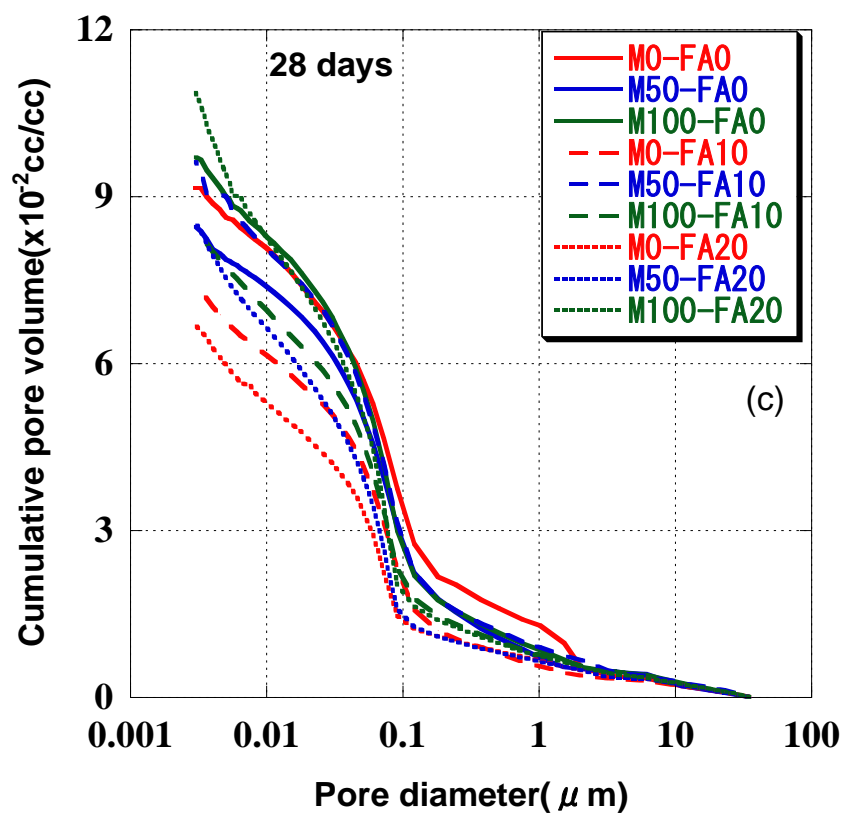
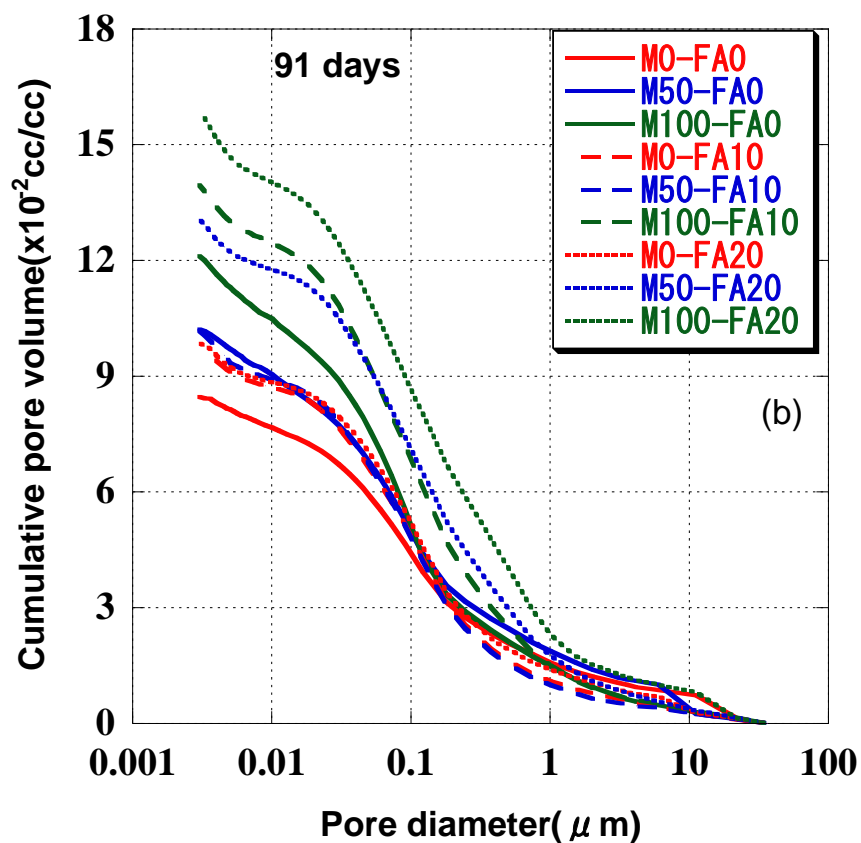
5.3.3 Cumulative pore volume

The MIP tests were carried out at 28 and 90 days. Fig. 3 show the cumulative pore volume with a W/B ratio of 0.55 at 28 and 91 days. The results show that the pore volume, for pore diameters of 0.003–36 μ m, increased with the RFA replacement ratio.

At 28 days, the cumulative pore volume of M50-FA0 was 23% higher than that of M0-FA0 and at 91

days, the cumulative pore volumes of M50-FA and M100-FA0 were respectively 15% and 43% higher than that of M0-FA0. This shows that the use of RFA increases the cumulative pore volume of concrete. As shown in Fig.5.3a and b, the cumulative pore volume increased with the RFA replacement ratio of pore diameters of 0.003–36 μm . This may be due to the fact that when RAC is produced, pores of various shapes are formed as a result of the old cement mortar present at the interfacial transition zone of the recycled aggregate, which is likely to affect the compressive strength of the RAC [40]. As shown in Figs.3b and d, the cumulative pore volume of concrete with a W/B of 0.40 is smaller than that with a W/B of 0.55. This observation is consistent with previous studies [41].





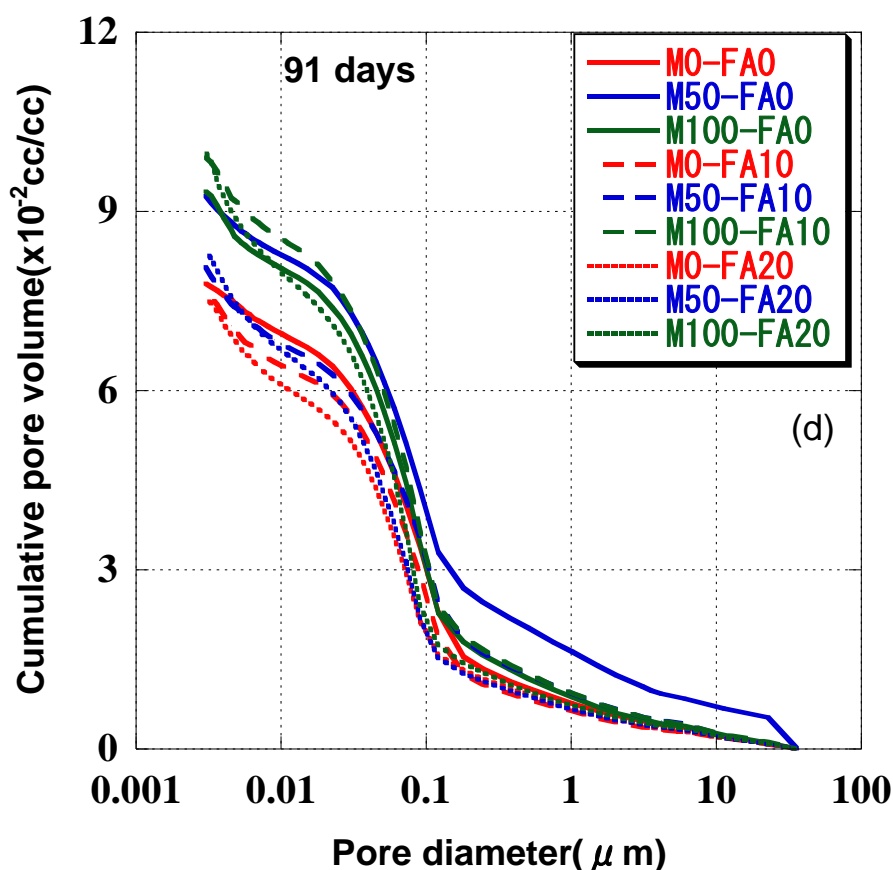
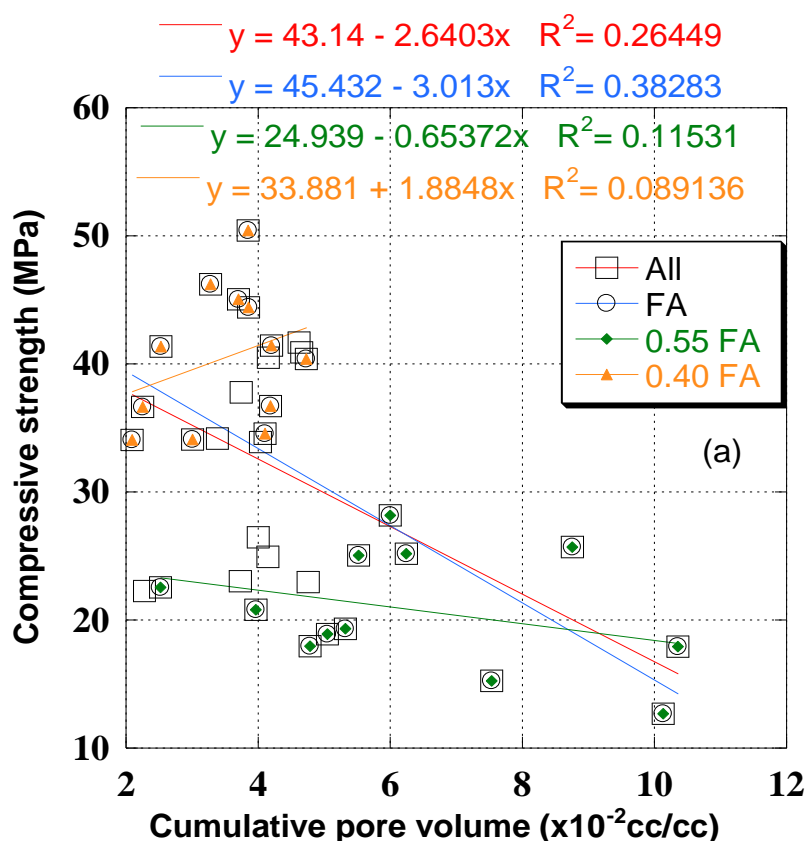


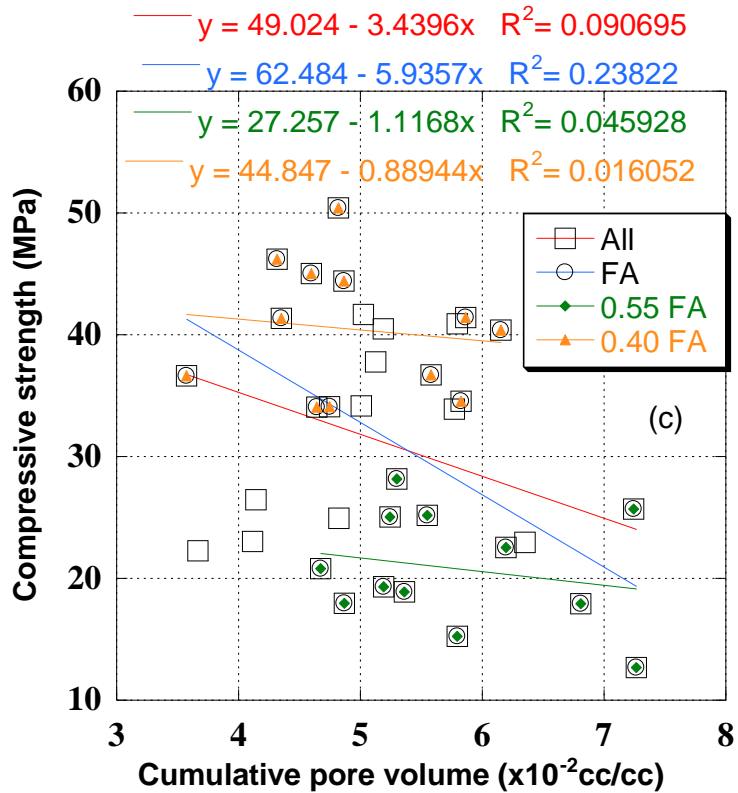
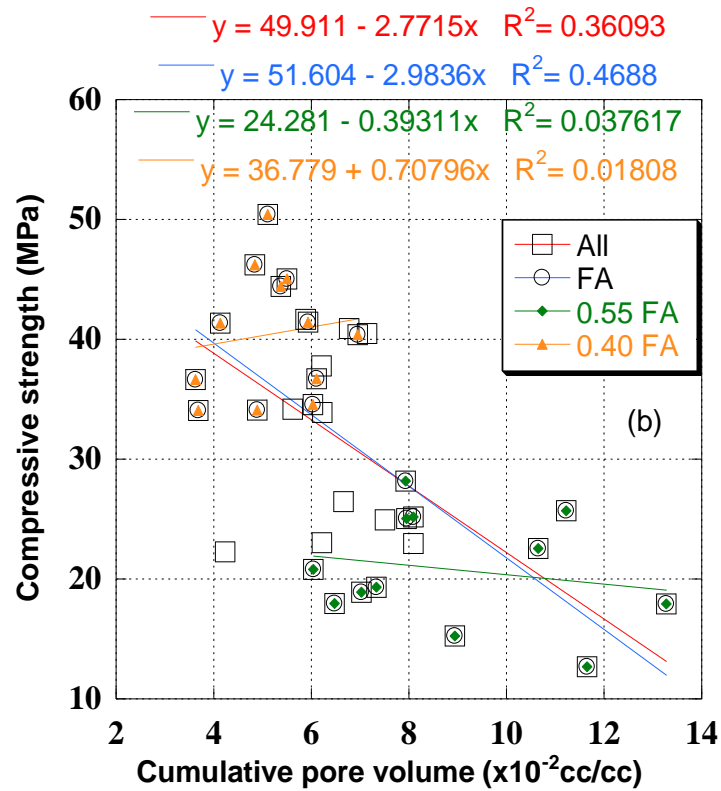
Fig.5.3 Cumulative pore volume at different W/B ratio: (a) and (b), W/B 0.55; (c) and (d), W/B 0.40. In Fig.5.3, each cumulative curve has three different pore volume intervals at points a and b because the pore size distributions of all the samples followed a similar pattern [42]. One with a gentle slope of cumulative pore volume between a range of pore diameter at 0.003–a μm ; the second within a range between point a and b with a significant increase in cumulative pore volume; and the last being between a range of b–36 μm with a gentle increase. Compressive strength was related to pore diameter interval to the right of point a. Drying shrinkage was related to pore diameter interval up to left of point b. As each curve in Fig.3 same pore diameter interval, the pore diameter intervals' left endpoint was point a, to look for the correlation between the pore volume and compressive strength in this interval. And the pore diameter intervals' right endpoint was point b, to look for the correlation between the pore volume and drying shrinkage in this interval.

The researchers studied the porosity and pore structure of cement paste. P.K. Mehta thought pores have four intervals: < 4.5nm, 4.5–50nm, 50–100nm, >100nm, and reported that the pore which diameter no more than 132nm had a slight impact on the properties of concrete [43]; Z.W. Wu thought pores have four intervals: < 20nm which named after harmless pore, 20–50nm which named after less-harm pore, 50–200nm which named after harmful pore, > 200nm which named after much-harm pore [44]. Capillary pores with a diameter greater than 0.011 μm affect the strength, and gel pores with a diameter less than 0.01 μm affect the durability of mortar [45]. Consequently, the correlation between the properties of the RAC and the pore volume can be evaluated by dividing various pore intervals. Wu's theory was used for comparison; therefore the left and right points of the pore diameter intervals

were defined as 0.02 and 0.2 μm , respectively. Simple linear regression also was performed to evaluate the correlation between the results of MIP and the results of compressive strength or drying shrinkage tests under different interval division methods.

Fig.5.4 shows the coefficients of determination between the pore volume and compressive strength at the following interval divisions: a- μm , a-36 μm , 0.02-0.2 μm , 0.02-36 μm . The pore size range of MIP test was 0.003-36 μm . The symbols "All", "FA", "0.55FA" and "0.40FA" shown in Fig. 4 indicate that the fitted line used the data of the compressive strength and cumulative pore volume of all mixes, mixes with FA, mixes with FA at W/B 0.55 and mixes with FA at W/B 0.40, respectively.





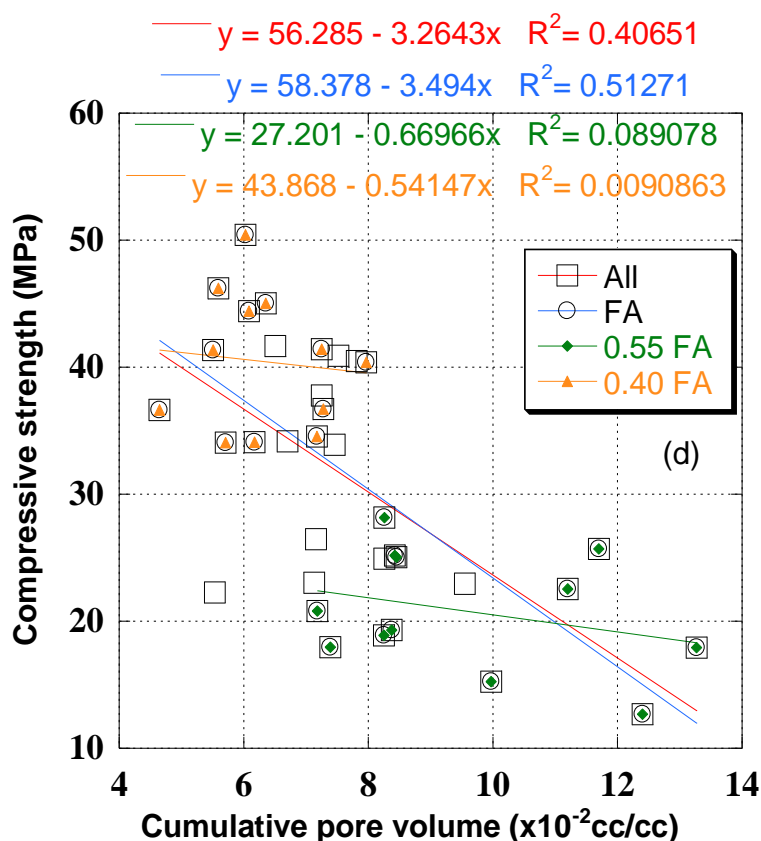
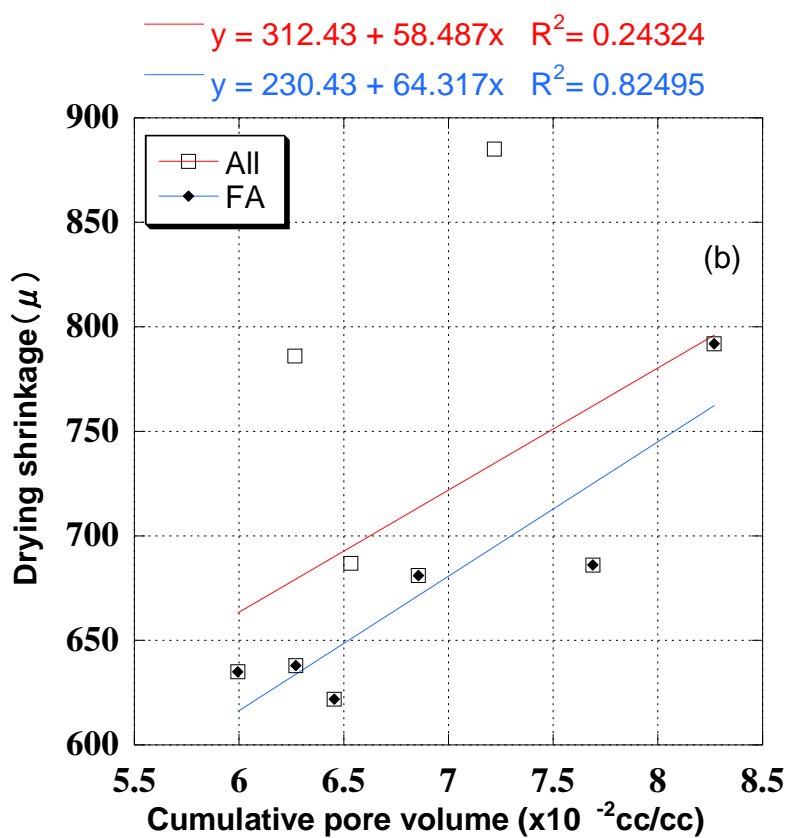
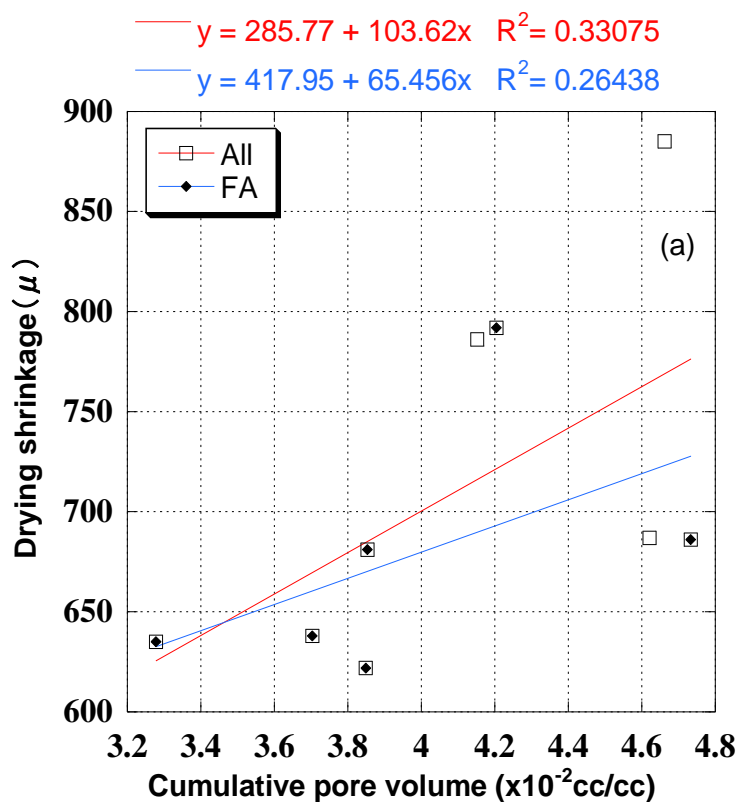


Fig.5.4 Coefficients of determination (R^2) of compressive strength and cumulative pore volume at interval division: (a) a–b μm ; (b) a–36 μm ; (c) 0.02–0.2 μm ; (d) 0.02–36 μm .

For RFA concrete incorporating FA, there was no interval with a high correlation coefficient between the compressive strength and the cumulative pore volume because the correlation coefficients of the four types of intervals ranged between 0 and 0.6 (Fig.5.4). In other words, there was no significant correlation between cumulative pore volume and compressive strength. Moreover, simple linear regression cannot use cumulative pore volume in a specific interval to determine or predict the strength of recycled concrete. Some researchers use quadratic [4] or exponential [46] regression equations to predict concrete strength. Concrete with FA should be considered separately when considering the correlation between compressive strength and cumulative pore volume because the correlation coefficients of the “FA” lines are higher than that of “All” line for the four intervals.

Fig.5 shows the coefficients of determination between the cumulative pore volume and drying shrinkage at interval divisions: a–b, a–36 μm , 0.02–0.2 μm , 0.02–36 μm . The symbols “All” and “FA” shown in Fig. 5 indicate that the fitted line used the data of the compressive strength and cumulative pore volume of all mixes and mixes with FA, respectively.



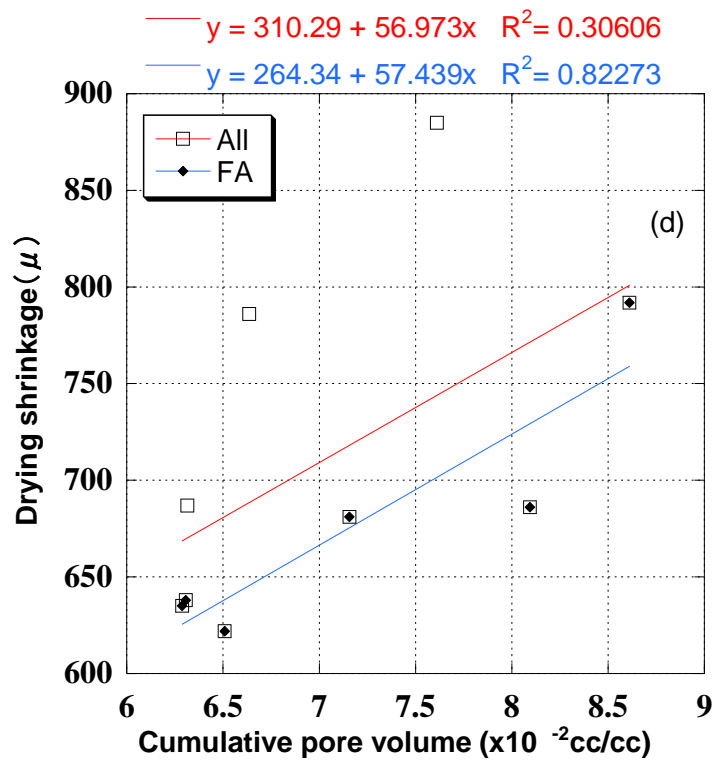
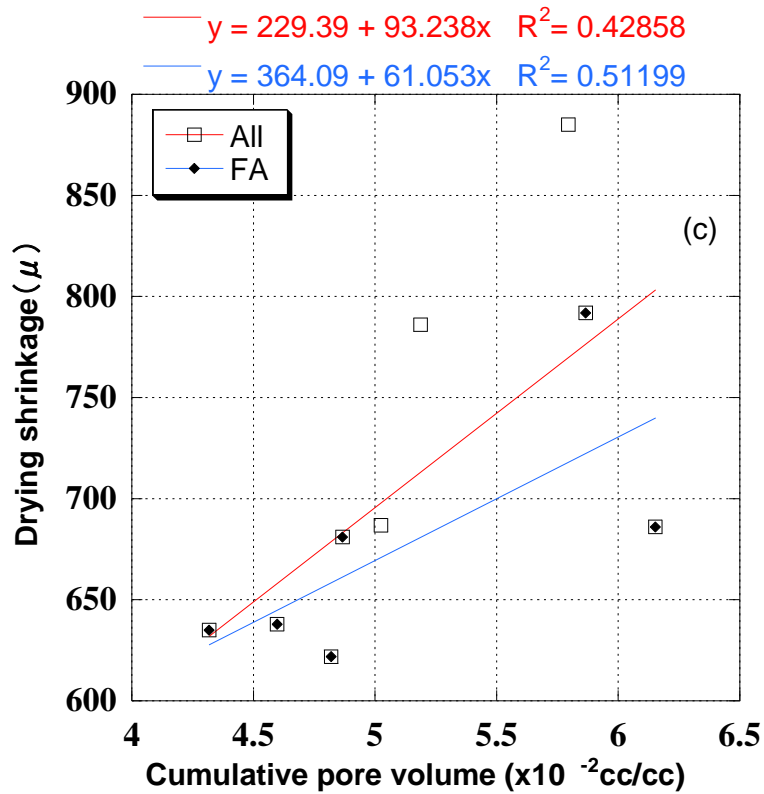


Fig.5.5 Coefficients of determination (R^2) of drying shrinkage and cumulative pore volume at different interval divisions: (a) a–b μ m; (b) 0.03–b μ m; (c) 0.02–0.2 μ m; (d) 0.03–0.2 μ m.

Concrete with FA should be considered separately when investigating the correlation between drying

shrinkage and cumulative pore volume because there are no linear fits with high correlation coefficients in Fig. 5a and c, whereas the “FA” line shows high correlation coefficients in Fig. 5b and d. The drying shrinkage of the concrete incorporating FA is related to the cumulative pore volume of micropores due to the pore diameter of interval divisions shown in Fig. 5a and c, both of which start from 0.003 μm . In other words, there is correlation between cumulative pore volume and drying shrinkage due to the incorporation of FA in concrete. This can be explained by the fact that FA can reduce both the pore size of capillary pores and gel pores in concrete [47], and because the shrinkage rate depends on the amount of water lost in the mesopore, in which the resistance to water loss was determined by the size of the macropore [48]. Hence, the drying shrinkage of concrete with FA is relatively correlated with the pore volume of micropores and mesopores. 0.003–b μm is the optimal interval between the drying shrinkage and the cumulative pore volume of concrete incorporating FA because the “FA” line in Fig. 5b has the highest correlation coefficient of 0.82.

5.4. Conclusion

- Incorporating RFA or low amount of FA as into concrete reduces its initial strength, but the compressive strength of concrete incorporating an appropriate amount of FA can reach that of concrete without FA as the age of concrete increases or the W/B ratio decreases.
- The effect on the initial compressive strength of adding both FA and RFA to concrete is greater than adding either component alone. However, the pozzolanic reaction gradually produces a beneficial effect on the compressive strength of the concrete as time passes.
- Incorporating RFA into the concrete mixture increase the drying shrinkage of the concrete whereas FA which can inhibit the increase of drying shrinkage of concrete by RFA, decreases the drying shrinkage.
- Cumulative pore volume increases with an increase of RFA replacement ratio and decreases with a decrease of the W/B ratio.
- Concrete incorporating FA should be considered separately when investigating the correlation between cumulative pore volume and compressive strength or drying shrinkage.
- There is no linear correlation between compressive strength and cumulative pore volume in all interval divisions.
- There is a linear correlation between cumulative pore volume and drying shrinkage result from the incorporation of FA in concrete and the optimal interval division for investigating the correlation between drying shrinkage and the cumulative pore volume of concrete incorporating FA is 0.003–b μm . the smallest pore diameter that can be measured by the MIP test is 0.003 μm and point b is the right change point of pore diameter in a plot of cumulative pore volume.

References

- [1] Neville, A. M. "4th and final ed., Properties of Concrete." (1996).
- [2] Wijayasundara, Mayuri, Priyan Mendis, and Robert H. Crawford. "Integrated assessment of the use of recycled concrete aggregate replacing natural aggregate in structural concrete." *Journal of cleaner production* 174 (2018): 591-604.
- [3] Wijayasundara, Mayuri, Priyan Mendis, and Robert H. Crawford. "Methodology for the integrated assessment on the use of recycled concrete aggregate replacing natural aggregate in structural concrete." *Journal of cleaner production* 166 (2017): 321-334.
- [4] Gómez-Soberón, José MV. "Porosity of recycled concrete with substitution of recycled concrete aggregate: An experimental study." *Cement and concrete research* 32.8 (2002): 1301-1311.
- [5] Wainwright, P. J. "Modifying the performance of concrete made with coarse and fine recycled concrete aggregates." *EIK Lauritezen (Ek.), Demolition and Reuse of Concrete, Guidelines for Demolition and Reuse of Concrete and Masonry* (1993).
- [6] Pedro, D., J. De Brito, and Luis Evangelista. "Influence of the use of recycled concrete aggregates from different sources on structural concrete." *Construction and Building Materials* 71 (2014): 141-151.
- [7] Etxeberria, Miren, et al. "Influence of amount of recycled coarse aggregates and production process on properties of recycled aggregate concrete." *Cement and concrete research* 37.5 (2007): 735-742.
- [8] Hansen, Torben C., and Erik Boegh. "Elasticity and drying shrinkage concrete of recycled-aggregate." *Journal Proceedings*. Vol. 82. No. 5. 1985.
- [9] Domingo-Cabo, Alberto, et al. "Creep and shrinkage of recycled aggregate concrete." *Construction and building materials* 23.7 (2009): 2545-2553.
- [10] Pacheco, João, et al. "Experimental investigation on the variability of the main mechanical properties of concrete produced with coarse recycled concrete aggregates." *Construction and Building Materials* 201 (2019): 110-120.
- [11] Matias, D., et al. "Mechanical properties of concrete produced with recycled coarse aggregates— Influence of the use of superplasticizers." *Construction and building materials* 44 (2013): 101-109.
- [12] González-Fonteboa, B., and F. Martínez-Abella. "Concretes with aggregates from demolition waste and silica fume. Materials and mechanical properties." *Building and Environment* 43.4 (2008): 429-437.
- [13] Tabsh, Sami W., and Akmal S. Abdelfatah. "Influence of recycled concrete aggregates on strength properties of concrete." *Construction and building materials* 23.2 (2009): 1163-1167.
- [14] de Oliveira Andrade, Jairo José, et al. "Performance of rendering mortars containing sludge from water treatment plants as fine recycled aggregate." *Journal of Cleaner Production* 192 (2018): 159-168.
- [15] Giergiczny, Zbigniew. "Fly ash and slag." *Cement and Concrete Research* 124 (2019): 105826.
- [16] Environment, U. N., et al. "Eco-efficient cements: Potential economically viable solutions for a low-CO₂ cement-based materials industry." *Cement and Concrete Research* 114 (2018): 2-26.
- [17] Matthes, Winnie, et al. "Ground granulated blast-furnace slag." *Properties of Fresh and Hardened Concrete Containing Supplementary Cementitious Materials*. Springer, Cham, 2018.

CHAPTER 5: EFFECT OF INCORPORATING FLY ASH AND RECYCLED FINE AGGREGATE
ON PROPERTIES AND CUMULATIVE PORE VOLUME OF CONCRETE

1-53.

- [18] Giergiczny, Z. "Fly ash in cement and concrete composition." *Золошлаки ТЭС: удаление, транспорт, переработка, складирование*. 2014.
- [19] Le Cornec, Domitille, et al. "Greening effect in slag cement materials." *Cement and Concrete Composites* 84 (2017): 93-98.
- [20] Kou, S. C., et al. "Hardened properties of recycled aggregate concrete prepared with fly ash." *Sustainable Waste Management and Recycling: Construction Demolition Waste*. Thomas Telford Publishing, 2004. 189-197.
- [21] Kou, Shi-Cong, and Chi-Sun Poon. "Properties of concrete prepared with crushed fine stone, furnace bottom ash and fine recycled aggregate as fine aggregates." *Construction and Building Materials* 23.8 (2009): 2877-2886.
- [22] Kurda, Rawaz, Jorge de Brito, and José D. Silvestre. "Influence of recycled aggregates and high contents of fly ash on concrete fresh properties." *Cement and Concrete Composites* 84 (2017): 198-213.
- [23] Gonzalez-Corominas, Andreu, Miren Etxeberria, and Chi Sun Poon. "Influence of steam curing on the pore structures and mechanical properties of fly-ash high performance concrete prepared with recycled aggregates." *Cement and Concrete Composites* 71 (2016): 77-84.
- [24] Namarak, Charin, Weerachart Tangchirapat, and Chai Jaturapitakkul. "Bar-concrete bond in mixes containing calcium carbide residue, fly ash and recycled concrete aggregate." *Cement and Concrete Composites* 89 (2018): 31-40.
- [25] Leite, M. B., and P. J. M. Monteiro. "Microstructural analysis of recycled concrete using X-ray microtomography." *Cement and Concrete Research* 81 (2016): 38-48.
- [26] Garboczi, Edward J. "Permeability, diffusivity, and microstructural parameters: a critical review." *Cement and concrete research* 20.4 (1990): 591-601.
- [27] Leite, M. B., and V. M. Santana. "Evaluation of an experimental mix proportion study and production of concrete using fine recycled aggregate." *Journal of Building Engineering* 21 (2019): 243-253.
- [28] Fan, Cheng-Chih, et al. "The effects of different fine recycled concrete aggregates on the properties of mortar." *Materials* 8.5 (2015): 2658-2672.
- [29] Fan, Cheng-Chih, et al. "Properties of concrete incorporating fine recycled aggregates from crushed concrete wastes." *Construction and Building Materials* 112 (2016): 708-715.
- [30] Bilir, Turhan, Osman Gencel, and Ilker Bekir Topcu. "Properties of mortars with fly ash as fine aggregate." *Construction and Building Materials* 93 (2015): 782-789.
- [31] Hwang, Kwangryul, Takafumi Noguchi, and Fuminiro Tomosawa. "Prediction model of compressive strength development of fly-ash concrete." *Cement and Concrete Research* 34.12 (2004): 2269-2276.
- [32] Chindaprasirt, Prinya, Chai Jaturapitakkul, and Theerawat Sinsiri. "Effect of fly ash fineness on compressive strength and pore size of blended cement paste." *Cement and Concrete Composites* 27.4 (2005): 425-428.
- [33] Cho, Young Keun, Sang Hwa Jung, and Young Cheol Choi. "Effects of chemical composition of fly ash on compressive strength of fly ash cement mortar." *Construction and Building Materials* 204 (2019): 255-264.

CHAPTER 5: EFFECT OF INCORPORATING FLY ASH AND RECYCLED FINE AGGREGATE
ON PROPERTIES AND CUMULATIVE PORE VOLUME OF CONCRETE

- [34] Limbachiya, Mukesh, Mohammed Seddik Meddah, and Youssef Ouchagour. "Use of recycled concrete aggregate in fly-ash concrete." *Construction and Building Materials* 27.1 (2012): 439-449.
- [35] Kurda, Rawaz, Jorge de Brito, and José D. Silvestre. "Combined influence of recycled concrete aggregates and high contents of fly ash on concrete properties." *Construction and Building Materials* 157 (2017): 554-572.
- [36] Kim, Kyuhun, Myoungsu Shin, and Soowon Cha. "Combined effects of recycled aggregate and fly ash towards concrete sustainability." *Construction and Building Materials* 48 (2013): 499-507.
- [37] Poon, C. S., L. Lam, and Y. L. Wong. "A study on high strength concrete prepared with large volumes of low calcium fly ash." *Cement and concrete research* 30.3 (2000): 447-455.
- [38] Tam, Vivian WY, X. F. Gao, and Chi M. Tam. "Microstructural analysis of recycled aggregate concrete produced from two-stage mixing approach." *Cement and concrete research* 35.6 (2005): 1195-1203.
- [39] Atiş, Cengiz Duran, Alaettin Kilic, and Umur Korkut Sevim. "Strength and shrinkage properties of mortar containing a nonstandard high-calcium fly ash." *Cement and Concrete Research* 34.1 (2004): 99-102.
- [40] Tavakoli, Mostafa, and Parviz Soroushian. "Drying shrinkage behavior of recycled aggregate concrete." *Concrete International* 18.11 (1996): 58-61.
- [41] Liu, Jun, et al. "Chloride transport and microstructure of concrete with/without fly ash under atmospheric chloride condition." *Construction and Building Materials* 146 (2017): 493-501.
- [42] Gonzalez-Corominas, Andreu, Miren Etxeberria, and Chi Sun Poon. "Influence of steam curing on the pore structures and mechanical properties of fly-ash high performance concrete prepared with recycled aggregates." *Cement and Concrete Composites* 71 (2016): 77-84.
- [43] Mehta, P. Kumar, and Paulo JM Monteiro. *Concrete microstructure, properties and materials*. 2017.
- [44] WU ZW, LIAN H. Z. "High Performance Concrete." *Beijing: China Railway Publication House* (1999).
- [45] Ho, Hsin-Lung, et al. "Pore-structures and durability of concrete containing pre-coated fine recycled mixed aggregates using pozzolan and polyvinyl alcohol materials." *Construction and Building Materials* 160 (2018): 278-292.
- [46] Lian, Chunqi, Y. Zhuge, and S. Beecham. "The relationship between porosity and strength for porous concrete." *Construction and Building Materials* 25.11 (2011): 4294-4298.
- [47] Chindaprasirt, Prinya, Chai Jaturapitakkul, and Theerawat Sinsiri. "Effect of fly ash fineness on microstructure of blended cement paste." *Construction and Building Materials* 21.7 (2007): 1534-1541.
- [48] Collins, Frank, and Jay G. Sanjayan. "Effect of pore size distribution on drying shrinking of alkali-activated slag concrete." *Cement and Concrete Research* 30.9 (2000): 1401-140

Chapter 6

***A STUDY ON PROPERTIES, STATIC AND DYNAMIC
ELASTIC MODULUS OF RECYCLED CONCRETE
UNDER THE INFLUENCE OF MODIFIED FLY ASH***

CHAPTER 6: A STUDY ON PROPERTIES, STATIC AND DYNAMIC ELASTIC MODULUS OF
RECYCLED CONCRETE UNDER THE INFLUENCE OF MODIFIED FLY ASH

6.1 Introduction

Environmental protection continues to be an important issue. The construction production process consumes large amounts of natural resources, including concrete, which requires cement and aggregates [1]. This requires us to use more renewable, environmentally friendly materials. Construction waste can be recycled into stable aggregates needed in the concrete production process [2]. However, concrete made from recycled fine aggregates (RFA) often exhibits poor workability because the aggregates have extremely high water absorption and undesirable properties, such as mortar attached to the surface [3]. The effects of RFA on the properties of concrete are more complex, and it is difficult to formulate a uniform law, for example, Kirthika et al [4]. believes that RFA will produce modifications to concrete properties, while other studies [5, 6] found that RFA has less effect on the compressive strength (f_c) of concrete. Therefore, it is essential to study the effect of RFA on concrete properties.

Fly ash (FA) can replace cement as a concrete admixture [7]. Most fly ash comes from coal burned in boilers in coal-fired power plants. The coal is first processed into fine pulverized coal and burned in the boiler, at which time the FA from the boiler to the chimney can be collected by the collector. The loss on ignition (LOI) of FA is particularly important because the change in the carbon content of 3% FA affects the strength of about 13% [8] of the concrete in which it is used. The flotation method has been used for efficient carbon removal [9]. In this experiment, we use an independently developed flotation device [10] that has been verified by continuous experiments. This flotation machine can efficiently remove unburned carbon from high carbon content FA in a short time using a new microbubble generation device. Therefore, the modified fly ash (MFA) obtained by flotation needs more data to show whether it meets the industrial requirements of each country and to increase the effective use of resources.

The strength of concrete is its most important and necessary property. Generally, only concrete that meets the f_c criteria can be used for building production. The strength of concrete is closely linked to Young's modulus, which is known as the static elastic modulus (E_c) and dynamic elastic modulus (E_d). E_c is the ratio of the axial stress to the axial strain of a material subjected to uniaxial loading [11]. Building codes usually require that specific E_c values be met to ensure satisfactory structural integrity of the building and to prevent unsatisfactory deformation; thus, Young's modulus is always required to analyze the deflection of the structure. Concrete structural members must be properly designed to prevent lateral and longitudinal deformations and to ensure that the applied loads do not exceed the load-carrying capacity of the members. E_c and E_d increase rapidly in the early stages of concrete curing same as compressive strength [12]. Design codes [13-21] recommend that E_c is often estimated from the f_c of concrete at day 28, but those formulas provide overly conservative results. Selecting concrete with much higher strengths than required may result in higher material costs. There are dynamic non-destructive testing methods [22] for estimating the E_d ; however, E_d is usually found to be higher than E_c [23]. The stress-strain relationship in concrete can be complex due to the water held in the concrete and the gel structure formed within it [24]. The static modulus is derived by loading the concrete and measuring the slope of the stress-strain curve. The dynamic testing method applies very small forces compared with static loading. The dynamic test method does not result in any additional deformation of the concrete, which is why measuring E_d is more convenient and environmentally friendly than measuring E_c . Although empirical relationships between E_c and E_d of

CHAPTER 6: A STUDY ON PROPERTIES, STATIC AND DYNAMIC ELASTIC MODULUS OF RECYCLED CONCRETE UNDER THE INFLUENCE OF MODIFIED FLY ASH

concrete have been proposed for conventional concrete [25-27], it is important to establish the relationship for recycled concrete using cementitious admixtures, which can also validate and refine the role of MFA in concrete.

This study aimed to establish the relationship among E_c , E_d , and f_c for recycled concrete containing MFA. The equations of E_c - E_d for the modified fly ash recycled concrete were based on experimental values. New equations for the relationship between E_c and f_c were proposed based on equations from different national standards and comparing these predicted values with the actual values obtained from E_c tests. The same relationship between E_d and f_c was also determined for concrete mixtures based on different covariates of RFA of different quality. Finally, we extended the applicability of E_d by using porosity as a bridge to exploring the relationship between E_d and drying shrinkage (ϵ_d).

6.2 Materials and experiments

6.2.1 Materials

The raw FA with high LOI was collected from power plants, and the carbon in the raw FA was removed by a self-developed fly ash flotation device [10] to bring the LOI to industrial standards. Table 6.1 shows the properties of the FA.

Table 6.1
Standards and properties of FA and MFA.

Type	Raw FA	MFA	JIS Class II	ASTM class F	GB Class I
LOI (%)	13	1.75	< 5	< 6	< 5
Density (g/cm ³)	2.32	2.33	> 1.95	2.45±5%	< 2.6
Blaine (cm ² /g)	4830	3220	> 2500	-	-
Active index (%)	86	81	> 80	> 75	> 70

In this experiment, different RFA was used to replace the normal aggregate, i.e., sand, in the concrete. Recycled coarse aggregate (RCA) was also used for comparison, some physical properties of aggregates were shown in Table 2.

Table 6.2
Physical Properties of aggregates.

Property	Coarse aggregate	RCA	Fine aggregate	RFA-M	RFA-L
Density-SSD (g/cm ³)	2.70	2.53	2.67	2.45	2.30
Fineness	6.72	6.65	2.20	2.95	2.09
Water absorption (%)	0.59	3.08	1.06	6.98	9.91

6.2.2 Experiments

In table 6.3, fifteen mix proportions were designed to investigate the influence of fly ash weight content, recycled aggregate volume content, and recycled aggregate type on the f_c . The water to binder ratio was 0.55 for all mixture proportions. The cement of F15 and M15 was replaced by 15% of their mass by FA and MFA, respectively. The aggregates of F100M15, FL100M15, and C100M15 used

CHAPTER 6: A STUDY ON PROPERTIES, STATIC AND DYNAMIC ELASTIC MODULUS OF RECYCLED CONCRETE UNDER THE INFLUENCE OF MODIFIED FLY ASH

RFA-M, RFA-L, and RCA respectively. The mass ratio of air-entraining water-reducing admixture and cement was about 0.4% was added to achieve a normal slump. Defoamer was also added to achieve the air content to $4.5\pm 1\%$.

Table 6.3
Mix proportions.

Type	Unit (kg/m ³)								
	W/C (%)	C	FA	MFA	S	RSM	RSL	G	RG
N	55	327	-	0	857	-	-	945	-
F15	65	278	49		840	-	-	945	-
F30	79	229	98		824	-	-	945	-
M15	65	278	-	49	842	-	-	945	-
M30	79	229	-	98	828	-	-	945	-
F50M15	65	278	-	49	421	386	-	945	-
F50M30	79	229	-	98	414	380	-	945	-
FL50M15	65	278	-	49	421	-	363	945	-
FL50M30	79	229	-	98	414	-	357	945	-
F100M15	65	278	-	49	0	773	-	945	-
F100M30	79	229	-	98	0	759	-	945	-
FL100M15	65	278	-	49	0	-	727	945	-
FL100M30	79	229	-	98	0	-	714	945	-
C100M15	65	278	-	49	842	-	-	-	885
C100M30	79	229	-	98	828	-	-	-	885

6.2.3 Test methods

The mixing procedure is shown below: Fine aggregate and cement are put in and mixed for the 30s; Insert water and mix for 60s; Input coarse aggregate and mix for 60s. During the experiment, high-performance water reducing agent was added to meet the air volume and slump specified by JIS A 1101 [28].

According to JIS A 1108 [29], the compressive strength test is performed with a cylinder ($\varnothing=100$ mm \times h=200 mm). For each series, plastic molds were used for casting 12 cylinders and before demolding, stored in a chamber at 20 °C and 60% RH for 24 hours. According to JIS A 1129-3 [30], the drying shrinkage test was performed with a cuboid (100 \times 100 \times 400 mm). Three cuboids were cast in a steel mold for each combination and demolded after 24 hours in a chamber at 20 °C and 60% RH.

As shown in Picture 6.1, during each strength test, a device for measuring longitudinal and transverse strains is installed around each concrete specimen. The strain measuring instrument shall be able to measure the longitudinal strain (strain degree) of the specimen with an accuracy of 10×10^{-6} or less. The length of the strain measuring instrument shall be at least 3 times the maximum size of the coarse aggregate used for concrete and at least 1/2 the height of the specimen. Once the deformations were calculated, E_c can then be calculated based on the slope of the stress-strain curve. According to JIS A 1149 [31] and ASTM C469 [32], the formula for E_c is seen in the Equation below:

$$E_c = \frac{S_1 - S_2}{\varepsilon_1 - \varepsilon_2} \times 10^{-3} \quad (1)$$

E_c : Static elastic modulus of each specimen (kN / mm²)

S_1 : Stress corresponding to 1/3 of the maximum load (N / mm²)

S_2 : Stress when the longitudinal strain of the specimen is 50×10^{-6} (N / mm²)

ε_1 : Vertical strain of the specimen caused by stress

ε_2 : 50×10^{-6}

In this study, resonant frequency testing was also performed to calculate E_d . Measuring resonant frequencies to determine material properties is a relatively new method of non-destructive testing. The resonant frequency of vibration is related to the density and E_d of the material. The resonant frequencies of concrete specimens were determined by exciting the specimens in longitudinal, transverse, or torsional mode and then measuring the resulting free vibration. The dynamic elastic modulus experiments, as illustrated in Picture 6.2, were carried out using a cylinder positioned on a support base such that both ends could vibrate freely without being restricted. According to JIS A 1127 [33], the major resonance frequency of the longitudinal vibration was defined as the frequency at which the amplified pickup's output voltage showed a distinct maximum vibration. The dynamic elastic modulus is calculated by the following equation.

$$E_d = 4.00 \times 10^{-6} \frac{L}{A} m f_1^2 \quad (2)$$

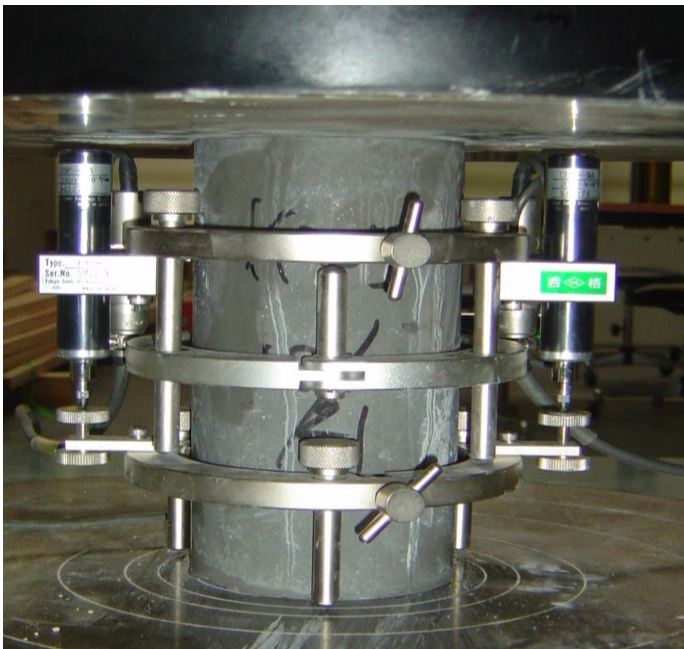
E_d : Dynamic elastic modulus (kN / mm²)

L : Specimen length (mm)

A : Specimen cross-sectional area (mm²)

m : Specimen mass (kg)

f_1 : Longitudinal vibration resonance frequency (Hz)



Picture 6.1. Test setups for E_c .



Picture 6.2. Test device for E_d .

The samples for mercury intrusion porosimetry (MIP) were extracted from the center of a cylinder that had dried in a curing room for either 28 or 91 days. Three specimens were tested under each set of conditions. The cylinder was then cut with a vise to obtain particles of 2–5 mm in diameter. The samples were dehydrated by submerging them in acetone for 2 h, after which they were dried for 1 h in an oven at 105°C and then put under a vacuum pump for 48 h. The MIP tests were done on AutoPore V, which subjected the samples to a maximum pressure of 60,000 psi and measured pore diameters of 3–3.6×10⁴ nm in this study. With MIP, numerous sample properties could be calculated, such as pore diameter distributions, total pore volume, and sample densities.

6.3 Result and discussion

6.3.1 Result of f_c and ε_d

At 7–91 days, the f_c of recycled concrete with FA or MFA was shown in Fig. 6.1. Using FA or MFA reduced the f_c of concrete at 7–91 days. At 7, 28, and 91 days, f_c of concrete containing 15% FA were 81.1%, 84.7%, and 97.5%, whereas f_c of concrete containing 15% MFA were 71.2%, 79.1%, and 92.5%, respectively. Although f_c of concrete containing MFA was lower than that of concrete containing FA, it increased faster. In addition, the use of recycled aggregates leads to a reduction in f_c , while the use of RFA with lower quality has a greater impact on f_c , and this difference could even reach 20% at a replacement level of 100% found by Khatib [34].

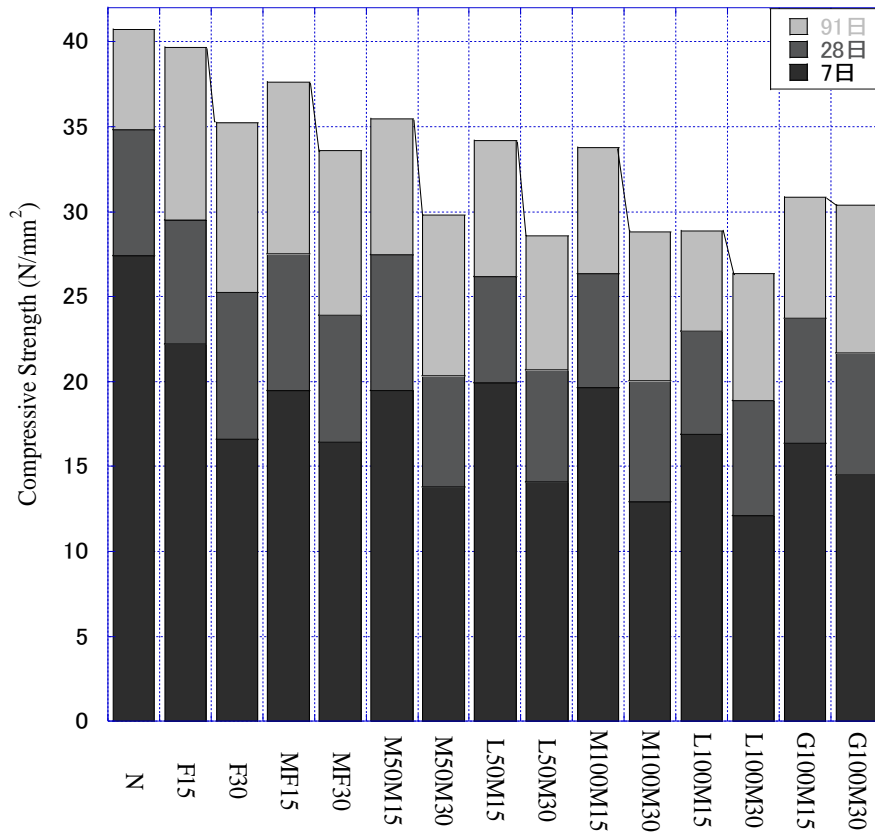


Fig. 6.1 Compressive strength of 7, 28, and 91 days.

Fig. 6.2 showed the ϵ_d of concrete specimens containing recycled aggregate and FA or MFA that lasted 181 days. Using FA or MFA increased the ϵ_d of concrete compared with the control concrete. The MFA replacement ratio had no significant effect on the ϵ_d at an RFA replacement ratio of 100%—the distance between lines of concrete containing 15% and 30% MFA, which are both below the red line, was tiny. This shows that, for recycled concrete, the impact of MFA on ϵ_d is consistent within a particular MFA content range (15-30%). This was attributed to the type of aggregate having a large effect on ϵ_d [35], and excess of an optimal FA content increasing ϵ_d [36].

CHAPTER 6: A STUDY ON PROPERTIES, STATIC AND DYNAMIC ELASTIC MODULUS OF RECYCLED CONCRETE UNDER THE INFLUENCE OF MODIFIED FLY ASH

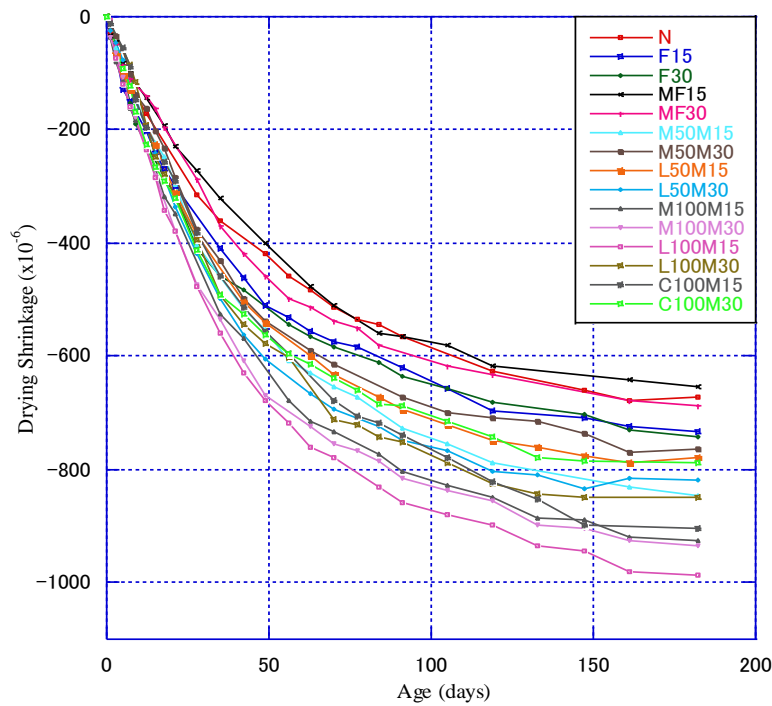


Fig. 6.2 Drying shrinkage lasted 181 days.

6.3.2 Result of E_c and E_d

Fig. 6.3 showed the box plot of the contrasting values of E_c based on the 91-day control concrete under the influence of different factors. The different factors had different effects on E_c , which increases with time, due to the increase in the concrete strength. The use of RFA and the decrease in the quality of the RFA decreased E_c , although the use of MFA decreased E_c only slightly. In other words, the effect of the factors on E_c was like the effect on the compressive strength.

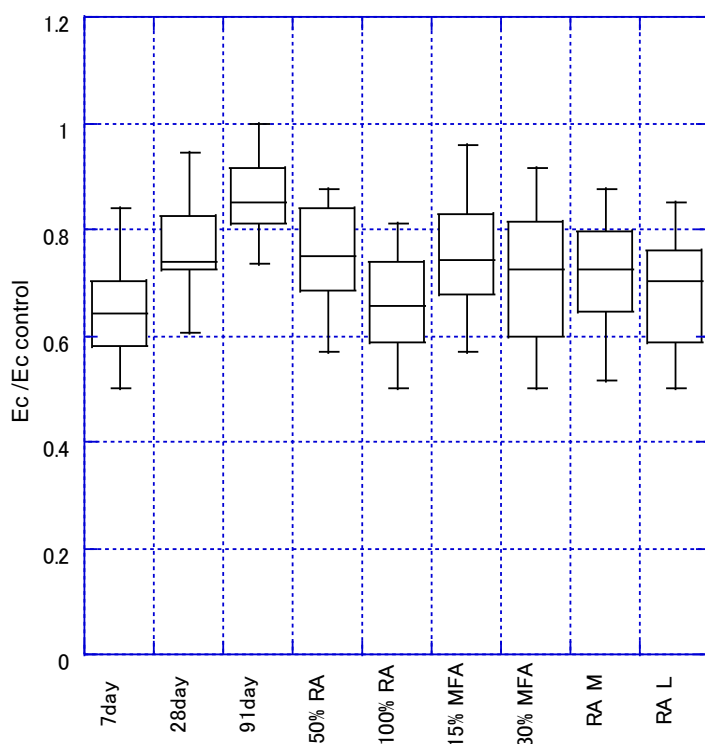


Fig. 6.3 Effect of age, incorporating MFA or RFA content and RFA quality on E_c .

The E_d was measured over a period of 7-91 days and each measurement was made one week apart, and the trend is shown in Fig. 6.4. The difference in the effect of using 15% and 30% FA or MFA on E_d was within 5%. For example, with equal amounts of MFA, E_d for concrete with 50% and 100% of class M or class L RFA was about 10% and 19% lower, respectively, on average at 91 days than with 0% admixture. This indicated that E_d was affected by RFA for all aggregate types which were consistent with results published in the literature [37, 38]. In other words, if the relationships of E_d with E_c and f_c are to be established for recycled concrete, RFA must be considered. According to Poon et al. [39], the change in E_d overtime is usually small and E_d in this experiment may have increased due to the FA being used instead of cement, which decreased water and hydration reactions in the early stage.

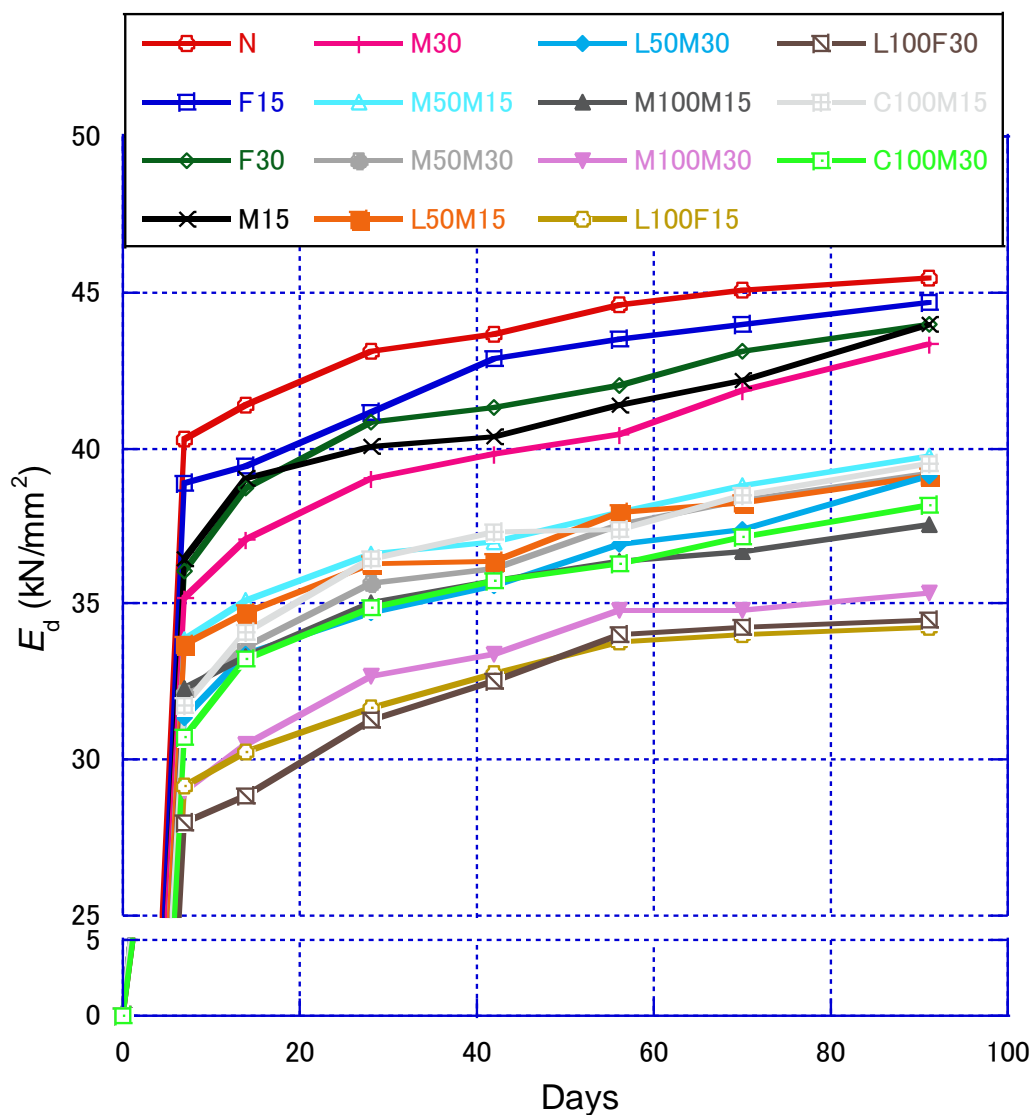


Fig. 6.4 Development of E_d of all mix.

6.3.3 Relationship between E_c and E_d

A linear relationship between E_c and E_d [40] has existed. In a study conducted by John S. Popovics [11], several empirical relationships were developed between E_c and E_d , and he developed the following equation.

$$E_d = 1.20E_c \quad (3)$$

E_c = Static Modulus of Elasticity (kN/mm^2)

E_d = Dynamic Modulus of Elasticity (kN/mm^2)

Based on the above discussion, in this experiment, the following equation would be used

$$E_d = aE_c \quad (4)$$

where a are coefficients.

E_c and E_d of each concrete specimen were plotted on the x-axis and y-axis, respectively. A trend line

was also inserted from the origin to show the best correlation values, and finally, the values of the trend line equation and R^2 were generated.

As shown in Fig. 6.5, the relationship between E_c and E_d was linear. Based on this data, the following empirical equation was determined and used to establish the relationship between E_c and E_d .

$$E_d = 1.31E_c \quad (5)$$

From this equation, it could be estimated that E_d was approximately 31% greater than the E_c , based on the analysis of all different concrete batches.

Unlike static testing, dynamic testing only applied a small amount of force to the specimen, and thus did not deform the specimen during the testing phase. This might be why E_d was higher than E_c , as observed in the present research. The composite nature of concrete might also cause the difference in Young's modulus. Homogeneous materials, such as steel [41] and paste samples did not exhibit this behavior. Concrete consisted of aggregates and sand particles, which greatly alter its homogeneity.

The R^2 value after linear fitting was 0.82265, which was close to 1 but did not exceed 0.9. The data plotted in Fig 6.5 was from all samples of all ages. Therefore, the equation for the linear trend line was based on the average correlation for the Young's moduli for samples of all ages. The same analysis was performed for the concrete data at different ages, which showed how the empirical equations for the early concrete changed.

As the equations in Table 4 shown, Young's modulus began to converge as the concrete matured. The R^2 values also increased with the age of the concrete, which indicated that the linear relationship between Young's modulus increased with age. This was due to the increase in the degree of hydration of the concrete in the later stages [42]. Early concrete was less hydrated and the free water in the concrete has a greater effect on E_c test. This resulted in a greater separation of these values at early ages. As the concrete matures and hydration increases, the axial static load did not deform the concrete specimens as much. This resulted in the convergence of the two Young's modulus over time.

The British Code of concrete structures CP110:1972 [43] gives the following equation:

$$E_d = 0.8E_c + 15.2 \quad (6)$$

Zhou [44] showed that at each age, E_d was always greater than E_c . A linear relationship between E_c and E_d was investigated, and this relationship was described by the equation

$$E_d = bE_c + c \quad (7)$$

where b and c are coefficients.

This indicated that there was more than one linear relationship between E_d and E_c . Based on the above analysis, in this experiment, unlike before, a trend line that did not cross the origin was added to show the best correlation values between the two methods, and the values of the trend line equation and R^2 were determined. The R^2 value was 0.9579, which was close to 1 (Fig. 5). This indicated that the data were close to the fitted regression line with little variability. Based on this data, the following empirical equation was determined and used to establish the relationship between E_c and E_d .

$$E_d = 0.95E_c + 10 \quad (8)$$

Based on this equation, it could be estimated that E_d was approximately 10 (N/mm²) larger than the E_c .

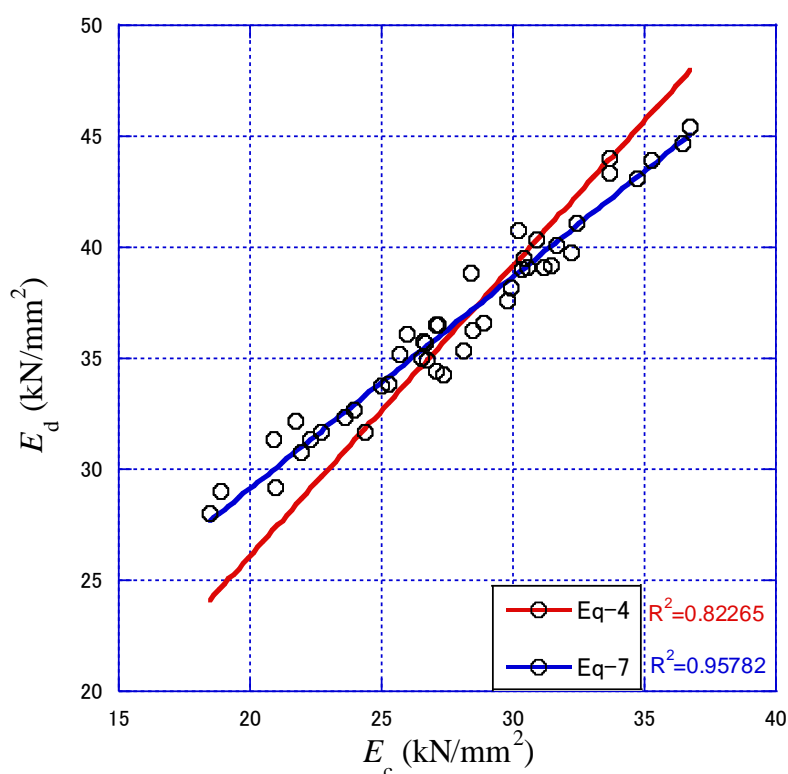


Fig. 6.5 Relationship between E_c and E_d of all mix.

The same analysis was performed for concrete data of different ages, as shown in the equation in Table 6.4, where the fixed difference between Young's moduli decreased as the concrete matured, which was consistent with the equation. However, R^2 remained constant, which showed that this equation was suitable for concrete of different ages, but it was difficult to write a single equation to express the relationship between E_d and E_c for all ages due to the large difference in fixed difference c . However, this result showed that the effect of age on coefficient b , which controls the shape and convergence of the relationship in this formula, was smaller than that on coefficient c . After calculation, the coefficient b is close to 1. Hence, we assume that the coefficient b is 1 to calculate the value of the coefficient c . The detailed relationship was as follows.

$$c = 9.28 - 0.01T \quad (9)$$

T : Age of concrete (days)

Table 6.4

Influence of age on the relationship between E_c and E_d .

Days	Equation	R^2	Equation	R^2
7	$E_d = 1.39E_c$	0.8134	$E_d = E_c + 9.43$	0.9589
28	$E_d = 1.310E_c$	0.8710	$E_d = E_c + 8.63$	0.9513
91	$E_d = 1.26E_c$	0.9546	$E_d = E_c + 8.25$	0.9373

6.3.4 Relationship between f_c and E_c

The relationship between E_c and f_c is provided in the design codes of many countries (Table 5). Fig. 6

compares the actual data from this experiment using the equations from these design codes. Most of the experimental values were higher than the normative standards of most countries because the equations tend to provide conservative values. The BS equation does not pass through the origin because this equation is designed for f_c , the 28-day compressive strength. Using RA and MFA reduces the strength of the concrete, which results in the strength not increasing as fast as E_c , which is also consistent with Fig. 6.1 and Fig. 6.3. The increases in strength between 7 and 28 days and 28 and 91 days were 27%–52% and 16%–47%, respectively, whereas the increases in E_c between 7 and 28 days and 28 and 91 days were 12%–27% and 5%–21%, respectively. The difference between the growth rates resulted in the calculated E_c being smaller than the actual value when the predicted equation was used.

The type of formulas in Table 6.5 showed that all formulas were power functions of the strength, except for the GB formula. Based on the regulations of each country, an equation with R^2 of 0.8699, which was closest to the experiment data, was obtained by calculating.

$$E_c = 5600 \times \sqrt{f_c} \quad (10)$$

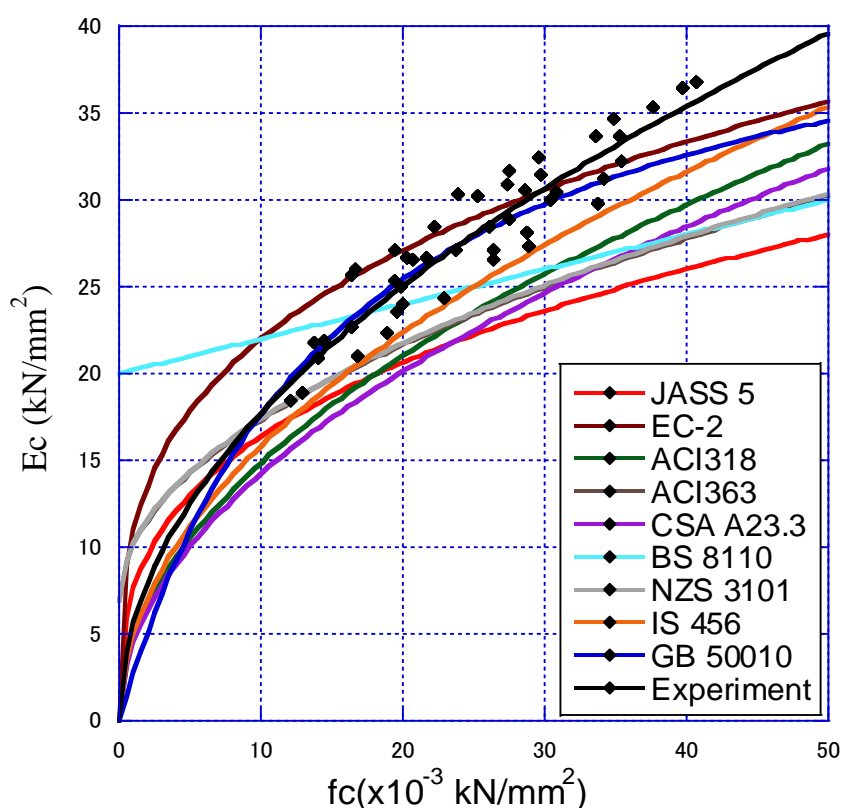


Fig. 6.6 Comparison of the calculated values and the experimental data.

However, the GB prediction equation was close to the experimental value (Fig. 6.6), and the GB equation was calculated (Table 6.5). The RMSE (root-mean-square error) of this equation was slightly larger than that of Eq. (10), which indicated that the GB equation could be used for recycled concrete with cement-based admixtures, although the values predicted by Eq. (10) were still closer to the

experimental values.

Table 6.5
Estimating equations for design codes of different countries.

Code	Equation	RMSE
JASS 5	$E_c = 3.35 \times 10^4 \times \left(\frac{\gamma}{2.4}\right)^2 \times \left(\frac{f_c}{60}\right)^{\frac{1}{3}}$	6.3630
EC-2	$E_c = 22000 \times \left(\frac{f_c}{10}\right)^{0.3}$	2.3908
ACI 318-14	$E_c = 4700 \times \sqrt{f_c}$	4.9305
ACI 363-08	$E_c = 3300 \times \sqrt{f_c} + 6900$	5.1941
CSA A23.3-04	$E_c = 4500 \times \sqrt{f_c}$	5.8839
BS 8110	$E_c = 20000 + 200 \times f_c$	4.2533
NZS 3101	$E_c = 3320 \times \sqrt{f_c} + 6900$	5.1012
IS 456	$E_c = 5000 \times \sqrt{f_c}$	3.5486
GB 50010	$E_c = \frac{10^5}{2.2 + \frac{34.7}{f_c}}$	1.9447
Experiment-based on GB	$E_c = \frac{10^5}{1.8 + \frac{42.2}{f_c}}$	1.67076
Experiment	$E_c = 5600 \times \sqrt{f_c}$	1.62980

γ : Density of concrete(t/m^3); f_c : Compressive strength(N/mm^2); E_c : Static modulus of elasticity(N/mm^2).

6.3.5 Relationship between f_c and E_d

According to Eq. (5) and Eq. (8), there was a linear correlation between E_c and E_d , and this result showed that E_d is always greater than E_c at each specific age. Table 5 shows that there is a power function correlation between E_c and f_c , and the predicted E_c values were always smaller than the experimental values. Thus, the equation in Table 5 could be modified to accommodate experimental E_d values. The equation was rewritten as follows.

$$E_d = d \times \sqrt{f_c} + e \quad (11)$$

where d and e are coefficients.

Fig. 6.7 showed the results of Eq. (11), which was a suitable relationship for all the concretes used. The values of d and e were affected by the different types and amounts of RA used in MFA (Table 6). These results correspond to Figure 4, which shows that different admixtures and types of RA led to different E_d values, although the trend in E_d over time was similar for each type of concrete.

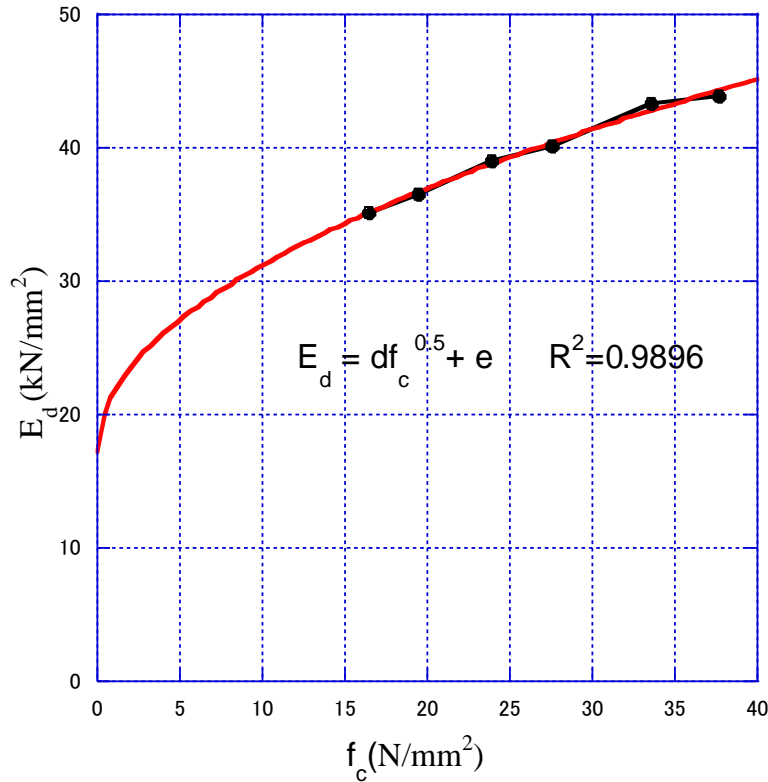


Fig. 6.7 Relationship between E_d and f_c of no recycled aggregate used concretes.

Table 6.6

Coefficients d and e for each series

RA Class M (%)	RA Class L (%)	d	c	R^2
0	0	4.41	17.25	0.9896
0	50	3.90	16.99	0.9115
0	100	3.59	15.21	0.9357
50	0	3.27	20.11	0.9200
100	0	3.73	15.74	0.9925

According to the results of the preceding study, d and e in Eq. (11) were influenced by the different containing and the quality of RFA. The linear coefficients d or e was determined by Multiple regression analysis under the influencing factors listed above. They were listed as follows.

$$d = 4.15 - 0.691V_{-M} - 0.551V_{-L} \quad (12)$$

$$c = 18.5 - 1.56V_{-M} - 3.24V_{-L} \quad (13)$$

where V_{-M} is volume content of recycled fine aggregate class M, ranges from 0 to 1, V_{-L} is content of recycled fine aggregate class L, ranges from 0 to 1.

6.3.6 Influence of pore diameter on the correlation between Porosity and ε_d or E_d

Mindess et al. [45] gave the following definitions based on experiments determined by MIP: capillary

pores were larger than 10 nm and gel pores were smaller than 10 nm. In addition, the researchers studied the porosity and pore structure of the cement paste. PK Mehta [46] considered four intervals of pores: < 4.5 nm; 4.5–50 nm; 50–100 nm; >100 nm, and reported that pores up to 132 nm in diameter have a slight effect on concrete properties; Wu [47] considered four intervals of pores: <20 nm named as harmless pores, 20–50 nm named as small harmful pores, 50–200 nm named as harmful pores and >200 nm named as large harmful pores.

MIP was not suitable for determining the pore diameter distribution of cementitious materials because of "ink bottle" pores [48] of which large pores were only penetrated when higher pressures are reached. Pores smaller than the threshold diameter [49] above which pores form disconnected paths throughout the sample were accurately determined by MIP [50]. 10 nm was the dividing pore diameter between the gel pore and the capillary pore, while the threshold diameter (Fig. 6.8) existed in the typical pore diameter distribution curve determined by the MIP experiment and was closer to 75 nm. The capillary pore is around 75 nm, while the gel pore was less than 5 nm based on the experimental data on drying shrinkage and weight loss [51].

The measurement range of MIP in this experiment was $3\text{--}3.6 \times 10^4$ nm, the gel pore was considered to have 5 or 10 nm, and the threshold pore diameter is taken as 75 nm, thus the pore diameter of the specimen was divided into five intervals of 3–10 nm; 10–20 nm; 20–50 nm; 50–75 nm; >75nm; as shown in Fig. 6.9. Overall, the pore volume in the 3–75 nm interval accounts for 84%–92% of the total pore volume, which also corresponds to Fig. 6.8.

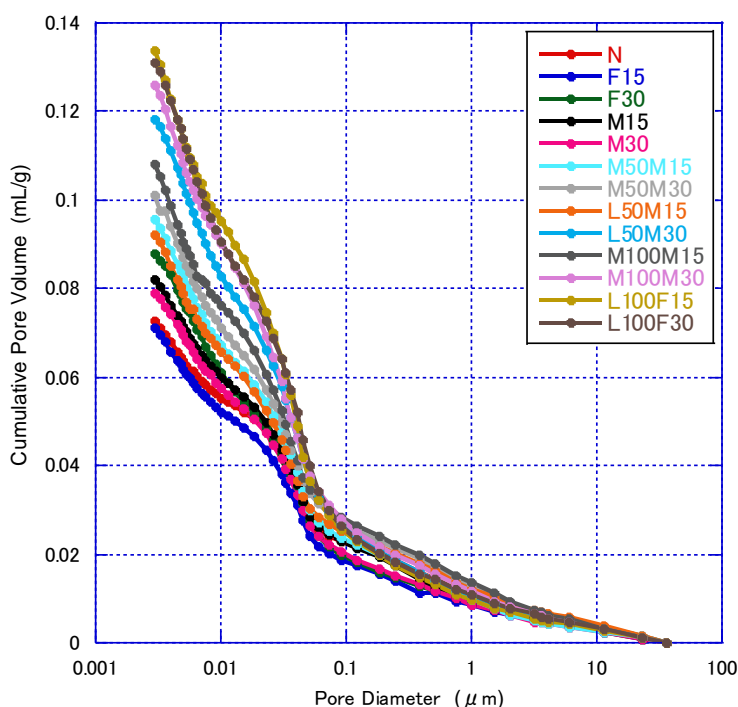


Fig. 6.8 Cumulative pore volume at 91 days

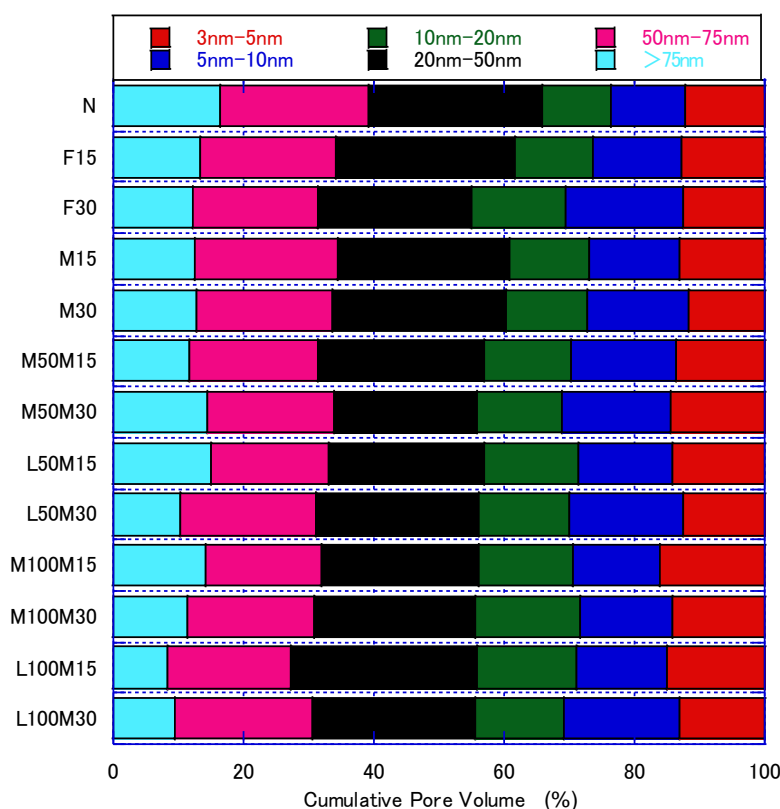


Fig. 6.9 Pore volume over different pore diameter intervals

In this experiment, E_d was measured for a maximum of 91 days, and thus 91 days of experimental data were used to establish the relationship. In concrete, ε_d is greatly influenced by the aggregate, particularly the water absorption rate of the aggregate, and the RFA has a substantially greater water absorption than the typical fine aggregate [52]. The quality of the RFA also affects some durability of the concrete; thus, the quality of the RFA and the admixture amount are separated to calculate the R^2 between ε_d and the pore volume at different pore diameters (Table 6.7).

Overall, the correlation between pore volume and ε_d gradually strengthened as the pore diameter increased, with R^2 reaching a maximum value of 0.92 at a pore diameter of 10–20 nm (Fig. 6.10). However, the correlation decreased when the pore diameter was 20–50 nm and increased when the pore diameter was greater than 50 nm. This was because ε_d is mainly affected by the volume occupied by the gel pores [53]. When the substitution rate of the RFA increased, the correlation depended on the pore diameter interval, and the correlation coefficient was higher at substitution rates of 50% and 100%. This may be due to the high water absorption of the RFA, where the higher the water absorption of the aggregate, the greater the effect on ε_d [54]. The effect of the high quality of the RFA on the correlation tended to be consistent. There was no clear pattern in the high and low correlation coefficients for MFA substitution rates of 15% and 30%.

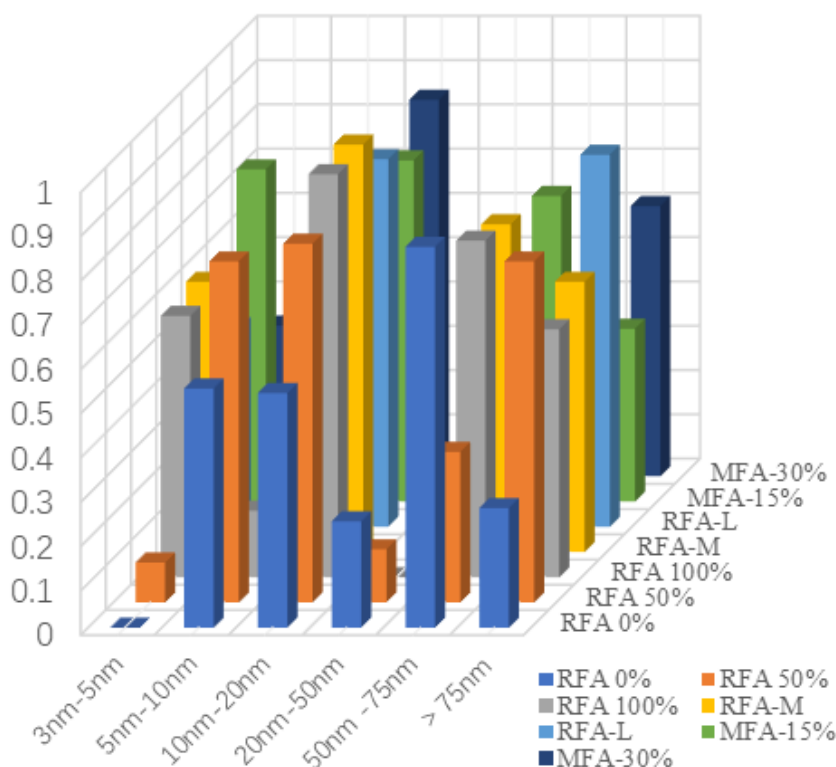


Fig.6.10 Influence of different pore diameters on R^2 between ϵ_d and pore volume

Table.6.7

R^2 between ϵ_d and the pore volume at different pore diameters

Interval	RFA 0%	RFA 50%	RFA 100%	RFA-M	RFA-L	MFA-15%	MFA-30%
3nm-5nm	0	0.09	0.59	0.61	0.45	0.75	0.34
5nm-10nm	0.54	0.77	0.15	0.07	0.24	0.14	0.24
10nm-20nm	0.53	0.81	0.91	0.92	0.83	0.77	0.85
20nm-50nm	0.24	0.12	0	0.11	0.09	0	0.2
50nm -75nm	0.86	0.34	0.76	0.74	0.34	0.69	0.35
> 75nm	0.27	0.77	0.56	0.61	0.84	0.39	0.61

Ho [53] argued that capillary pores affected strength and gel pores affected the durability of the mortar. Thus, the pore volume within a certain pore diameter range including both gel pores and capillary pores affected both the mechanical properties and durability of concrete. The correlation coefficients between the dynamic elastic modulus of concrete and the volume of pores at different pore diameters were calculated and the data are listed in Table 6.8.

The correlation between pore volume and ϵ_d gradually increased as the pore diameter increased, with R^2 reaching a maximum value of 0.95 at pore diameters up to 10–20 nm (Fig. 6.11). However, the correlation decreased when the pore diameter was 20–50 nm and increased when the pore diameter was greater than 50 nm, similar to the trend in Fig. 6.10. This result also implied that the pore volume and E_d at pore diameters of 10–20 nm had a high correlation; in other words, this confirmed that E_d

could be correlated with ε_d . The different fine aggregate substitution rates, fine aggregate qualities, and MFA substitution rates in Table 8 had similar effects on the correlation coefficients as those in Table 6.7, indicating that E_d and ε_d were still correlated despite changes in RFA substitution rate or quality or MFA substitution rate. Therefore, the pore volumes at a certain pore diameter interval (considered as 10–20 nm in this experiment) could be correlated as a bridge to establish a predictive equation for ε_d of recycled concrete with MFA as a variable by using E_d .

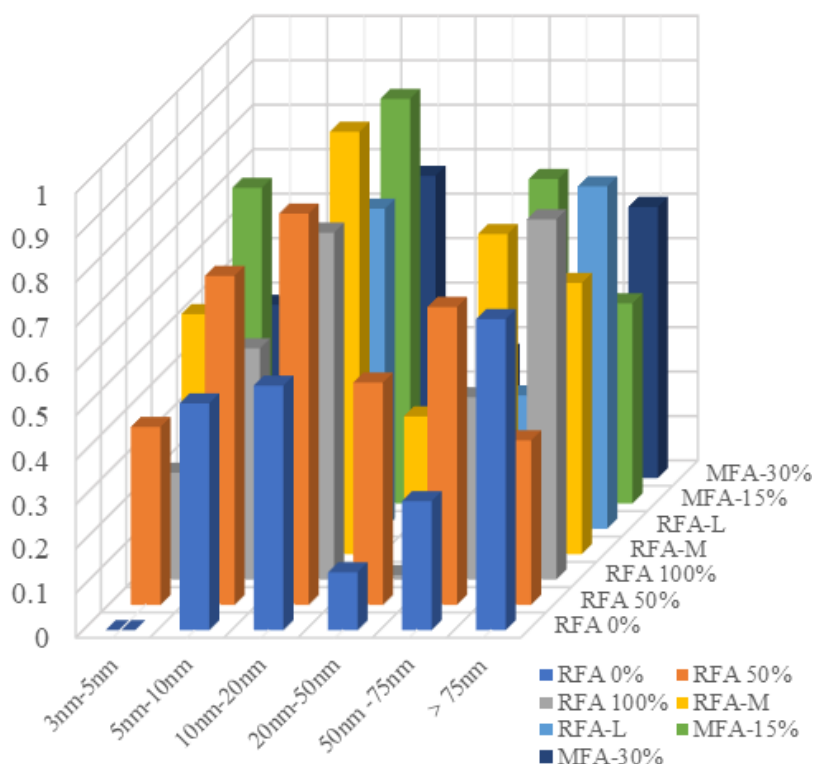


Fig.6.11 Influence of different pore diameters on R^2 between E_d and pore volume

Table.6.8

R^2 between E_d and the pore volume at different pore diameters

Interval	RFA 0%	RFA 50%	RFA 100%	RFA-M	RFA-L	MFA-15%	MFA-30%
3nm-5nm	0	0.40	0.24	0.54	0.37	0.71	0.39
5nm-10nm	0.51	0.74	0.52	0.21	0.37	0.18	0.36
10nm-20nm	0.55	0.88	0.78	0.95	0.72	0.91	0.68
20nm-50nm	0.13	0.50	0.01	0.31	0	0	0.28
50nm-75nm	0.29	0.67	0.41	0.72	0.30	0.73	0.35
>75nm	0.70	0.37	0.81	0.61	0.77	0.45	0.61

From the mentioned above, it is found that there is a correlation between the drying shrinkage and the dynamic modulus. Therefore, based on the prediction equation Eq. (14) defined by ACI

209 [58] for drying shrinkage, it is considered to adding a coefficient related to the dynamic modulus and test time.

$$\varepsilon_{t} = t / (35 + t) \cdot \varepsilon_{\mu}$$

(14)

$$\varepsilon_{\mu} = 780 \times 10^{-6} \gamma$$

ε_t : The drying shrinkage strain at drying time t

ε_{μ} : The final value of drying shrinkage strain

t : The drying time

γ : The influence correction coefficient

Fitting by bringing in the experimental values to obtain following equation:

$$\varepsilon_{t} = T / E_d \cdot t / (35 + t) \cdot \varepsilon_{\mu}$$

(15)

$$T = 39 + 1.13 \sqrt{t(E_d)}$$

$t(E_d)$: Dynamic elastic modulus testing time.

6.4 Conclusions

In this study, the relationship between the compressive strength, static modulus, and dynamic modulus of concrete with RFA and MFA was confirmed.

The following conclusions can be drawn:

- 1) There are two types of linear correlations between the static modulus E_c and the dynamic modulus E_d , one of which is affected by age of concrete.
- 2) The relationship between the compressive strength and static modulus of elasticity is recommended by an equation derived based on the formula of each national standard.
- 3) A polynomial equation suggests a relationship between the compressive strength and dynamic modulus of elasticity. The $E_d - f_c$ connection is governed by two factors: recycled aggregate volume content and quality.
- 4) E_d or ε_d of concrete has the highest correlation for pore volumes in the 10 nm-20 nm pore diameter range, and there is a high degree of consistency in the cases affected by RFA volume content, RFA quality, and MFA volume content.

The above results are based on the recycled concrete with modified fly ash and other different types of concrete that may not be applicable due to the different parameters of correlation they may have.

References

- [1] M. Behera, S.K. Bhattacharyya, A.K. Minocha, R. Deoliya, S. Maiti, Recycled aggregate from C&D waste & its use in concrete – A breakthrough towards sustainability in construction sector: A review, *Construction and Building Materials* 68 (2014) 501-516. <https://doi.org/10.1016/j.conbuildmat.2014.07.003>
- [2] M. Etxeberria, A.R. Marí, E. Vázquez, Recycled aggregate concrete as structural material, *Materials and Structures* 40(5) (2007) 529-541. <https://doi.org/10.1617/s11527-006-9161-5>
- [3] M.E. Sosa, Y.A. Villagrán Zaccardi, C.J. Zega, A critical review of the resulting effective water-to-cement ratio of fine recycled aggregate concrete, *Construction and Building Materials* 313 (2021) 125536. <https://doi.org/https://doi.org/10.1016/j.conbuildmat.2021.125536>
- [4] S.K. Kirthika, S.K. Singh, Durability studies on recycled fine aggregate concrete, *Construction and Building Materials* 250 (2020) 118850. <https://doi.org/https://doi.org/10.1016/j.conbuildmat.2020.118850>
- [5] R. Kurda, J. de Brito, J.D. Silvestre, Combined influence of recycled concrete aggregates and high contents of fly ash on concrete properties, *Construction and Building Materials* 157 (2017) 554-572. <https://doi.org/https://doi.org/10.1016/j.conbuildmat.2017.09.128>
- [6] C.J. Zega, Á.A. Di Maio, Use of recycled fine aggregate in concretes with durable requirements, *Waste Management* 31(11) (2011) 2336-2340. <https://doi.org/https://doi.org/10.1016/j.wasman.2011.06.011>
- [7] T. Uygunoğlu, I.B. Topcu, O. Gencil, W. Brostow, The effect of fly ash content and types of aggregates on the properties of pre-fabricated concrete interlocking blocks (PCIBs), *Construction and Building Materials* 30 (2012) 180-187. <https://doi.org/https://doi.org/10.1016/j.conbuildmat.2011.12.020>
- [8] H.-J. Chen, N.-H. Shih, C.-H. Wu, S.-K. Lin, Effects of the Loss on Ignition of Fly Ash on the Properties of High-Volume Fly Ash Concrete, *Sustainability* 11(9) (2019) 2704. <https://doi.org/10.3390/su11092704>
- [9] M. Ejtemaei, M. Gharabaghi, M. Irannajad, A review of zinc oxide mineral beneficiation using flotation method, *Advances in Colloid and Interface Science* 206 (2014) 68-78. <https://doi.org/https://doi.org/10.1016/j.cis.2013.02.003>
- [10] H. Lin, K. Takasu, H. Koyamada, H. Suyama, Development of Flotation Device for Removing Unburnt Carbon in Fly Ash for Use in Hardened Cementitious Materials, *Materials (Basel)* 14(21) (2021) 6517. <https://doi.org/10.3390/ma14216517>
- [11] J.S. Popovics, J. Zemajtis, I. Shkolnik, A study of static and dynamic modulus of elasticity of concrete, *ACI-CRC Final Report* (2008).
- [12] J.K. Kim, Y.H. Moon, S.H. Eo, Compressive strength development of concrete with different curing time and temperature, *Cement and Concrete Research* 28(12) (1998) 1761-1773. [https://doi.org/https://doi.org/10.1016/S0008-8846\(98\)00164-1](https://doi.org/https://doi.org/10.1016/S0008-8846(98)00164-1)
- [13] Architectural Institute of Japan, JASS 5: Japanese Architectural Standard Specification for Reinforced Concrete Work, Japan, 2018.
- [14] European Committee for Standardization, Eurocode 2: Design of Concrete Structures, Brussels, Belgium, 2004.
- [15] American Concrete Institute, ACI 318-08 Building Code for Structural Concrete, Detroit,

USA, 2008.

[16] American Concrete Institute, ACI 363R-08 State of the Art Report on High Strength Concrete, Detroit, USA, 2008.

[17] CSA Technical Committee, Reinforced Concrete Design, A23.3-04, Design of Concrete Structures, Rexdale, Ontario, Canada, 2004.

[18] British Standards Institution, BS 8110-2: 1985, Code of practice for special circumstances, UK, 1985.

[19] New Zealand Standard, Concrete Structures Standard, NZS 3101:2006, The Design of Concrete Structures, Wellington, New Zealand, 2006.

[20] BUREAU OF INDIAN STANDARDS, IS 456: 2000, Indian Standard PLAIN AND REINFORCED CONCRETE - CODE OF PRACTICE, 2000.

[21] Code For Design of Concrete Structures (GB 50010-2010), State Development Planning Commission of the People's Republic of China, Beijing.

[22] X. Lu, Q. Sun, W. Feng, J. Tian, Evaluation of dynamic modulus of elasticity of concrete using impact-echo method, Construction and Building Materials 47 (2013) 231-239. <https://doi.org/https://doi.org/10.1016/j.conbuildmat.2013.04.043>

[23] A.I. Marques, J. Morais, P. Morais, M.d.R. Veiga, C. Santos, P. Candeias, J.G. Ferreira, Modulus of elasticity of mortars: Static and dynamic analyses, Construction and Building Materials 232 (2020) 117216. <https://doi.org/https://doi.org/10.1016/j.conbuildmat.2019.117216>

[24] P.P. Chavhan, M.R. Vyawahare, Correlation of static and dynamic modulus of elasticity for different SCC mixes, International Journal on Recent and Innovation Trends in Computing and Communication 3(7) (2015) 4914-4919.

[25] M. Safiuddin, M. Abdus Salam, M.Z. Jumaat, Correlations between Different Hardened Properties of High-Strength Self-Consolidating Concrete Including Palm Oil Fuel Ash, Applied Mechanics and Materials 117-119 (2012) 1215-1222. <https://doi.org/10.4028/www.scientific.net/AMM.117-119.1215>

[26] B.J. Lee, S.-H. Kee, T. Oh, Y.-Y. Kim, Effect of Cylinder Size on the Modulus of Elasticity and Compressive Strength of Concrete from Static and Dynamic Tests, Advances in Materials Science and Engineering 2015 (2015) 580638. <https://doi.org/10.1155/2015/580638>

[27] P. Smarzewski, D. Barnat-Hunek, Property Assessment of Hybrid Fiber-Reinforced Ultra-High-Performance Concrete, International Journal of Civil Engineering 16(6) (2018) 593-606. <https://doi.org/10.1007/s40999-017-0145-3>

[28] Japanese Industrial Standard Committee, JIS A 1101 Method of test for slump of concrete, Japan, 2020.

[29] Japanese Industrial Standard Committee, JIS A 1108 Method of Test for Compressive Strength of Concrete, Japan, 2018.

[30] Japanese Industrial Standard Committee, JIS A 1129-3 Methods of Measurement for Length Change of Mortar and Concrete—Part 3: Method with Dial Gauge, Japan, 2010.

[31] Japanese Industrial Standard Committee, JIS A 1149 Method of Test for Static Modulus of Elasticity of Concrete, Japan, 2017.

[32] American Society for Testing Material, ASTM C469/C469M-14 Standard Test Method For Static Modulus of Elasticity and Poisson's Ratio of Concrete in Compression, West Conshohocken,

Pennsylvania, USA, 2014.

[33] Japanese Industrial Standard Committee, JIS A 1127 Methods of Test for Dynamic Modulus of Elasticity, Rigidity and Poisson's Ratio of Concrete by Resonance Vibration, Japan, 2010.

[34] J.M. Khatib, Properties of concrete incorporating fine recycled aggregate, *Cement and Concrete Research* 35(4) (2005) 763-769.
<https://doi.org/https://doi.org/10.1016/j.cemconres.2004.06.017>

[35] R.W. Carlson, Drying shrinkage of concrete as affected by many factors, *American Soc Testing & Materials Proc* (1938).

[36] J. Liu, R. An, Z. Jiang, H. Jin, J. Zhu, W. Liu, Z. Huang, F. Xing, J. Liu, X. Fan, T. Sui, Effects of w/b ratio, fly ash, limestone calcined clay, seawater and sea-sand on workability, mechanical properties, drying shrinkage behavior and micro-structural characteristics of concrete, *Construction and Building Materials* 321 (2022) 126333.
<https://doi.org/https://doi.org/10.1016/j.conbuildmat.2022.126333>

[37] V. Corinaldesi, G. Moriconi, Influence of mineral additions on the performance of 100% recycled aggregate concrete, *Construction and Building Materials* 23(8) (2009) 2869-2876.
<https://doi.org/https://doi.org/10.1016/j.conbuildmat.2009.02.004>

[38] J.M.V. Gómez-Soberón, Porosity of recycled concrete with substitution of recycled concrete aggregate: An experimental study, *Cement and Concrete Research* 32(8) (2002) 1301-1311.
[https://doi.org/https://doi.org/10.1016/S0008-8846\(02\)00795-0](https://doi.org/https://doi.org/10.1016/S0008-8846(02)00795-0)

[39] P. Chisun, K.O.U. Shicong, Effects of fly ash on mechanical properties of 10-year-old concrete prepared with recycled concrete aggregates, RILEM Publications SARL, pp. 46-59.

[40] S.-H. Han, J.-K. Kim, Effect of temperature and age on the relationship between dynamic and static elastic modulus of concrete, *Cement and Concrete Research* 34(7) (2004) 1219-1227.
<https://doi.org/https://doi.org/10.1016/j.cemconres.2003.12.011>

[41] W.-y. Wang, B. Liu, V. Kodur, Effect of temperature on strength and elastic modulus of high-strength steel, *Journal of materials in civil engineering* 25(2) (2013) 174-182.

[42] A.L.A. Fraay, J.M. Bijen, Y.M. de Haan, The reaction of fly ash in concrete a critical examination, *Cement and Concrete Research* 19(2) (1989) 235-246.
[https://doi.org/https://doi.org/10.1016/0008-8846\(89\)90088-4](https://doi.org/https://doi.org/10.1016/0008-8846(89)90088-4)

[43] British Standards Institution, CP 110:1972, Code of practice for the structural use of concrete, UK, 1972.

[44] Y. Zhou, J. Gao, Z. Sun, W. Qu, A fundamental study on compressive strength, static and dynamic elastic moduli of young concrete, *Construction and Building Materials* 98 (2015) 137-145. <https://doi.org/https://doi.org/10.1016/j.conbuildmat.2015.08.110>

[45] S. Mindess, F.J. Young, D. Darwin, *Concrete* 2nd Editio, Technical Documents (2003).

[46] P.K. Mehta, P.J.M. Monteiro, *Concrete microstructure, properties and materials*, 2017.

[47] Z.W. WU, H.Z. LIAN, *High Performance Concrete*, Beijing: China Railway Publication House (1999).

[48] S. Diamond, Mercury porosimetry: An inappropriate method for the measurement of pore size distributions in cement-based materials, *Cement and Concrete Research* 30(10) (2000) 1517-1525. [https://doi.org/https://doi.org/10.1016/S0008-8846\(00\)00370-7](https://doi.org/https://doi.org/10.1016/S0008-8846(00)00370-7)

[49] L. Cui, J.H. Cahyadi, Permeability and pore structure of OPC paste, *Cement and Concrete*

CHAPTER 6: A STUDY ON PROPERTIES, STATIC AND DYNAMIC ELASTIC MODULUS OF RECYCLED CONCRETE UNDER THE INFLUENCE OF MODIFIED FLY ASH

- Research 31(2) (2001) 277-282. [https://doi.org/https://doi.org/10.1016/S0008-8846\(00\)00474-9](https://doi.org/https://doi.org/10.1016/S0008-8846(00)00474-9)
- [50] C. Pichler, R. Lackner, H.A. Mang, A multiscale micromechanics model for the autogenous-shrinkage deformation of early-age cement-based materials, *Engineering Fracture Mechanics* 74(1) (2007) 34-58. <https://doi.org/https://doi.org/10.1016/j.engfracmech.2006.01.034>
- [51] H.M. Jennings, Colloid model of C–S–H and implications to the problem of creep and shrinkage, *Materials and Structures* 37(1) (2004) 59-70. <https://doi.org/10.1007/BF02481627>
- [52] Y. Mao, J. Liu, C. Shi, Autogenous shrinkage and drying shrinkage of recycled aggregate concrete: A review, *Journal of Cleaner Production* 295 (2021) 126435. <https://doi.org/https://doi.org/10.1016/j.jclepro.2021.126435>
- [53] H.-L. Ho, R. Huang, W.-T. Lin, A. Cheng, Pore-structures and durability of concrete containing pre-coated fine recycled mixed aggregates using pozzolan and polyvinyl alcohol materials, *Construction and Building Materials* 160 (2018) 278-292. <https://doi.org/https://doi.org/10.1016/j.conbuildmat.2017.11.063>
- [54] S.-c. Kou, C.-s. Poon, Effect of the quality of parent concrete on the properties of high performance recycled aggregate concrete, *Construction and Building Materials* 77 (2015) 501-508. <https://doi.org/https://doi.org/10.1016/j.conbuildmat.2014.12.035>

CHAPTER 6: A STUDY ON PROPERTIES, STATIC AND DYNAMIC ELASTIC MODULUS OF
RECYCLED CONCRETE UNDER THE INFLUENCE OF MODIFIED FLY ASH

Chapter 7

***STRENGTH AND DRYING SHRINKAGE OF HIGH-
STRENGTH CONCRETE WITH RECYCLED
AGGREGATES USING FLY ASH WITH THE
FLOTATION OF DECARBONIZATION***

CHAPTER 7: STRENGTH AND DRYING SHRINKAGE OF HIGH-STRENGTH CONCRETE
WITH RECYCLED AGGREGATES USING FLY ASH WITH THE FLOTATION OF
DECARBONIZATION

7.1. Introduction

Many environmental problems may be traced back to the construction industry, particularly those that are the result of the manufacturing and transportation of various building materials (e.g., aggregates and cement). As a result, environmental protection organizations have been applying pressure to the cement and aggregate sectors, demanding that they reduce their use of raw materials and energy. The annual need for fine and coarse aggregates around the globe has climbed to more than 52 billion tons [1]. The extraction of aggregate has a number of negative effects on environmental quality, including the destruction of habitats for a variety of living species and the loss of fertile land, as well as increased levels of noise and air pollution, soil erosion, and changes in the area's aesthetic scenery [2].

On the other hand, construction and demolition waste (often abbreviated as CDW) have also seen significant increases over the last ten years. Loss of essential areas, a lack of landfills, and other issues in solid waste management are only some of the environmental impacts that may be attributed to CDW. CDW has the potential to raise the already hazardous amounts found in soils [3]. As an example, China created more than 15 billion tons of construction and demolition waste in 2016 [4]. The yearly production of CDW in Europe is between 320 and 380 million tons [5].

It is possible to recycle CDW so that it may be used again in RC. Therefore, the aforementioned problems may be partly remedied by including CRA into the manufacturing of concrete [6, 7], although at the expense of some of the material's mechanical behavior and durability [8-11]. Nevertheless, switching from CNA to CRA results in a reduction in the carbon emissions that are related with the production of concrete [12, 13].

The majority of the time, loads are not the cause of cracking in concrete buildings; rather, deformation is. A has hypothesized that deformation-induced fractures make up more than 80 percent of the total number of cracks. Cracking in concrete as a result of its deformation is caused by a complex set of elements, including structural design, material composition, building method, and environmental conditions. Changes in the composition and qualities of the concrete material itself, as well as the resultant changes in building procedures, are key reasons why contemporary concrete structures are prone to cracking. Related to these factors is the evolution of construction techniques.

The term "drying shrinkage of concrete" refers to the irreversible shrinkage that occurs after the concrete stops curing and loses the adsorbed water in the internal capillary pores and gel pores in unsaturated air. The mechanism behind the drying shrinkage of concrete is primarily based on the capillary tension theory as well as the disassembly pressure theory. Dry shrinkage is a significant contributor to early cracking, and the elements that influence it include the ratio of water to cement, the make-up of cementitious materials, the kind and amount of aggregates, as well as the temperature and humidity of the surrounding environment.

Quarrying is required to produce a significant volume of sand and gravel aggregates for use in concrete products. This practice contributes to the loss of natural aggregate resources and to environmental degradation. The environmental and resource sustainability issues that now exist may be helped significantly by finding new applications for old concrete. Because the drying shrinkage of concrete is directly connected to the danger of cracking in concrete buildings, it is a scientific and technological subject that deserves to be studied. The influence of recycled aggregate on the drying shrinkage of recycled concrete is a topic deserving of further investigation.

In this study, high-strength recycled concrete was produced by exchanging natural fine aggregates for

CHAPTER 7: STRENGTH AND DRYING SHRINKAGE OF HIGH-STRENGTH CONCRETE
WITH RECYCLED AGGREGATES USING FLY ASH WITH THE FLOTATION OF
DECARBONIZATION

recycled fine aggregates of varying doses, using a double-blending technique that combined fly ash and a high-efficiency water-reducing agent, and replacing natural fine aggregates with recycled fine aggregates. The findings of this study have implications, both theoretical and practical, for improving the performance of recycled concrete in terms of its high strength.

7.2. Materials and method of experiment

7.2.1 Materials

The properties of fly ash and modified fly ash after decarbonization by flotation are shown in Table 1. The properties of recycled aggregates are shown in Table 7.2. All aggregates are utilized in saturated-surface dried (SSD) conditions. Since the aggregates' absorption was already satisfied, effective water contents of both RC and NC families were kept the same and no additional-water was added.

Table 7.1

Standards and properties of FA and MFA.

Type	Raw FA	MFA	JIS Class II	ASTM class F	GB Class I
LOI (%)	13	1.75	< 5	< 6	< 5
Density (g/cm ³)	2.32	2.33	> 1.95	2.45±5%	< 2.6
Blaine (cm ² /g)	4830	3220	> 2500	-	-
Active index (%)	86	81	> 80	> 75	> 70

Table 7.2

Physical Properties of aggregates.

Property	Coarse aggregate	RCA	Fine aggregate	RFA-M	RFA-L
Density-SSD (g/cm ³)	2.70	2.53	2.67	2.45	2.30
Fineness	6.72	6.65	2.20	2.95	2.09
Water absorption (%)	0.59	3.08	1.06	6.98	9.91

7.2.2 Mix proportion

The same water/binder ratio of 0.30 was used for the other concrete mixes with the same amount of slump. Consequently, the dosage of superplasticiser changed due to the effect of the different levels of silica fume. The high performance air entraining superplasticizer was used.

The mix proportion and strength of the experiment are shown in Table 7.3

Table 7.3

	W/C	W/B	Unit (kg/m ³)						
	(%)	(%)	W	C	MFA	S	RSM	RSL	G
HM15	30	26.08695652	180	600	90	524	0		945
HM30	30	23.07692308		600	180	421	0		945
HF100M15	30	26.08695652		600	90	0	481		945
HF100M30	30	23.07692308		600	180	0	386		945
HL100M15	30	26.08695652		600	90	0		452	945
HL100M30	30	23.07692308		600	180	0		363	945

7.2.3 Test method

Method of drying shrinkage: the base length is the distance between the inner end faces of the gauge plug. This distance is referred to as the base length. Instructions for putting in the gauge plug. After attaching the gauge plug to the form in advance in order to position it at the center of both end faces of the specimen, the concrete test specimen is created. Alternatively, a tiny hole may be bored into the cured specimen using a drill or something similar.



Photo 7.1 The gauge plug in the specimen

The following is the approach that is used to measure:

- a) At the time of the measurement, the temperature that has been prescribed for each test should be applied to the specimen, the standard scale, and the measuring equipment. The temperature is often set at 20 degrees Celsius, plus or minus 2 degrees, especially when it is not fixed.
- b) Before measuring the length of the specimen, be sure that any foreign matter that has adhered to the gauge plug has been thoroughly removed.
- c) The measuring frame is brought back to the same position it was in when the specimen was being measured.
- d) The contact point of the measuring frame is brought into contact with one of the gauge plugs of the standard ruler. This causes the tip of the spindle of the dial gauge to move along the axis connecting the gauge plugs, the spindle to gradually come out of the dial gauge, and the other gauge plug to become engaged. And make sure you're familiar with the dial gauge's scale. In this instance, you should handle the spindle with care and check to see if the contact portion is comfortable and familiar.
- e) Remove the spindle and carry out step
- d) once again. Next, determine the value that is representative of an average of the second and subsequent measurements, and label this number X_{i1} .
- g) If required, measure the mass of the specimen.

CHAPTER 7: STRENGTH AND DRYING SHRINKAGE OF HIGH-STRENGTH CONCRETE WITH RECYCLED AGGREGATES USING FLY ASH WITH THE FLOTATION OF DECARBONIZATION

f) Replace the standard scale with a specimen, perform the same process as in d), e), and take the average value from the reading of the scale on the dial gauge. Let this value be X_{i2} . In the case of mortar, the weight must be less than 1 kilogram, and the eye size must be less than 0.2 grams or less; in the case of concrete, the weight must be greater than 15 kilograms, and the eye size must be less than 2 grams or less.



Photo 7.2 Drying shrinkage test equipment

The following equation is used to compute the drying shrinkage, and the results are rounded to three significant digits by rounding off.

$$\varepsilon = \frac{(X_{01} - X_{02}) - (X_{i1} - X_{i2})}{L_0} \quad (\text{Eq 3.1})$$

ε : Drying shrinkage ($\times 10^{-6}$)

L_0 : Original length

$X_{01} - X_{02}$: Measurement values of the standard scale and specimen at the reference time point

$X_{i1} - X_{i2}$: Measurements of the standard scale and specimen at time i

The unit of the length of L_0 , X_{01} , X_{02} , X_{i1} , X_{i2} is the same.

7.3. Result and discussion

7.3.1 Drying shrinkage test

The drying shrinkage of recycled coarse and fine aggregates together is larger than the drying shrinkage of recycled coarse aggregates only, according to the findings of a significant number of tests. Furthermore, the drying shrinkage of recycled coarse and fine aggregates together is larger than the drying shrinkage of recycled coarse aggregates only. The drying shrinkage of high-strength recycled concrete, on the other hand, does not completely adhere to the aforementioned norm.

Drying shrinkage of high-strength recycled concrete has a tendency to grow with an increase in the quantity of recycled aggregate, although the 90-day dry shrinkage values of any of the groups do not surpass 500. The drying shrinkage of RCI series high-strength recycled concrete is smaller than that of the base fly ash concrete, and the 90-d dry shrinkage value is less than 400 ; on the other hand, the drying shrinkage of RCI series high-strength recycled concrete is smaller than that of the base fly ash concrete when recycled coarse and fine aggregates are used together, and the 90-d dry shrinkage value is less than 400.

When only recycled coarse aggregate is used, the drying When recycled coarse and fine aggregates are used together, the dry shrinkage of RCII series high-strength recycled concrete is larger than that

of the base fly ash concrete, and the 90-d dry shrinkage values are over 400. This occurs because the dry shrinkage of recycled coarse aggregates is greater than the dry shrinkage of recycled fine aggregates.

(1) the actual water-cement ratio of the high performance concrete with low water-cement ratio increases at the beginning of hardening because of the slow initial hydration of fly ash, and the hydration conditions of cement are improved; (2) the effect of fly ash can effectively refine the pore size of concrete, especially the pore content of 3.2 to 100 nm pore size, which increases the density of cohesion; and (3) the actual water-cement ratio of the high performance concrete with low water- (3) Because fly ash does not take part in the hydration reaction during the early stage, it is equivalent to microaggregate. Additionally, the strength of fly ash particles is very high, and the strength of microbeads can reach more than 700 MPa, which means that it can effectively impede the deformation of concrete.

In the first stages, the shrinkage caused by vitrified concrete was much less than that caused by regular concrete. When the water on the surface of the concrete evaporates in the early stage, the water contained within the vitrified concrete migrates to the cement stone, thereby compensating for the water that is lost as a result of drying the concrete.

It attributed the aforementioned phenomenon to the fact that vitrified concrete is a porous material that absorbs water during the process of mixing concrete. He said this explains how the phenomenon occurs. Because of the low stiffness of the ceramic pellets themselves, the shrinkage and deformation of the concrete are less inhibited, which results in the shrinkage of ceramic concrete being accelerated and even exceeding that of ordinary concrete.

However, because water evaporates, the amount of water that can be replenished by ceramic pellets is limited. Because recycled aggregates are porous and have a low degree of stiffness, the shrinkage of recycled concrete is very comparable to that of vitrified concrete. The "internal curing" effect of water release from recycled aggregates has a positive effect on the drying shrinkage of concrete, while the low degree of stiffness of recycled aggregates has a negative effect on the drying shrinkage of concrete. In addition to this, it was discovered that the actual water-cement ratio has a significant influence on the amount of dry shrinkage that occurs in concrete.

Since the large water absorption rate of recycled aggregate has the ability to significantly lower the actual water-cement ratio of concrete, this factor also has a positive impact on the amount of dry shrinkage that occurs in concrete. In general, the positive effect is greater than the negative effect; however, as the amount of recycled aggregate increases, the drying shrinkage of RCI series high-strength recycled concrete increases; however, it is still less than the drying shrinkage of the base fly ash concrete.

This is because the negative effect of recycled aggregate increases as the amount of recycled aggregate increases; as a result, the drying shrinkage of high-strength recycled concrete increases. As for the RCII series of high-strength recycled concrete with coarse and fine aggregates, the excessive content of fine powder in the recycled aggregate lessens the inhibiting effect of the aggregate on the shrinkage of cement stone, and at the same time, the fine powder itself is easy to shrink, which leads to a significant increase in the drying shrinkage and exceeds that of the base fly ash concrete. This is because the fine powder itself is easy to shrink. This is seen in figure 7.3, which depicts the drying shrinkage of high-strength recycled concrete.

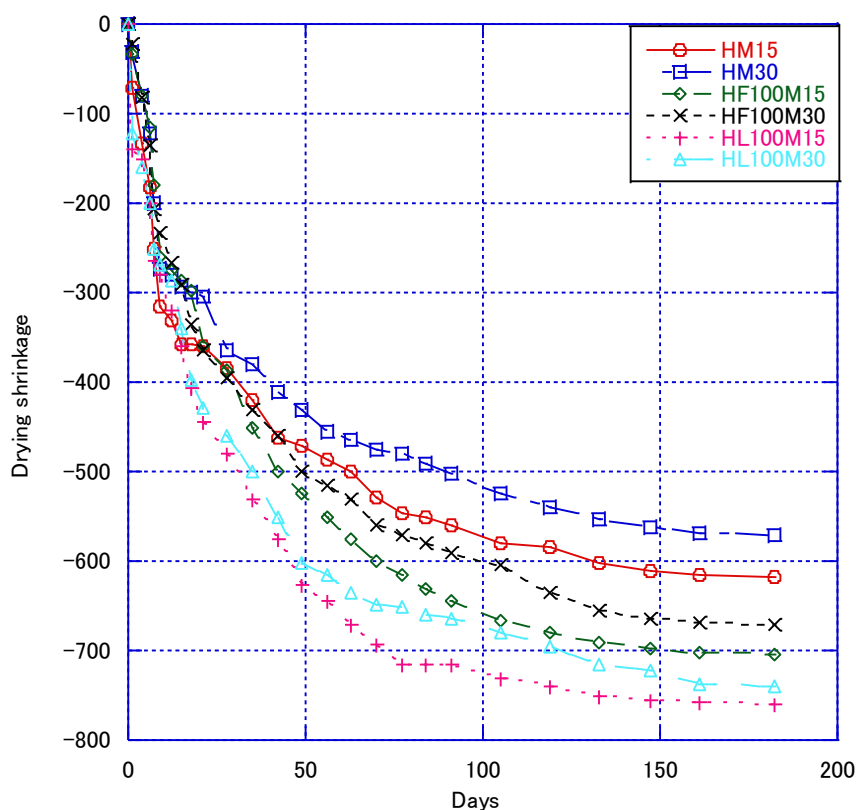


Fig 7.1 Dry shrinkage of high strength recycled concrete

7.3.2 Dry shrinkage prediction model

Because the drying shrinkage time of concrete is so lengthy, it is extremely difficult to quantify it in the laboratory. Additionally, the temperature and humidity of the concrete components in the real project are different from those in the test room, and the concrete mix ratio also changes.

As a result, many of the variables that influence the shrinkage of concrete should be taken into consideration when applying the results of an indoor shrinkage test to practical projects. Different estimate formulae for the drying shrinkage strain of concrete have been presented in a variety of technical publications and standards both in the United States and internationally. These formulas are based on a variety of experimental research and experiences.

Among them are the ACI formula proposed by the ACI209 committee, the European CEB/FIP Model Both the Code 1990 (MC-90) and the predictive formula that was developed by JCI TC911 are included. [14]

The aforementioned empirical formulae are developed by apprehending a variety of aspects via real measurement data. Because of this, the correctness of the formulas is going to be impacted to some degree. Scholars from a variety of nations are continuously refining and polishing the empirical formula in order to increase the accuracy of prediction even further.

The successful steps done both at home and abroad to improve the accuracy of prediction may be summed up as follows: I the process of developing drying shrinkage based on the theory of diffusion; and (ii) the use of short-term (28 day or 1 year) measured drying shrinkage to predict the final value of concrete drying shrinkage, which can be measured more accurately. Both of these processes are based on the diffusion theory. The following sets of forecasting models are often used.

1) ACI 209[15]

$$\varepsilon_t = \frac{t}{35 + t} \cdot \varepsilon_\mu$$

$$\varepsilon_\mu = 780 \times 10^{-6} \gamma$$

ε_t is the drying shrinkage strain at drying time t

ε_μ is the final value of drying shrinkage strain

t is the drying time

γ is the influence correction coefficient

2) CEB-FIP [16]

$$\varepsilon_t = \varepsilon_0 \beta_s (t - t_s)$$

ε_t is the drying shrinkage strain at drying time t

Notional shrinkage coefficient: $\varepsilon_0 = \beta_{RH} \cdot [160 + \beta_{sc}(90 - fc)] \cdot 10^{-6}$

β_{sc} : 5 for normal or rapid hardening cements, 8 for rapid hardening high strength cements

β_{RH} : Depends on ambient relative humidity

$\beta_s(t - t_s)$ is the coefficient to describe the development of shrinkage with time

3) The JCI TC911[14] Committee proposes the following equations for relative humidity and concrete drying shrinkage:

$$\varepsilon_t = \frac{\varepsilon_0 \cdot (t - t_0)}{\beta + (t - t_0)}$$

ε_0 : The final value of drying shrinkage strain

β : Drying shrinkage over time indicates the term

t: The drying time

t_0 : Age at which the drying shrinkage of the concrete is started to be measured

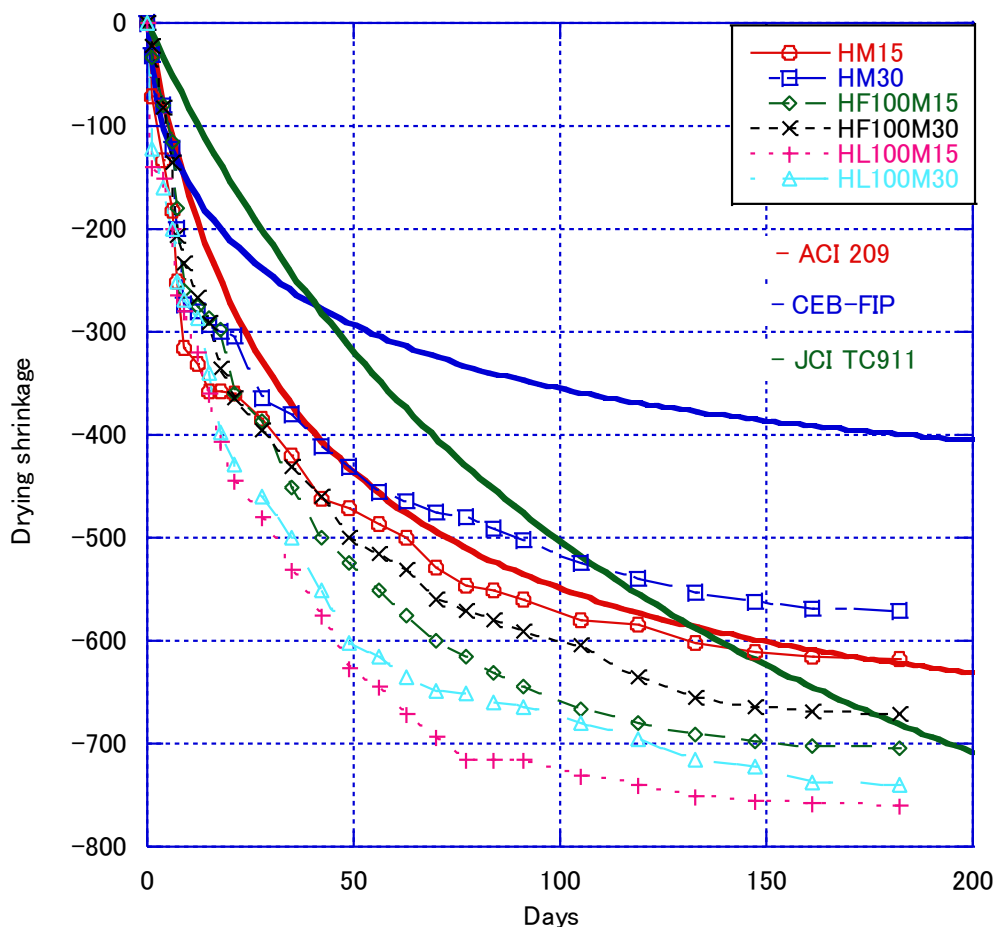


Fig 7.2 Predictive formula and experimental value of drying shrinkage

It can be seen from Figure 7.2 that the predicted value of the ACI formula is the closest to the actual value. According to the Chinese paper [17], the recommended formula is

$$\varepsilon_t = \frac{t}{a + bt} \cdot 10^{-3}$$

According to different concrete types and strength grades, the test coefficients a and b in the formula obtained by the regression are also different. When the initial age is 3 days, the basic equation of the drying shrinkage of ordinary concrete is:

$$\varepsilon_t = \frac{t}{71.84 + 1.47t} \cdot 10^{-3}$$

The linear regression analysis of the drying shrinkage of high-strength fly ash recycled concrete is carried out by the hyperbolic function model shown in the formula, and the results are shown in Table 7.4

Table 7.4 Hyperbolic regression analysis of drying shrinkage

Type	$\varepsilon_t = \frac{t}{a + bt} \cdot 10^{-3}$		Correlation coefficient
	a	b	R ²
HM15	21.67	1.56	0.98

CHAPTER 7: STRENGTH AND DRYING SHRINKAGE OF HIGH-STRENGTH CONCRETE
WITH RECYCLED AGGREGATES USING FLY ASH WITH THE FLOTATION OF
DECARBONIZATION

HM30	29.52	1.83	0.98
HF100M15	33.80	1.25	0.99
HF100M30	31.85	1.09	0.99
HL100M15	22.41	1.07	0.99
HL100M30	23.49	1.04	0.99

From the results of regression analysis shown in Table 4, it can be seen that the hyperbolic function model can be used to estimate the drying shrinkage of fly ash high-strength recycled concrete, and the relevant indices are all 0.0. However, its coefficients (a, b) are quite different from those of ordinary concrete. The coefficient a of the series with high quality recycled aggregate is greater than that of the series of high-strength recycled concrete with low quality of raw aggregate.

7.4. Conclusion

- Due to the effect of fly ash, high-strength recycled concrete has better volume stability.
- In the range of 30%, with the increase of recycled aggregate content, the drying shrinkage of high-strength recycled concrete tends to decrease.
- By comparing the predicted formulas of various countries, the predicted formula of ACI is the closest to the actual value of this experiment.
- The coefficients a and b in the Chinese hyperbolic function model are used for correction, so that it can better estimate the drying shrinkage of high-strength recycled concrete, and the relevant indexes are all 0. Above 90, the estimation accuracy is high.

Reference

- [1] Freedonia-Group, Global Construction Aggregates - Demand and Sales Forecasts, Market Share, Market Size, Market Leaders (2016)
- [2] W.H. Langer, B.F. Arbogast, Environmental impacts of mining natural aggregate, Deposit and Geoenvironmental Models for Resource Exploitation and Environmental Security, Springer (2002), pp. 151-169
- [3] R. Kurda, J.D. Silvestre, J. de Brito, Toxicity and environmental and economic performance of fly ash and recycled concrete aggregates use in concrete: a review
- [4] J. Tai, M. An, X. Wang, Annual Research Report on the Development of Urban 637 Environmental and Sanitation Industry in China: 2015–2016 (2017), Shanghai, China
- [5] J. Pacheco, J. de Brito, J. Ferreira, D. Soares, Dynamic characterization of full-scale structures made with recycled coarse aggregates, J. Clean. Prod., 142 (2017), pp. 4195-4205
- [6] E. Benhelal, G. Zahedi, E. Shamsaei, A. Bahadori, Global strategies and potentials to curb CO2 emissions in cement industry, J. Clean. Prod., 51 (2013), pp. 142-161
- [7] R. Kurda, J. de Brito, J. Silvestre, Combined economic and mechanical performance optimization of recycled aggregate concrete with high volume of fly ash, Appl. Sci., 8 (2018), p. 1189
- [8] B. Ali, L.A. Qureshi, Durability of recycled aggregate concrete modified with sugarcane molasses, Constr. Build. Mater., 229 (2019), Article 116913
- [9] B. Ali, L.A. Qureshi, Influence of glass fibers on mechanical and durability performance of concrete with recycled aggregates, Constr. Build. Mater., 228 (2019), Article 116783
- [10] R. Kurad, J.D. Silvestre, J. de Brito, H. Ahmed, Effect of incorporation of high volume of recycled concrete aggregates and fly ash on the strength and global warming potential of concrete, J. Clean. Prod., 166 (2017), pp. 485-502

CHAPTER 7: STRENGTH AND DRYING SHRINKAGE OF HIGH-STRENGTH CONCRETE
WITH RECYCLED AGGREGATES USING FLY ASH WITH THE FLOTATION OF
DECARBONIZATION

- [11] B. Masood, A. Elahi, S. Barbhuiya, B. Ali, Mechanical and durability performance of recycled aggregate concrete incorporating low calcium bentonite, *Constr. Build. Mater.*, 237 (2019), Article 117760,
- [12] A.M. Braga, J.D. Silvestre, J. de Brito, Compared environmental and economic impact from cradle to gate of concrete with natural and recycled coarse aggregates, *J. Clean. Prod.*, 162 (2017), pp. 529-543
- [13] C.F. Hendriks, G.M.T. Janssen, Use of recycled materials in constructions, *Mater. Struct.*, 36 (2003), pp. 604-608
- [14] Japan Concrete Association Concrete structure creep, And Time-Dependent Deformation due to Shrinkage Research Committee Report, pp.101-121,2001
- [15] ACI Committee 209, Prediction of creep, shrinkage and temperature effects in concrete structures, *ACI Manual of concrete practice, Part 1*, 1997, 209R 1-92.
- [16] CEB-FIP Model Code for concrete structures, Evaluation of the time dependent behavior of concrete, *Bulletin d'Information No. 199*, Comite European du Beton/Federation Internationale de la Precontrainte, Lausanne, 1999.
- [17] Pan Liben, & Zhang Sujun. (1997). Experimental study on shrinkage and creep of concrete. *Journal of Hohai University: Natural Science Edition*, 25(5), 84-89.

Chapter 8

CONCLUSION

8.1 Conclusion

CHAPTER 1 RESEARCH BACKGROUND AND PURPOSE OF THE STUDY focuses on the production of fly ash and the hazards, briefly describes the classification system of fly ash, and discusses the development status of the flotation method of fly ash. The background and significance of the study of fly ash recycled concrete are discussed, while the significance of the study is reflected by introducing the mechanical and physical properties of concrete. Finally, the purpose and innovation of this study are briefly described.

CHAPTER 2 PREVIOUS LITERATURE REVIEW mainly introduces the current status of research on fly ash concrete at home and abroad. The development of fly ash decarbonization technology is reflected through the development of fly ash flotation method and the international utilization of fly ash. The development status of recycled aggregates and the development status of compressive strength, drying shrinkage, and elastic modulus of concrete are also introduced.

CHAPTER 3 RESEARCH METHOD mainly describes the experimental methods of this study. It includes the development process of the flotation method and the design of the concrete mix ratio introducing the development method of the new equipment. The experiments for measuring the concrete properties are also introduced, which include the mix design, slump experiment, air volume determination experiment, compressive strength experiment, drying shrinkage experiment, elastic modulus experiment and porosity determination experiment.

CHAPTER 4 DEVELOPMENT OF FLOTATION DEVICE FOR REMOVING UNBURNT CARBON IN FLY ASH FOR USE IN HARDENED CEMENTITIOUS MATERIALS concluded that: We developed a prototype device for removing unburned carbon from fly ash by means of the flotation method and examined the operating conditions of the device experimentally. The fly ash was used in Portland cement concrete and the concrete properties were measured. Our findings are summarized as follows. The base model, which used a circulating microbubble generator with a spiral pump, removed unburned carbon from fly ash by means of the froth flotation method without affecting the chemical composition of the fly ash. The removal efficiency was increased by adding a collecting agent to 60 wt% fly ash slurry and pre-stirring with a concrete mixer for 30 min. The LOI was greatly reduced within 10 min, and a treatment time of 30 min was sufficient. Flotation was improved by pre-stirring the sample and adding water to form a slurry with a concentration of 20 wt%. MFAS was used in the mortar, and its properties were better than those of dry fly ash. MFAS reduced the compressive strength of concrete at 7–91 days. The drying shrinkage of concrete containing fly ash was greater than that of ordinary concrete; however, at fly ash replacement ratios of 15–30%, the replacement ratio did not affect the drying shrinkage. Our results demonstrate that it is feasible to use modified fly ash prepared using the flotation method in concrete.

CHAPTER 5 EFFECT OF INCORPORATING FLY ASH AND RECYCLED FINE AGGREGATE ON PROPERTIES AND CUMULATIVE PORE VOLUME OF CONCRETE concluded that: Incorporating RFA or low amount of FA as into concrete reduces its initial strength, but the compressive strength of concrete incorporating an appropriate amount of FA can reach that of

concrete without FA as the age of concrete increases or the W/B ratio decreases. The effect on the initial compressive strength of adding both FA and RFA to concrete is greater than adding either component lone. However, the pozzolanic reaction gradually produces a beneficial effect on the compressive strength of the concrete as time passes. Incorporating RFA into the concrete mixture increase the drying shrinkage of the concrete whereas FA which can inhibit the increase of drying shrinkage of concrete by RFA, decreases the drying shrinkage. Cumulative pore volume increases with an increase of RFA replacement ratio and decreases with a decrease of the W/B ratio. Concrete incorporating FA should be considered separately when investigating the correlation between cumulative pore volume and compressive strength or drying shrinkage. There is no linear correlation between compressive strength and cumulative pore volume in all interval divisions. There is a linear correlation between cumulative pore volume and drying shrinkage result from the incorporation of FA in concrete and the optimal interval division for investigating the correlation between drying shrinkage and the cumulative pore volume of concrete incorporating FA is $0.003\text{--}b \mu\text{m}$. the smallest pore diameter that can be measured by the MIP test is $0.003 \mu\text{m}$ and point b is the right change point of pore diameter in a plot of cumulative pore volume.

CHAPTER 6 A STUDY ON PROPERTIES, STATIC AND DYNAMIC ELASTIC MODULUS OF RECYCLED CONCRETE UNDER THE INFLUENCE OF MODIFIED FLY ASH concluded that: There are two types of linear correlations between the static modulus E_c and the dynamic modulus E_d , one of which is affected by age of concrete. The relationship between the compressive strength and static modulus of elasticity is recommended by an equation derived based on the formula of each national standard. A polynomial equation suggests a relationship between the compressive strength and dynamic modulus of elasticity. The $E_d - f_c$ connection is governed by two factors: recycled aggregate volume content and quality. E_d or ε_d of concrete has the highest correlation for pore volumes in the 10 nm-20 nm pore diameter range, and there is a high degree of consistency in the cases affected by RFA volume content, RFA quality, and MFA volume content.

CHAPTER 7 STRENGTH AND DRYING SHRINKAGE OF HIGH-STRENGTH CONCRETE WITH RECYCLED AGGREGATES USING FLY ASH WITH THE FLOTATION OF DECARBONIZATION concluded that: Due to the effect of fly ash, high-strength recycled concrete has better volume stability. In the range of 30%, with the increase of recycled aggregate content, the drying shrinkage of high-strength recycled concrete tends to decrease. By comparing the predicted formulas of various countries, the predicted formula of ACI is the closest to the actual value of this experiment. The coefficients a and b in the Chinese hyperbolic function model are used for correction, so that it can better estimate the drying shrinkage of high-strength recycled concrete, and the relevant indexes are all 0. Above 90, the estimation accuracy is high.

CHAPTER 8 CONCLUSION presents the key findings of each chapter and the conclusion of the general paper. Finally the future of this study is looked forward.

In general, this paper starts with the development of new flotation equipment to bring fly ash up to industrial standards by reducing the carbon content in fly ash. After that the mechanical and physical

properties of concrete with different proportions and different aggregates are measured by different experiments, compared with normal concrete and an attempt is made to find out the connection between some of these properties. By comparing the measurements of compressive strength, drying shrinkage, static modulus of elasticity and dynamic modulus of elasticity of normal concrete with the predicted values of drying shrinkage of high strength concrete, it can be concluded that the application of fly ash in concrete after decarbonization using the new flotation method makes good results.

8.2 Prospect

(1) in the process of incorporating fly ash instead of cement, the optimal value of the various properties of concrete corresponding to the ratio is often mismatched, and it is even possible that when a certain performance is optimal when the other performance has been affected, resulting in fly ash concrete performance defects, many scholars only consider the optimal ratio of some of the properties often ignore the optimal ratio of the overall performance. Therefore, the optimal ratio of comprehensive performance is how to maximize the problem that we need to solve in the concrete industry today.

(2) Although the compressive strength of fly ash concrete is improved compared with ordinary concrete, its strength is still not high. The combination of graphene and fly ash on the various properties of concrete does not seem to be too much involved in the study, the relevant research found that [13 graphene can not only promote the hydration rate of fly ash concrete, improve the early strength and can significantly improve the compressive strength of concrete, etc., but there are many properties that many scholars have not started research. For the time being, the addition of graphene in fly ash is a new trend in the future of concrete, it can significantly improve the strength of concrete, the preparation of new high-performance concrete.

(3) Fly ash is a hydrophobic material, its water retention properties are not enough, in the study of good water retention properties and can also enhance the mechanical properties of the material problem, has not found a better way. As a green and highly active organic fertilizer, many scholars do not associate it with concrete, and using earthworm manure as a new material for the construction industry is certainly a new path. Firstly, during the digestion process, earthworms produce organic acids, which chemically bond with the silica carboxyl groups in the concrete system to enhance the mechanical properties of the system, and secondly, earthworm manure has good water retention properties, which can promote the full hydration of concrete and thus enhance the mechanical properties of the system [1". At present, the study of applying earthworm manure to concrete has not been carried out.

(4) Fly ash as an active material with volcanic ash properties, has replaced part of the cement. As an emerging building material, the combination of its own properties of fly ash and cement in the application of concrete and research has been comprehended by many scholars, only fly ash as a single admixture can no longer meet the innovative requirements of the concrete industry, the future will be fly ash as the main material, other admixtures as auxiliary materials and admixtures compounded into the cement to make concrete structure and study the properties of concrete; Research the most suitable ratio to meet the requirements of concrete performance. Secondly, fly ash will also be improved to obtain better performance of environmentally friendly concrete.